Towards quantifying the role of hydrogen bonding within amphiphile self-association and resultant aggregate formation.

L. J. White,[a] N. J. Wells,[b] L. R. Blackholly,[a] H. J. Shepherd,[a] B. Wilson,[a] G. P. Bustone,[a] T. J. Runacres,[c] and J. R. Hiscock*[a]

[a] *School of Physical Sciences, University of Kent, Park Wood Road, Canterbury, Kent, CT2 7NH, UK; Email: J.R.Hiscock@Kent.ac.uk; Tel: +44 (0)1227 823043.*

[b] *School of Chemistry, University of Southampton, Southampton, UK, SO17 1BJ.*

[c] *School of Biosciences, University of Kent, Park Wood Road, Canterbury, Kent, CT2 7NH, UK.*

Electronic Supplementary Information

Table of Contents

Chemical structures

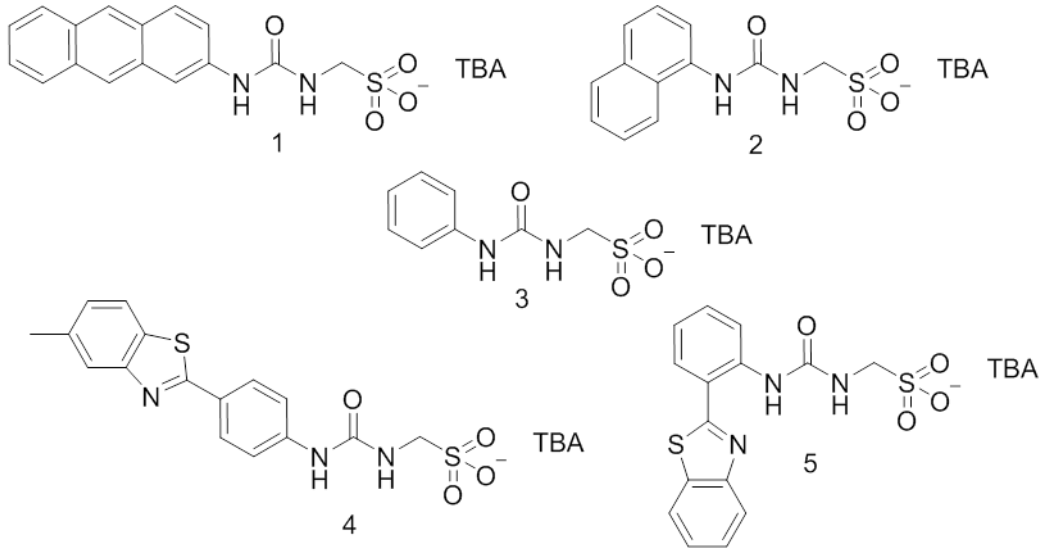

Experimental

General remarks: All reactions were performed under slight positive pressure of nitrogen using oven dried glassware. NMR spectra were determined using a Jeol ECS-400, Burker AV2 500, Burker AV2 400 or Bruker AV3 600 MHz spectrometer with the chemical shifts reported in parts per million (ppm), calibrated to the centre of the solvent peak set. All solvents and starting materials were purchased from commercial sources or chemical stores where available. High resolution mass spectra were collected using a Bruker micrOTOF-Q mass spectrometer or a SYNAPT G2-S Mass Spectrometer. Melting points were recorded in open capillaries using a Stuart SMP10 melting point apparatus and are uncorrected. Infrared (IR) spectra were recorded using a Shimadzu IR-Affinity 1, and reported in wavenumbers (cm^{-1}). DLS studies were performed using a Malvern Zetasizer Nano ZS. UV-Vis were recorded using a Shimadzu UV-1800, and reported in nm. Fluorometric measurements were obtained using a Perkin Elmer LS-50 Luminescence Spectrometer. Tensiometry performed using a Biolin Scientific Theta Attension optical tensiometer with data analysis conducted using one attension software.

Transmission and Fluorescence Microscopy: Samples were visualised using an Olympus IX71 microscope with PlanApo 100x OTIRFM-SP 1.49 NA lens mounted on a PIFOC *z*-axis focus drive (Physik Instrumente, Karlsruhe, Germany), fitted onto an ASI motorised stage (ASI, Eugene, OR), with the sample holder, objective lens and environmental chamber held at the required temperature. Samples were illuminated using LED light sources (Cairn Research Ltd, Faversham, UK) with appropriate filters (Chroma, Bellows Falls, VT). Samples were visualised using either a Zyla 5.5 (Andor) CMOS camera, and the system was controlled with Metamorph software (Molecular Devices). 10 µl of the appropriate sample was pipetted onto the centre of an agarose pad, covered with a coverslip and secured in place. Images were analysed using Metamorph software. Filters used to aid visualization within these studies: DAPI excitation 360 nm and emission 460 nm, and GFP excitation 480 nm and emission 510 nm.[1]

DLS studies: Studies conducted with compounds **1 - 5** were prepared in series with an aliquot of the most concentrated solution undergoing serial dilution. Sample sizes were kept to 1 mL. All solvents used for DLS studies were filtered to remove particulates from the solvents. Samples were heated to the appropriate temperature and allowed to equilibrate for 2 minutes and then a series of 10 'runs' were performed with each sample to give enough data to derive an appropriate average. In some instances, the raw correlation data indicated that a greater amount of time may be needed for the samples to reach a stable state. For this reason, only the last 9 'runs' were included in the average size distribution calculations.

Zeta potential studies: All solvents used for Zeta potential studies were filtered to remove particulates from the solvents. Samples were heated to the appropriate temperature and allowed to equilibrate for 2 minutes and then a series of 10 'runs' at 25 ^{o}C were performed with each sample to give enough data to derive an appropriate average. In some instances, the raw correlation data indicated that a greater amount of time may be needed for the samples to reach a stable state. For this reason, only the last 9 'runs' were included in the average size distribution calculations.

HRMS studies: Samples were dissolved in HPLC methanol at a concentration of 1 mg/ml before being diluted 1 in 100 in methanol. 10 µL of sample was injected into a flowing stream of 10 mM ammonium acetate in 95% methanol in water (flow rate: 0.02 ml/min) and the flow directed into the electrospray source of the mass spectrometer. Mass spectra were acquired in the negative ion mode and data processed in Bruker's Compass Data Analysis software or Mass Lynx software utilising a lock mass.

UV-Vis studies: Samples were prepared in series with an aliquot of the most concentrated solution undergoing serial dilution. All solutions underwent an annealing process and were allowed to rest for approximately 2 minutes before undergoing analysis. The absorbance of solutions was noted at equilibrium temperature of 298.15K.

Fluorometry studies: Samples were prepared in series with an aliquot of the most concentrated solution undergoing serial dilution. All solutions underwent an annealing process and were allowed to rest for approximately 2 minutes before undergoing analysis. Compounds **1**, **2** and **4** were analysed at a concentration of 0.003 mM and compound **5** at a concentration of 0.03 mM.

Tensiometry studies: Samples were prepared in series with an aliquot of the most concentrated solution undergoing serial dilution. All solutions underwent an annealing process and were allowed to rest for approximately 2 minutes before undergoing analysis. Surfactant adsorption behaviour and critical micelle concentrations (CMC's) are determined by surface tension measurements using axisymmetric drop shape analysis with a pendant-drop apparatus. A succession of 3 droplets were measured for each sample and an average for these measurements reported.

Self-association constant calculation: All association constants were calculated using the freely available bindfit programme (http://app.supramolecular.org/bindfit/). All the data relating to the calculation of the association constants can be accessed online, through the links given for each complexation event.

Compound 1: Triphosgene (0.445 g, 1.50 mM) was added to a stirring solution of 2-aminoanthracene (0.62 g, 3.01 mM) in ethyl acetate (30 mL). The mixture was heated at reflux overnight. Tetrabutylammonium (TBA) hydroxide (1N) in methanol (1.73 ml) was added to aminomethanesulfonic acid (0.19g, 1.73 mM) at room temperature and taken to dryness to give the tetrabutylammonium sulfonate salt. This salt was then added to the original reaction mixture, which was then heated for a further 4 hours at reflux. The resultant mixture was then filtered and the filtrate taken to dryness, re-dissolved in chloroform (10 mL) and washed with water (10 mL). The organic fraction was then taken to dryness. The pure product was obtained by flash chromatography 100 % ethyl acetate followed by 100 % methanol. The methanol fraction was taken to dryness with further addition of TBAOH as necessary to give the pure product as a dark yellow/brown solid. Yield 43 % (0.74 g, 1.29 mM); MP : 98 °C; ^{1}H NMR (400 MHz, DMSO-d_6): δ: 9.11 (br, s, 1H, NH), 8.41 (s, 1H), 8.30 (s, 1H), 8.21 (s, 1H), 7.97 (dd, *J* = 12.97, 8.00 Hz, 3H), 7.50 – 7.29 (m, 3H), 6.80 (t, *J* = 5.67 Hz, 1H), 3.98 (t, *J* = 8.12 Hz, 2H), 3.23 – 3.00 (m, 8H), 1.64 – 1.43 (m, 8H), 1.38 – 1.20 (m, 8H), 0.91 (t, *J* = 7.32 Hz, 12H); ^{13}C{^{1}H} NMR (100 MHz, DMSO-d_6): δ: 155.2 (CO), 138.1 (ArC), 132.7 (ArC), 132.2 (ArC), 130.3 (ArCH), 129.2 (ArC), 128.6 (ArCH), 128.5 (ArCH), 128.1 (ArCH), 126.3 (ArCH), 125.9 (ArC), 124.9 (ArCH), 124.5 (ArCH), 121.4 (ArCH), 111.1 (ArCH), 58.0 (CH_2), 56.6 (CH_2), 23.6 (CH_2), 19.7 (CH_2) , 14.0 (CH_3); IR (film): ν = 3290 (NH stretch), 1689, 1215, 1176, 887; HRMS for the sulfonate-urea ion ($C_{15}H_{22}N_3O_4S_2$) (ESI^-): m/z: act: 362.0261 $[M]^-$ cal: 362.0275 $[M]^-$.

Compound 2: Aminomethanesulfonic acid (0.330 g, 3 mM) was added to a stirring solution of 1-naphthyl isocyanate (0.282 mL**,** 3 mM) in pyridine (10 mL). The mixture was heated to 60 °C overnight and the precipitate removed by filtration and the filtrate taken to dryness. The resulting residue was dissolved in a solution of tetrabutylammonium (TBA) hydroxide (1N) in methanol (1.2 ml) and taken to dryness, dissolved in dichloromethane (40 mL) and washed with water (40 mL). The organic phase was then taken to dryness. The pure product was obtained through precipitation from ethyl acetate (30 mL) as pale brown solid with a yield of 31% (0.489g, 0.94 mM); Melting point: 78 °C; ^{1}H NMR (400 MHz, DMSO-d_6): δ: 8.80 (s, 1H), 8.17 (d, *J* = 7.99 Hz, 1H), 8.09 (d, *J* = 5.44 Hz, 1H), 7.88 (d, *J* = 8.18 Hz, 1H), 7.60 – 7.46 (m, 3H), 7.41 (t, *J* = 7.89 Hz, 1H), 7.11 (t, *J* = 5.68 Hz, 1H), 3.94 (d, *J* = 5.72 Hz, 2H), 3.21 – 3.05 (m, 8H), 1.64 – 1.40 (m, 8H), 1.41 – 1.21 (m, 8H), 0.92 (t, *J* = 7.31 Hz, 12H); ^{13}C{^{1}H} NMR (100 MHz, DMSO-d_6): δ: 155.40 (CO), 135.76 (ArC), 134.17 (ArC), 128.79 (ArCH), 126.37 (ArCH), 126.14(ArCH), 125.82(ArCH), 125.59 (ArCH), 122.21 (ArCH), 121.78 (ArCH), 116.10 (ArC), 57.99 (CH_2), 56.71 (CH_2), 23.53 (CH_2), 19.67 (CH_2), 13.95 (CH_3); IR (film): ν = 3321 (NH stretch), 1700, 1245, 1174, 879; HRMS for the sulfonate-urea ion ($C_{12}H_{11}N_2O_4S$) (ESI^-): m/z: act: 278.9615 $[M]^-$ cal: 279.0445$[M]^-$.

Compound 3: This compound was synthesised in line with previously published methods.[2]

Compound 4: Aminomethanesulfonic acid (0.23 g, 2.08 mM) was added to tetrabutylammonium (TBA) hydroxide (1N) in methanol (2.08 ml, 2.08 mM) and taken to dryness. Triphosgene (0.309 g, 1 mM) was added to a stirring solution of 4-(6-methylbenzothiazol)aniline (0.5 g, 2 mM) in ethyl acetate (30 mL) and the mixture heated at reflux for 4 hours. The tetrabutylammonium salt was then dissolved in ethyl acetate (10 mL) and added to the reaction mixture and heated at reflux overnight, filtered and the solid washed with ethyl acetate (10 mL). The impurities were removed through the recrystallization, followed by filtration of the solid from methanol. The filtration was then taken to dryness to give the pure product as a yellow solid with a yield of 65 % (0.806 g, 1.33 mM); Melting Point: 98 °C; ^{1}H NMR (400 MHz, DMSO-d_6): δ: 9.25 (s, 1H), 7.95 – 7.75 (m, 4H), 7.58 (d, *J* = 8.74 Hz, 2H), 7.37 – 7.20 (m, 1H), 6.98 (t, *J* = 5.88 Hz, 1H), 3.96 (d, *J* = 5.88 Hz, 2H), 3.20 – 3.01 (m, 9H), 2.43 (s, 3H), 1.63 – 1.43 (m, 9H), 1.40 – 1.17 (m, 9H), 0.91 (t, *J* = 7.32 Hz, 13H); ^{13}C{^{1}H} NMR (100 MHz, DMSO-d_6): δ: 166.7 (CO), 154.8 (ArC), 152.4 (ArC), 144.1 (ArC), 135.7 (ArC), 134.8 (ArC), 128.4 (ArCH, ArCH), 128.3 (ArCH, ArCH), 126.0 (ArC), 122.4 (ArCH), 122.2 (ArCH), 118.1 (ArCH), 60.0 (CH_2), 56.5 (CH_2), 23.6 (CH_2), 21.6 (CH_3), 19.7 (CH_2), 14.02 (CH_3); IR (film): ν = 2984 (NH stretch), 1697, 1176,

1035, 843; HRMS for the sulfonate-urea ion ($C_{16}H_{14}N_3O_4S_2$) (ESI^-): m/z: act: 376.0390 $[M]^-$ cal: 376.0431 $[M]^-$.

Compound 5: A mixture of 2-(2-Aminophenyl)benzothiazole (0.392 g, 1.73 mM) and 1,1'-Carbonyldiimidazole (0.281g, 1.73 mM) were heated at reflux for 3 hours in chloroform (10mL).A mixture of aminomethanesulfonic acid (0.19g, 1.73 mM) and tetrabutylammonium (TBA) hydroxide (1N) in methanol (1.73 ml) were added to anhydrous pyridine (2 mL) at room temperature. This solution was added to the original reaction mixture which was heated at reflux overnight. The resultant solid was removed by filtration and the filtrate taken to dryness, dissolved in methanol (30 mL) and a precipitate removed by filtration. The filtrate was taken to dryness, dissolved in ethyl acetate (20 mL) and washed with water (20 mL). The organic fraction was then taken to dryness then dissolved in ethyl acetate (30 mL) where precipitation occurred. The precipitate was removed by filtration to give the pure product a pale-yellow solid with a yield of 42% (0.255g, 0.42 mM); Melting Point: 168 ^oC; ^1H NMR (400 MHz, DMSO-d_6): δ: 10.67 (s, 1H) 8.45 (d, *J* = 7.77 Hz, 1H), 8.30 (d, *J* = 7.79 Hz, 1H), 8.15 (d, *J* = 7.92 Hz, 1H), 7.85 (br s,d, *J* = 7.72 Hz, 2H), 7.58 (t, *J* = 7.58 Hz, 1H), 7.47 (tt, *J* = 11.69, 7.49 Hz, 2H), 7.10 (t, *J* = 7.52 Hz, 1H), 3.96 (s, 2H), 3.23 – 2.99 (m, 8H), 1.62 – 1.44 (m, 8H), 1.41 – 1.19 (m, 8H), 0.92 (t, *J* = 7.32 Hz, 12H); $^3C\{^1H\}$ NMR (100 MHz, DMSO-d_6): δ: 167.9 (CO), 154.9 (ArC), 153.3 (ArC), 139.8 (ArC), 133.8 (ArC), 132.0 (ArCH), 130.5 (ArCH), 127.0 (ArCH), 126.3 (ArCH), 124.0 (ArCH), 122.4 (ArCH), 122.0 (ArCH), 120.9 (ArCH), 119.3 (ArC), 58.0 (CH_2), 56.8 (CH_2), 23.6 (CH_2), 19.7 (CH_2), 14.0 (CH_3); IR (film): ν = 3275 (NH stretch), 1670, 1186, 1041, 879; HRMS for the sulfonate-urea ion ($C_{15}H_{12}N_3O_4S_2$) (ESI^-): m/z: act: 362.0261 $[M]^-$ cal: 362.0275 $[M]^-$.

Characterisation NMR

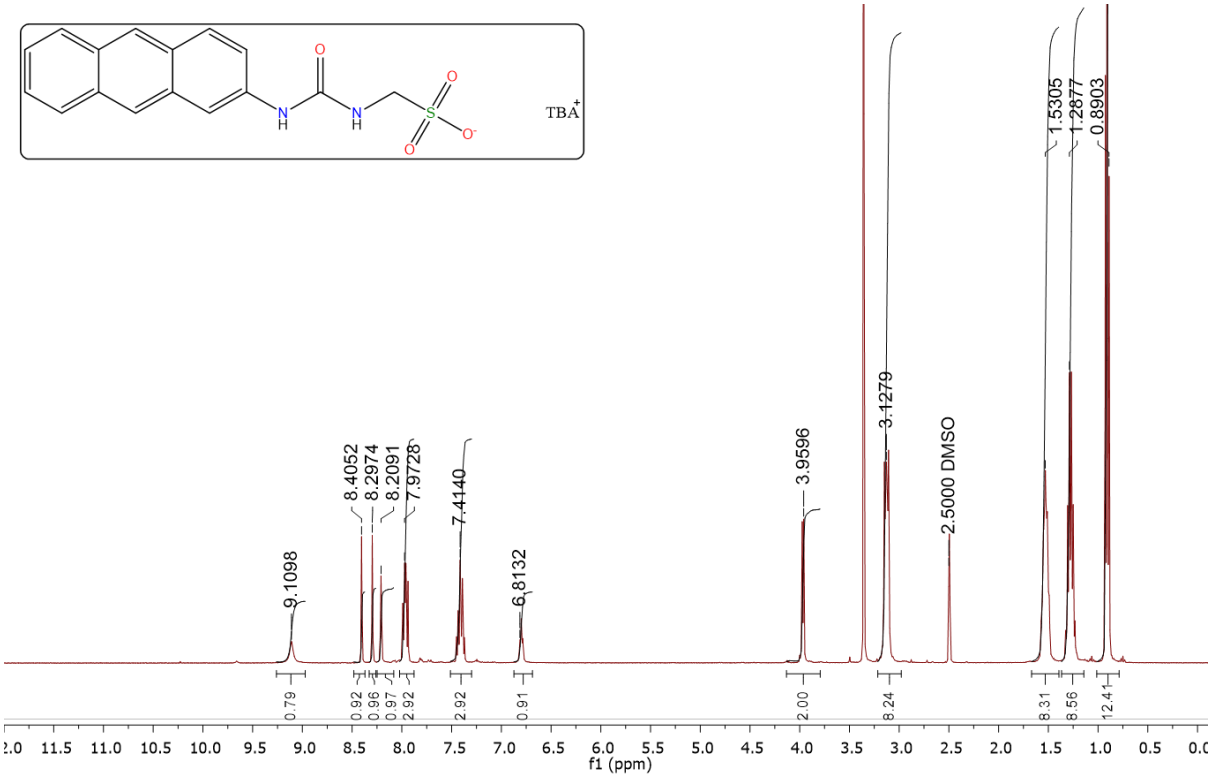

Figure S1 – ^{1}H NMR of compound **1** in DMSO-d_6.

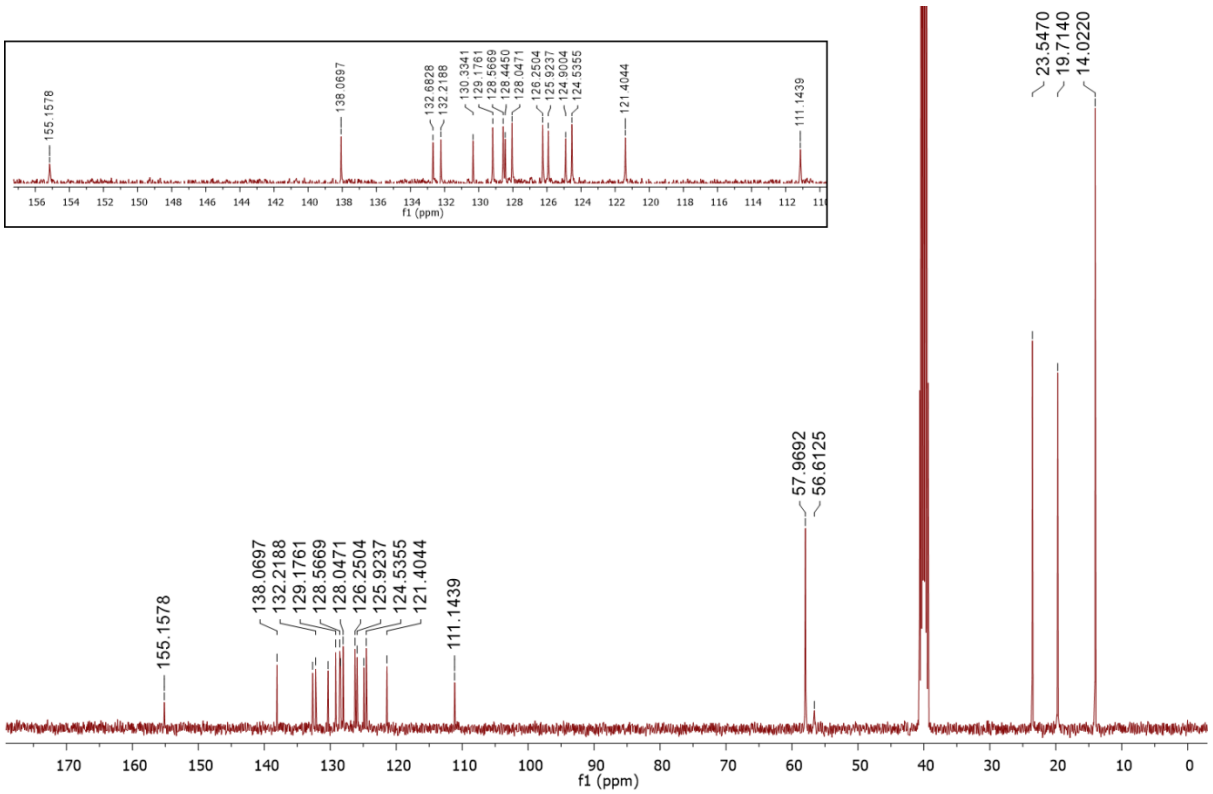

Figure S2 – ^{13}C NMR of compound **1** in DMSO-d_6.

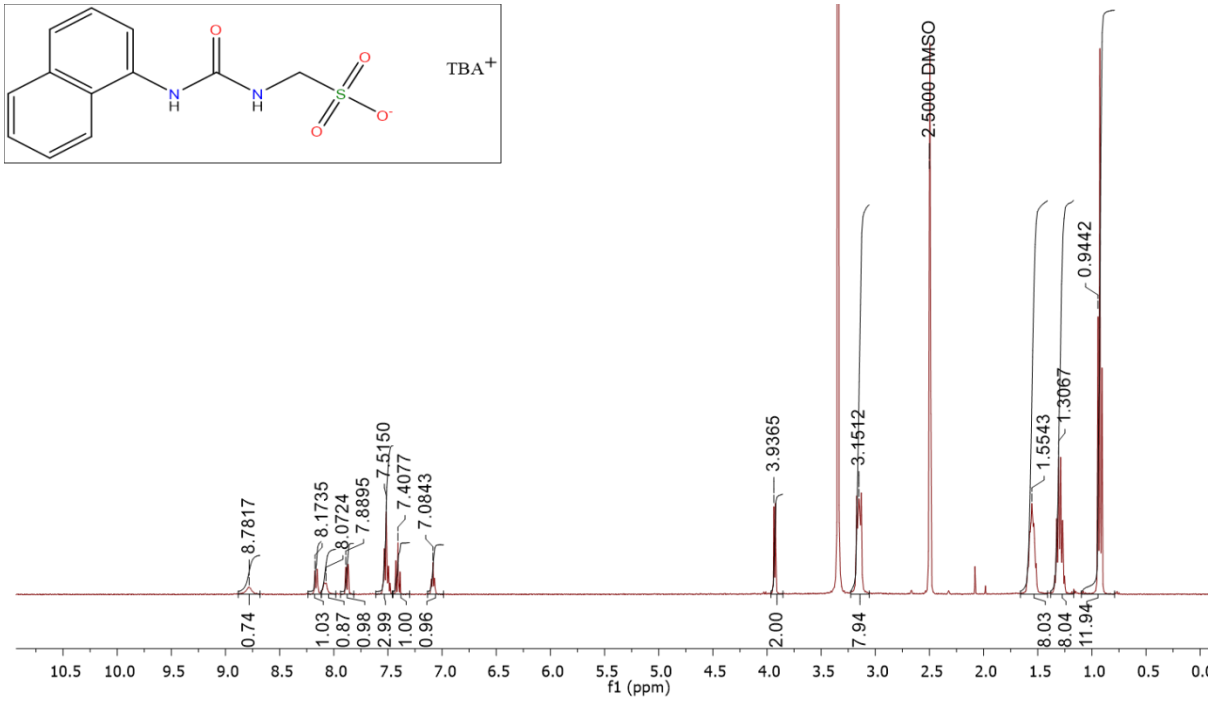

Figure S3 – ^{1}H NMR of compound **2** in DMSO-d_6.

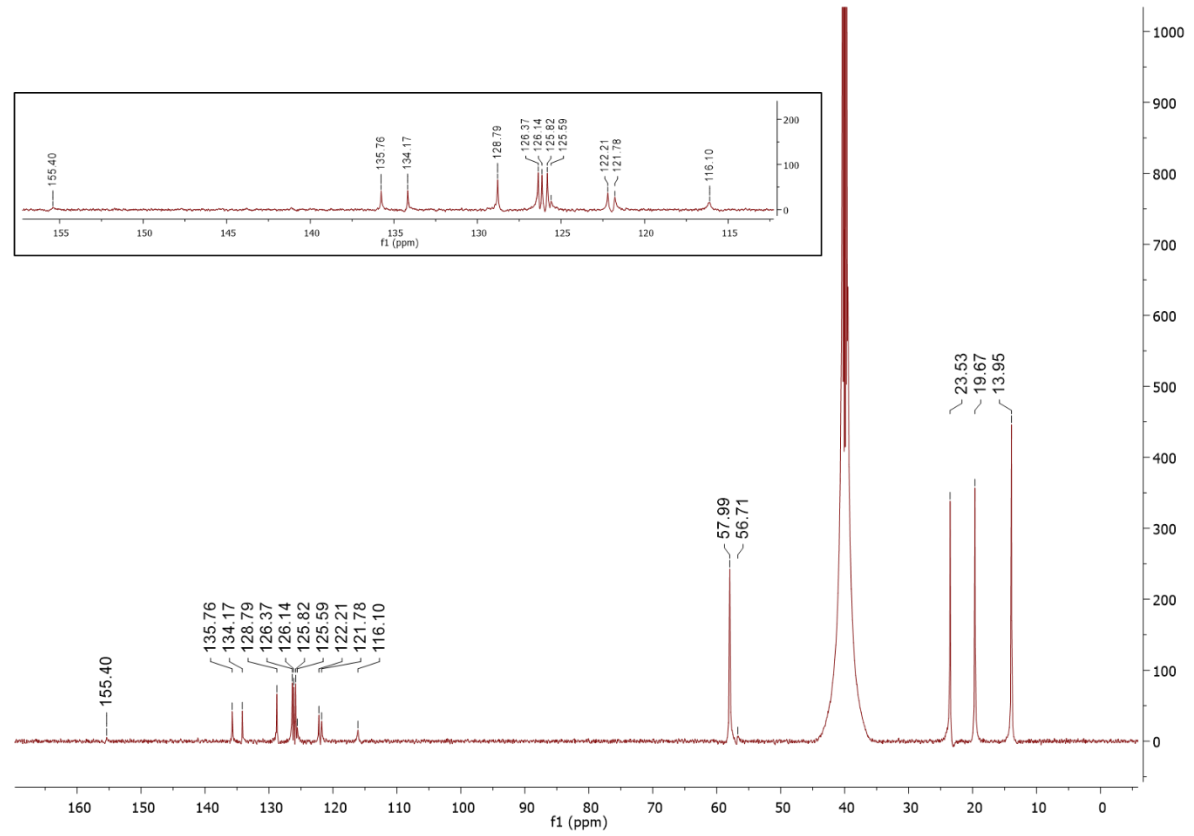

Figure S4 – ^{13}C NMR of compound **2** in DMSO-d_6.

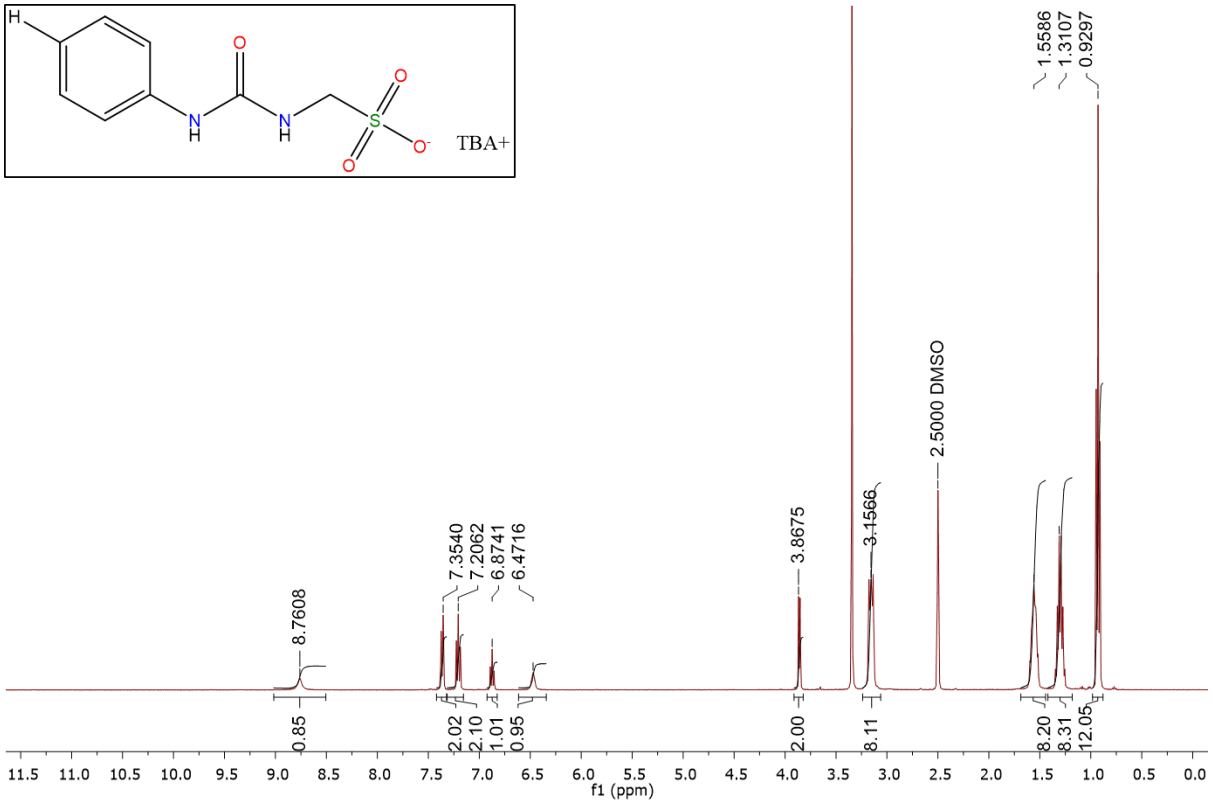

Figure S5 – ^{1}H NMR of compound **3** in DMSO-d_6.

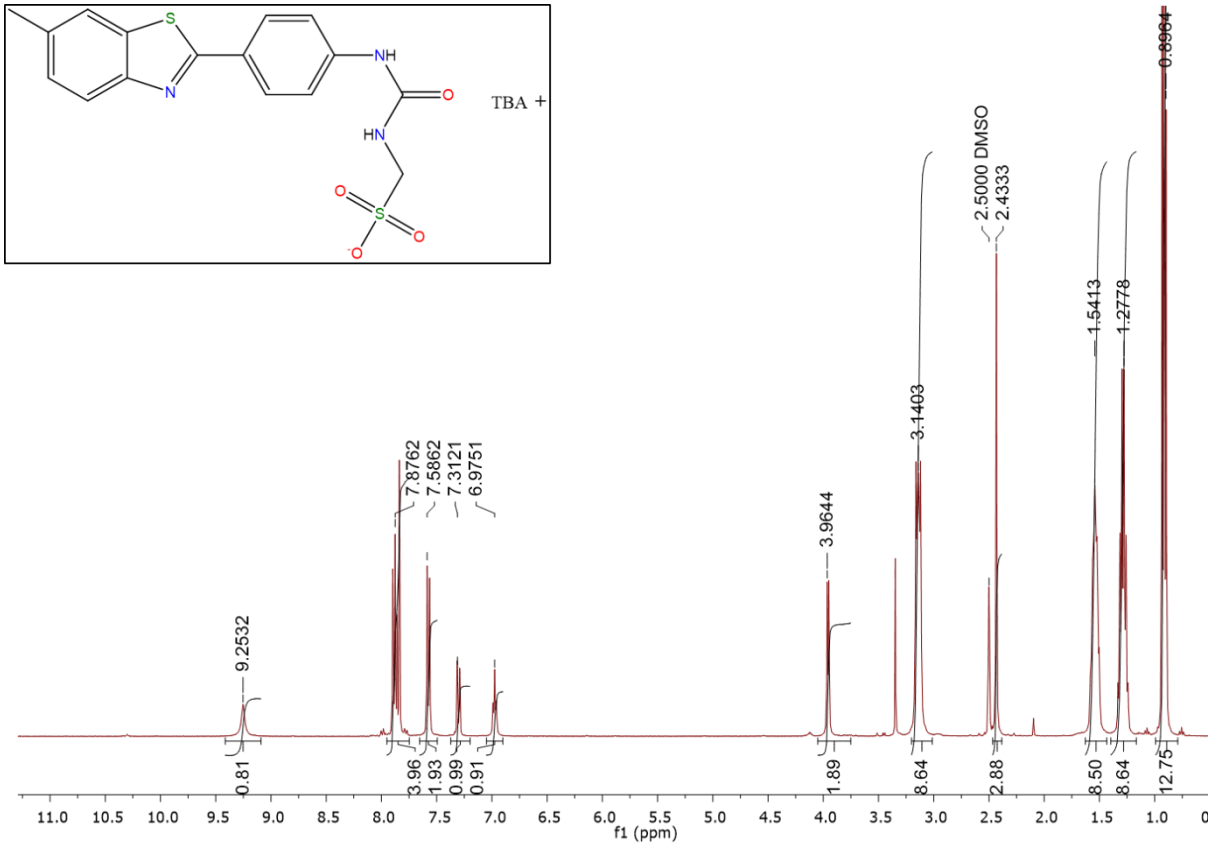

Figure S6 – ^{1}H NMR of compound **4** in DMSO-d_6.

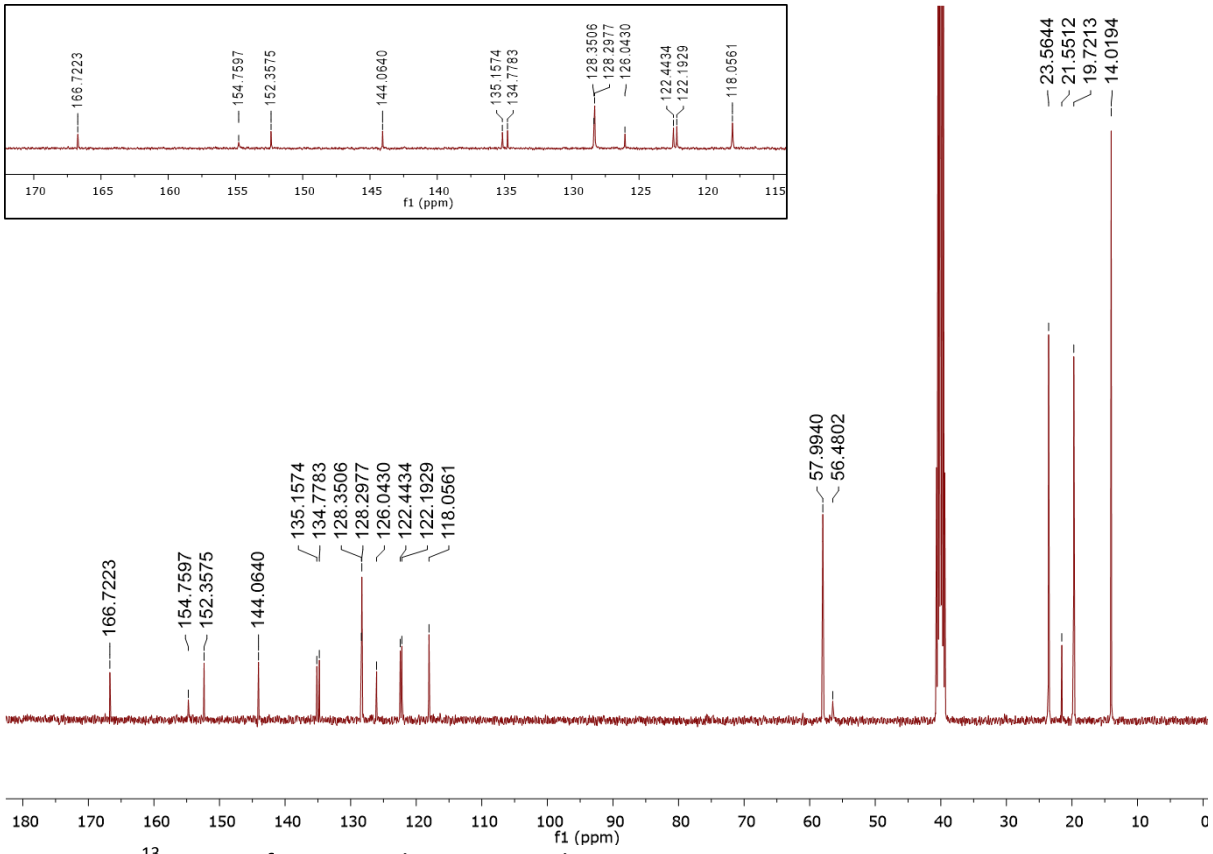

Figure S7 – ^{13}C NMR of compound **4** in DMSO-d_6.

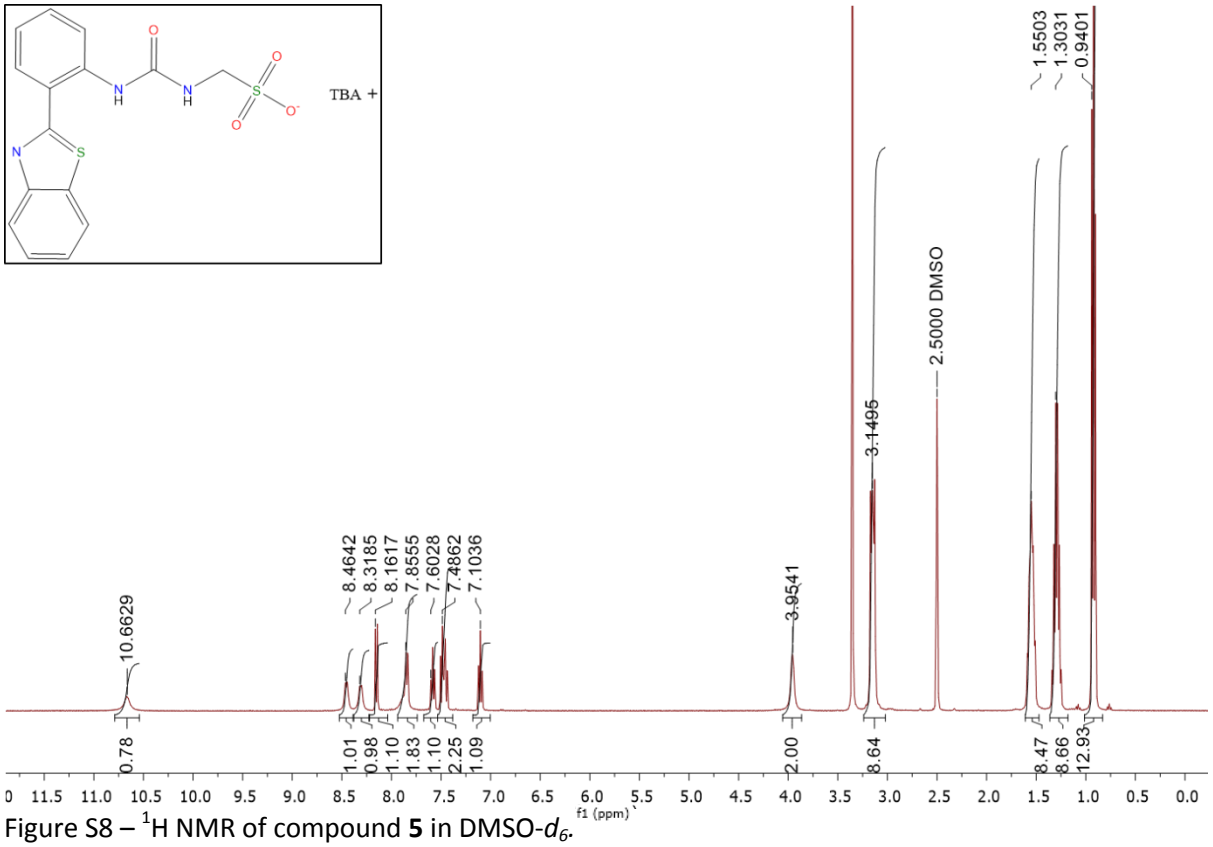

Figure S8 – ^{1}H NMR of compound **5** in DMSO-d_6.

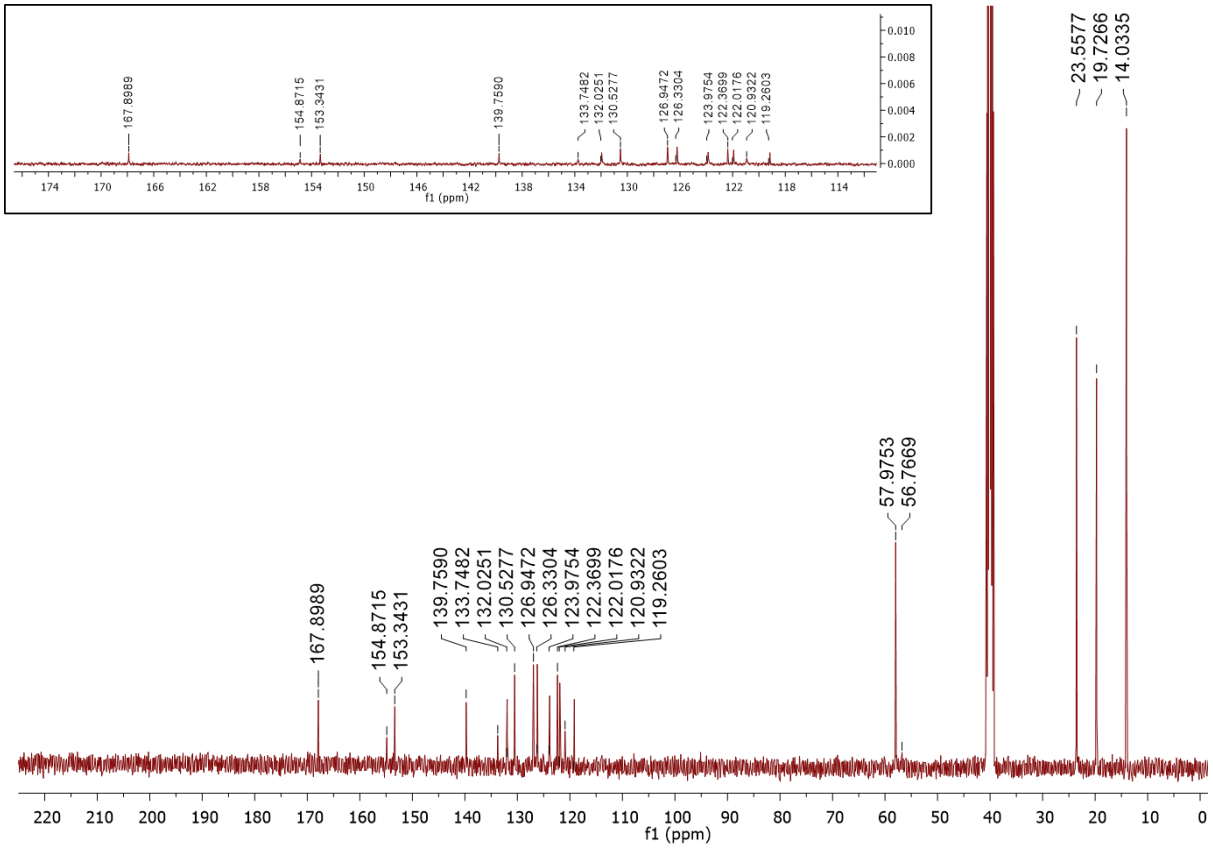

Figure S9 – ^{13}C NMR of compound **5** in DMSO-d_6.

^{1}H DOSY NMR experiments

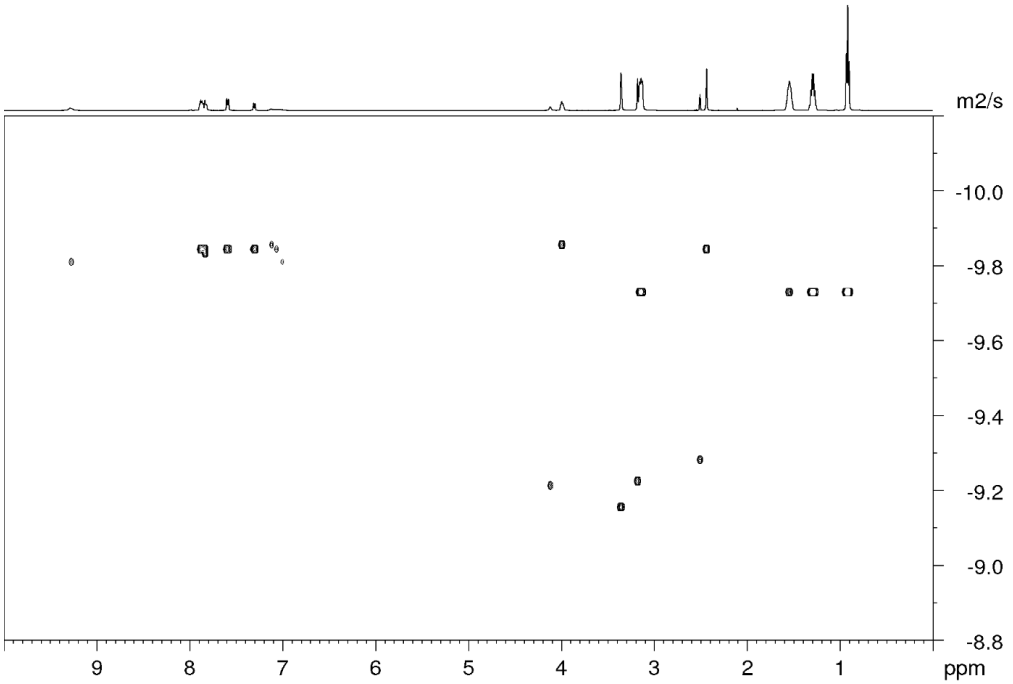

Figure S10 – ^{1}H DOSY of compound **4** (55.56 mM) in DMSO-d_6 conducted at 299.3 K.

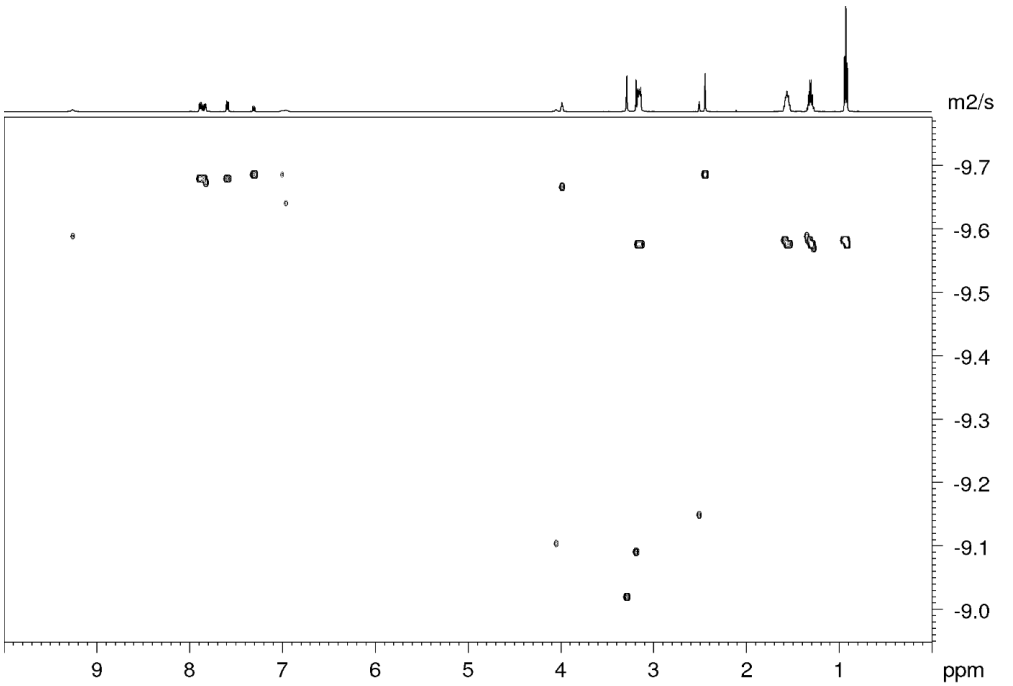

Figure S11 – ^{1}H DOSY of compound **4** (55.56 mM) in DMSO-d_6 conducted at 311.8 K.

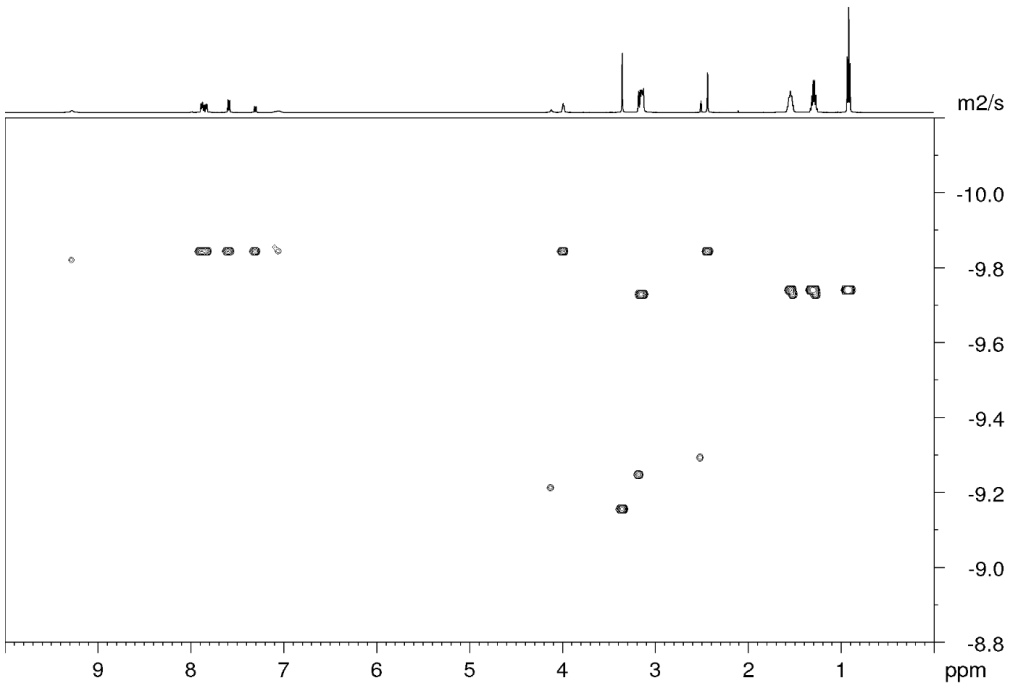

Figure S12 – ^{1}H DOSY of compound **4** (55.56 mM) in DMSO-d_6 conducted at 299.1 K after heating to 311.8 K.

Quantitative ^{1}H NMR experiments

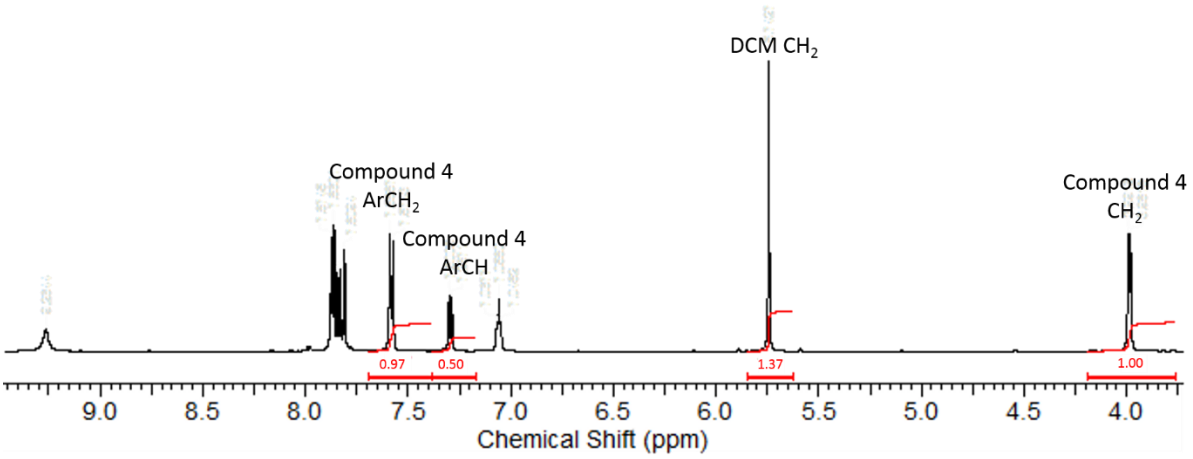

Figure S13 - ^{1}H NMR of compound **4** (0.035 g, 0.05 mM) and dichloromethane (0.007 mg, 0.08 mM) in DMSO-d_6.

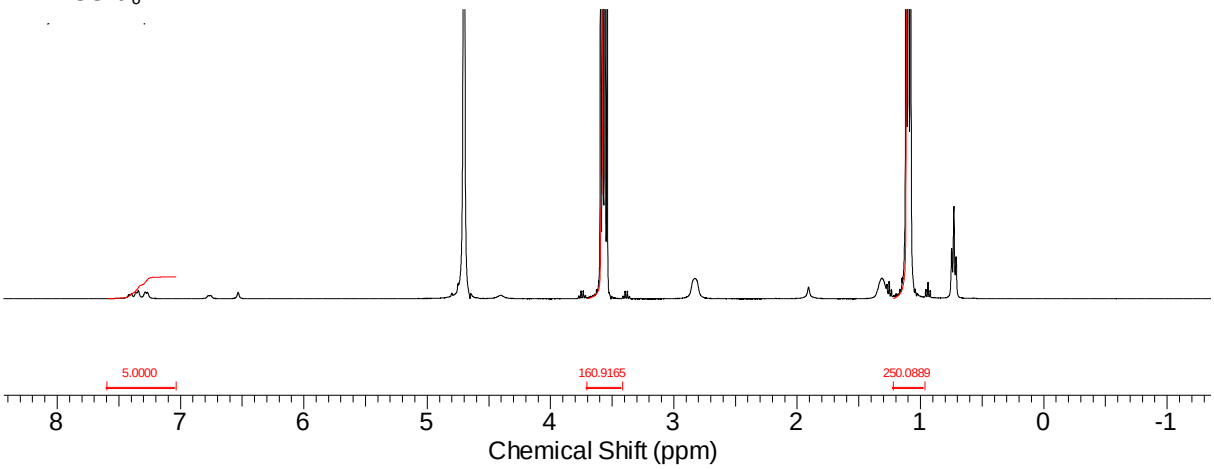

Figure S14 – ^{1}H NMR spectrum with a delay (d_1 = 60 s) of compound **4** (0.037 g, 5.91 mM) and ethanol (25 µl, 0.43 mM) in D_2O. An apparent 9.99% loss of compound was observed upon comparative signal integration.

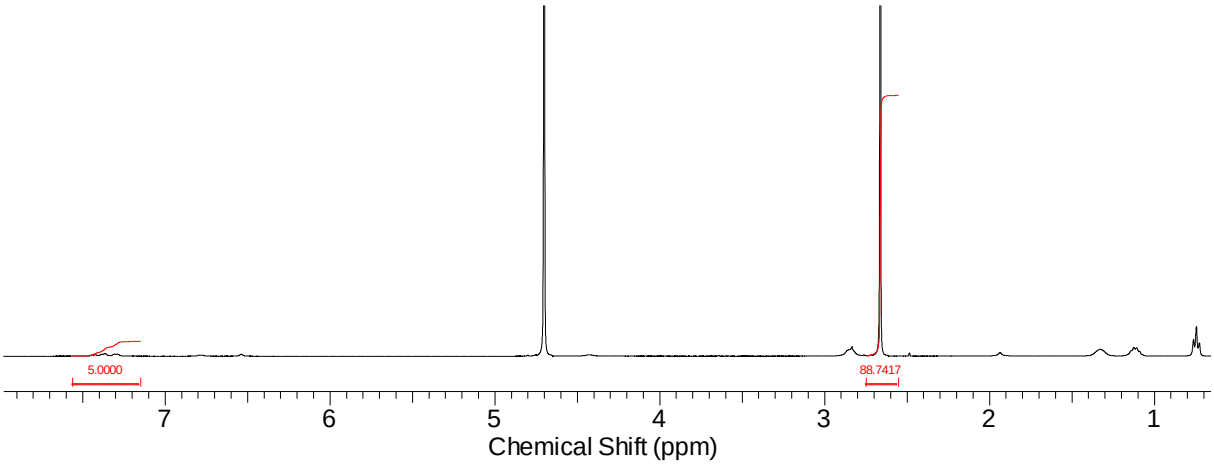

Figure S15 – ^{1}H NMR spectrum with a delay (d_1 = 60 s) of compound **4** (0.035 g, 5.57 mM) and DMSO (5 µl, 0.07 mM) in D_2O. An apparent 13.52 % loss of compound was identified upon comparative signal integration.

^{1}H NMR self-association studies

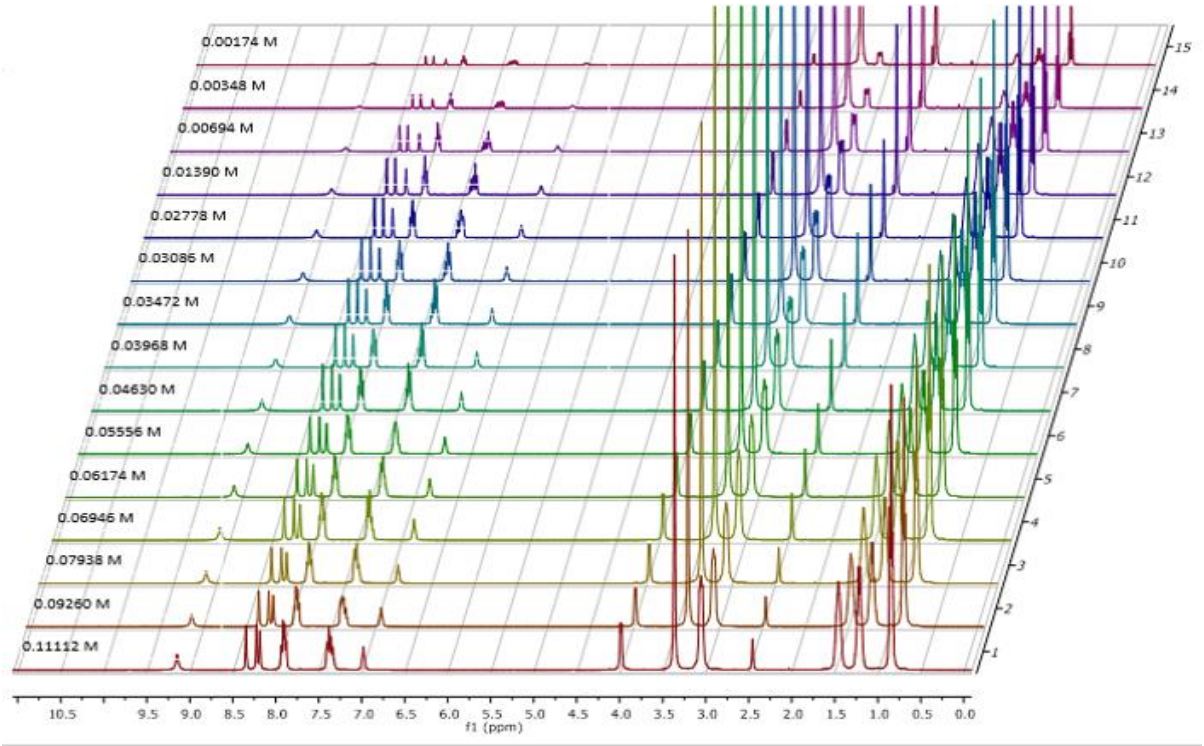

Figure S16 – ^{1}H NMR stack plot of compound **1** in a DMSO-d_6 0.5% H_2O solution. Samples were prepared in series with an aliquot of the most concentrated solution undergoing serial dilution.

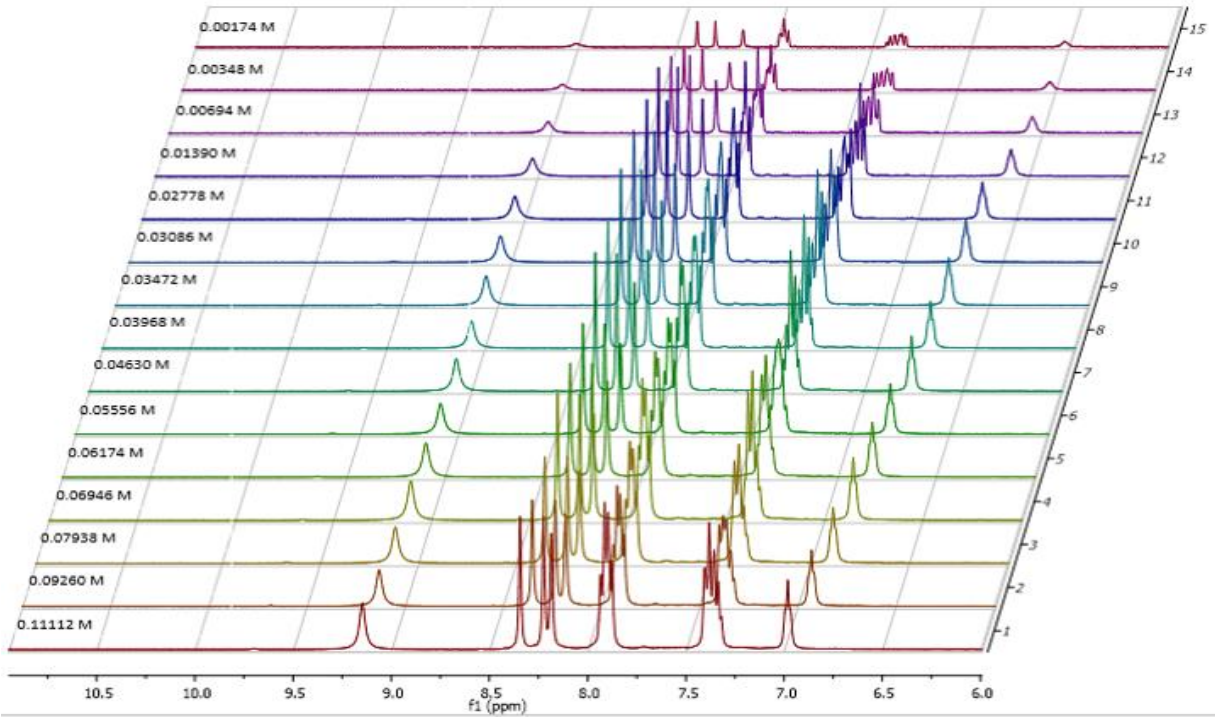

Figure S17 – Enlarged ^{1}H NMR stack plot of compound **1** in a DMSO-d_6 0.5% H_2O solution. Samples were prepared in series with an aliquot of the most concentrated solution undergoing serial dilution.

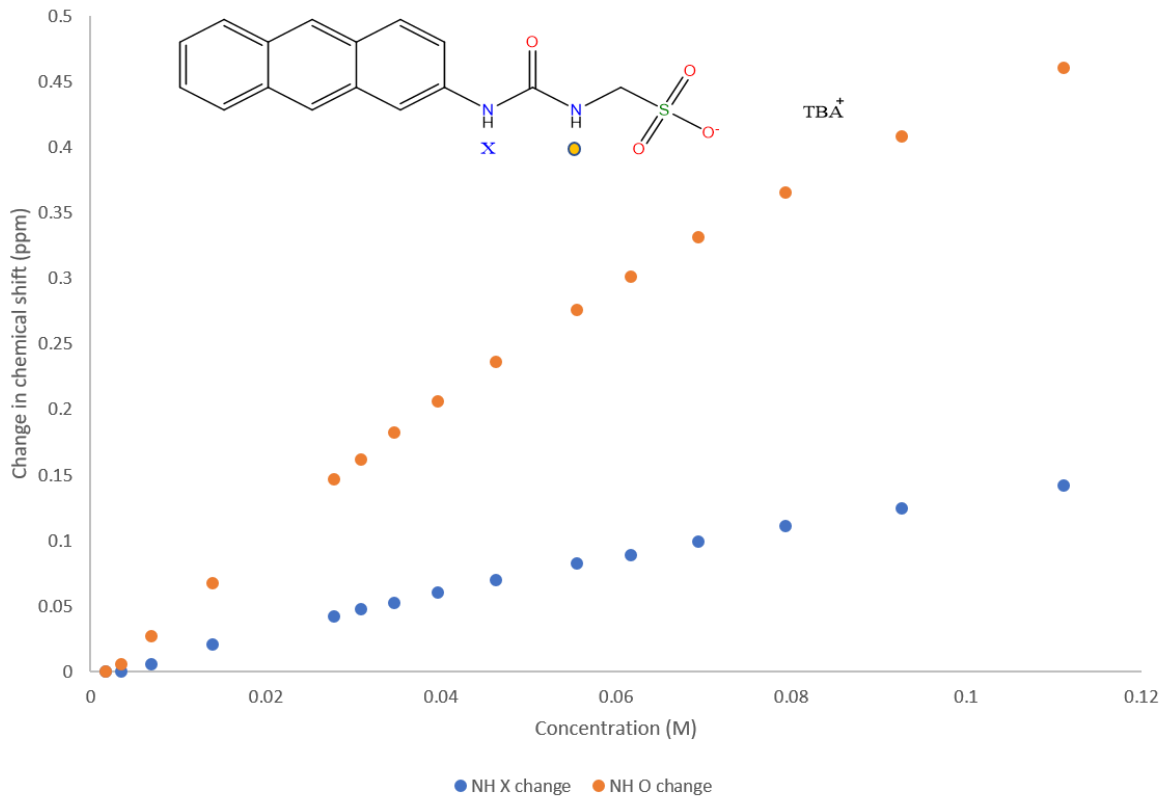

Figure S18 - Graph illustrating the ^{1}H NMR down-field change in chemical shift of urea NH resonances with increasing concentration of compound **1** in DMSO- d_6 0.5% H_2O (298 K).

Self-association constant calculation

Compound **1** – Dilution study in DMSO-d_6 0.5% H_2O. Values calculated combining the data gathered from both NH 1 and 2.

Equal K/Dimerization model

K_e = 2.90 M^{-1} ± 0.4983 % K_{dim} = 1.45 M^{-1} ± 0.2492 %

http://app.supramolecular.org/bindfit/view/230dfa2b-daa3-44e5-bdea-65ce98de9d06

CoEK model

K_e = 8.62 M^{-1} ± 1.0817 % K_{dim} = 4.31 M^{-1} ± 0.5409 % ρ = 0.50 ± 2.5165 %

http://app.supramolecular.org/bindfit/view/d404f32d-a98a-4dd2-a513-3611349b02ee

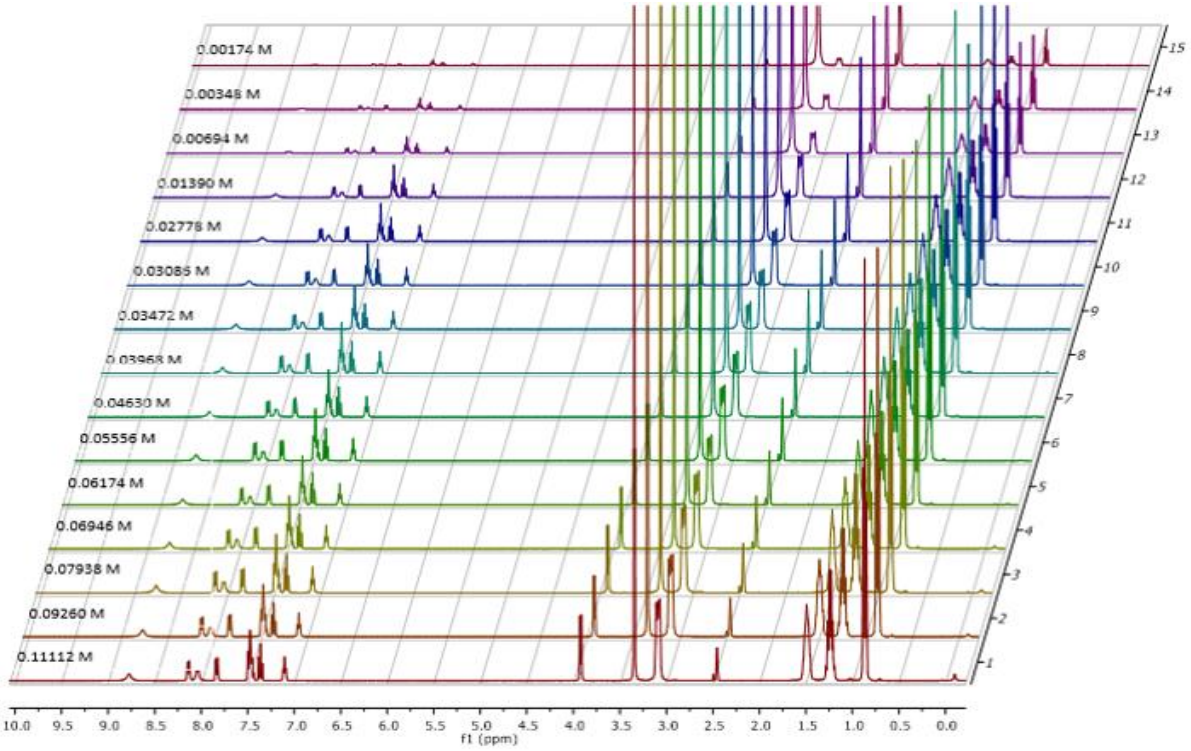

Figure S19 - ^{1}H NMR stack plot of compound **2** in a DMSO-d_6 0.5% H_2O solution. Samples were prepared in series with an aliquot of the most concentrated solution undergoing serial dilution.

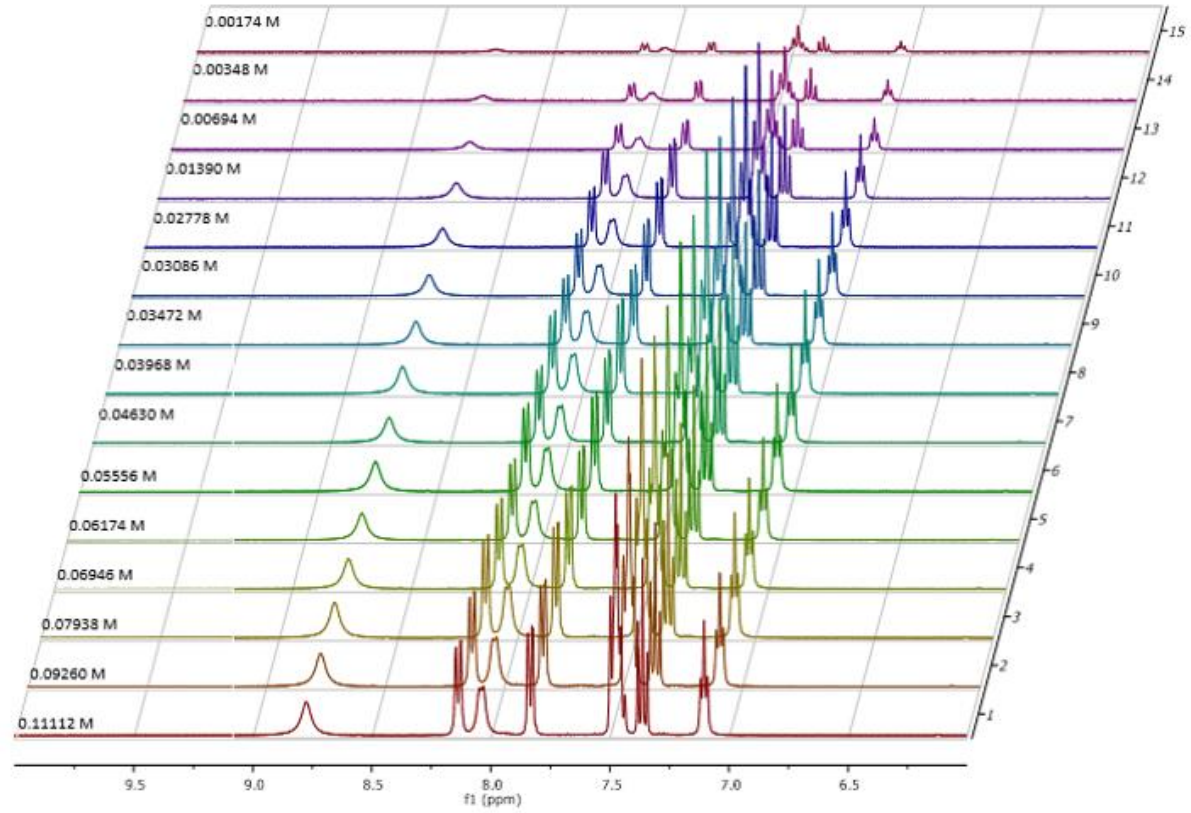

Figure S20 – Enlarged ^{1}H NMR stack plot of compound **2** in a DMSO-d_6 0.5% H_2O solution. Samples were prepared in series with an aliquot of the most concentrated solution undergoing serial dilution.

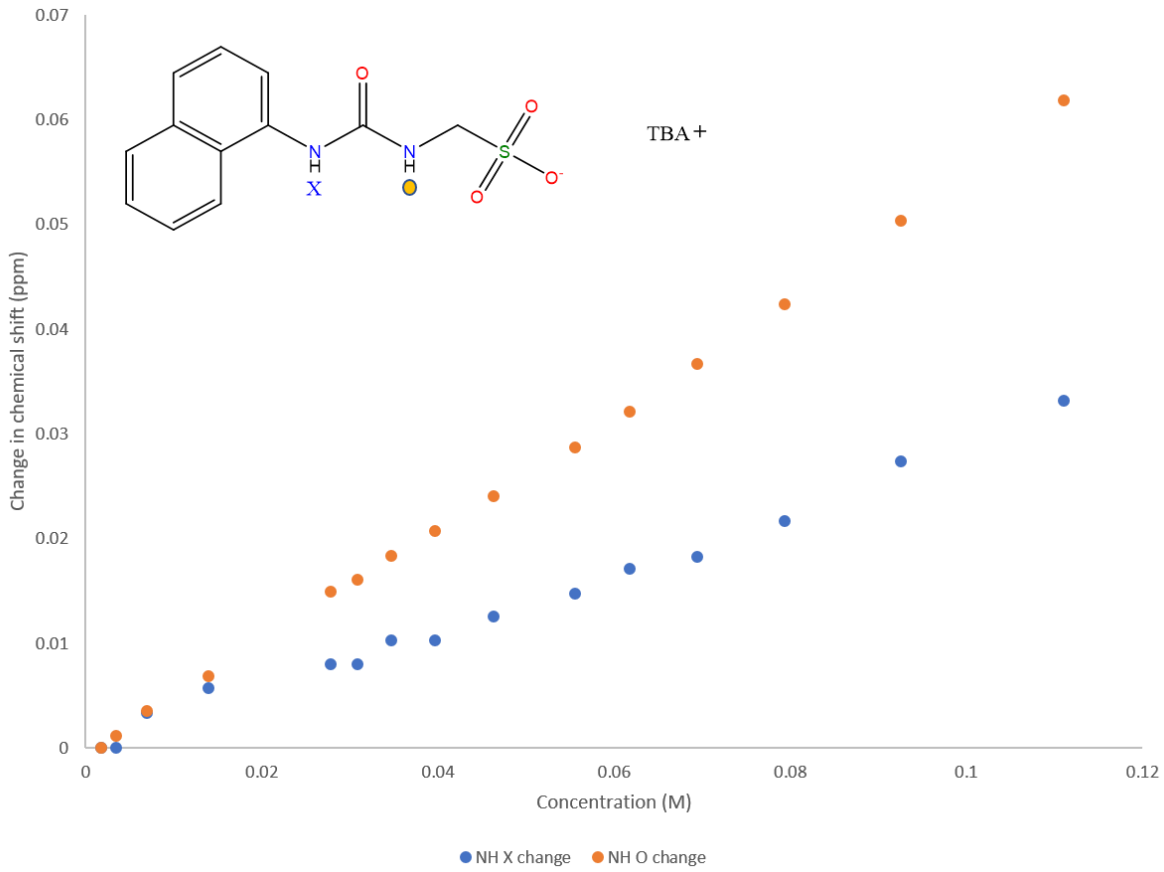

Figure S21 - Graph illustrating the ^{1}H NMR down-field change in chemical shift of urea NH resonances with increasing concentration of compound **2** in DMSO- d_6 0.5% H_2O (298 K).

Self-association constant calculation

Compound **2** – Dilution study in DMSO-d_6 0.5% H_2O. Values calculated combining the data gathered from both NH 1 and 2.

Equal K/Dimerization model

K_e = 0.03 M^{-1} ± 1.5195 % K_{dim} = 0.01 M^{-1} ± 0.7597 %

http://app.supramolecular.org/bindfit/view/b1102806-e844-49bc-84b3-bafd8a2dbcbb

CoEK model

K_e = 0.53 M^{-1} ± 43.0910 % K_{dim} = 0.27 M^{-1} ± 21.5455 % ρ = 0.00 ± 47.0444 %

http://app.supramolecular.org/bindfit/view/a4df1a0a-4903-4624-b2f5-d2ecc5edd3ed

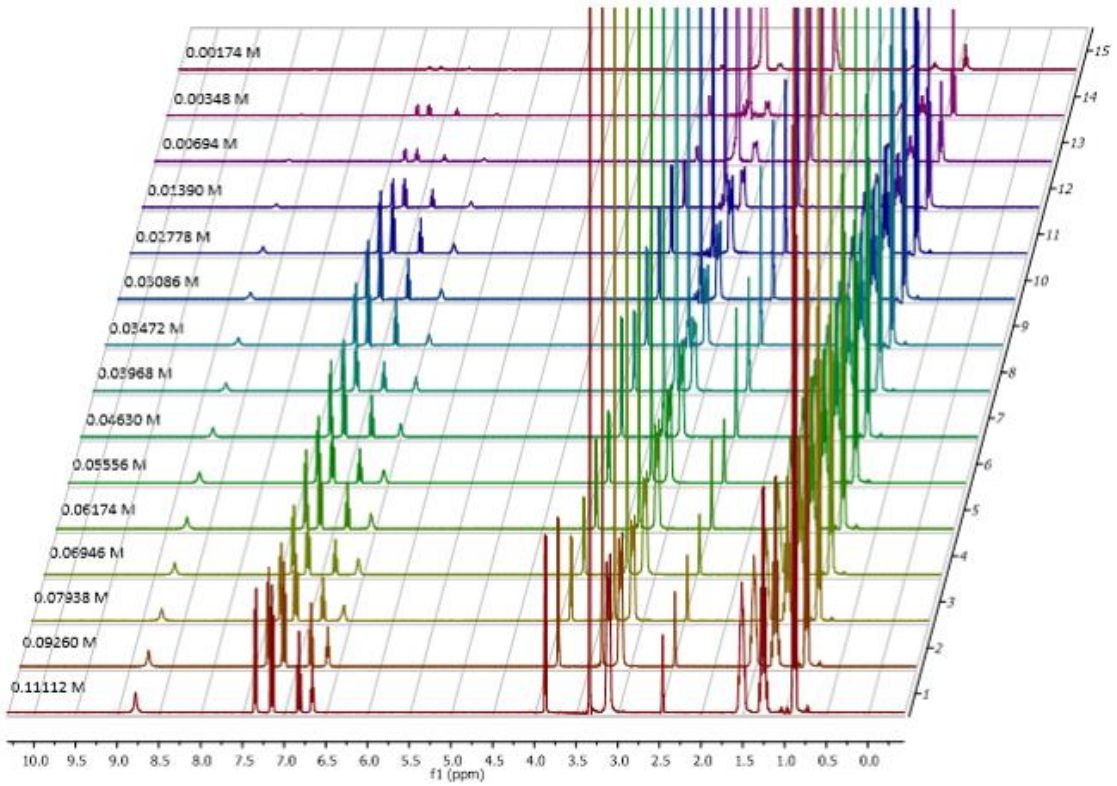

Figure S22 - ^{1}H NMR stack plot of compound **3** in a DMSO-d_6 0.5% H_2O solution. Samples were prepared in series with an aliquot of the most concentrated solution undergoing serial dilution.

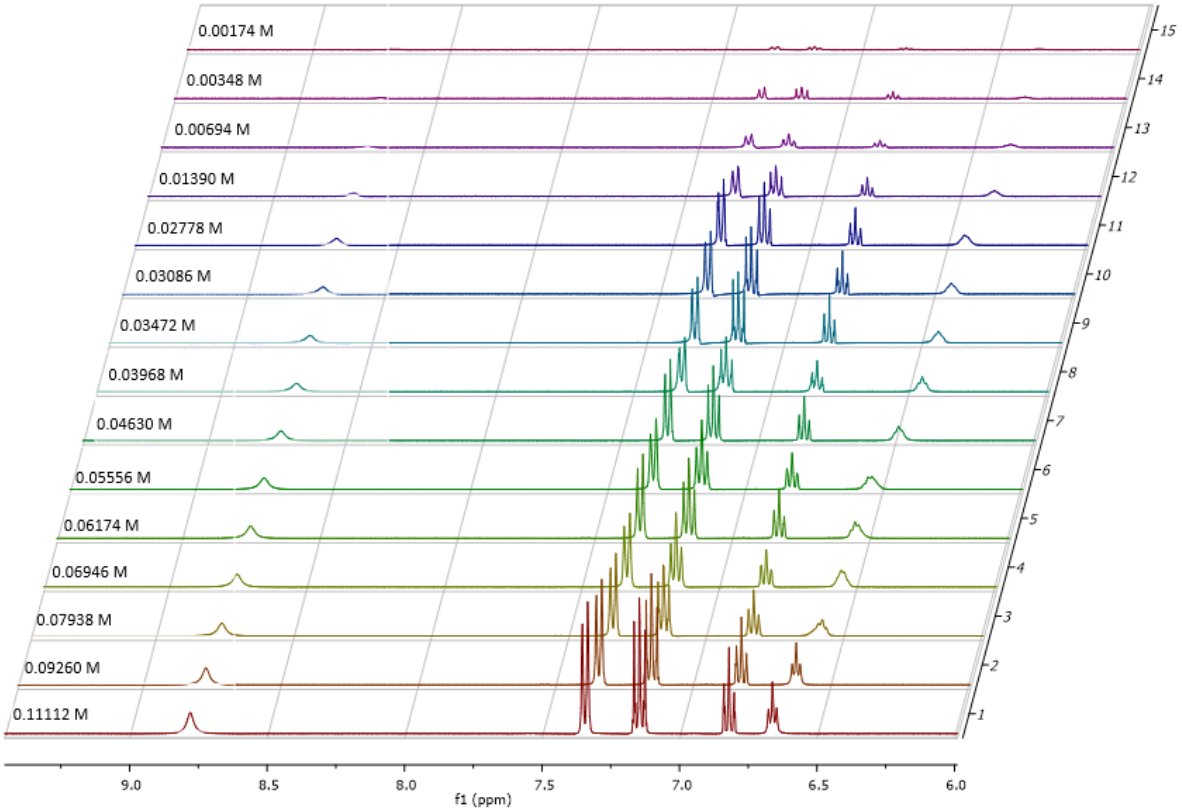

Figure S23 – Enlarged ^{1}H NMR stack plot of compound **3** in a DMSO-d_6 0.5% H_2O solution. Samples were prepared in series with an aliquot of the most concentrated solution undergoing serial dilution.

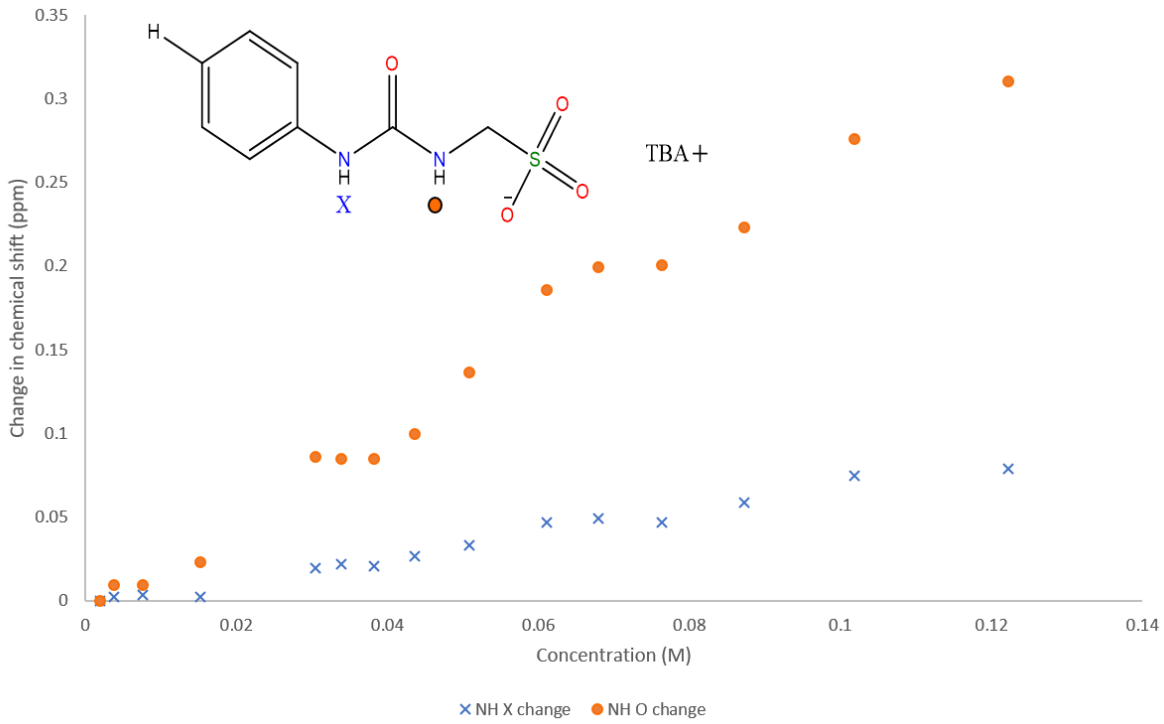

Figure S24 - Graph illustrating the ^{1}H NMR down-field change in chemical shift of urea NH resonances with increasing concentration of compound **3** in DMSO-d_6 0.5% H_2O (298 K).

Self-association constant calculation

Compound **3** – Dilution study in DMSO-d_6 0.5% H_2O. Values calculated combining the data gathered from both NH 1 and 2.

Equal K/Dimerization model

K_e = 0.61 M^{-1} ± 3.0255 % K_{dim} = 0.30 M^{-1} ± 1.5128 %

http://app.supramolecular.org/bindfit/view/82f6ee49-a329-40d1-8025-1adb091e0f87

CoEK model

K_e = 12.98 M^{-1} ± 5.7461 % K_{dim} = 6.49 M^{-1} ± 2.8731 % ρ = 0.17 ± 23.7749 %

http://app.supramolecular.org/bindfit/view/6fd2fbc5-dbb0-4e7d-b60d-e6620e47ceff

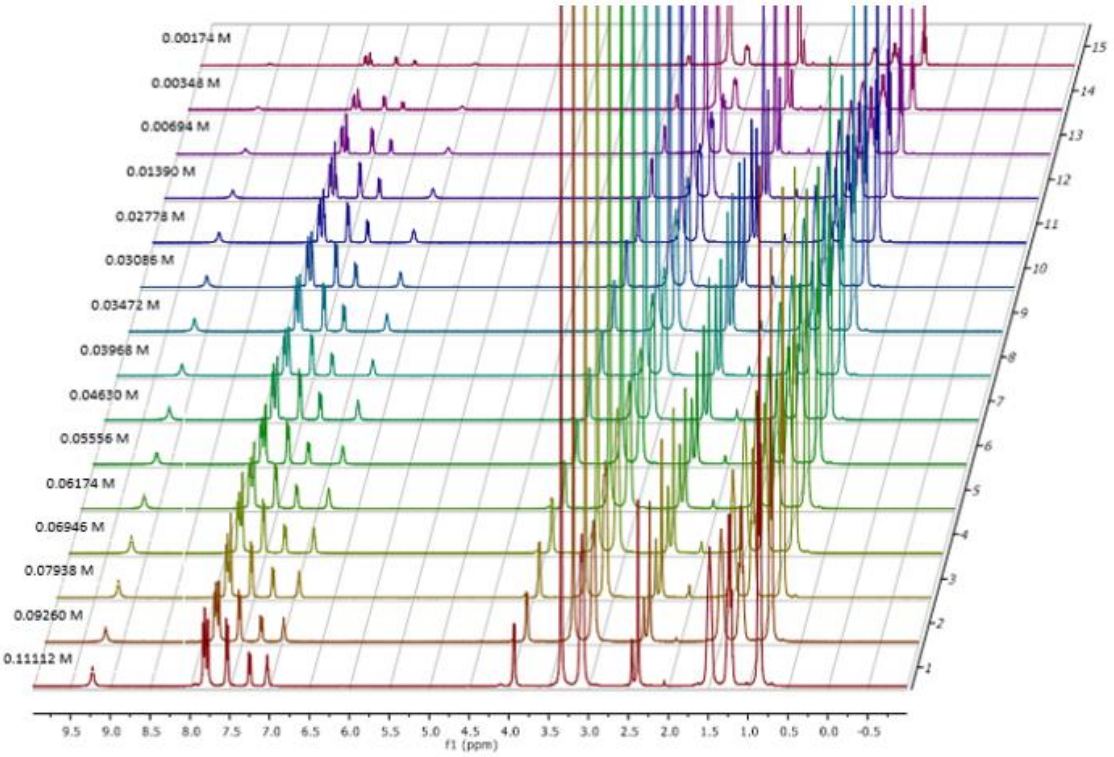

Figure S25 – ^{1}H NMR stack plot of compound **4** in a DMSO-d_6 0.5% H_2O solution. Samples were prepared in series with an aliquot of the most concentrated solution undergoing serial dilution.

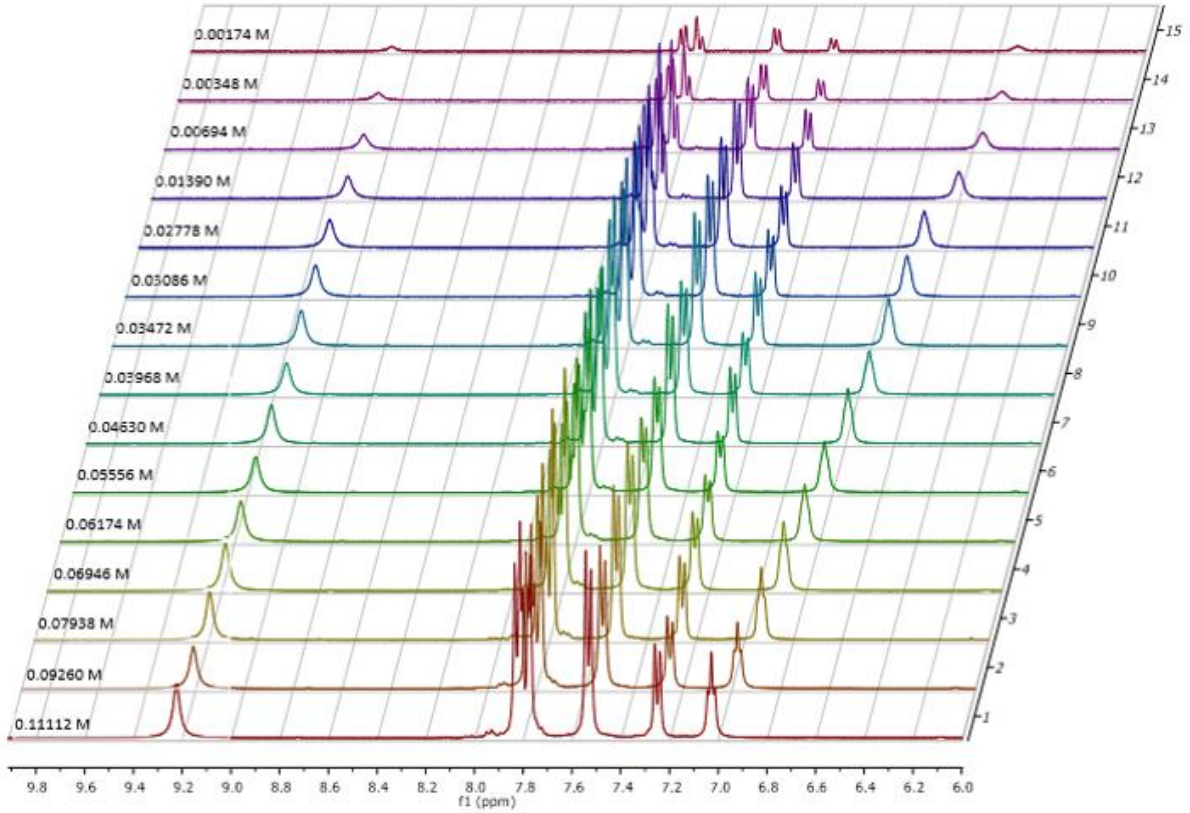

Figure S26 – Enlarged ^{1}H NMR stack plot of compound **4** in a DMSO-d_6 0.5% H_2O solution. Samples were prepared in series with an aliquot of the most concentrated solution undergoing serial dilution.

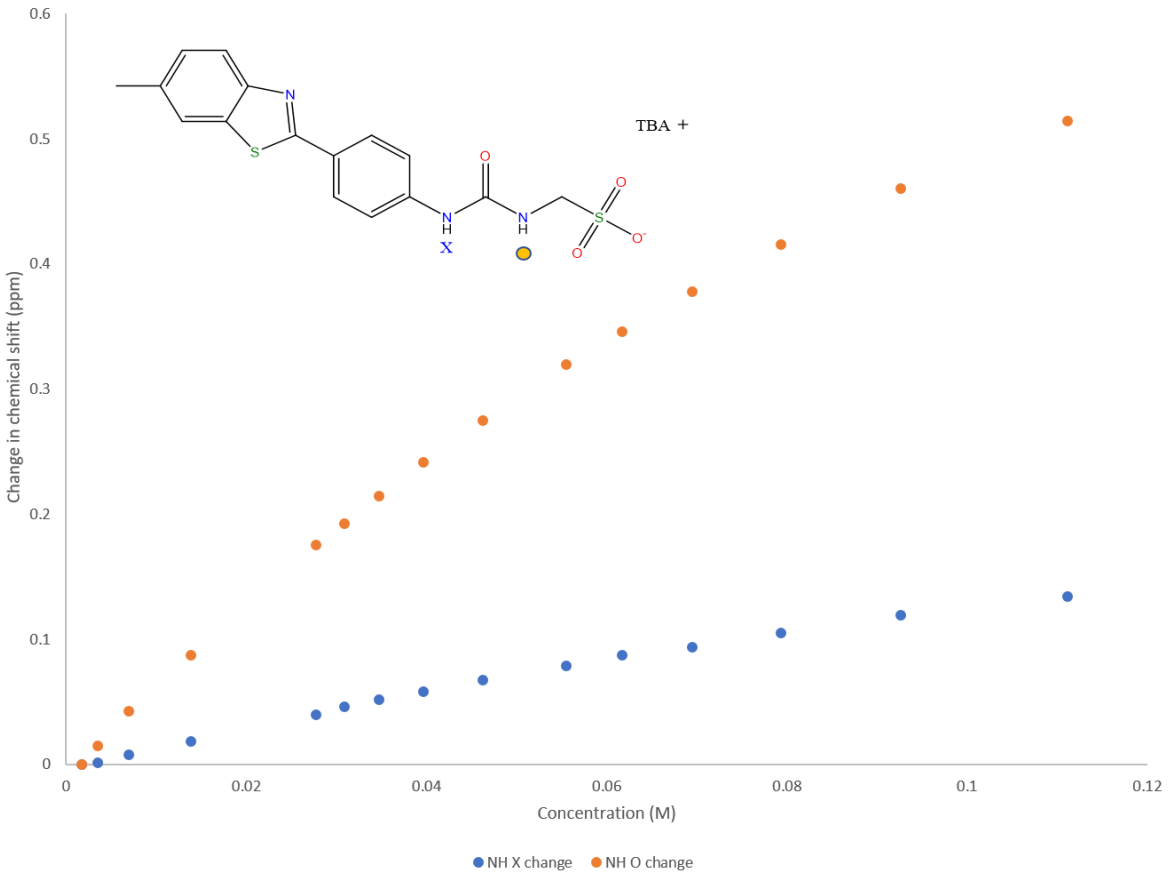

Figure S27 - Graph illustrating the ^{1}H NMR down-field change in chemical shift of urea NH resonances with increasing concentration of compound **4** in DMSO-d_6 0.5% H_2O (298 K).

Self-association constant calculation

Compound **4** – Dilution study in DMSO-d_6 0.5% H_2O. Values calculated combining the data gathered from both NH 1 and 2.

Equal K/Dimerization model

K_e = 5.34 M^{-1} ± 0.6112 % K_{dim} = 2.67 M^{-1} ± 0.3056 %

http://app.supramolecular.org/bindfit/view/ef5fa21f-a268-46aa-87ef-ebf751300648

CoEK model

K_e = 12.95 M^{-1} ± 0.6971 % K_{dim} = 6.47 M^{-1} ± 0.3485 % ρ = 0.50 ± 2.0433 %

http://app.supramolecular.org/bindfit/view/de1c6c54-3f86-4e43-8063-4ad17361d6da

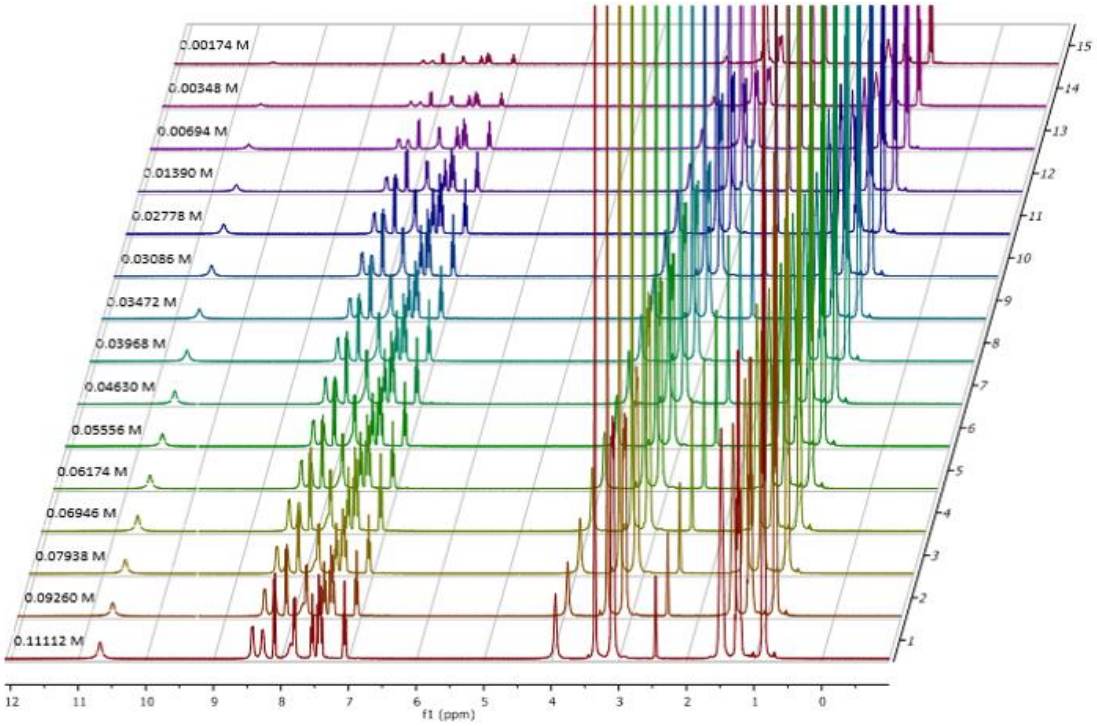

Figure S28 – ^{1}H NMR stack plot of compound **5** in a DMSO-d_6 0.5% H_2O solution. Samples were prepared in series with an aliquot of the most concentrated solution undergoing serial dilution.

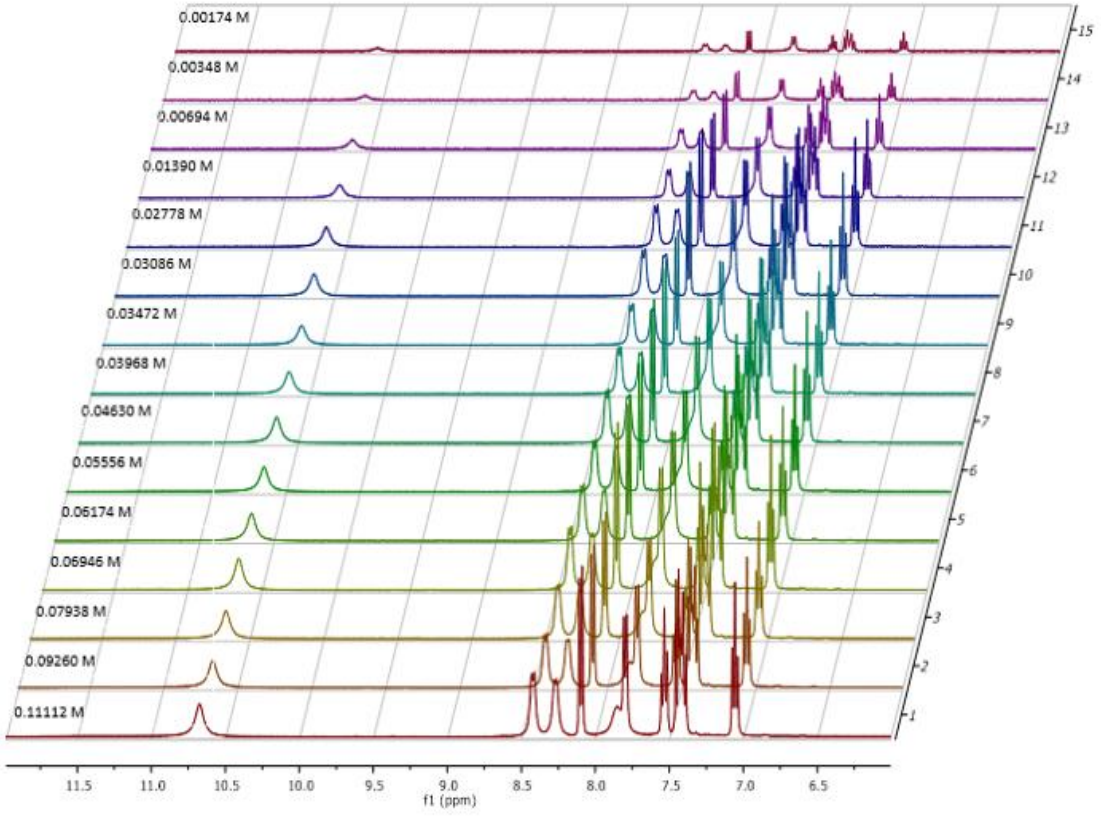

Figure S29 – Enlarged ^{1}H NMR stack plot of compound **5** in a DMSO-d_6 0.5% H_2O solution. Samples were prepared in series with an aliquot of the most concentrated solution undergoing serial dilution.

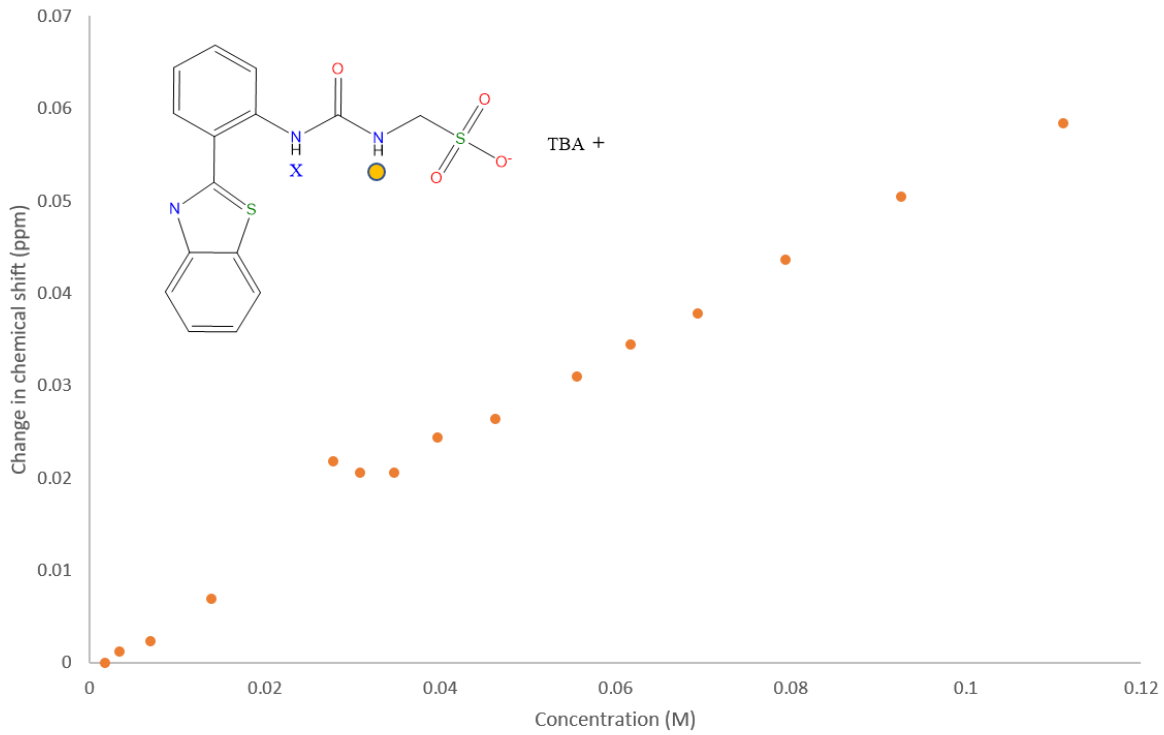

Figure S30 - Graph illustrating the ^{1}H NMR down-field change in chemical shift of urea NH resonances with increasing concentration of compound **5** in DMSO-d_6 0.5% H_2O (298 K).

Self-association constant calculation

Compound **5** – Dilution study in DMSO-d_6 0.5% H_2O. Values calculated from data gathered from NH 1

Equal K/Dimerization model

K_e = 1.15 M^{-1} ± 2.0521 % K_{dim} = 0.57 M^{-1} ± 1.0610 %

http://app.supramolecular.org/bindfit/view/0780d95f-ffc6-428d-b327-a9c32dbcce60

CoEK model

K_e = 6.19 M^{-1} ± 8.8173 % K_{dim} = 3.10 M^{-1} ± 4.4087 % ρ = 0.43 ± 17.8122 %

http://app.supramolecular.org/bindfit/view/101ed3ba-862a-4486-b8b7-af27b5cffdf0

DLS data

Correlation data

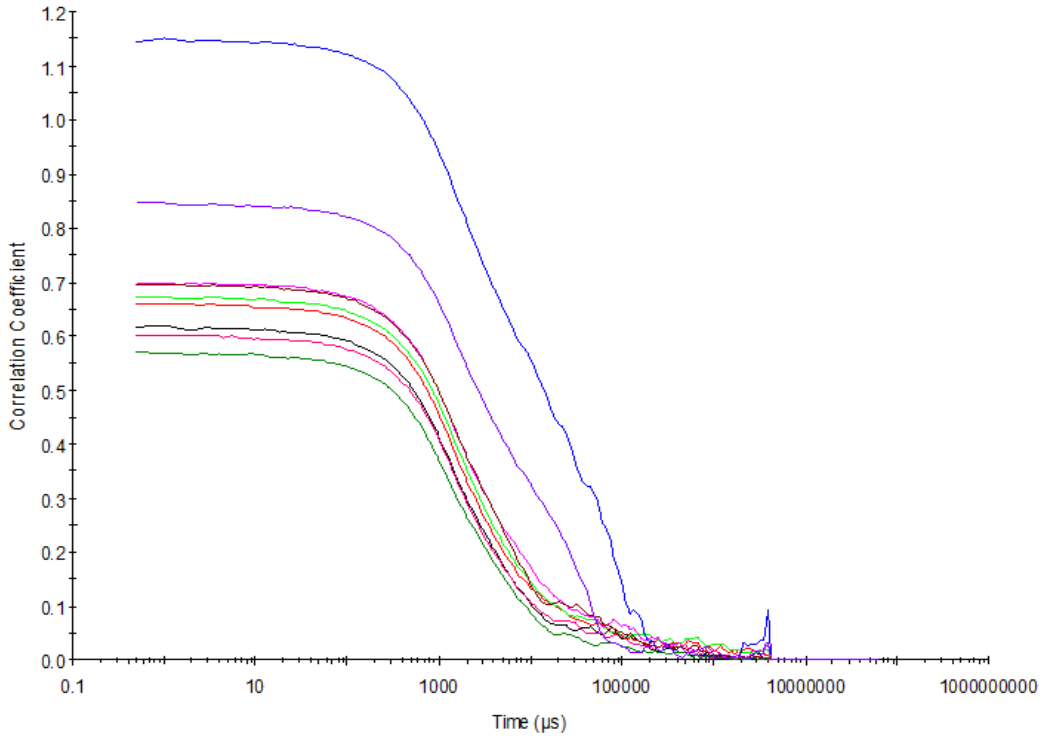

Figure S31 – Raw correlation data for 9 DLS runs at 25 °C before heating to 40 °C with compound **1** at a concentration of 111.12 mM in DMSO.

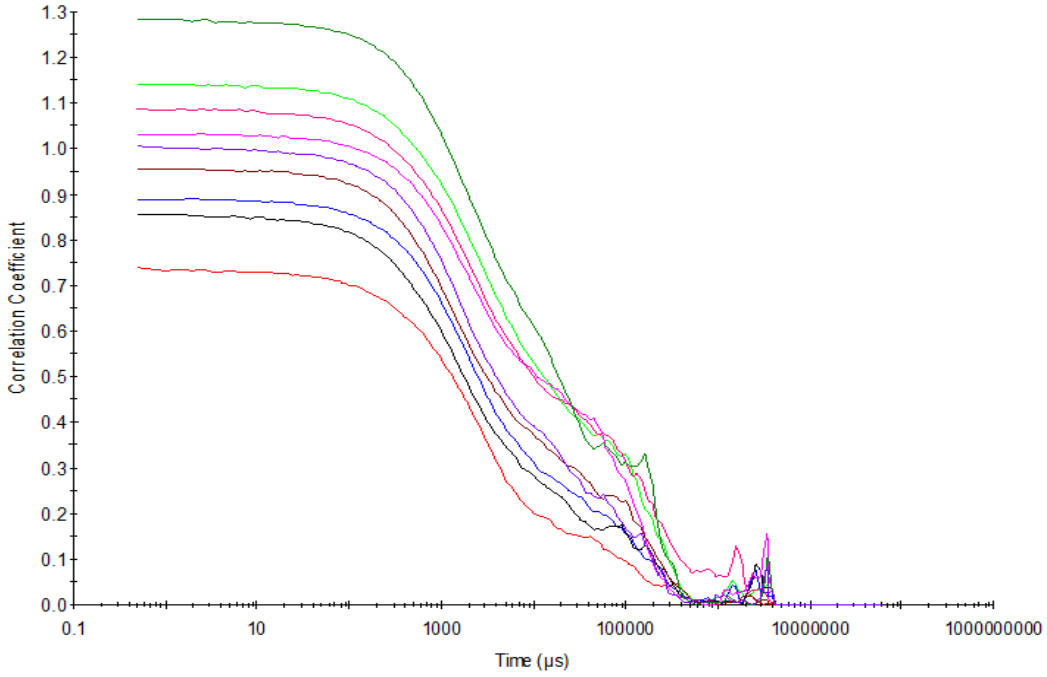

Figure S32 – Raw correlation data for 9 DLS runs at 40 °C with compound **1** at a concentration of 111.12 mM in DMSO.

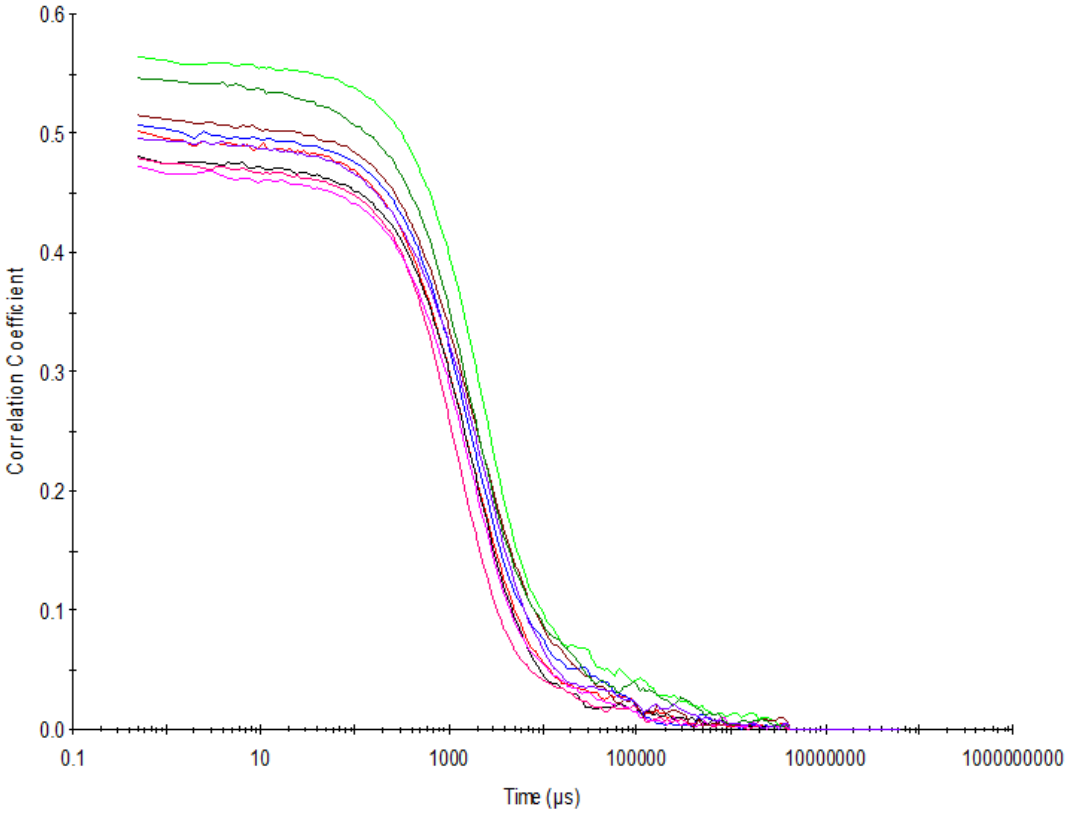

Figure S33 – Raw correlation data for 9 DLS runs at 25 °C after heating to 40 °C with compound **1** at a concentration of 111.12 mM in DMSO.

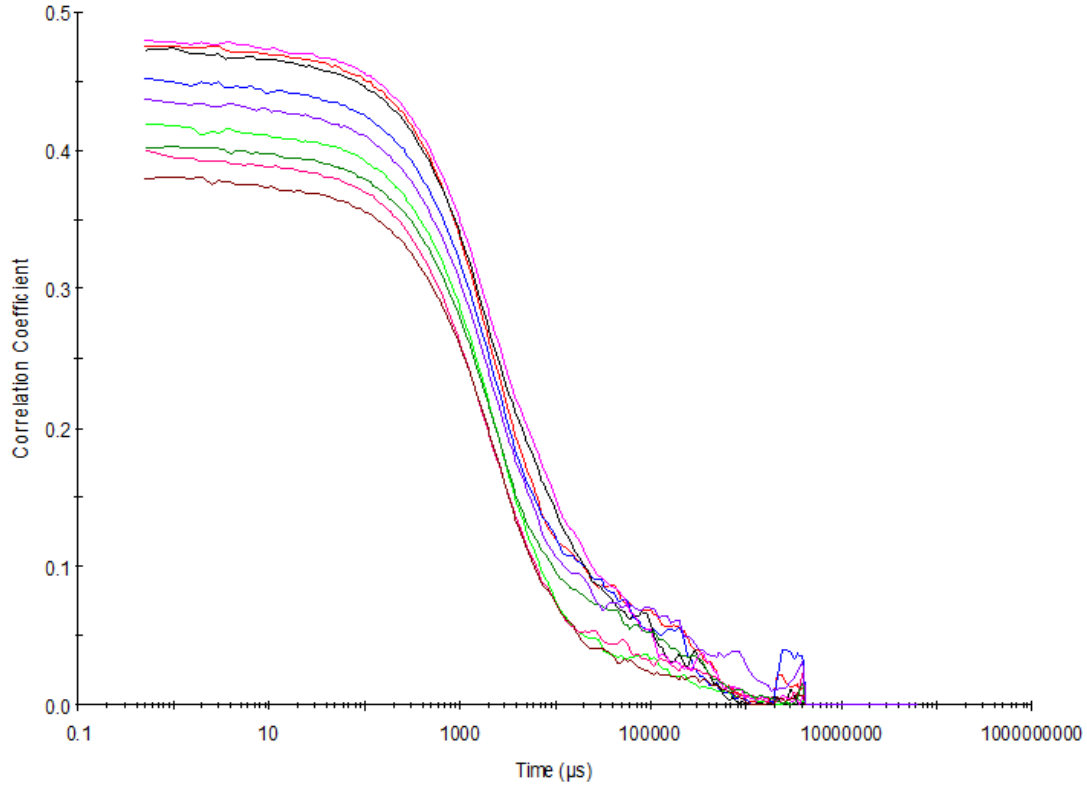

Figure S34 – Raw correlation data for 9 DLS runs at 25 °C before heating to 40 °C with compound **1** at a concentration of 55.56 mM in DMSO.

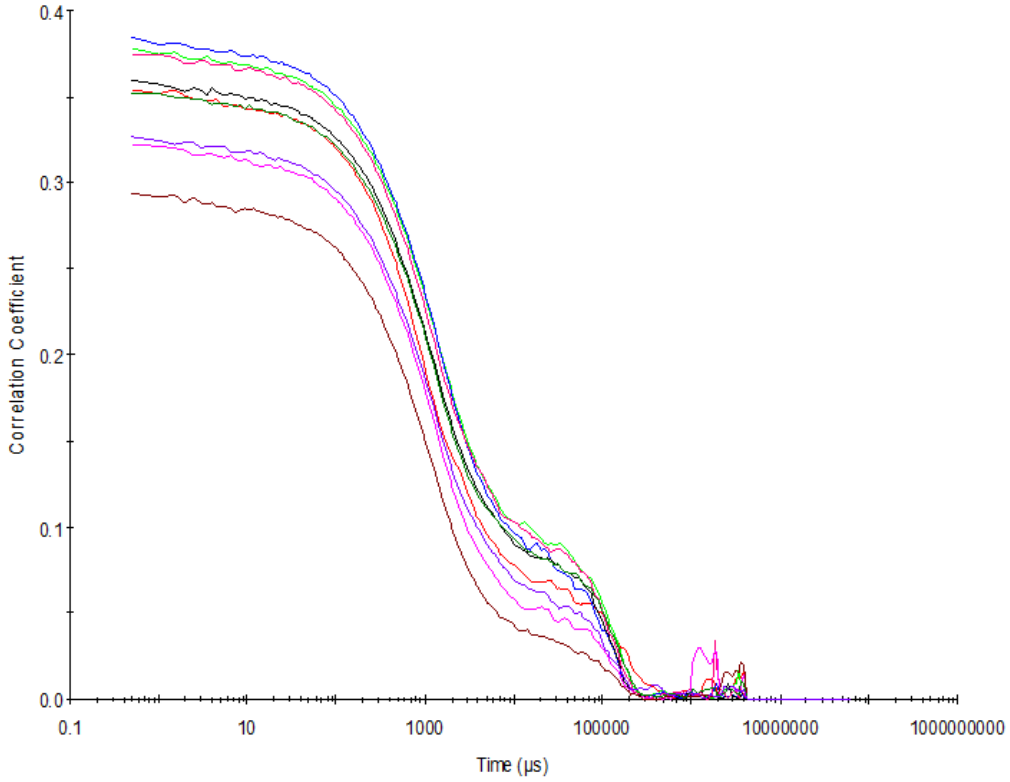

Figure S35 – Raw correlation data for 9 DLS runs at 40 °C with compound **1** at a concentration of 55.56 mM in DMSO.

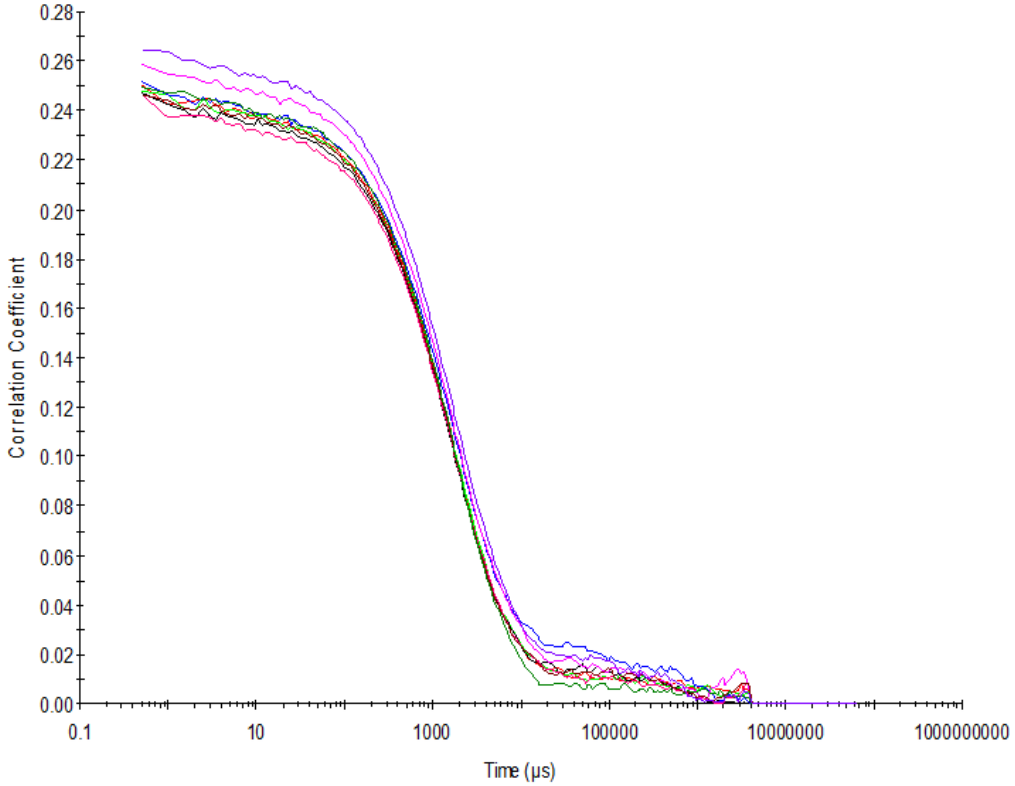

Figure S36 – Raw correlation data for 9 DLS runs at 25 °C after heating to 40 °C with compound **1** at a concentration of 55.56 mM in DMSO.

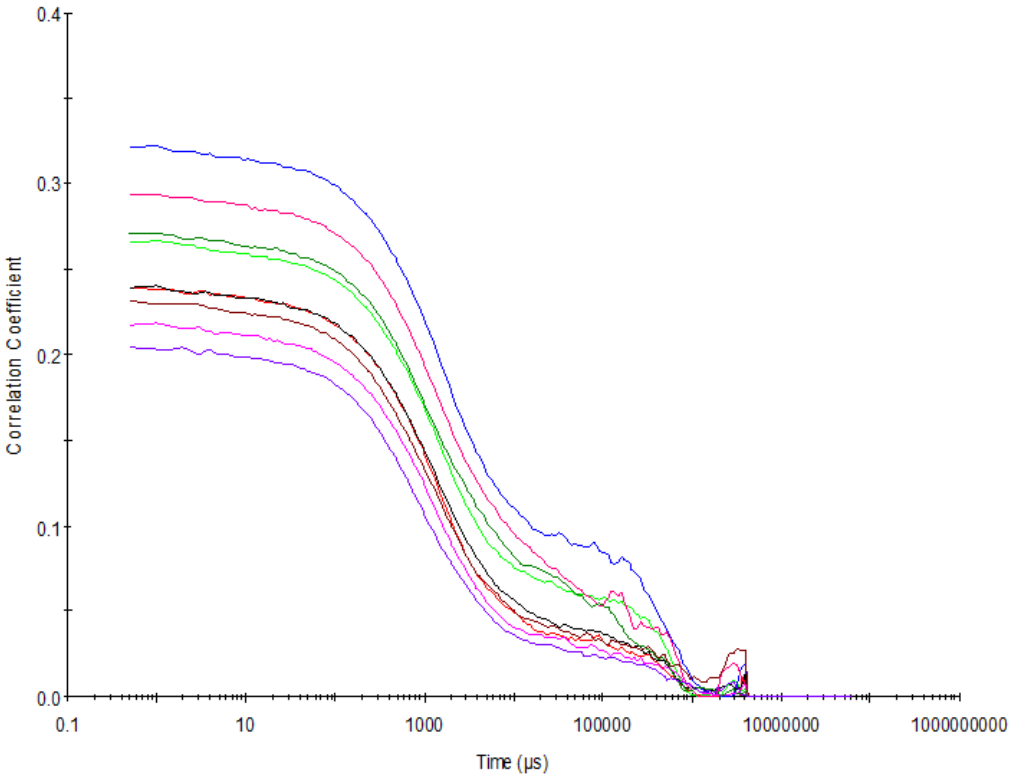

Figure S37 – Raw correlation data for 9 DLS runs at 25 °C before heating to 40 °C with compound **1** at a concentration of 5.56 mM in DMSO.

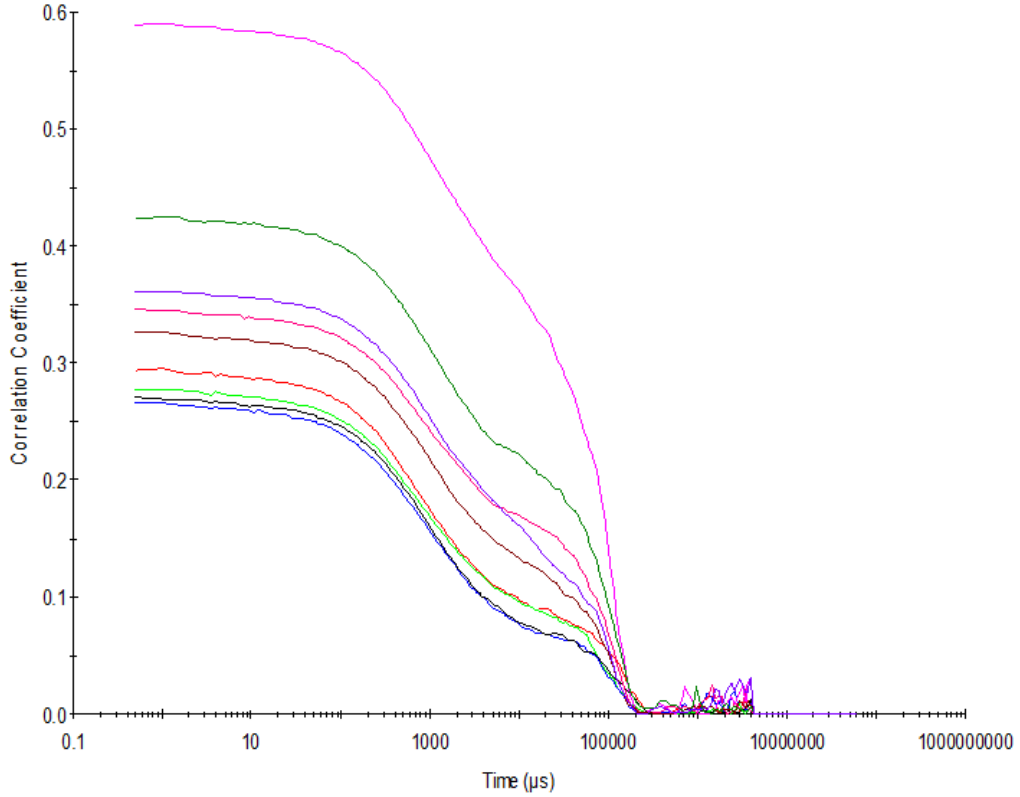

Figure S38 – Raw correlation data for 9 DLS runs at 40 °C with compound **1** at a concentration of 5.56 mM in DMSO.

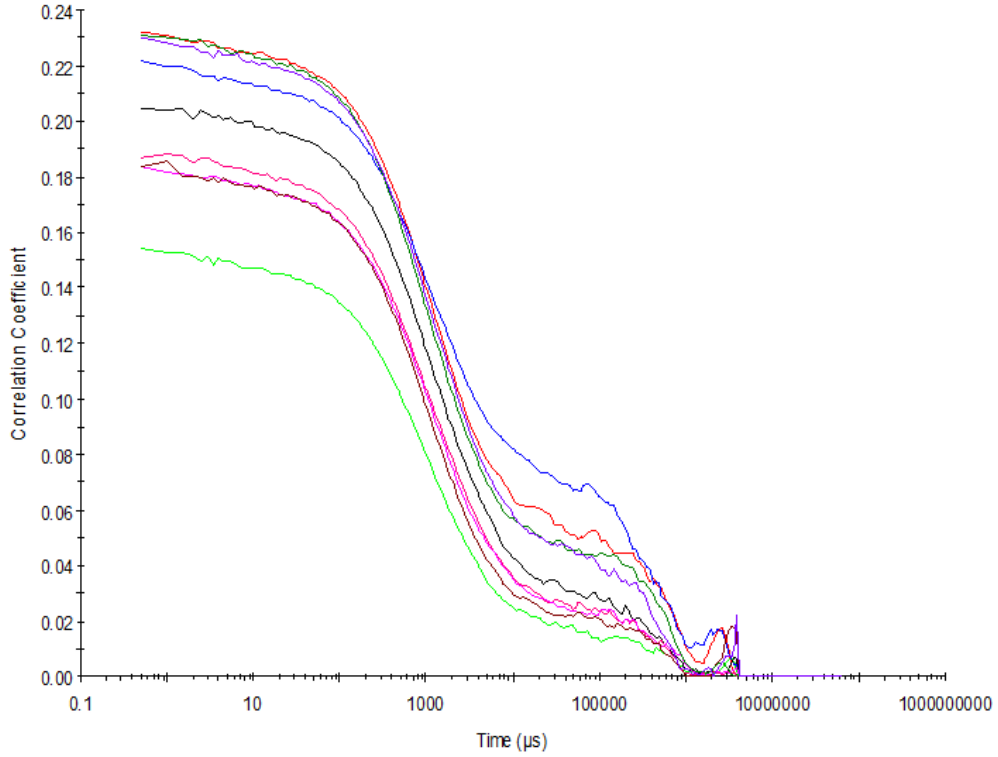

Figure S39 – Raw correlation data for 9 DLS runs at 25 °C after heating to 40 °C with compound **1** at a concentration of 5.56 mM in DMSO.

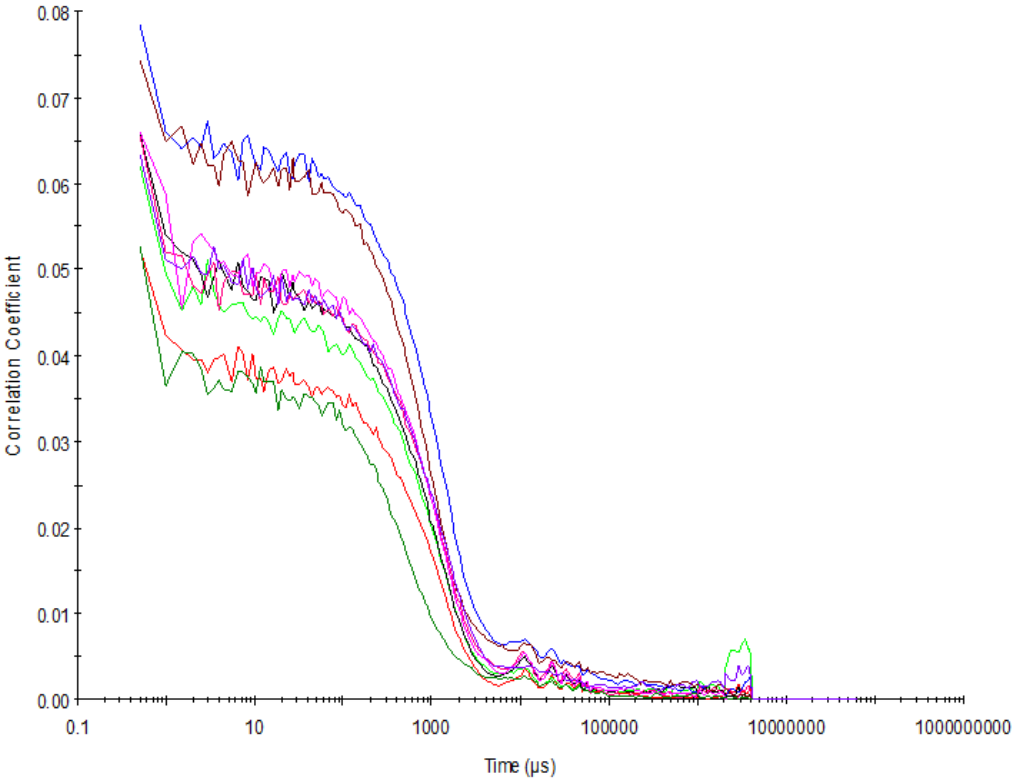

Figure S40 – Raw correlation data for 9 DLS runs at 25 °C before heating to 40 °C with compound **1** at a concentration of 0.56 mM in DMSO.

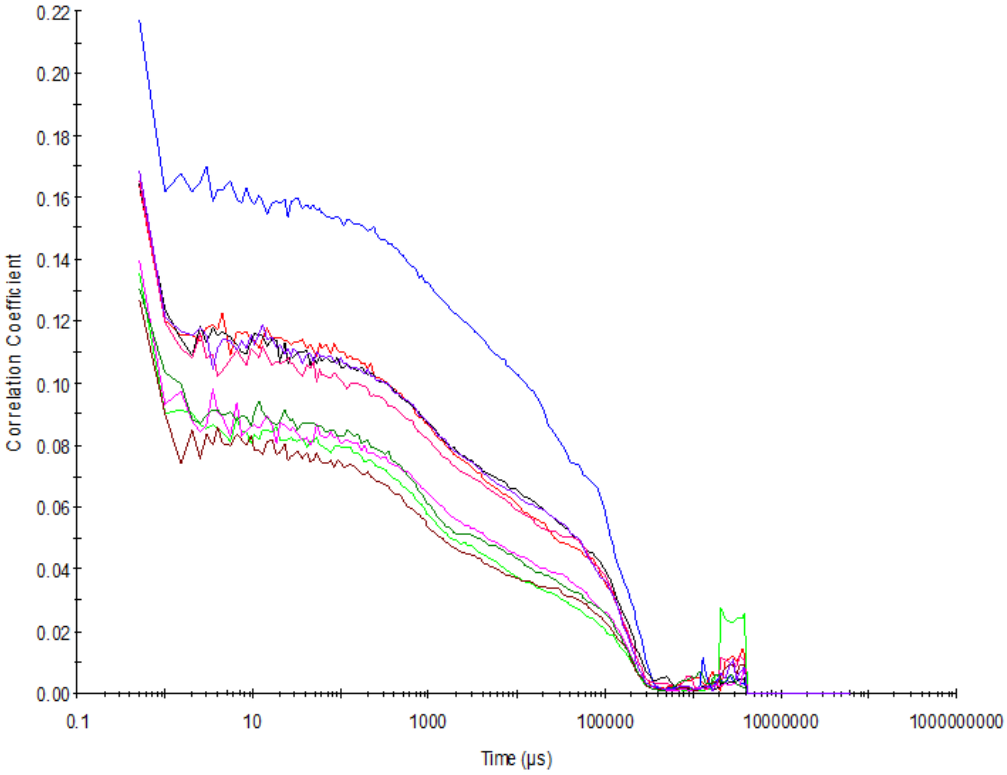

Figure S41 – Raw correlation data for 9 DLS runs at 40 °C with compound **1** at a concentration of 0.56 mM in DMSO.

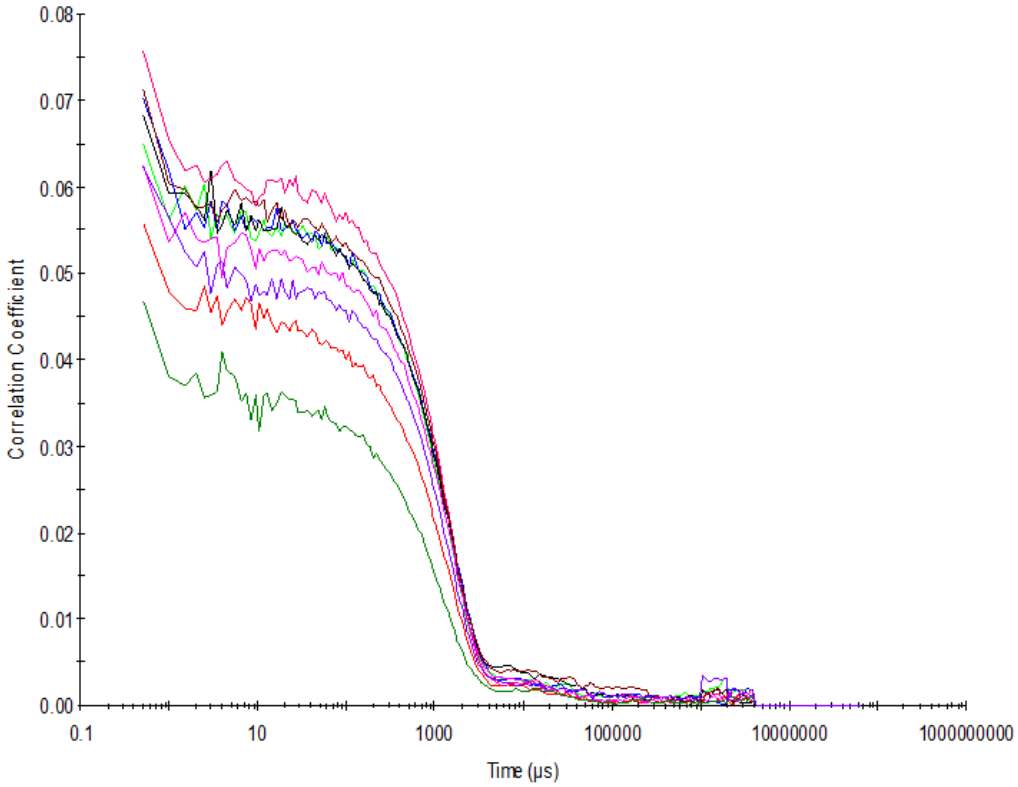

Figure S42 – Raw correlation data for 9 DLS runs at 25 °C after heating to 40 °C with compound **1** at a concentration of 0.56 mM in DMSO.

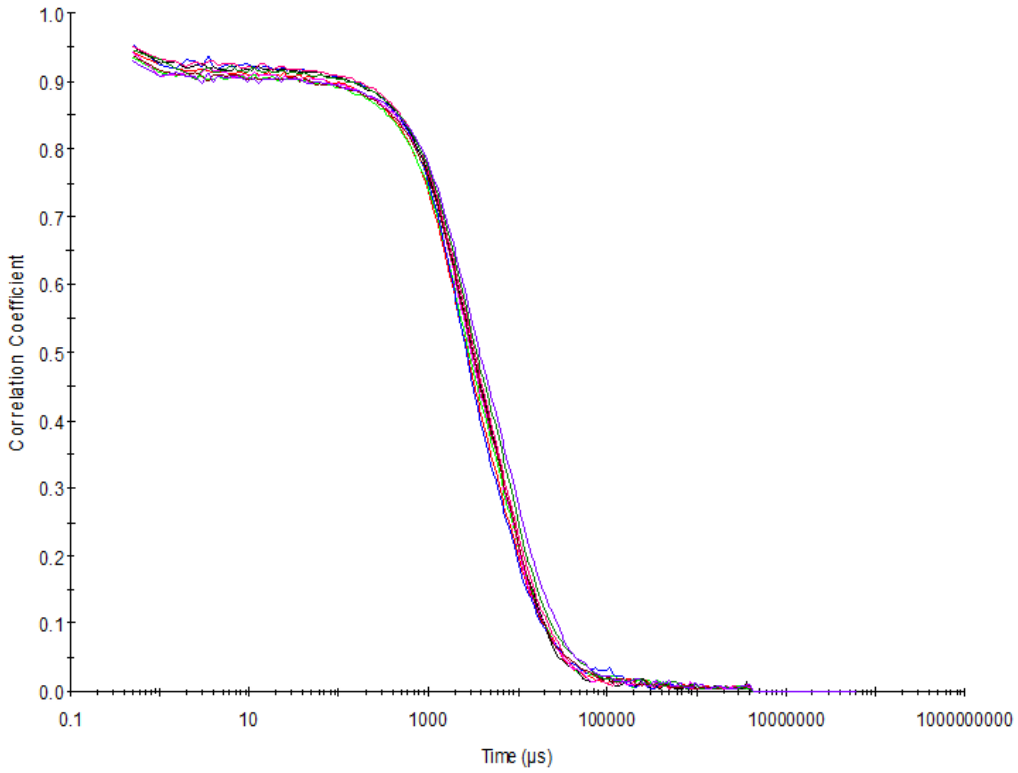

Figure S43 – Raw correlation data for 9 DLS runs at 25 °C after heating to 40 °C with compound **1** at a concentration of 55.56 mM in DMSO: H_2O 1: 1.

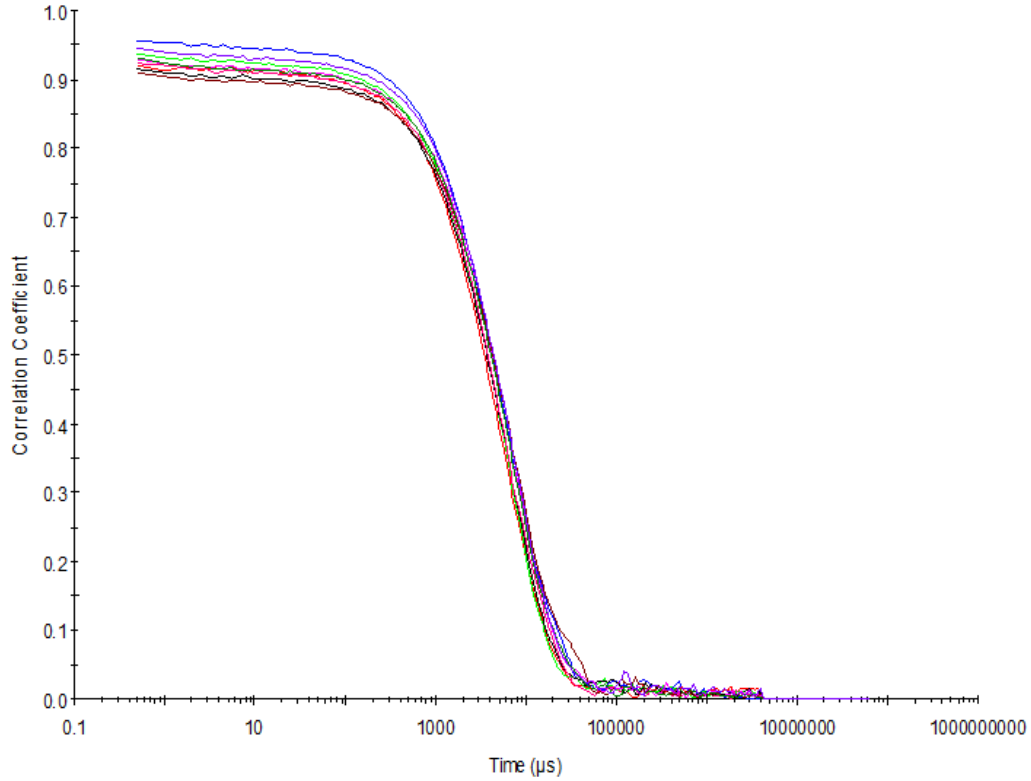

Figure S44 - Raw correlation data for 9 DLS runs at 25 °C after heating to 40 °C with compound **1** at a concentration of 5.56 mM in DMSO: H_2O 1: 1.

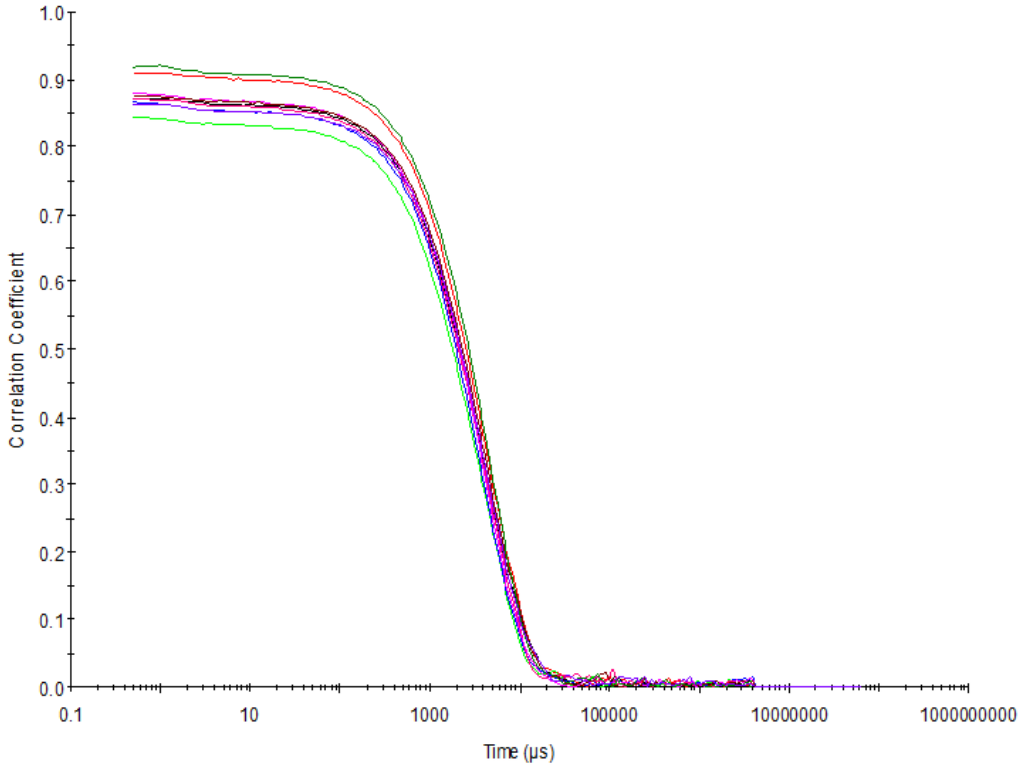

Figure S45 - Raw correlation data for 9 DLS runs at 25 °C after heating to 40 °C with compound **1** at a concentration of 0.56 mM in DMSO: H_2O 1: 1.

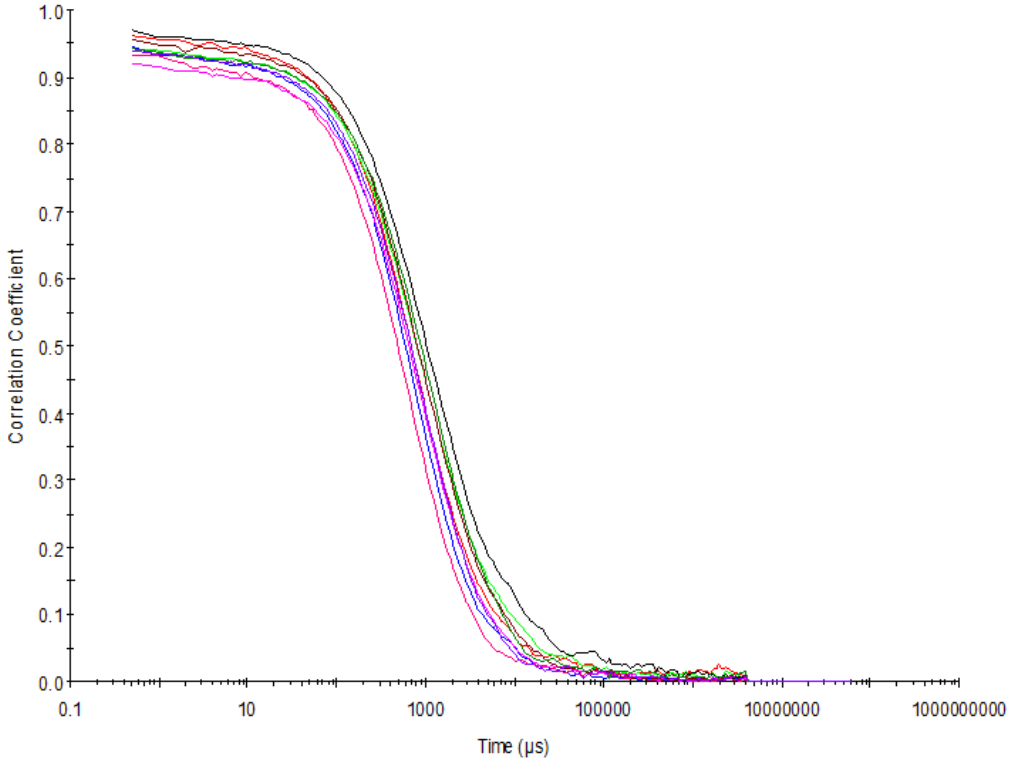

Figure S46 - Raw correlation data for 9 DLS runs at 25 °C after heating to 40 °C with compound **1** at a concentration of 5.56 mM in DMSO: H_2O 3: 7.

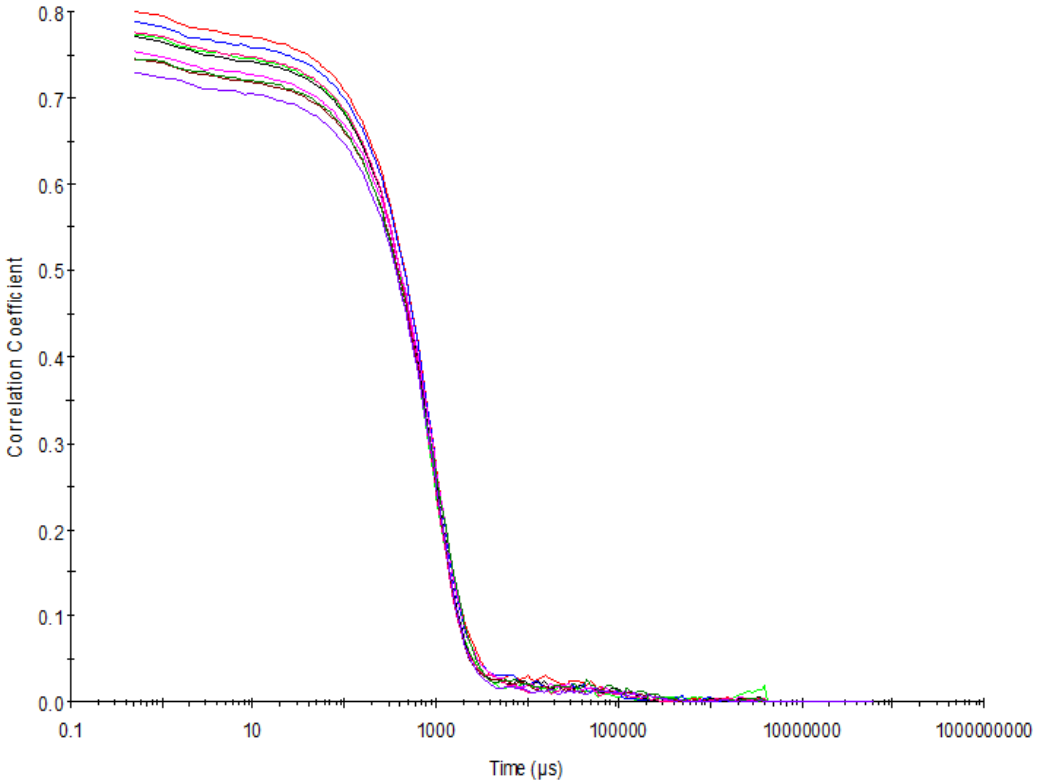

Figure S47 - Raw correlation data for 9 DLS runs at 25 °C after heating to 40 °C with compound **1** at a concentration of 0.56 mM in DMSO: H_2O 3: 7.

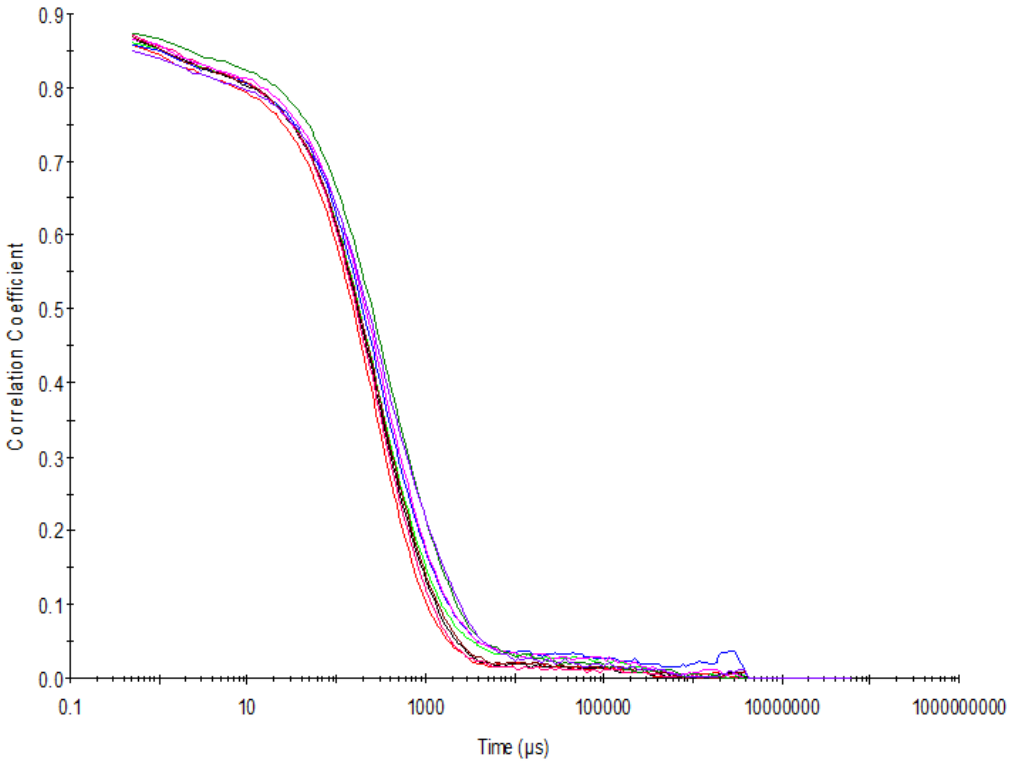

Figure S48 - Raw correlation data for 9 DLS runs at 25 °C after heating to 40 °C with compound **1** at a concentration of 0.56 mM in DMSO: H_2O 1: 4.

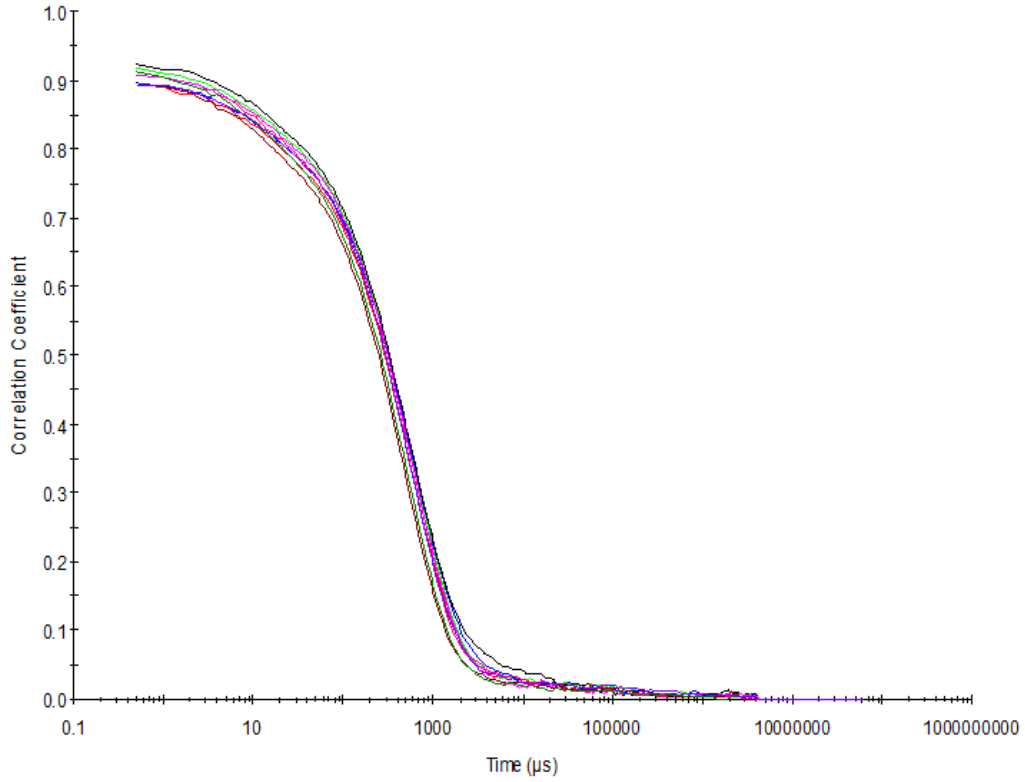

Figure S49 - Raw correlation data for 9 DLS runs at 25 °C after heating to 40 °C with compound **1** at a concentration of 5.56 mM in EtOH: H_2O 1: 19.

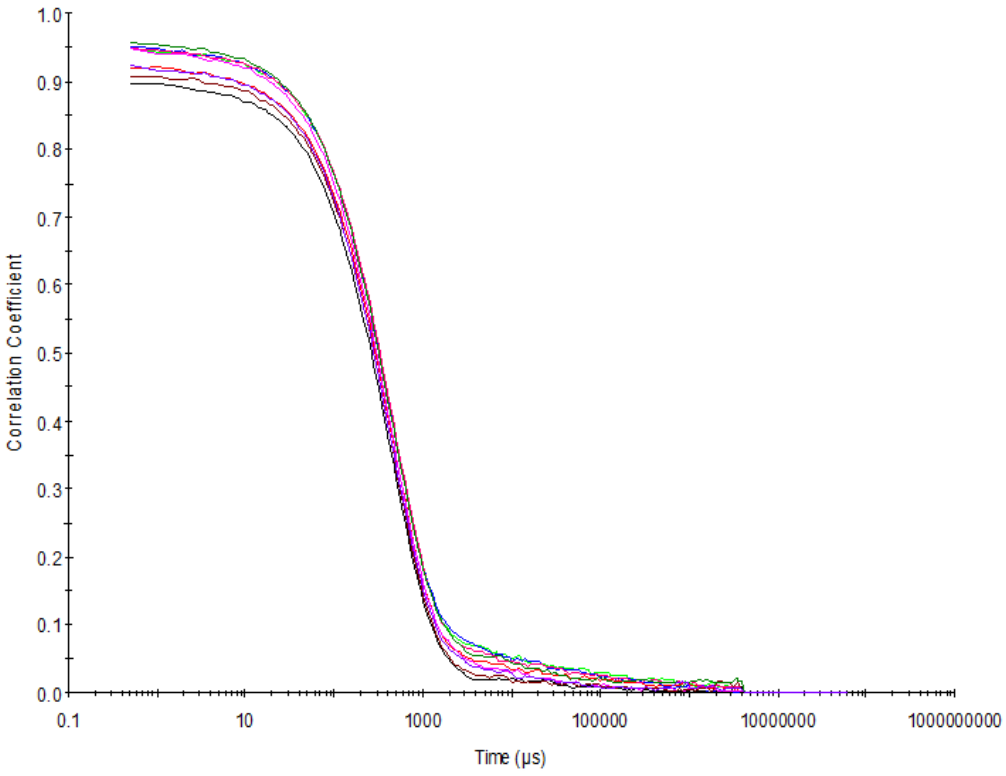

Figure S50 - Raw correlation data for 9 DLS runs at 25 °C after heating to 40 °C with compound **1** at a concentration of 0.56 mM in EtOH: H_2O 1: 19.

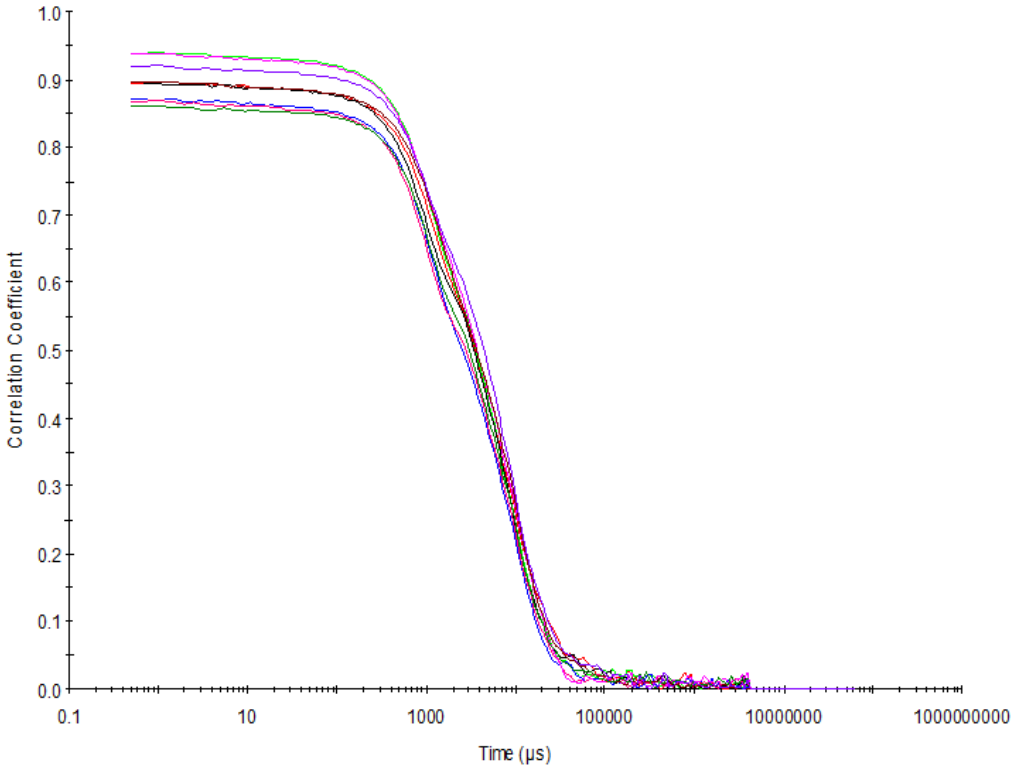

Figure S51 - Raw correlation data for 9 DLS runs at 25 °C after heating to 40 °C with compound **2** at a concentration of 55.56 mM in DMSO: H_2O 1: 1.

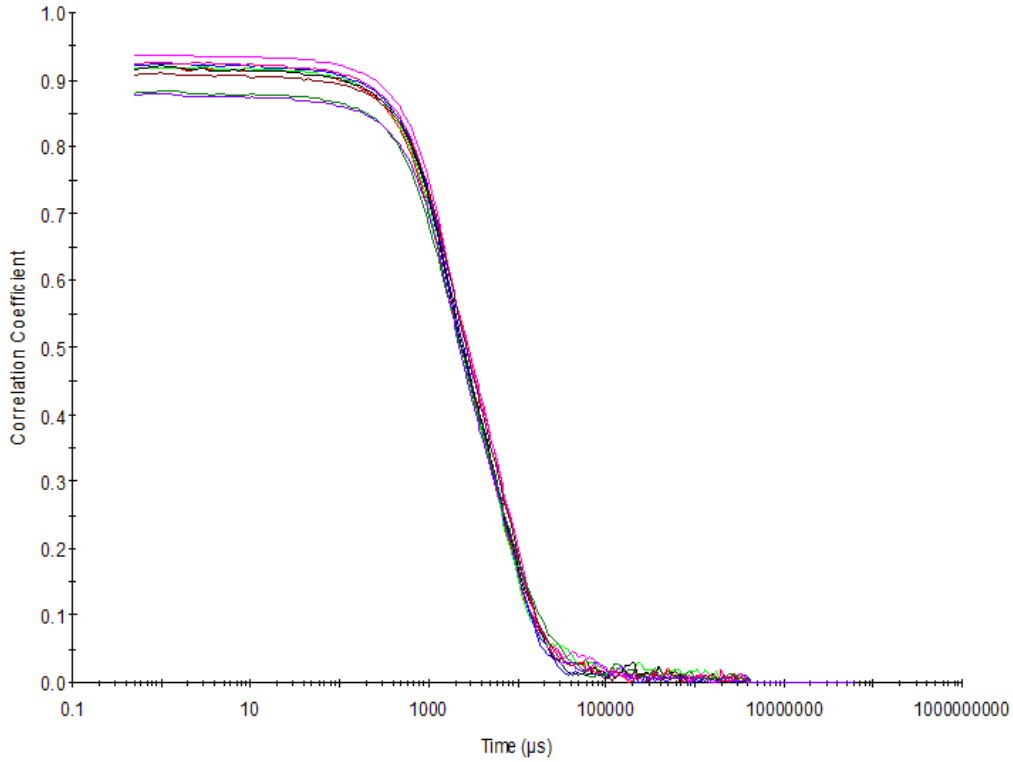

Figure S52 - Raw correlation data for 9 DLS runs at 25 °C after heating to 40 °C with compound **2** at a concentration of 5.56 mM in DMSO: H_2O 1: 1.

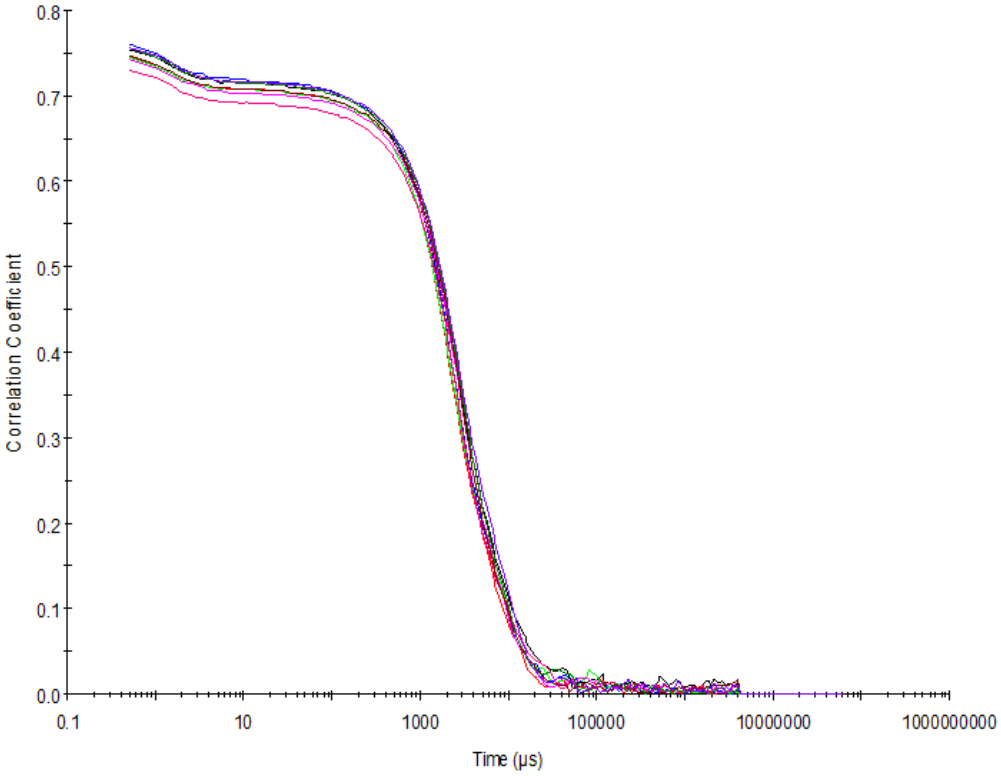

Figure S53 - Raw correlation data for 9 DLS runs at 25 °C after heating to 40 °C with compound **2** at a concentration of 0.56 mM in DMSO: H_2O 1: 1.

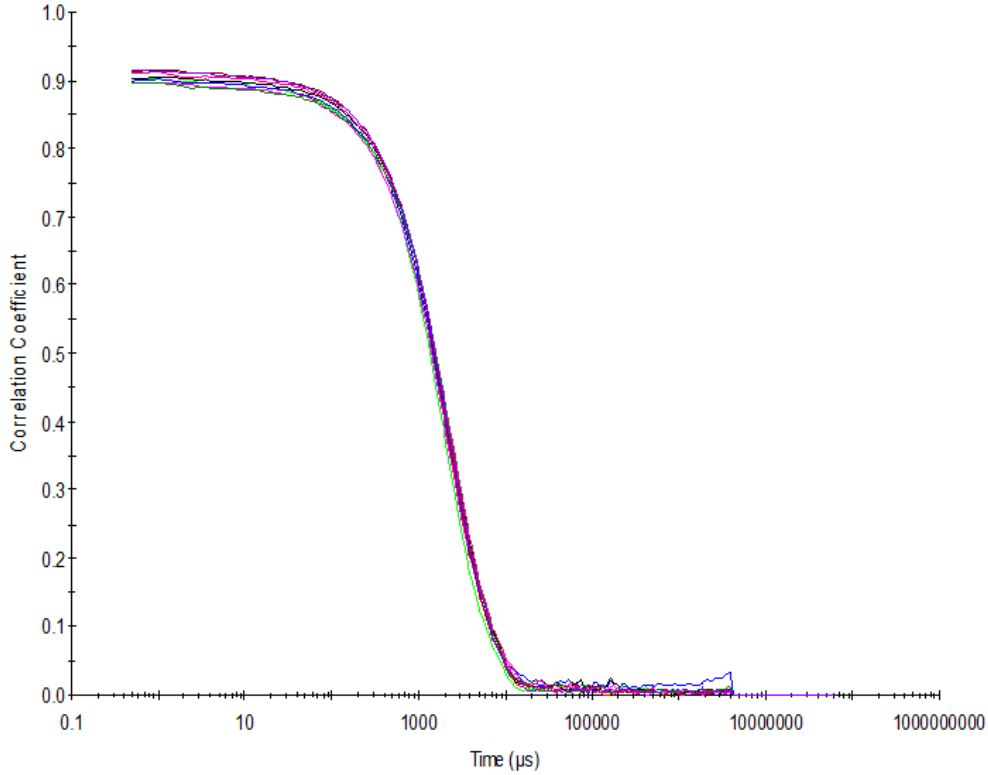

Figure S54 - Raw correlation data for 9 DLS runs at 25 °C after heating to 40 °C with compound **2** at a concentration of 5.56 mM in DMSO: H_2O 3: 7.

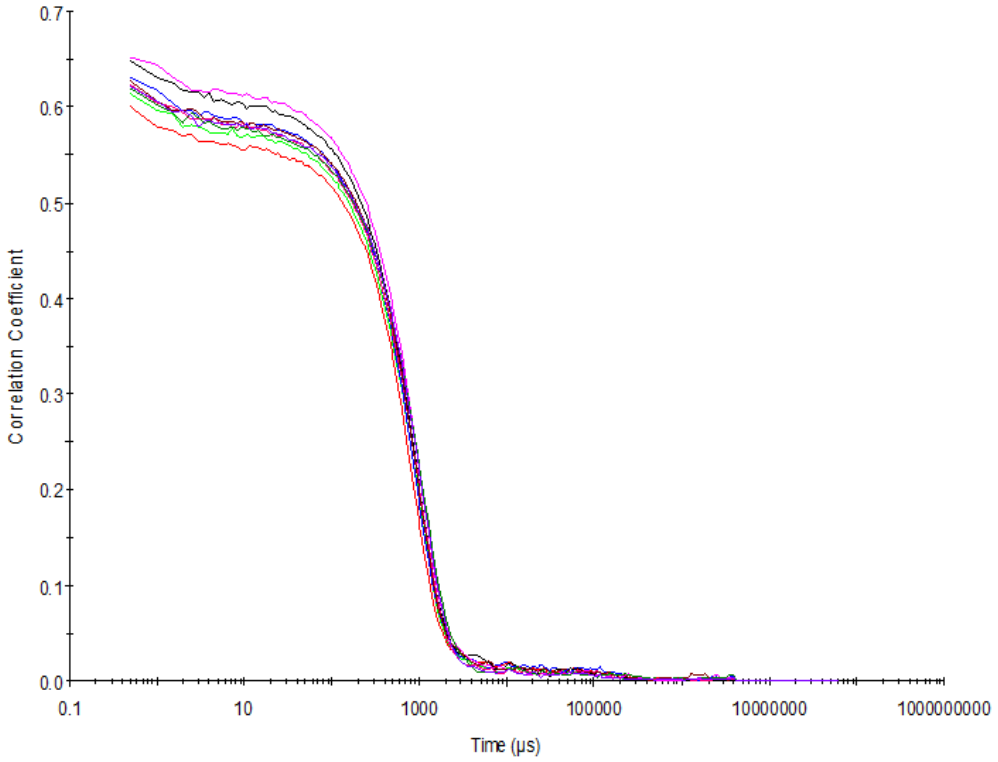

Figure S55- Raw correlation data for 9 DLS runs at 25 °C after heating to 40 °C with compound **2** at a concentration of 0.56 mM in DMSO: H_2O 3: 7.

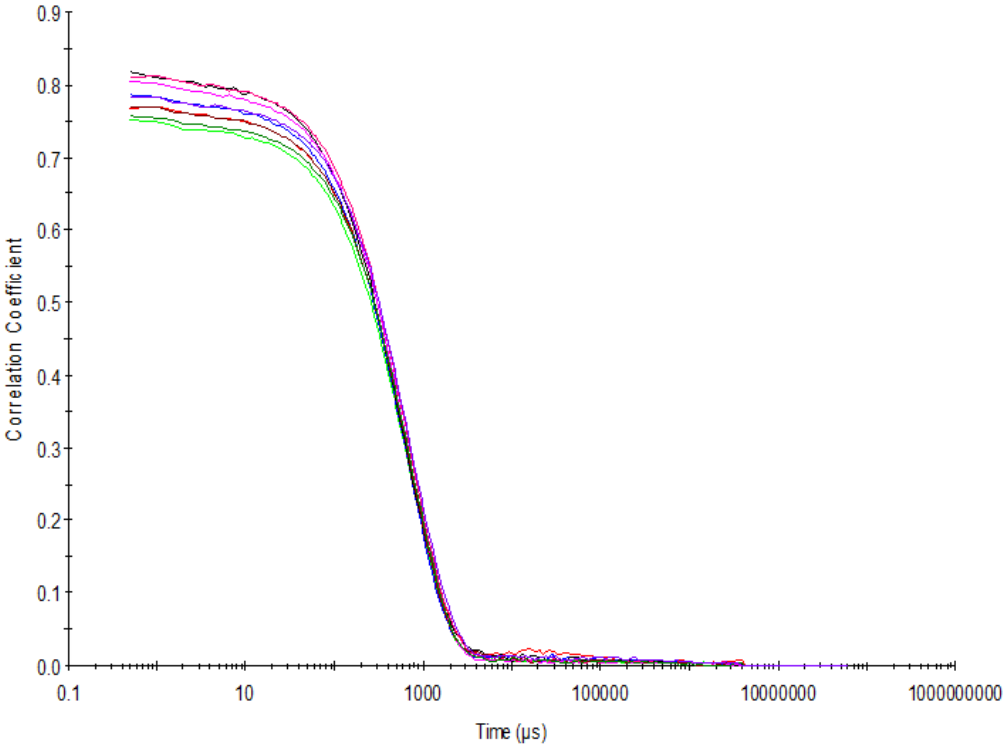

Figure S56 - Raw correlation data for 9 DLS runs at 25 °C after heating to 40 °C with compound **2** at a concentration of 0.56 mM in DMSO: H_2O 1: 4.

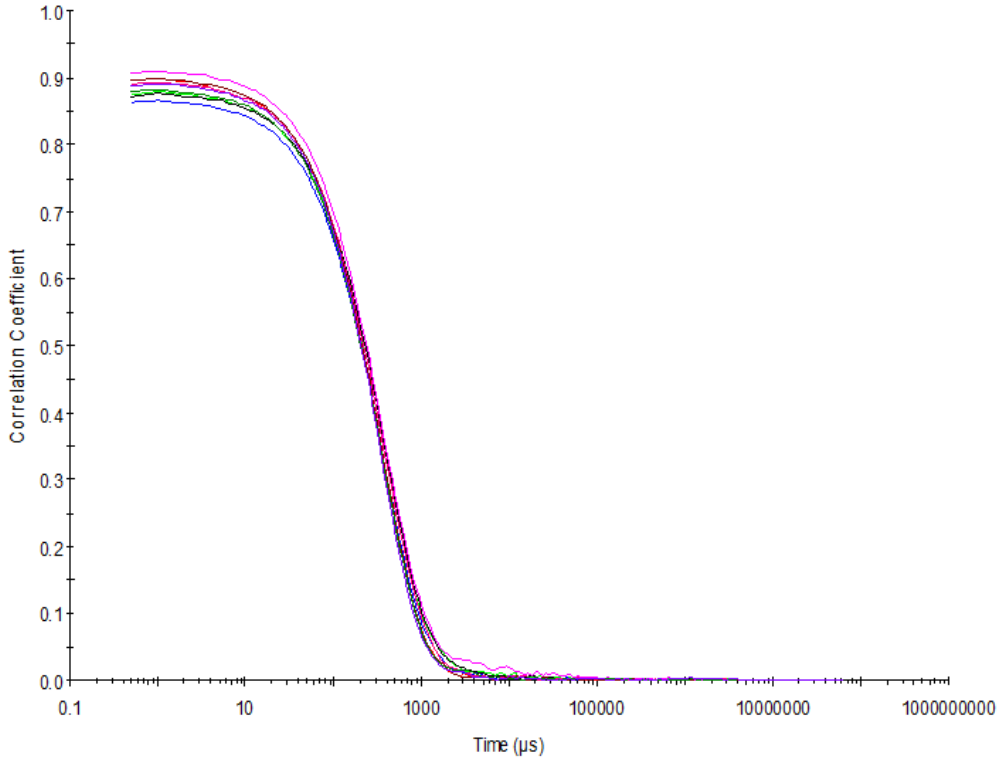

Figure S57 - Raw correlation data for 9 DLS runs at 25 °C after heating to 40 °C with compound **2** at a concentration of 5.56 mM in EtOH: H_2O 1: 19.

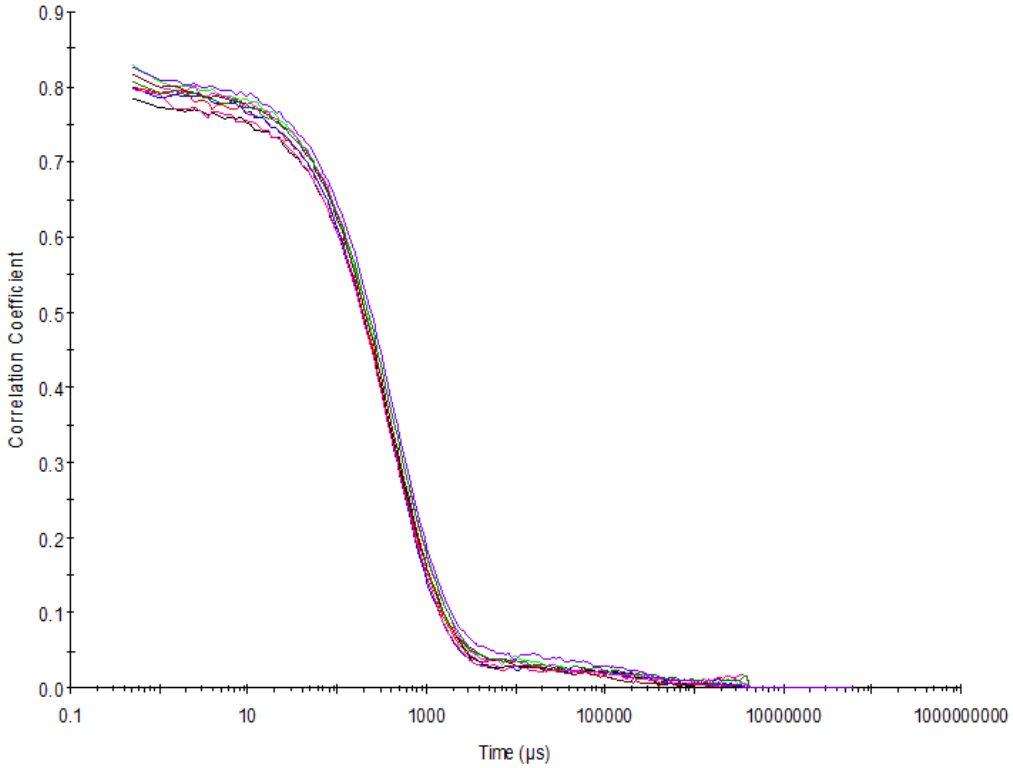

Figure S58 - Raw correlation data for 9 DLS runs at 25 °C after heating to 40 °C with compound **2** at a concentration of 0.56 mM in EtOH: H_2O 1: 19.

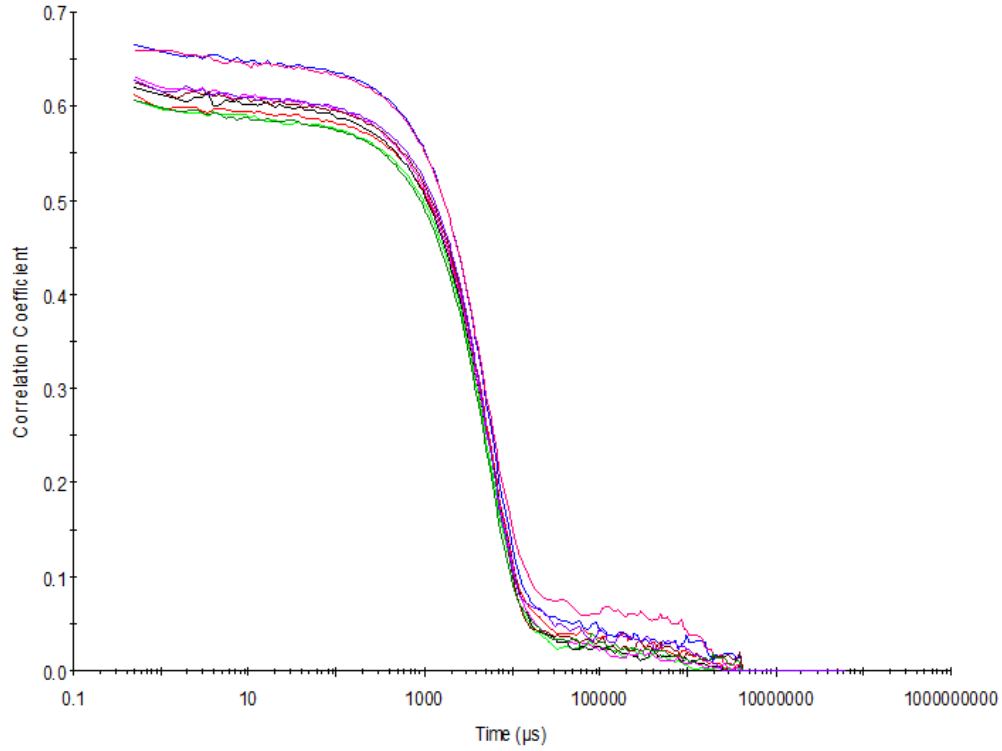

Figure S59 – Raw correlation data for 9 DLS runs at 25 °C before heating to 40 °C with compound **3** at a concentration of 111.12 mM in DMSO.

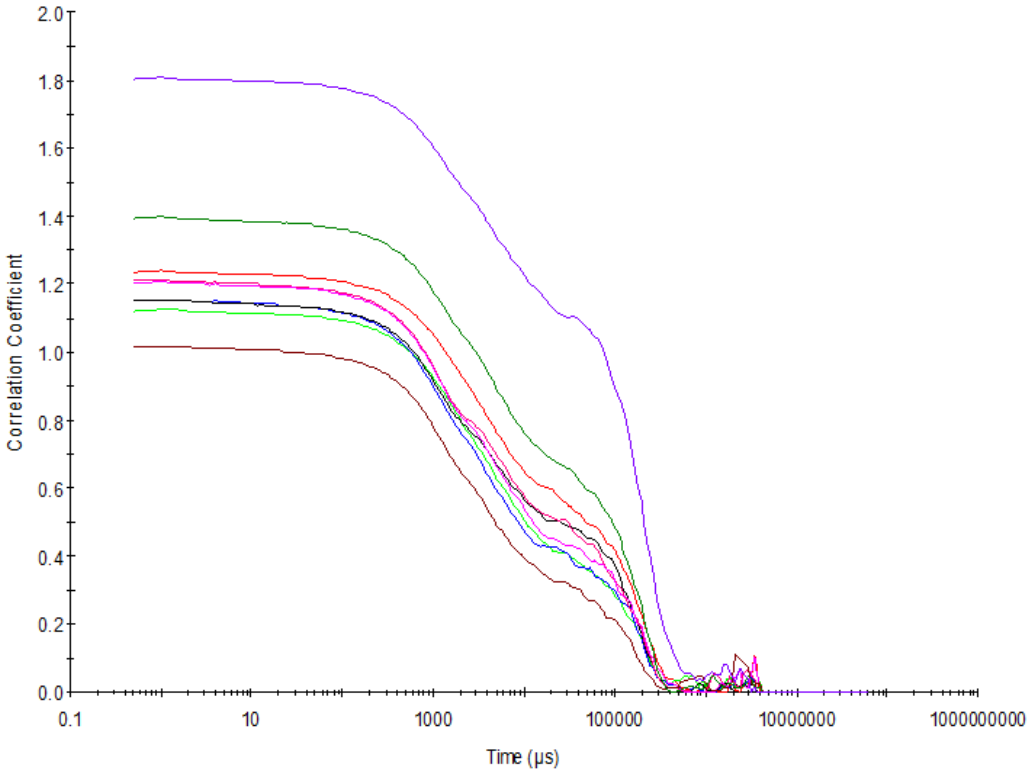

Figure S60– Raw correlation data for 9 DLS runs at 40 °C with compound **3** at a concentration of 111.12 mM in DMSO.

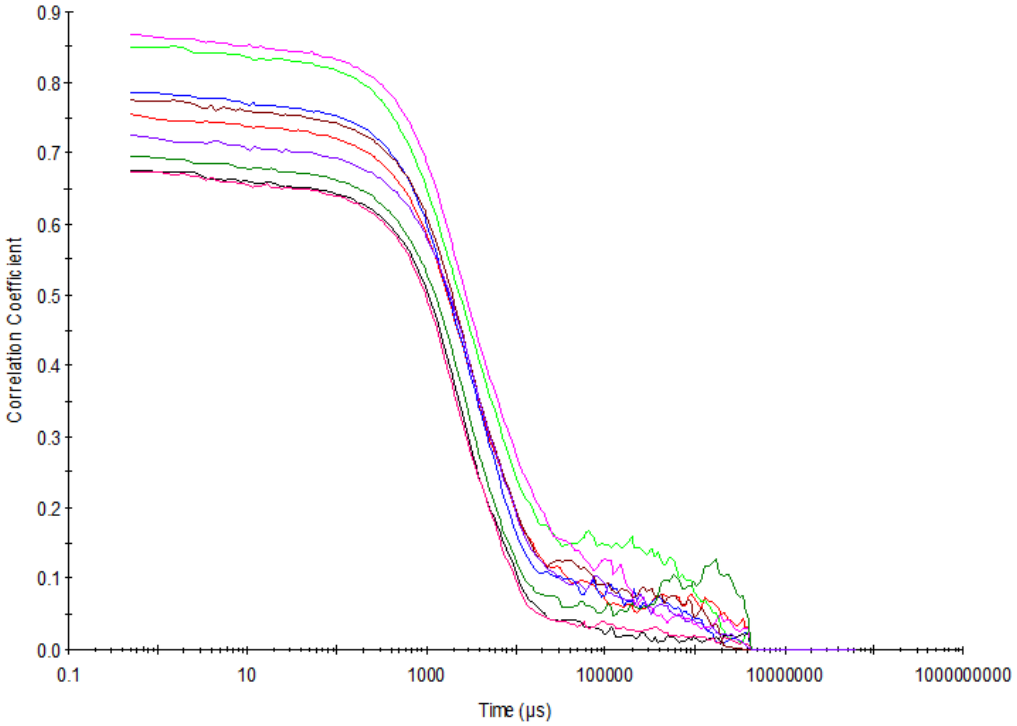

Figure S61 – Raw correlation data for 9 DLS runs at 25 °C after heating to 40 °C with compound **3** at a concentration of 111.12 mM in DMSO.

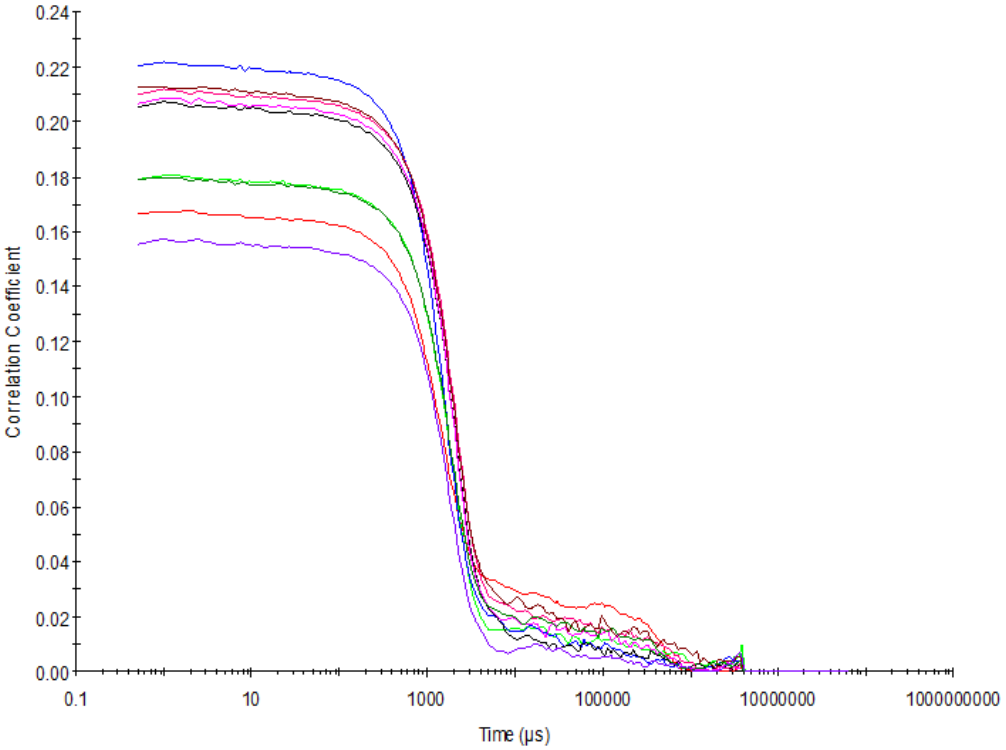

Figure S62– Raw correlation data for 9 DLS runs at 25 °C before heating to 40 °C with compound **3** at a concentration of 55.56 mM in DMSO.

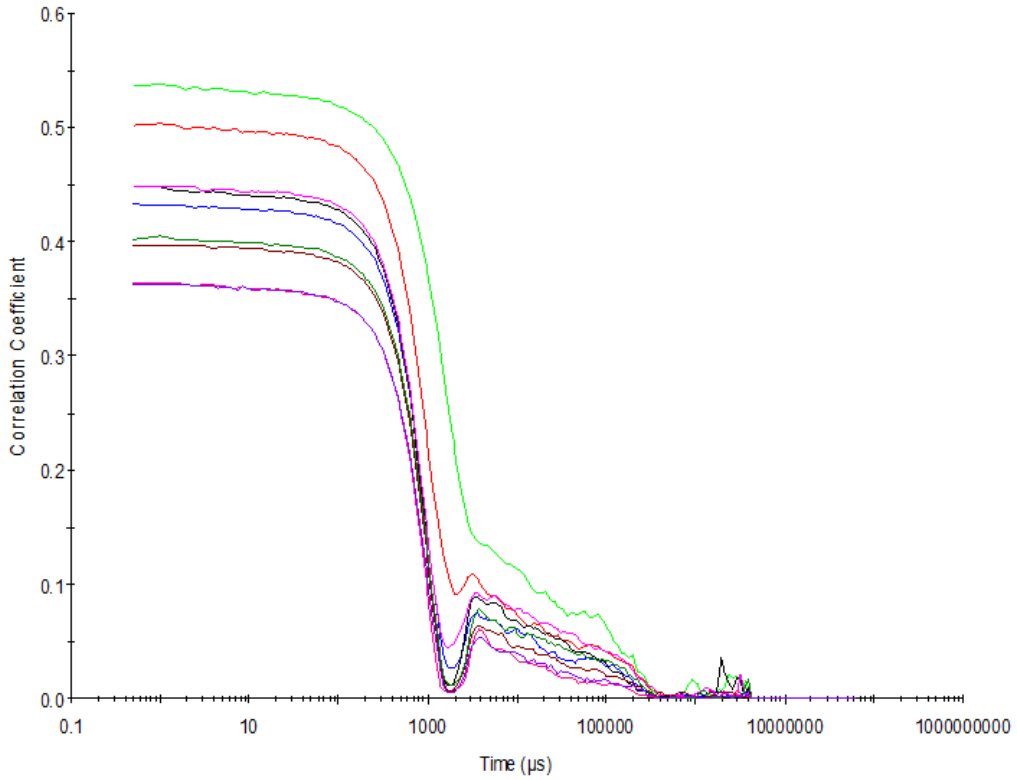

Figure S63 – Raw correlation data for 9 DLS runs at 40 °C with compound **3** at a concentration of 55.56 mM in DMSO.

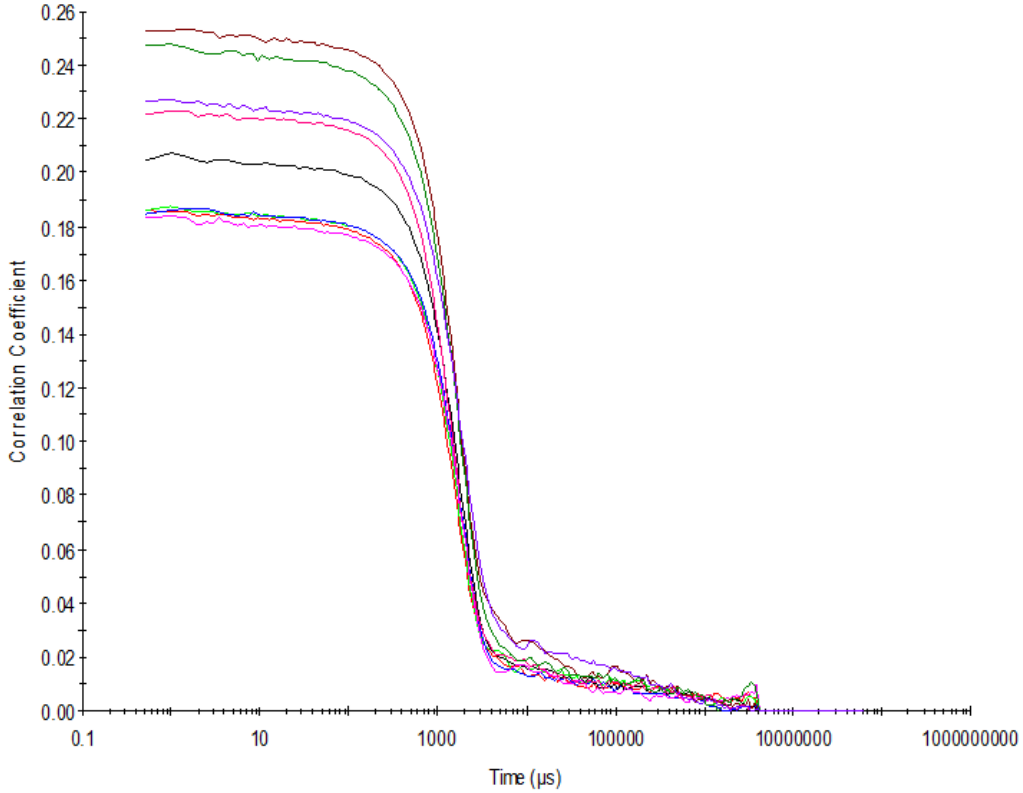

Figure S64 – Raw correlation data for 9 DLS runs at 25 °C after heating to 40 °C with compound **3** at a concentration of 55.56 mM in DMSO.

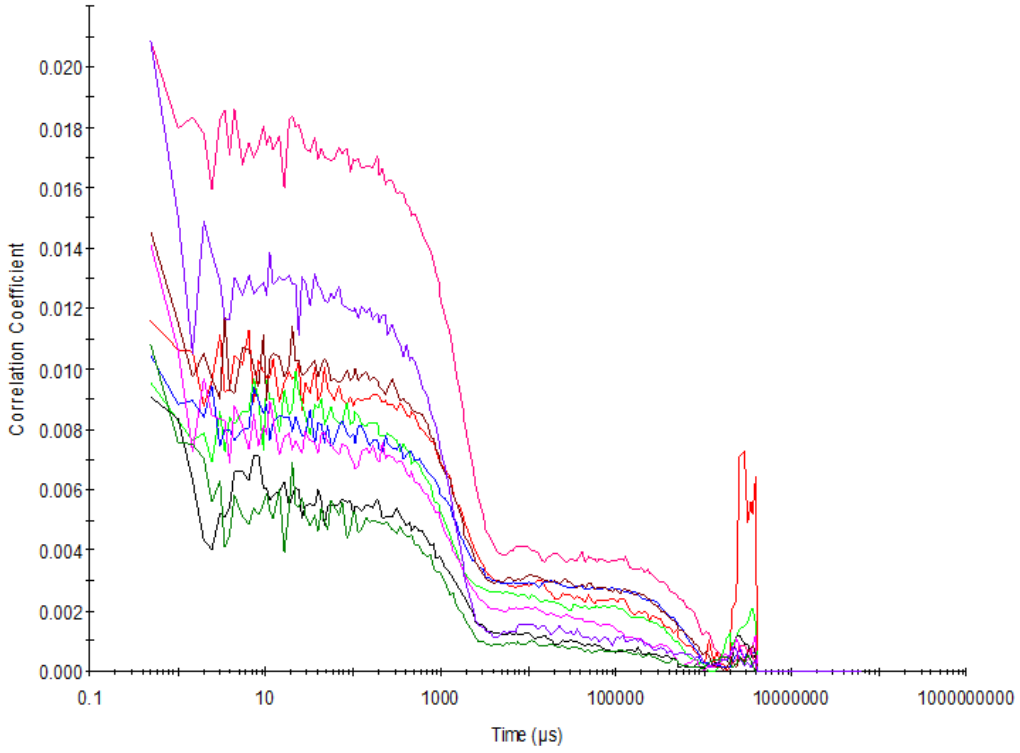

Figure S65 – Raw correlation data for 9 DLS runs at 25 °C before heating to 40 °C with compound **3** at a concentration of 5.56 mM in DMSO.

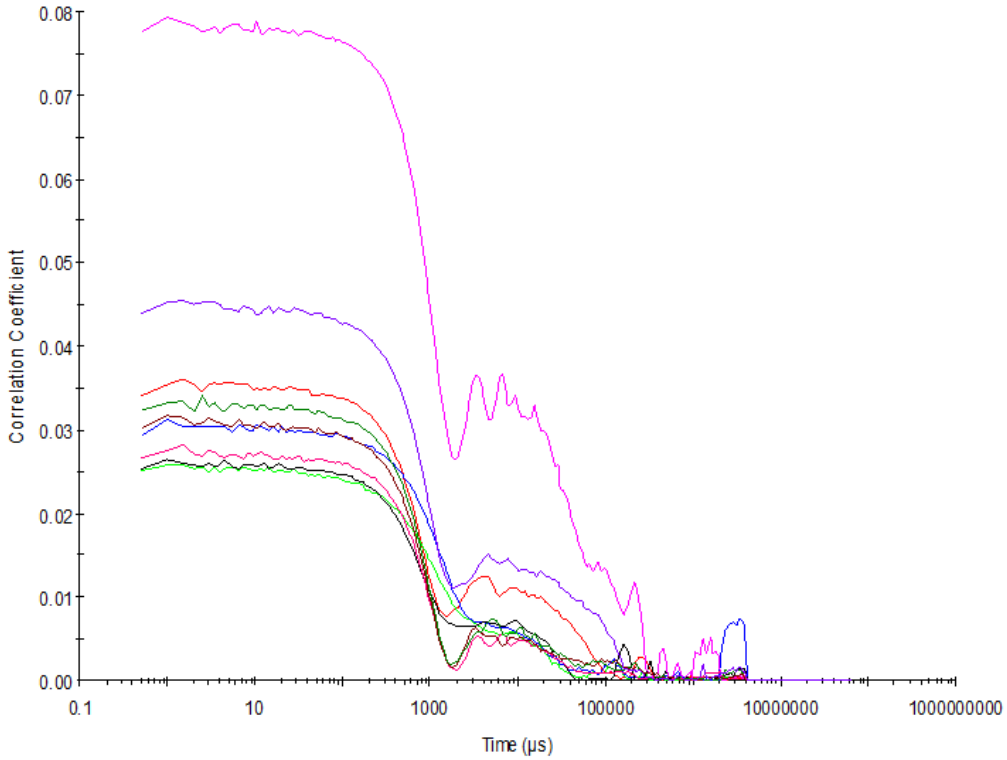

Figure S66 – Raw correlation data for 9 DLS runs at 40 °C with compound **3** at a concentration of 5.56 mM in DMSO.

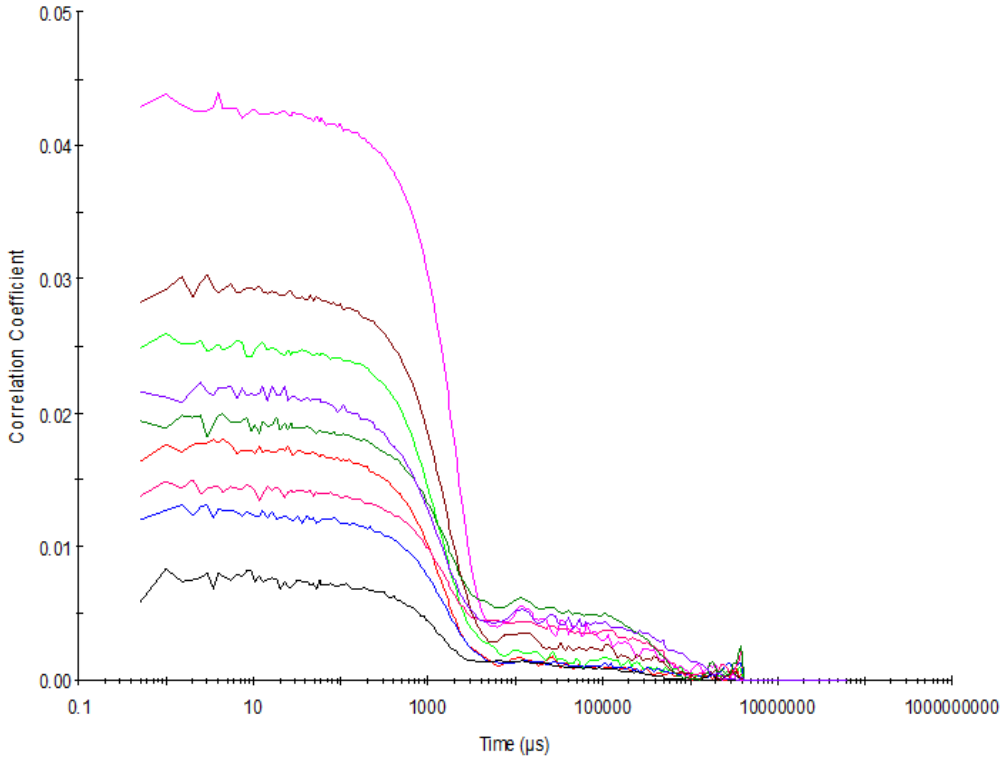

Figure S67 – Raw correlation data for 9 DLS runs at 25 °C after heating to 40 °C with compound **3** at a concentration of 5.56 mM in DMSO.

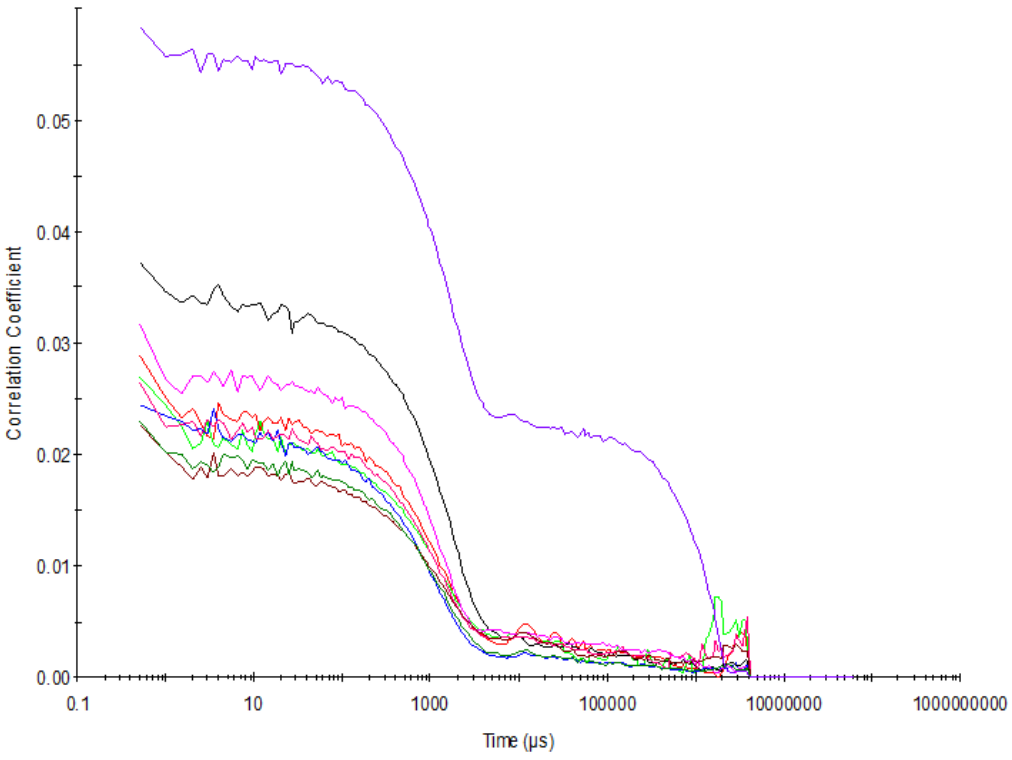

Figure S68 – Raw correlation data for 9 DLS runs at 25 °C before heating to 40 °C with compound **3** at a concentration of 0.56 mM in DMSO.

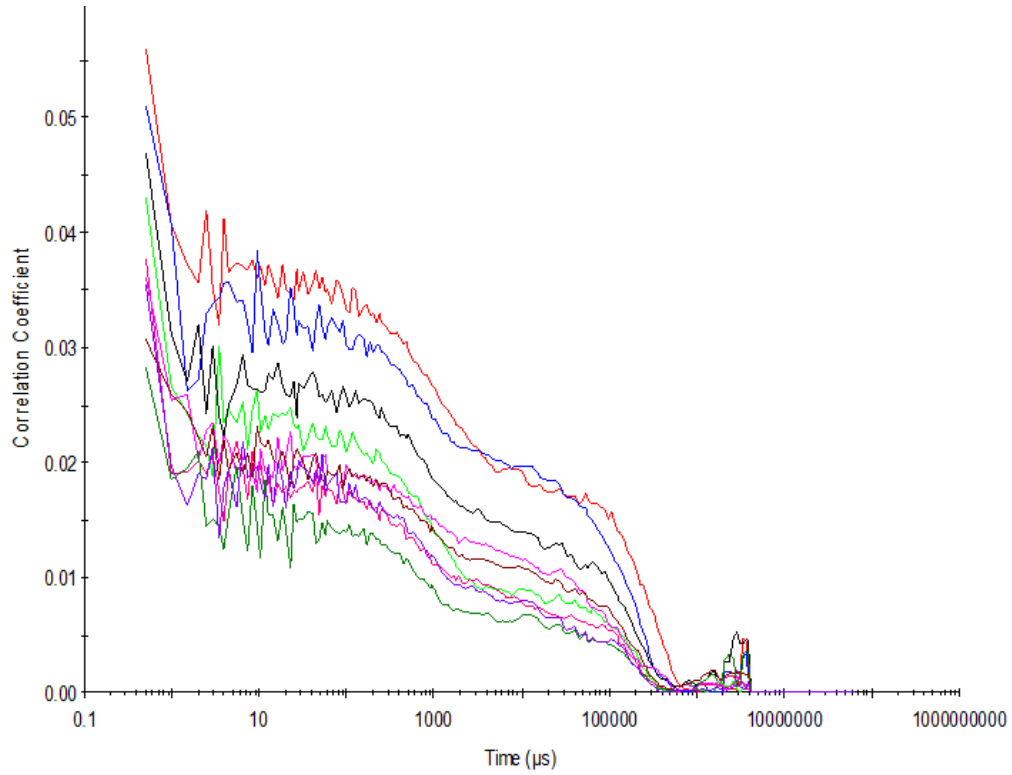

Figure S69 – Raw correlation data for 9 DLS runs at 40 °C with compound **3** at a concentration of 0.56 mM in DMSO.

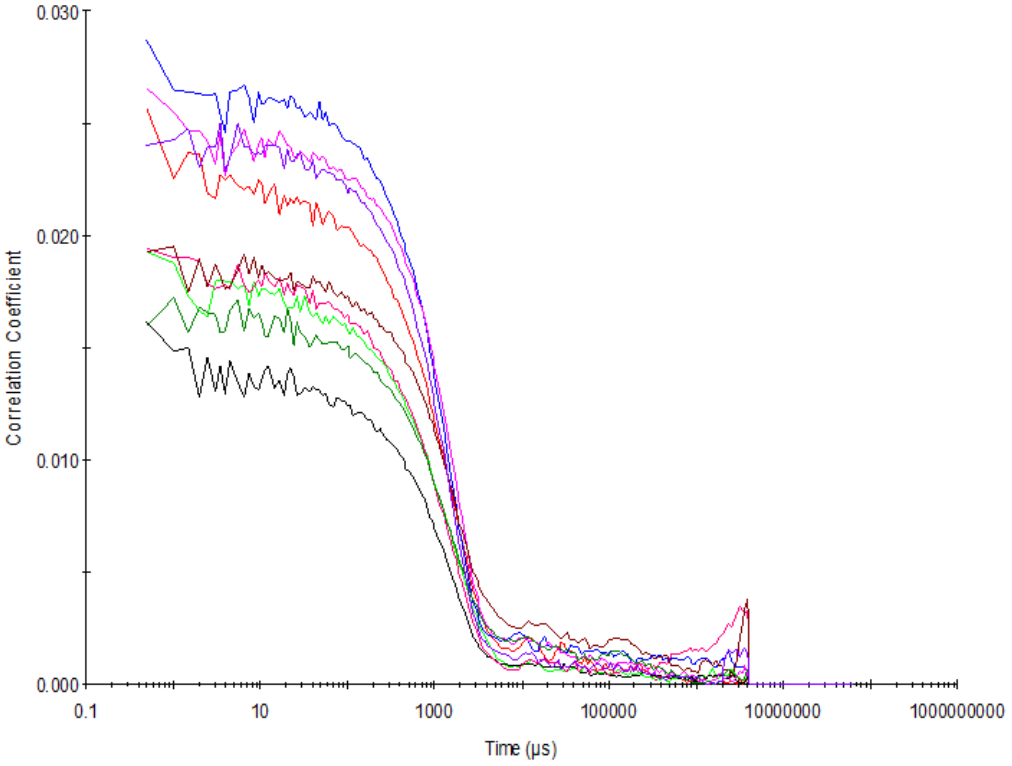

Figure S70 – Raw correlation data for 9 DLS runs at 25 °C after heating to 40 °C with compound **3** at a concentration of 0.56 mM in DMSO.

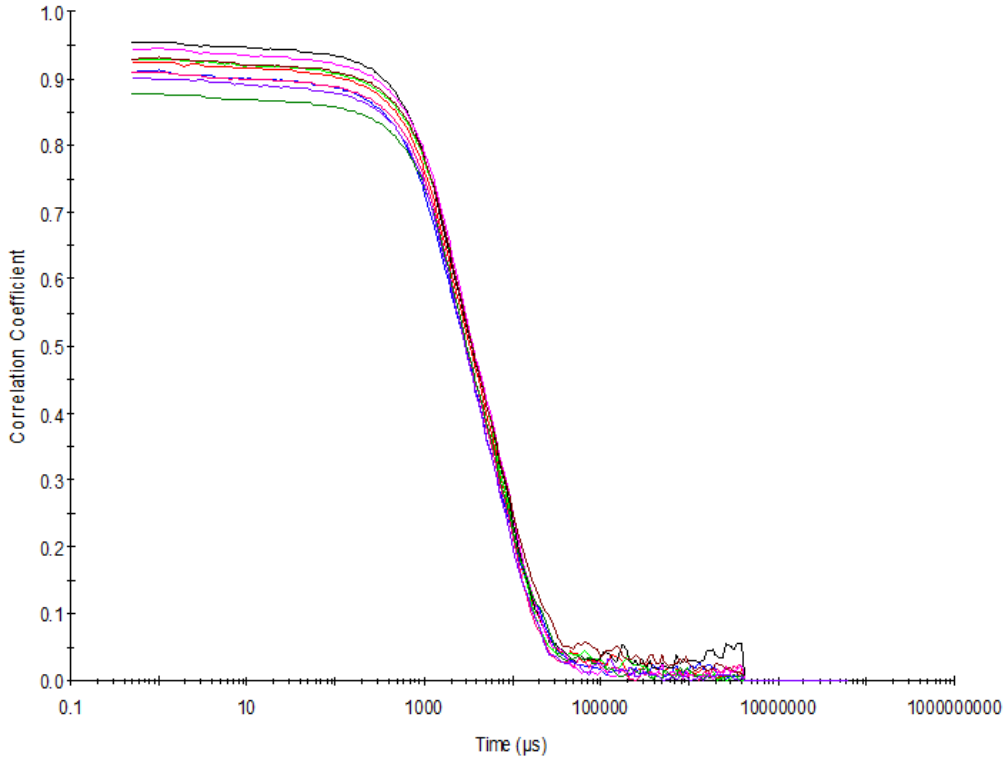

Figure S71 - Raw correlation data for 9 DLS runs at 25 °C after heating to 40 °C with compound **3** at a concentration of 55.56 mM in DMSO: H_2O 1: 1.

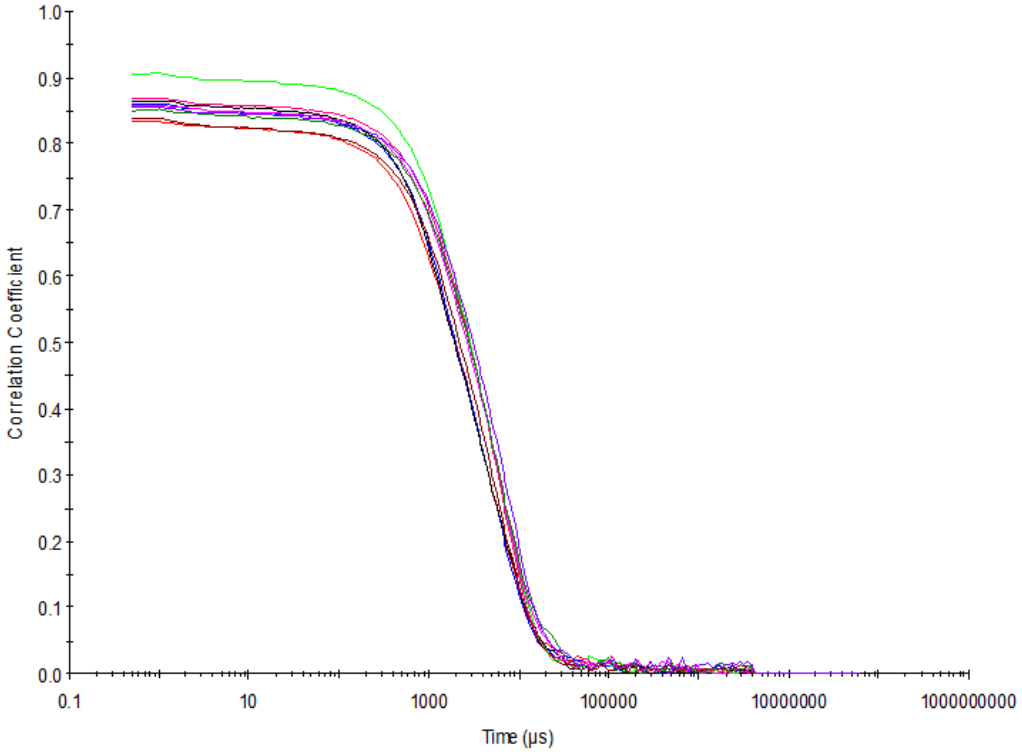

Figure S72 - Raw correlation data for 9 DLS runs at 25 °C after heating to 40 °C with compound **3** at a concentration of 5.56 mM in DMSO: H_2O 1: 1.

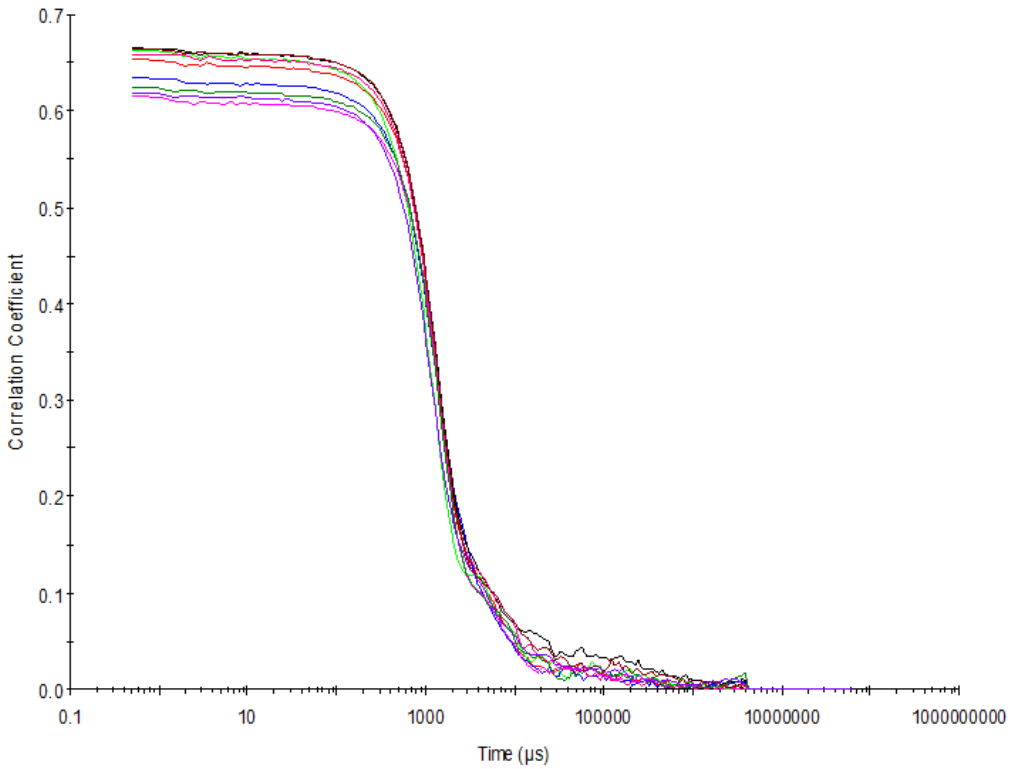

Figure S73 - Raw correlation data for 9 DLS runs at 25 °C after heating to 40 °C with compound **3** at a concentration of 0.56 mM in DMSO: H_2O 1: 1.

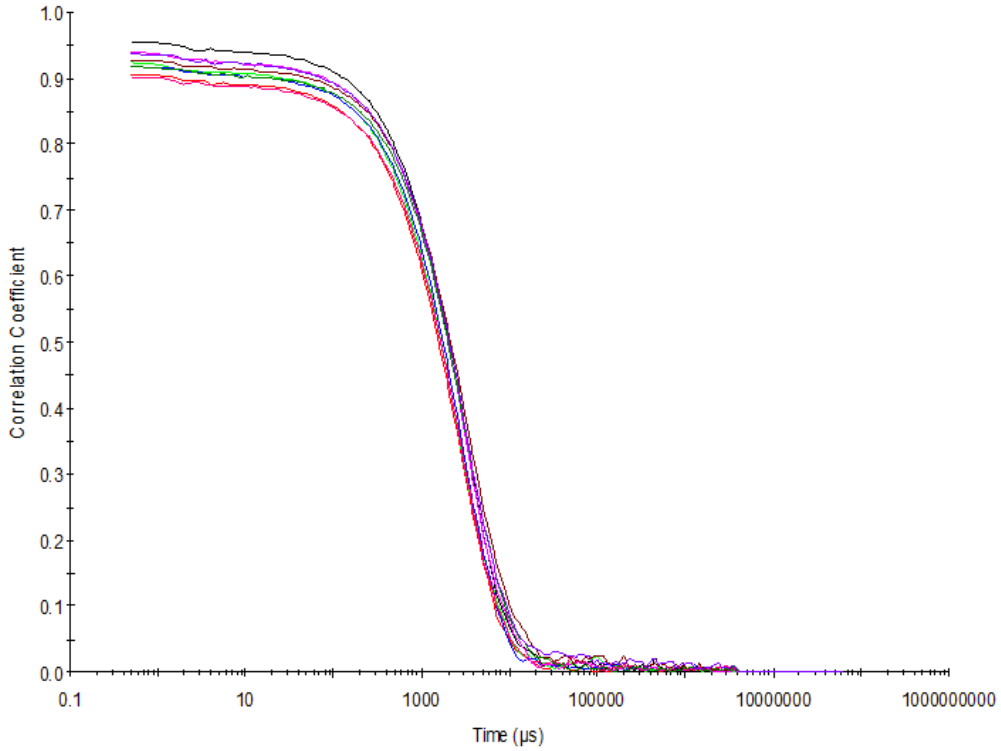

Figure S74 - Raw correlation data for 9 DLS runs at 25 °C after heating to 40 °C with compound **3** at a concentration of 5.56 mM in DMSO: H_2O 3: 7.

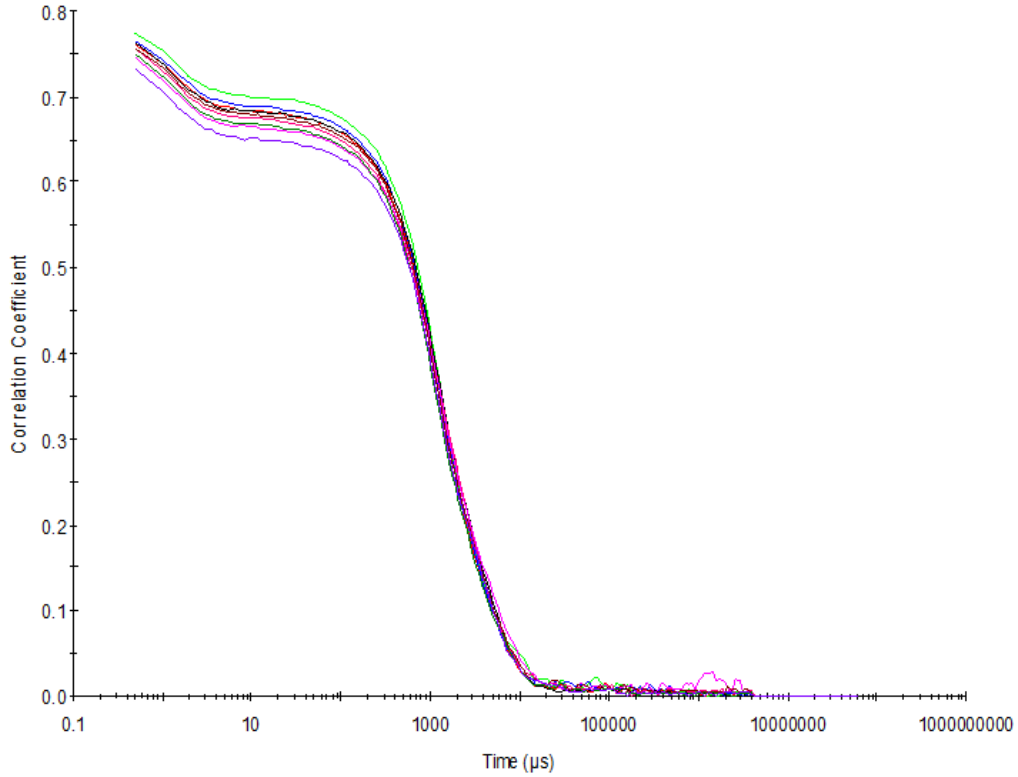

Figure S75 - Raw correlation data for 9 DLS runs at 25 °C after heating to 40 °C with compound **3** at a concentration of 0.56 mM in DMSO: H_2O 3: 7.

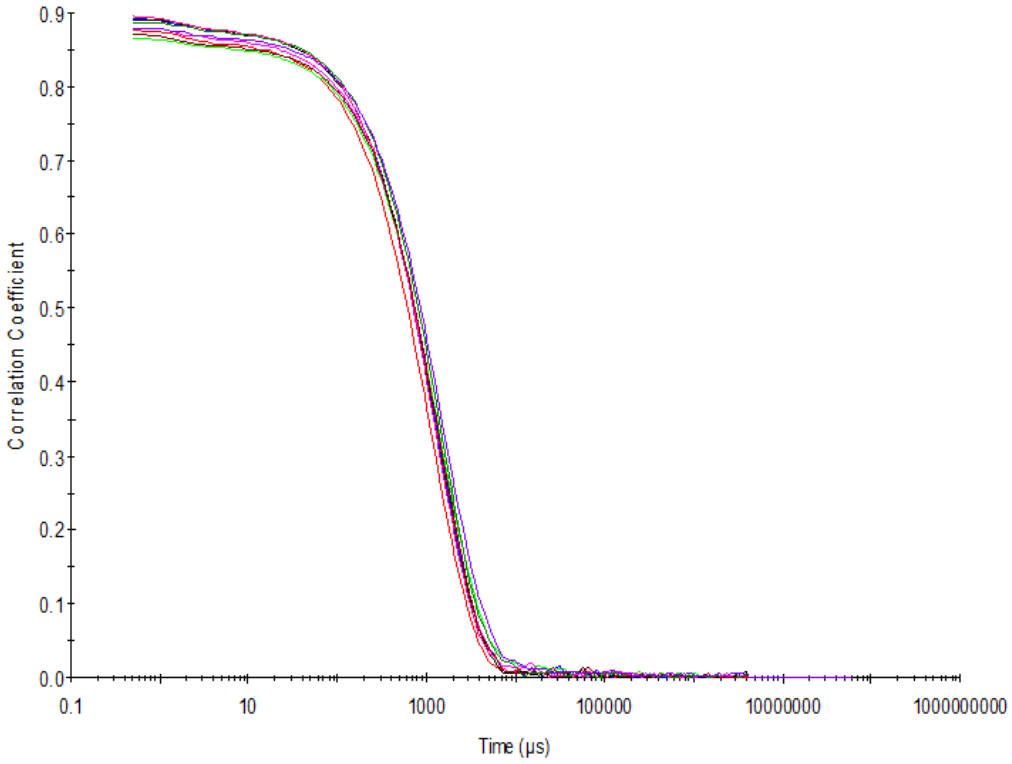

Figure S76 - Raw correlation data for 9 DLS runs at 25 °C after heating to 40 °C with compound **3** at a concentration of 0.56 mM in DMSO: H_2O 1: 4.

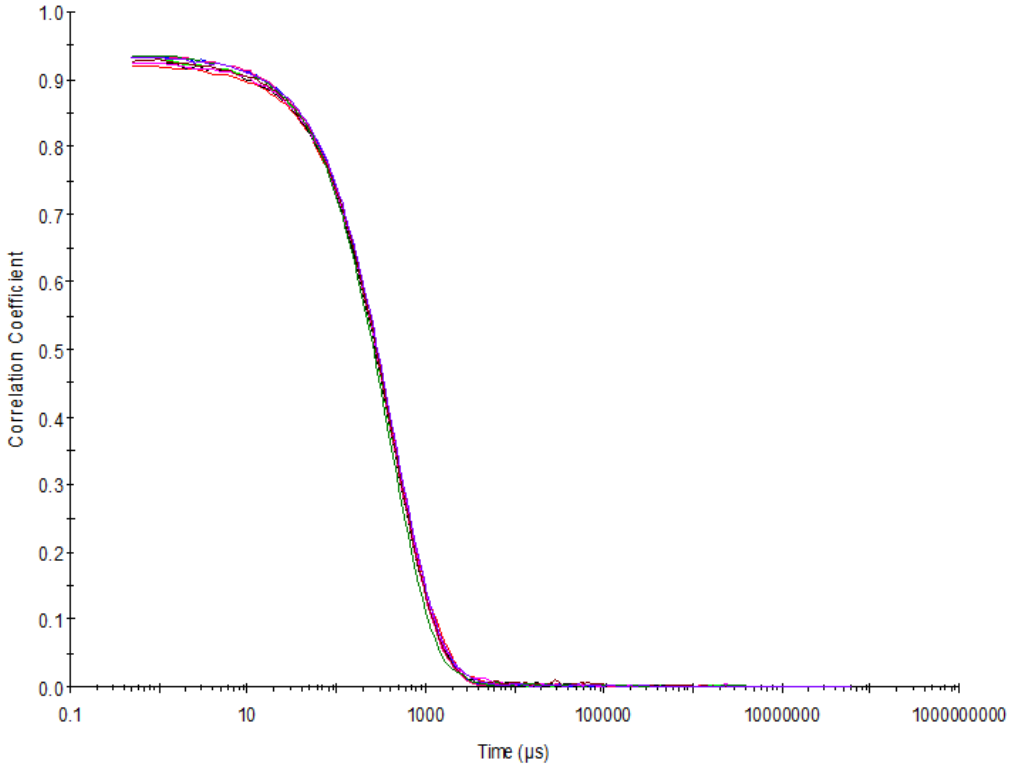

Figure S77 - Raw correlation data for 9 DLS runs at 25 °C after heating to 40 °C with compound 2 at a concentration of 5.56 mM in EtOH: H_2O 1: 19.

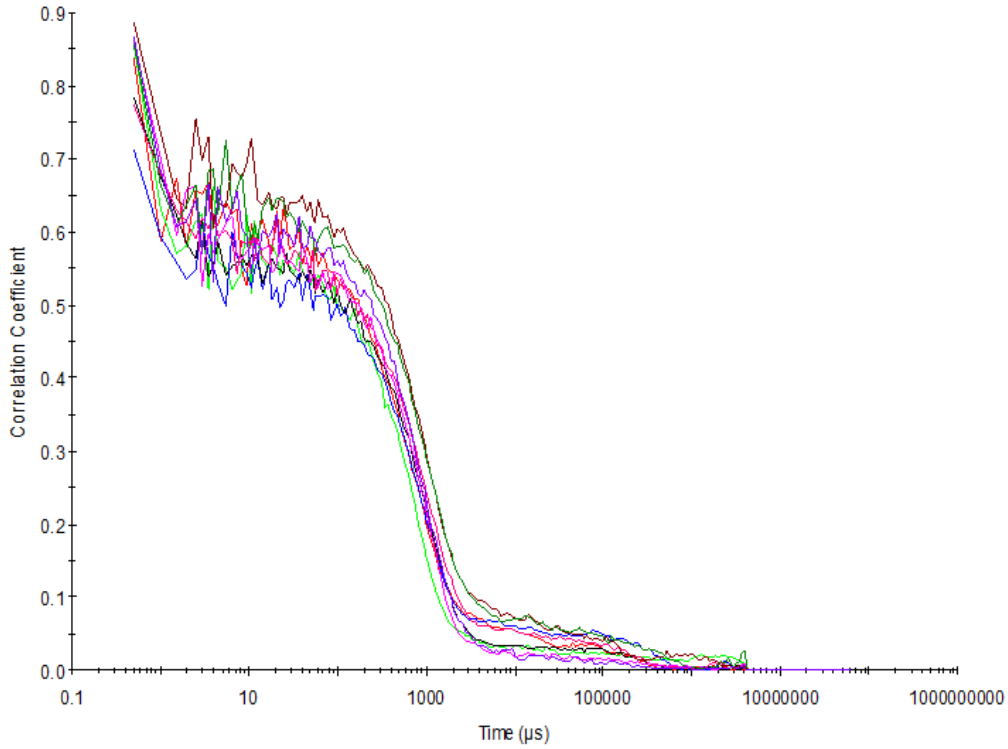

Figure S78 - Raw correlation data for 9 DLS runs at 25 °C after heating to 40 °C with compound **3** at a concentration of 0.56 mM in EtOH: H_2O 1: 19.

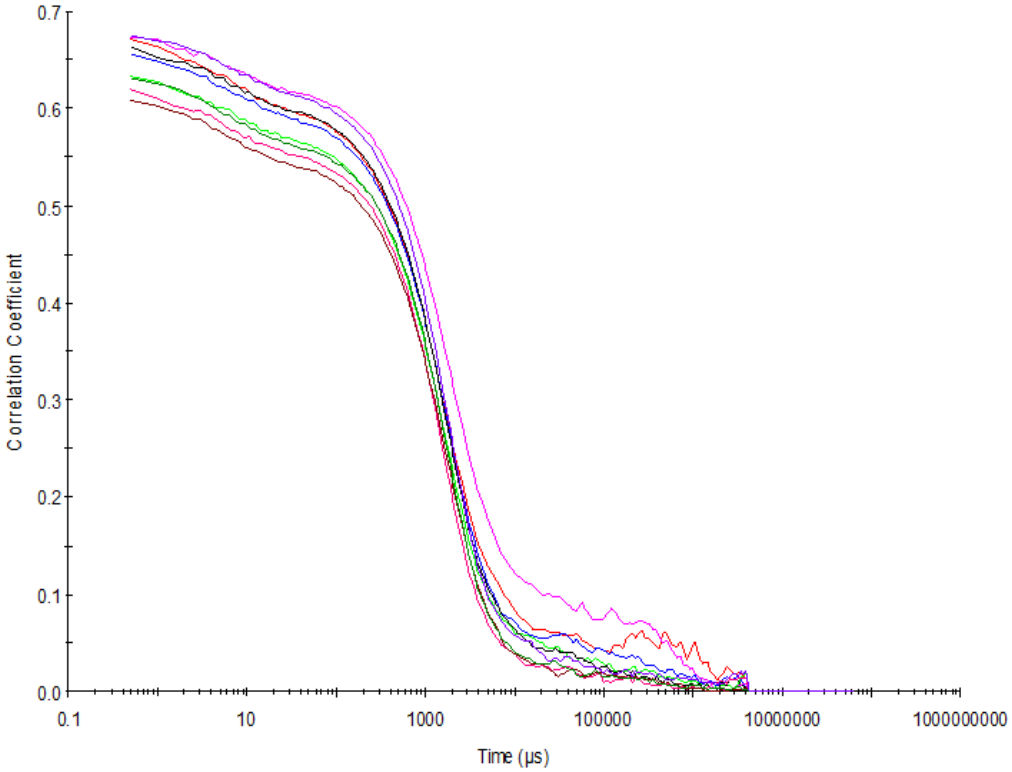

Figure S79 – Raw correlation data for 9 DLS runs at 25 °C before heating to 40 °C with compound **4** at a concentration of 111.12 mM in DMSO.

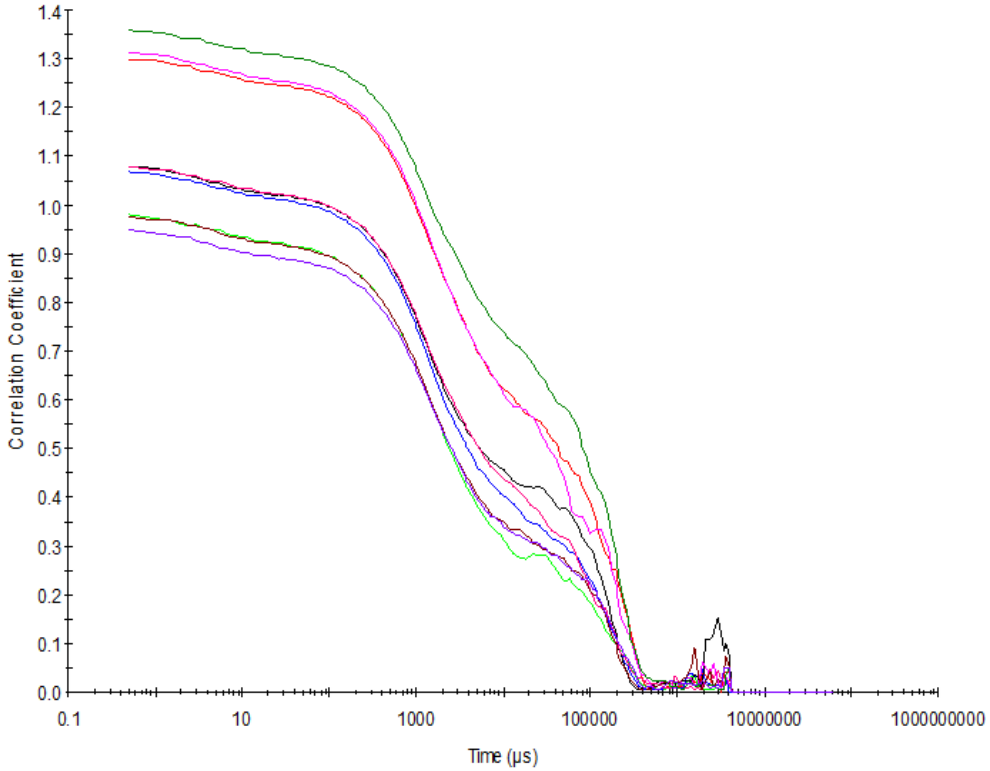

Figure S80 – Raw correlation data for 9 DLS runs at 40 °C with compound **4** at a concentration of 111.12 mM in DMSO.

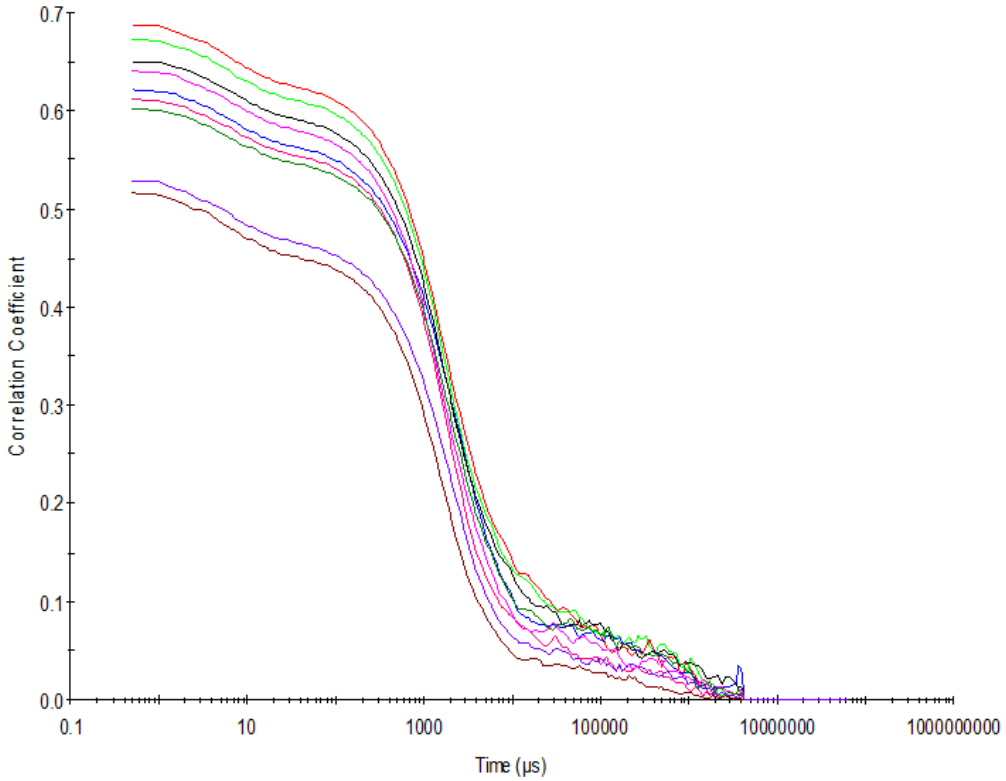

Figure S81 – Raw correlation data for 9 DLS runs at 25 °C after heating to 40 °C with compound **4** at a concentration of 111.12 mM in DMSO.

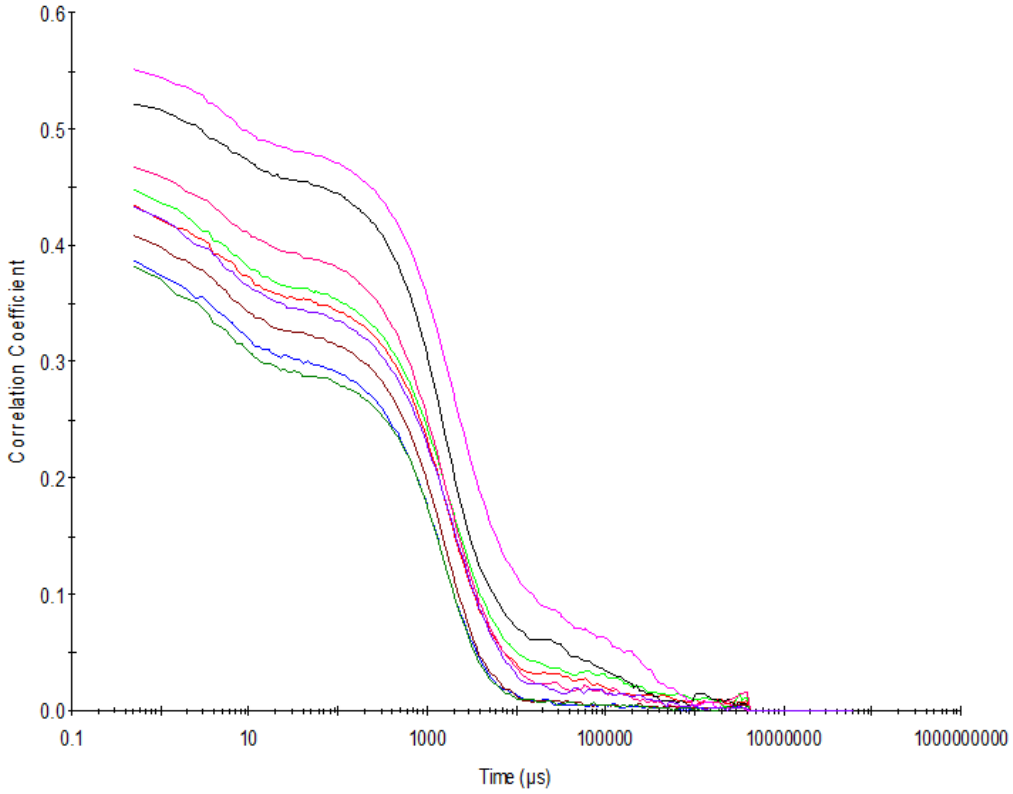

Figure S82 – Raw correlation data for 9 DLS runs at 25 °C before heating to 40 °C with compound **4** at a concentration of 55.56 mM in DMSO.

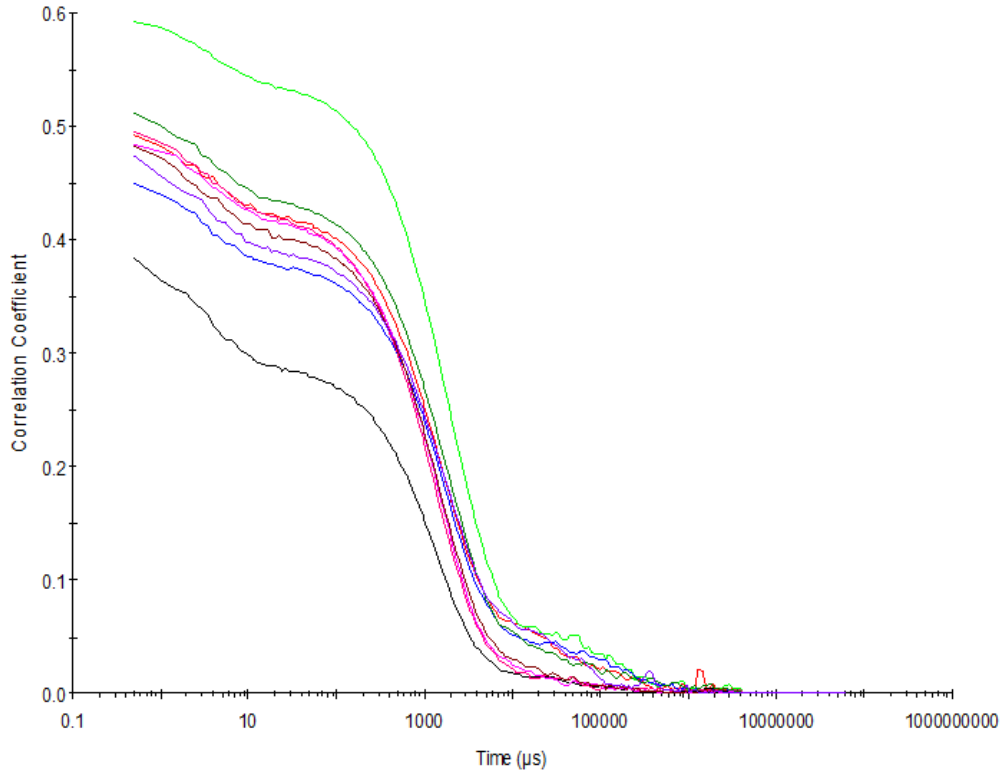

Figure S83– Raw correlation data for 9 DLS runs at 40 °C with compound **4** at a concentration of 55.56 mM in DMSO.

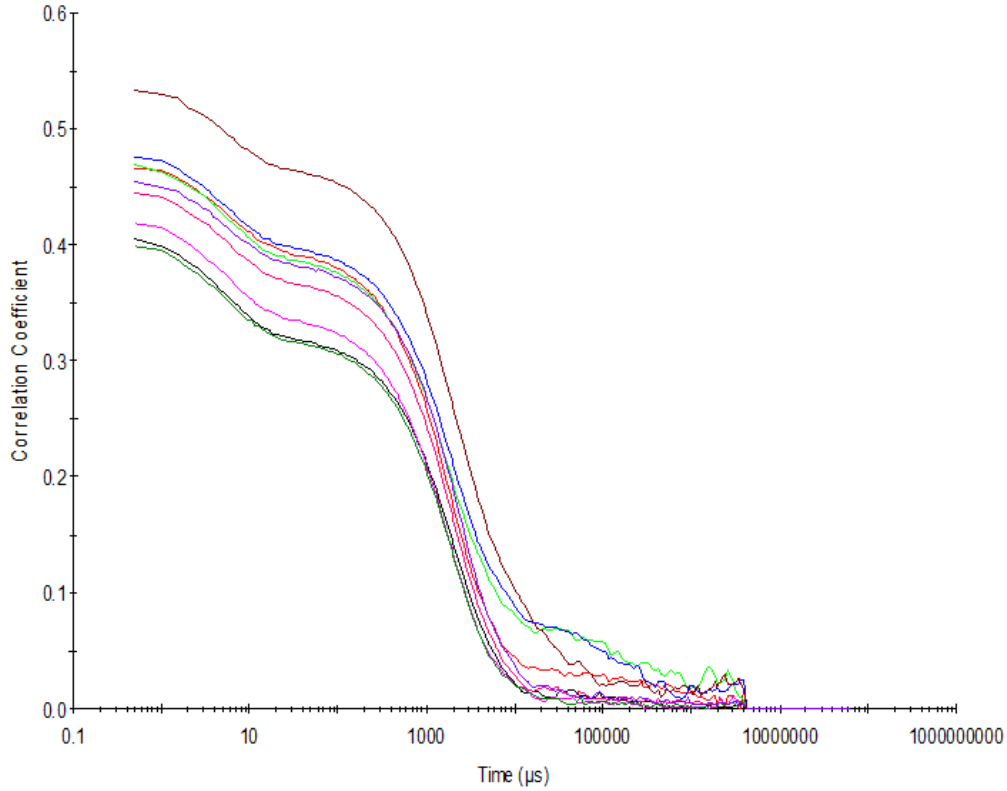

Figure S84 – Raw correlation data for 9 DLS runs at 25 °C after heating to 40 °C with compound **4** at a concentration of 55.56 mM in DMSO.

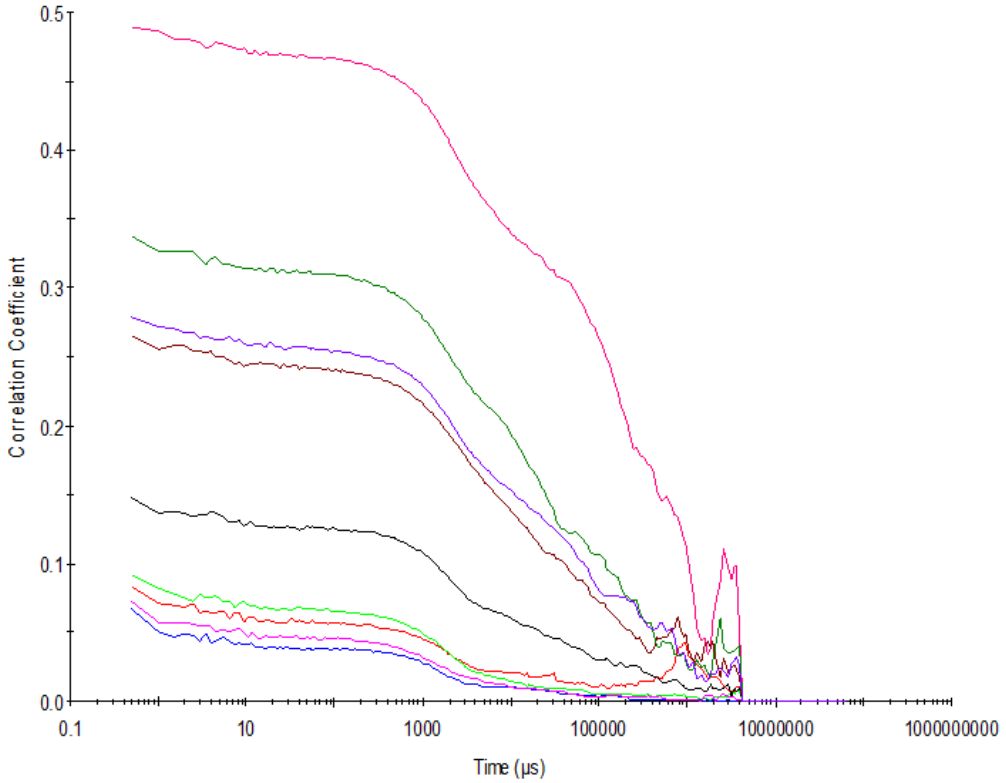

Figure S85 – Raw correlation data for 9 DLS runs at 25 °C before heating to 40 °C with compound **4** at a concentration of 5.56 mM in DMSO.

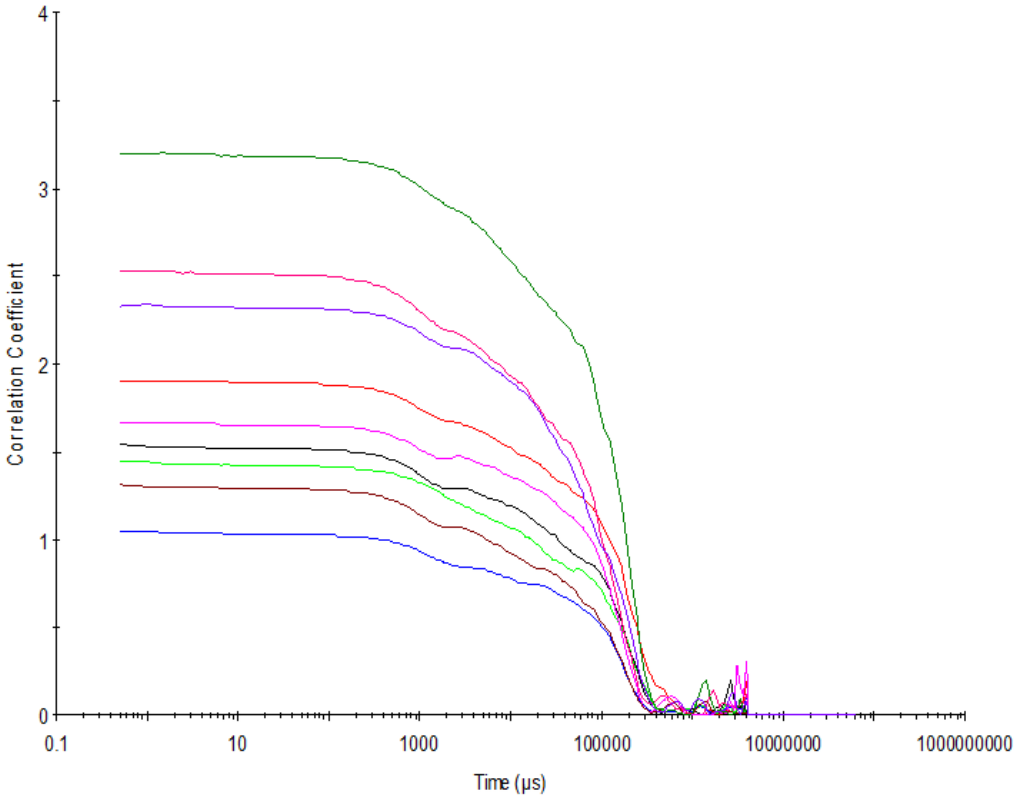

Figure S86 – Raw correlation data for 9 DLS runs at 40 °C with compound **4** at a concentration of 5.56 mM in DMSO.

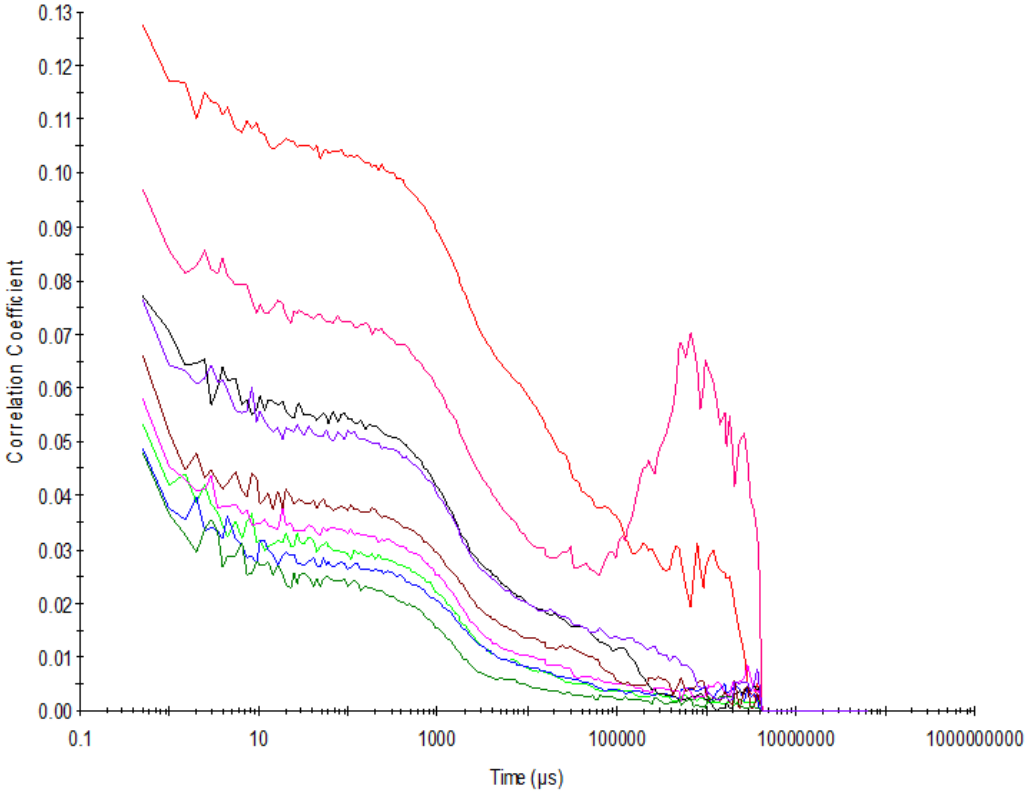

Figure S87 – Raw correlation data for 9 DLS runs at 25 °C after heating to 40 °C with compound **4** at a concentration of 5.56 mM in DMSO.

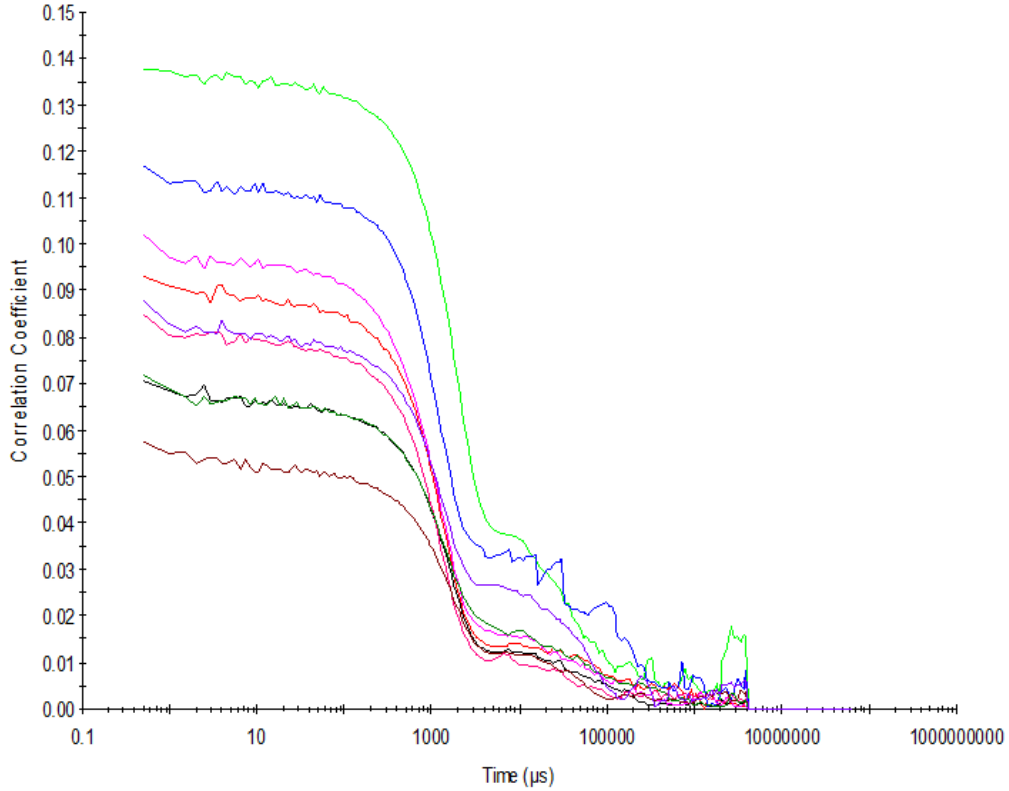

Figure S88 – Raw correlation data for 9 DLS runs at 25 °C before heating to 40 °C with compound **4** at a concentration of 0.56 mM in DMSO.

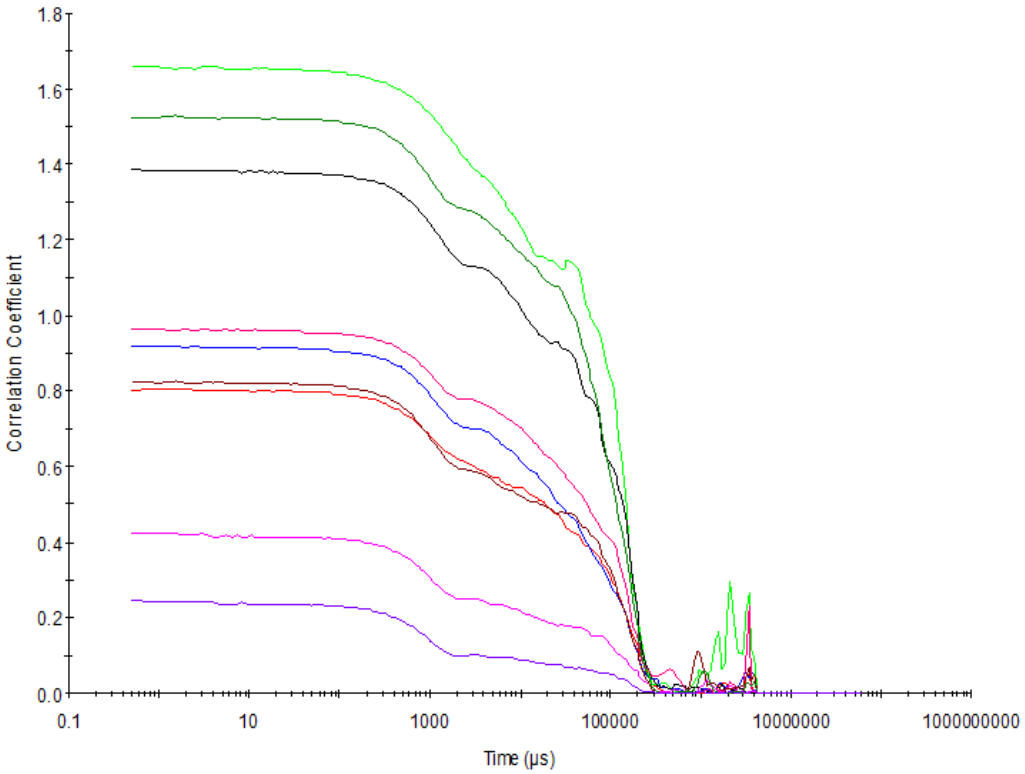

Figure S89 – Raw correlation data for 9 DLS runs at 40 °C with compound **4** at a concentration of 0.56 mM in DMSO.

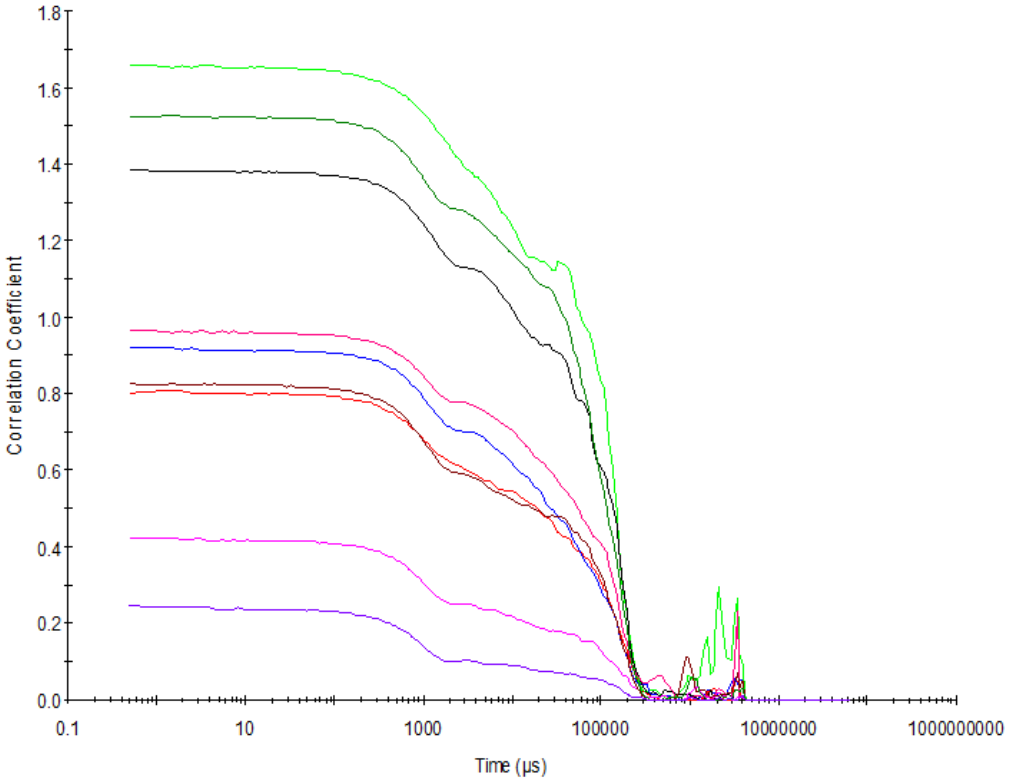

Figure S90 – Raw correlation data for 9 DLS runs at 25 °C after heating to 40 °C with compound **4** at a concentration of 0.56 mM in DMSO.

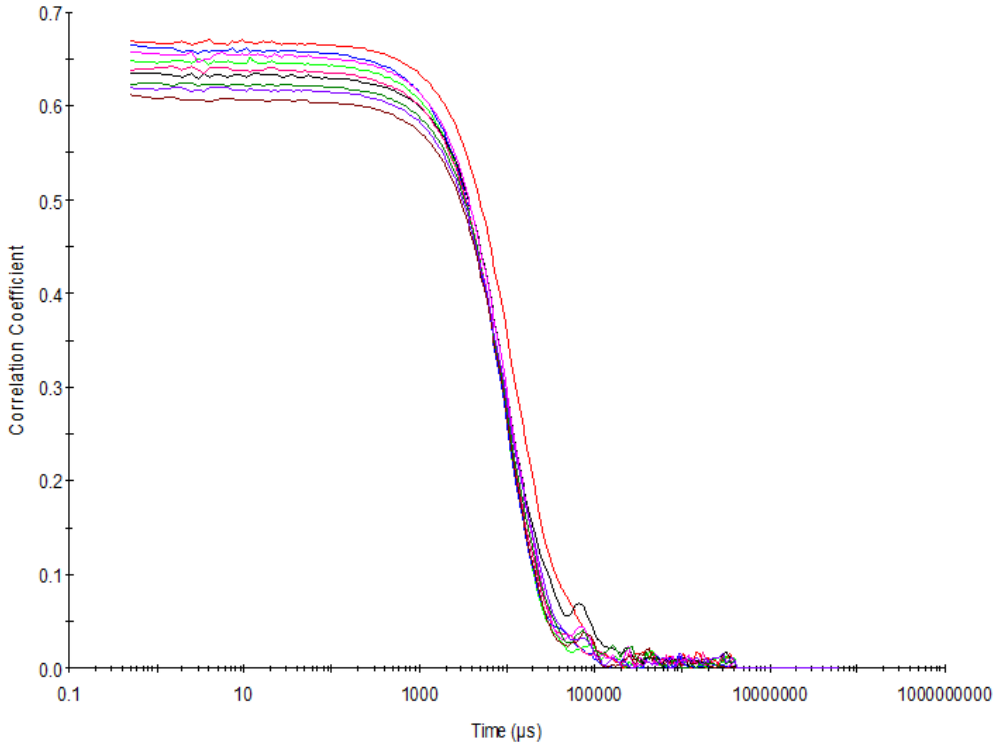

Figure S91 - Raw correlation data for 9 DLS runs at 25 °C after heating to 40 °C with compound **4** at a concentration of 55.56 mM in DMSO: H_2O 1: 1.

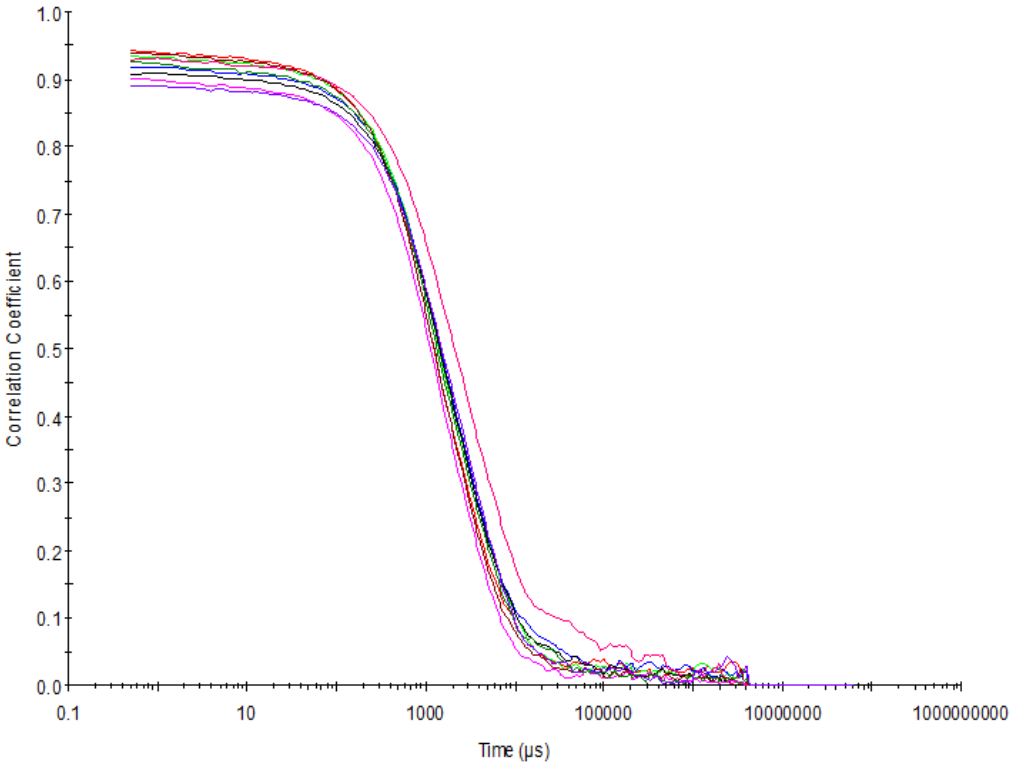

Figure S92 - Raw correlation data for 9 DLS runs at 25 °C after heating to 40 °C with compound **4** at a concentration of 5.56 mM in DMSO: H_2O 1: 1.

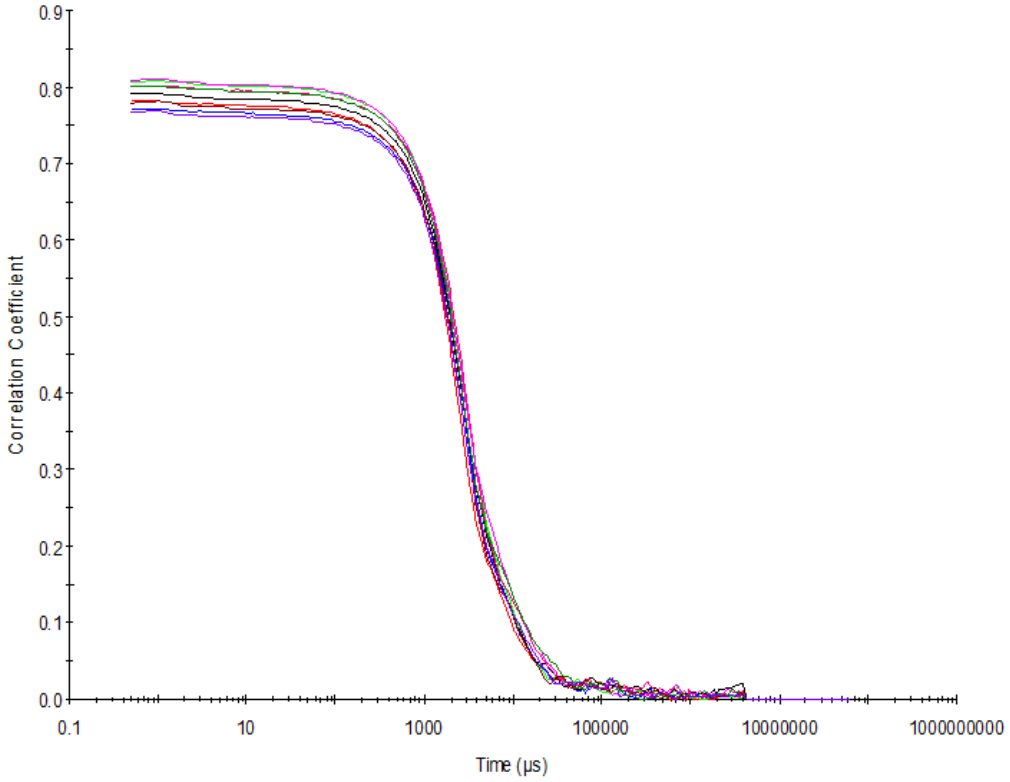

Figure S93 - Raw correlation data for 9 DLS runs at 25 °C after heating to 40 °C with compound **4** at a concentration of 0.56 mM in DMSO: H_2O 1: 1.

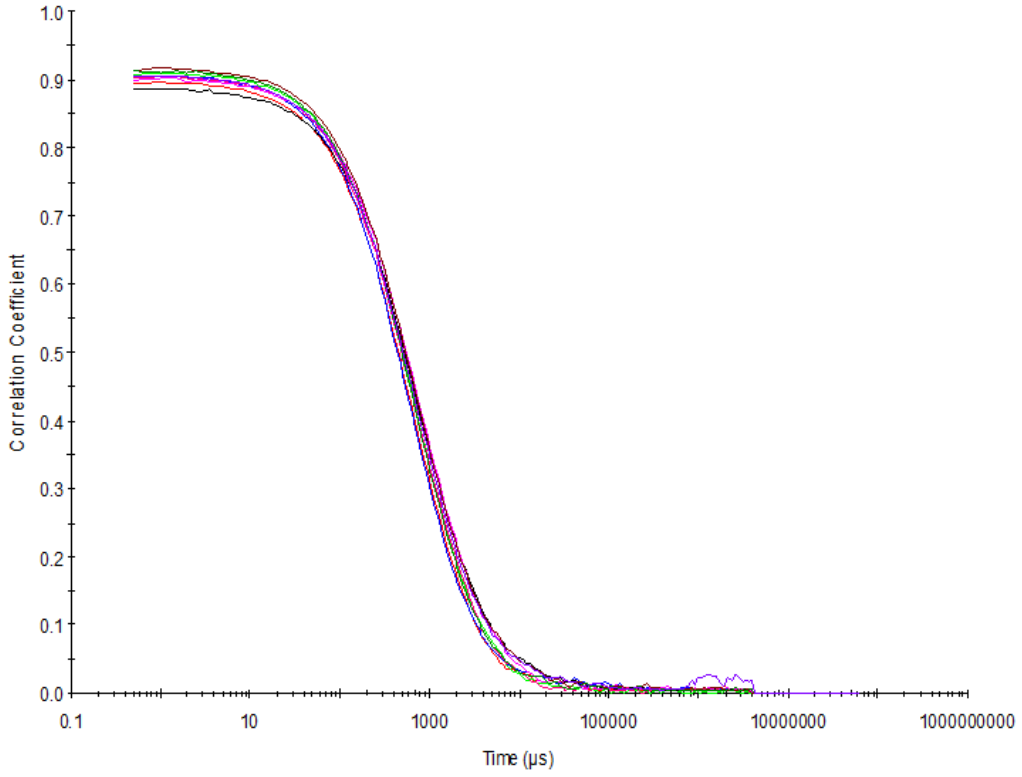

Figure S94 - Raw correlation data for 9 DLS runs at 25 °C after heating to 40 °C with compound **4** at a concentration of 5.56 mM in DMSO: H_2O 3: 7.

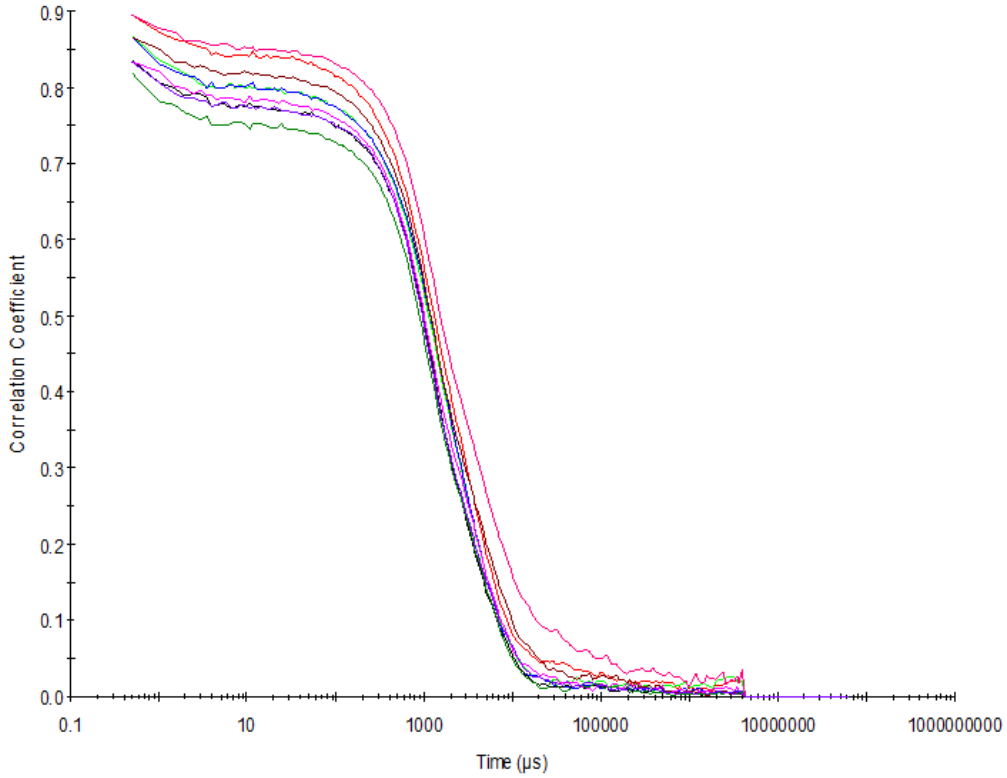

Figure S95 - Raw correlation data for 9 DLS runs at 25 °C after heating to 40 °C with compound **4** at a concentration of 0.56 mM In DMSO: H_2O 3: 7.

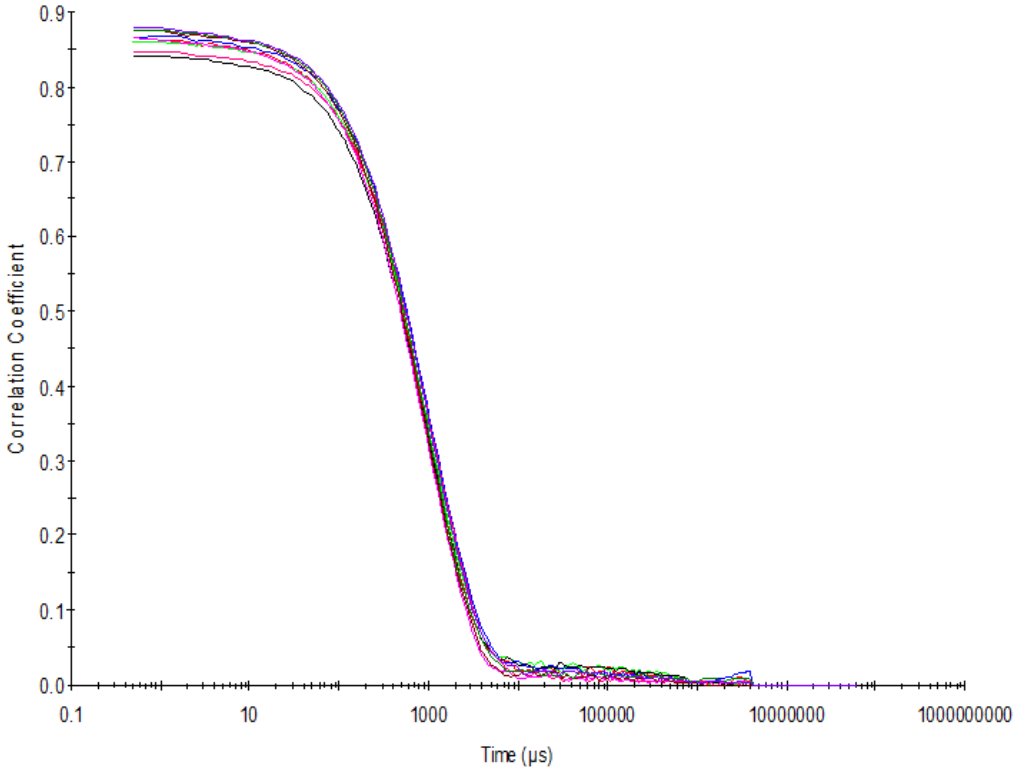

Figure S96 - Raw correlation data for 9 DLS runs at 25 °C after heating to 40 °C with compound **4** at a concentration of 0.56 mM in DMSO: H_2O 1: 4.

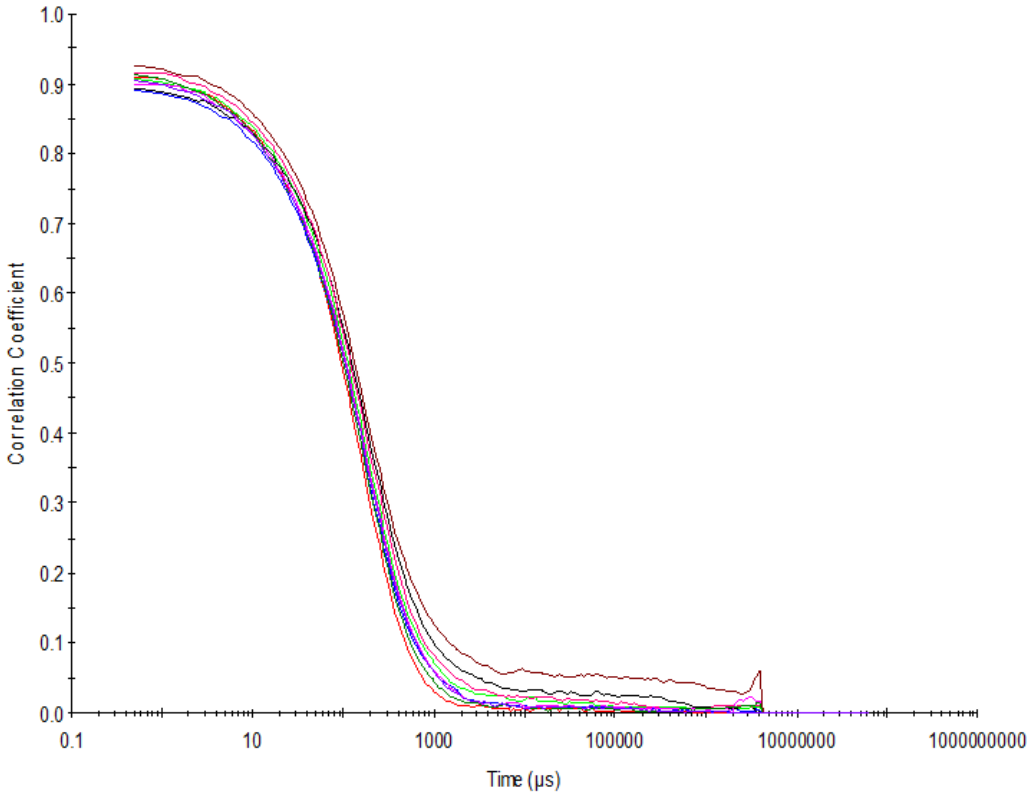

Figure S97 - Raw correlation data for 9 DLS runs at 25 °C after heating to 40 °C with compound **4** at a concentration of 5.56 mM in EtOH: H_2O 1: 19.

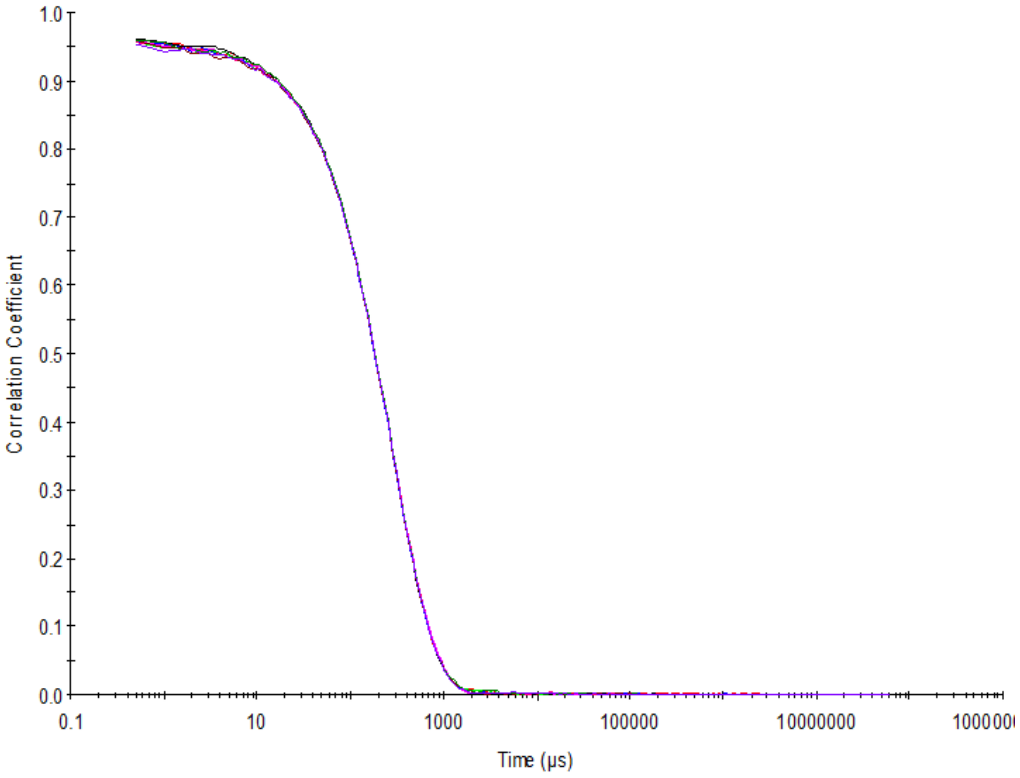

Figure S98 - Raw correlation data for 9 DLS runs at 25 °C after heating to 40 °C with compound **4** at a concentration of 0.56 mM in EtOH: H_2O 1: 19.

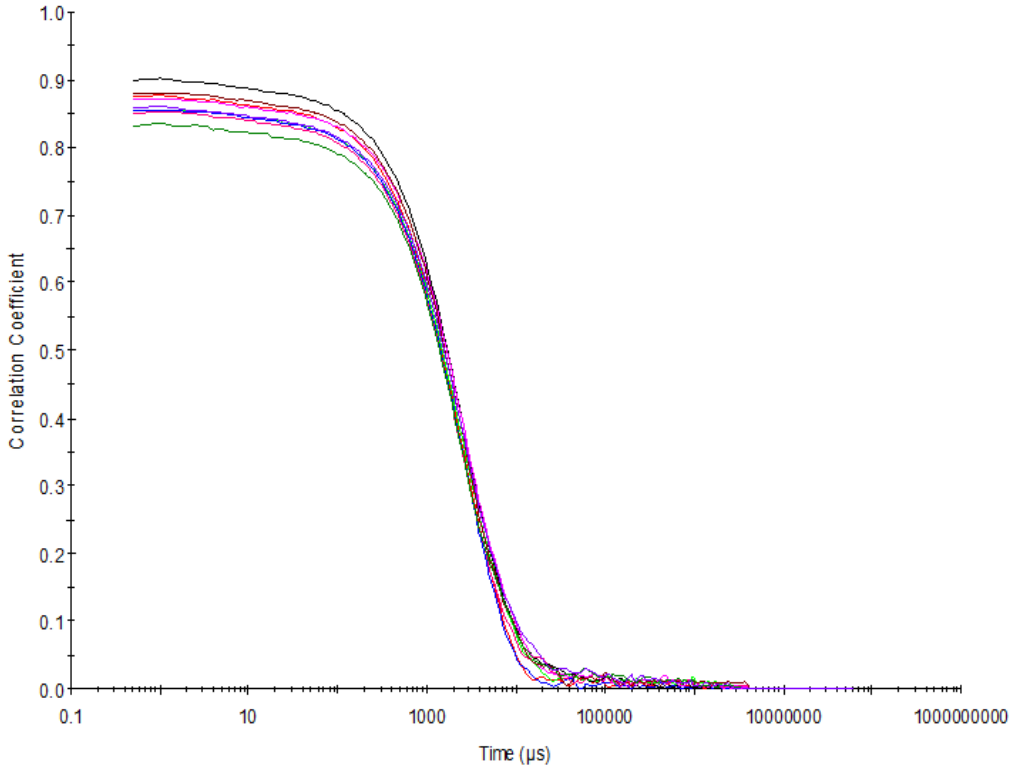

Figure S99 – Raw correlation data for 9 DLS runs at 25 °C before heating to 40 °C with compound **5** at a concentration of 111.12 mM in DMSO.

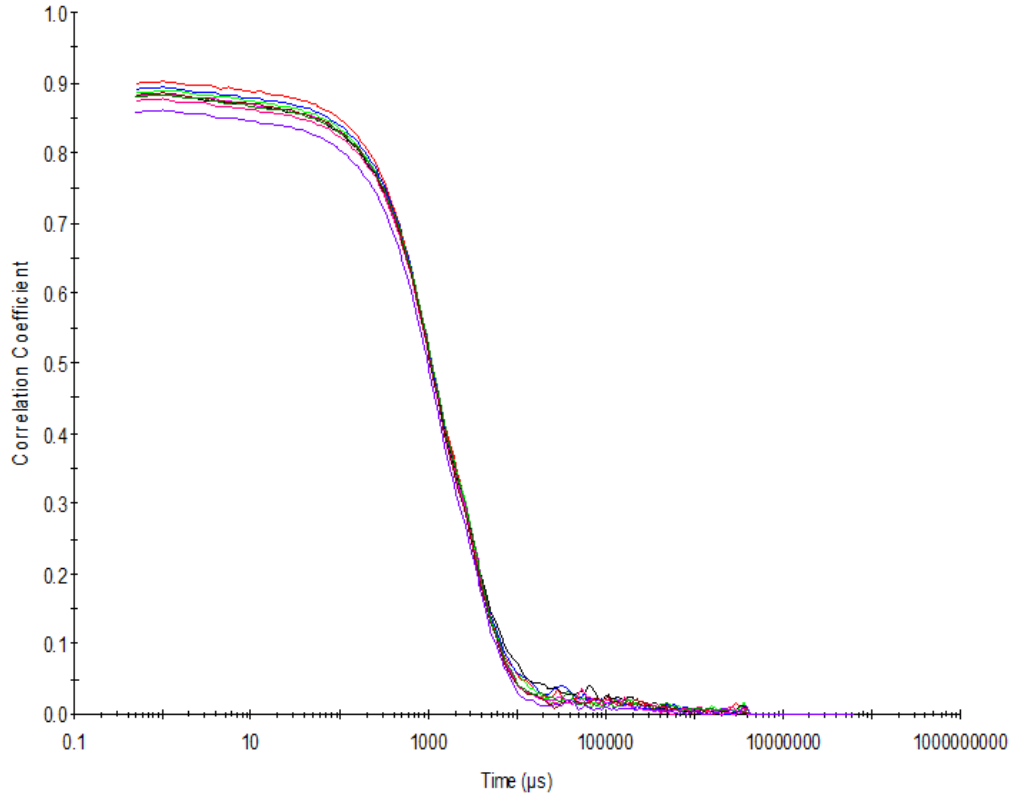

Figure S100 – Raw correlation data for 9 DLS runs at 40 °C with compound **5** at a concentration of 111.12 mM in DMSO.

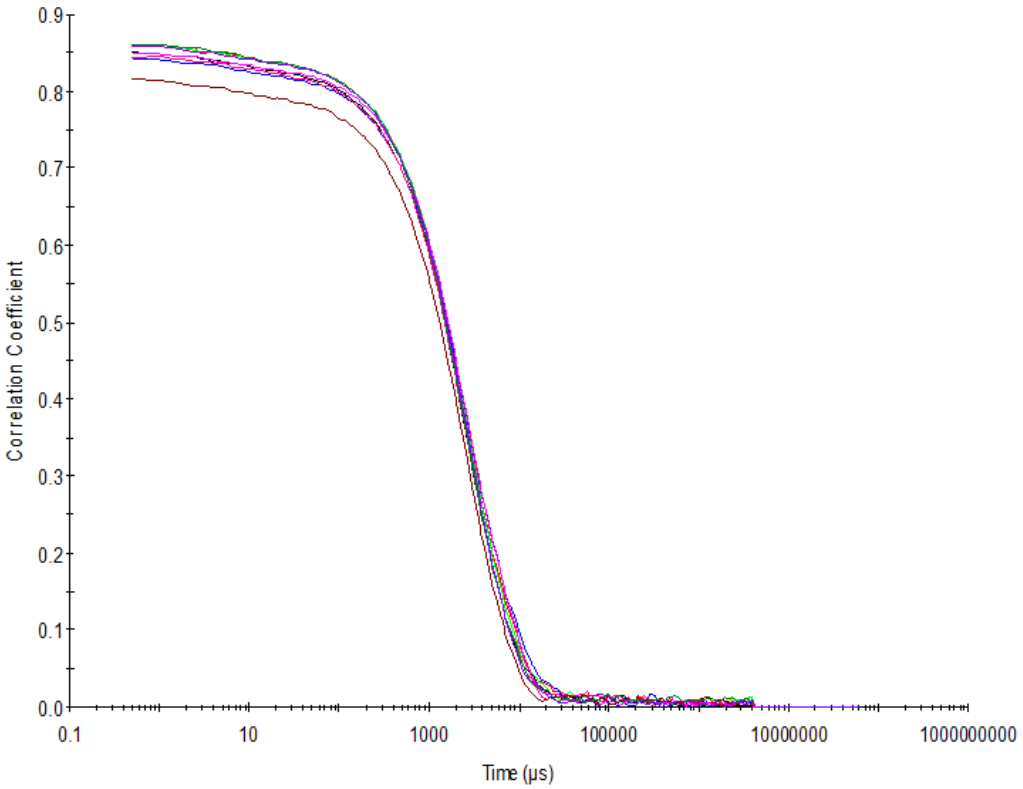

Figure S101 – Raw correlation data for 9 DLS runs at 25 °C after heating to 40 °C with compound **5** at a concentration of 111.12 mM in DMSO.

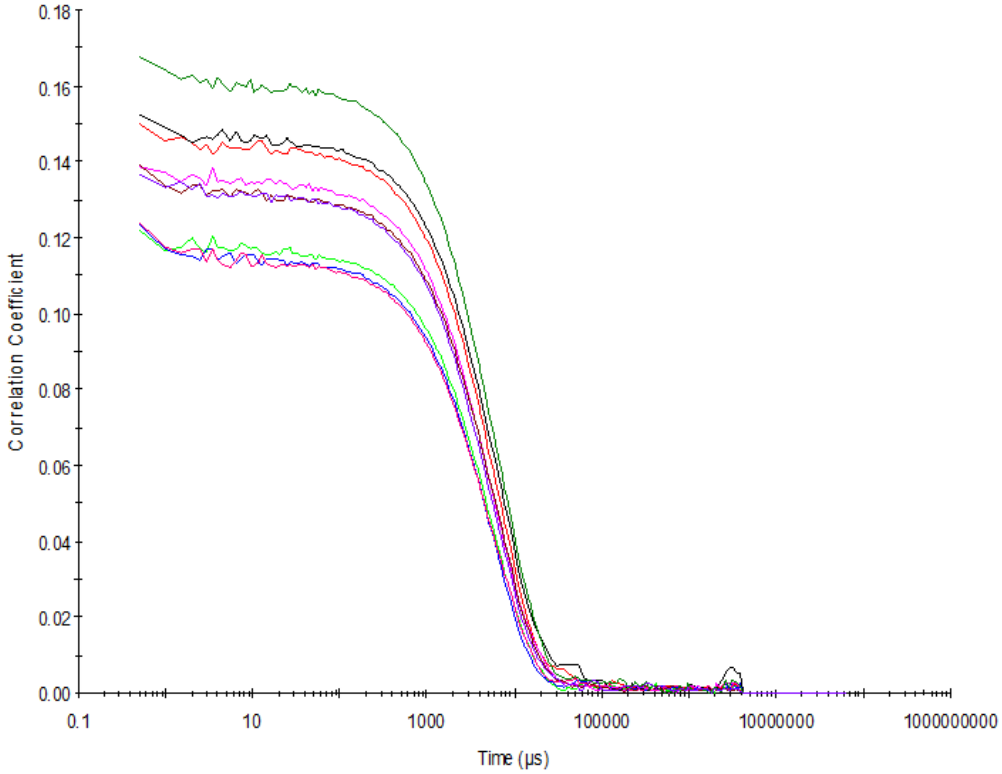

Figure S102 – Raw correlation data for 9 DLS runs at 25 °C before heating to 40 °C with compound **5** at a concentration of 55.56 mM in DMSO.

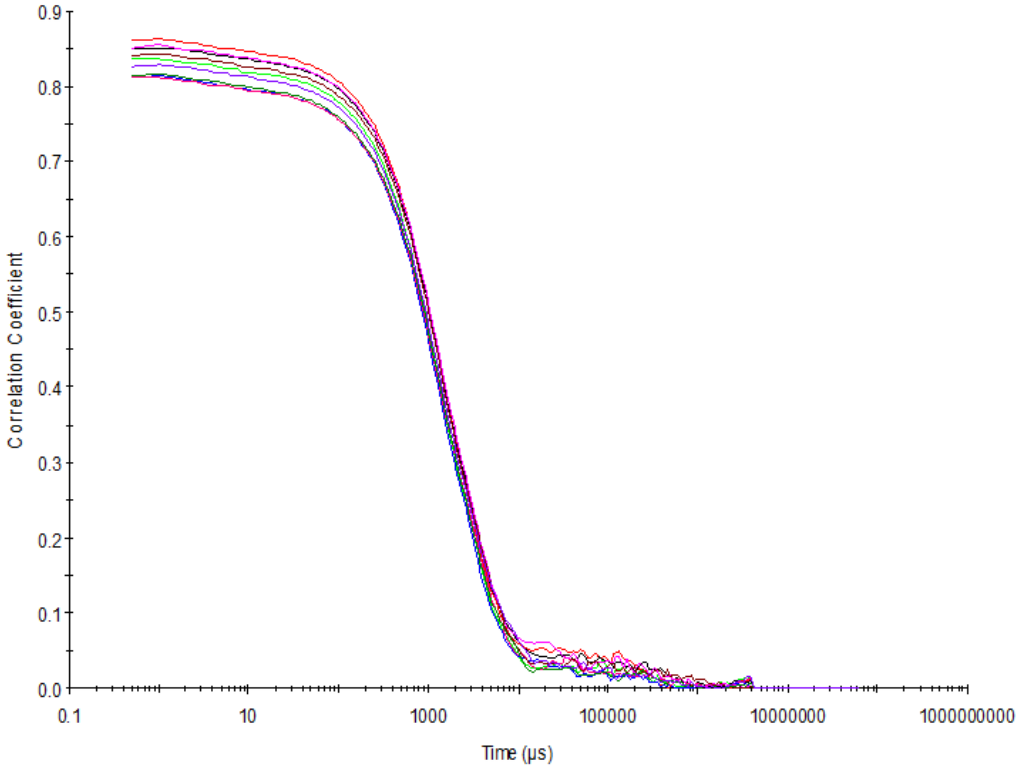

Figure S103 – Raw correlation data for 9 DLS runs at 40 °C with compound **5** at a concentration of 55.56 mM in DMSO.

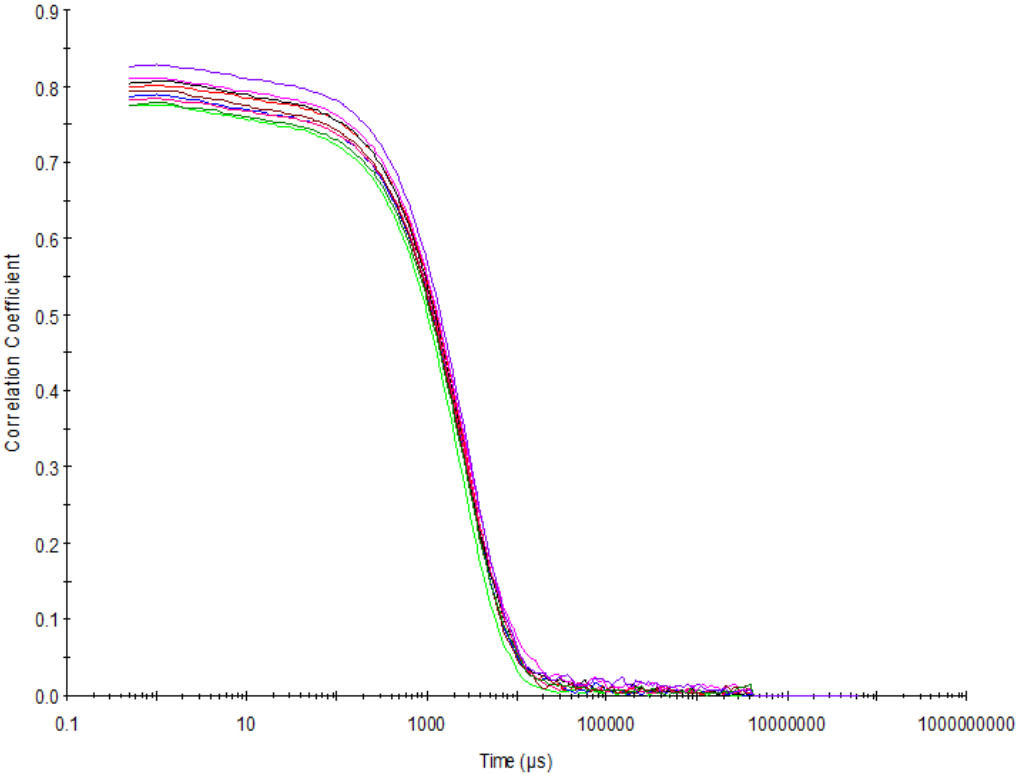

Figure S104 – Raw correlation data for 9 DLS runs at 25 °C after heating to 40 °C with compound **5** at a concentration of 55.56 mM in DMSO.

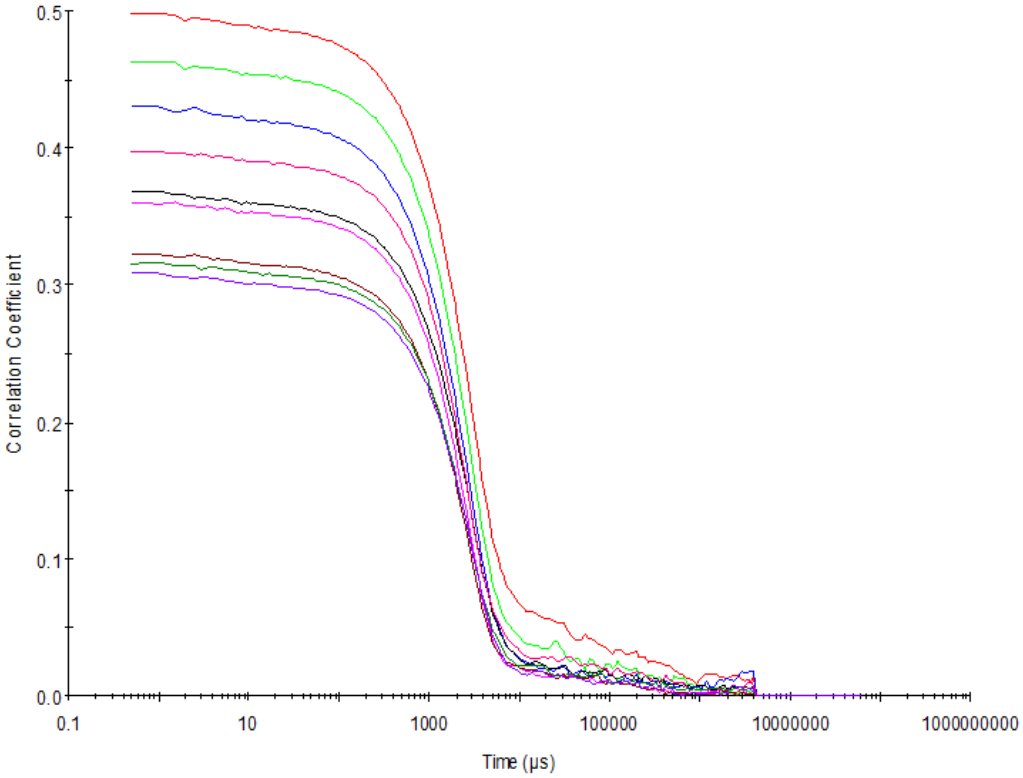

Figure S105 – Raw correlation data for 9 DLS runs at 25 °C before heating to 40 °C with compound **5** at a concentration of 5.56 mM in DMSO.

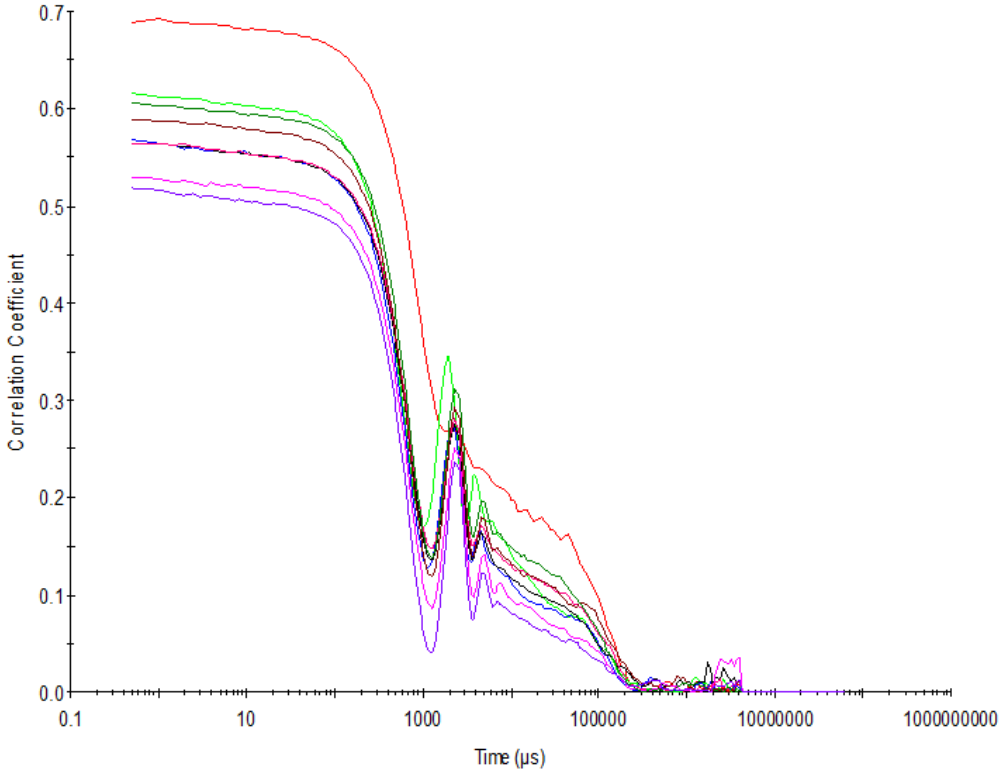

Figure S106 – Raw correlation data for 9 DLS runs at 40 °C with compound **5** at a concentration of 5.56 mM in DMSO.

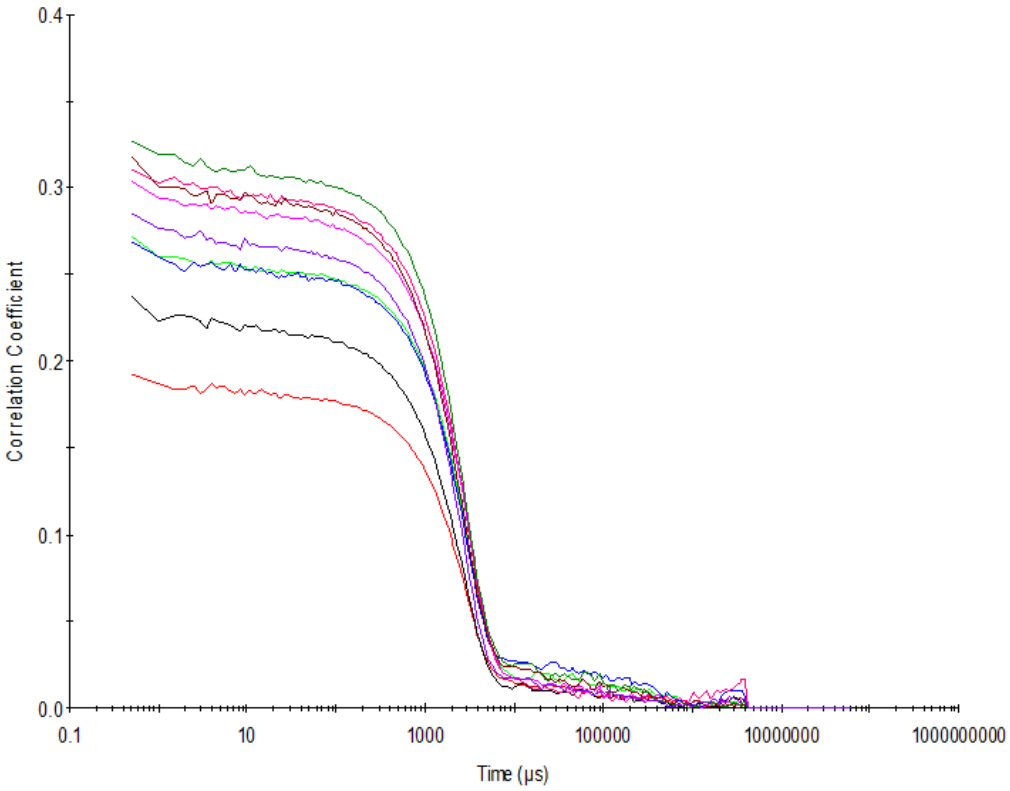

Figure S107 – Raw correlation data for 9 DLS runs at 25 °C after heating to 40 °C with compound **5** at a concentration of 5.56 mM in DMSO.

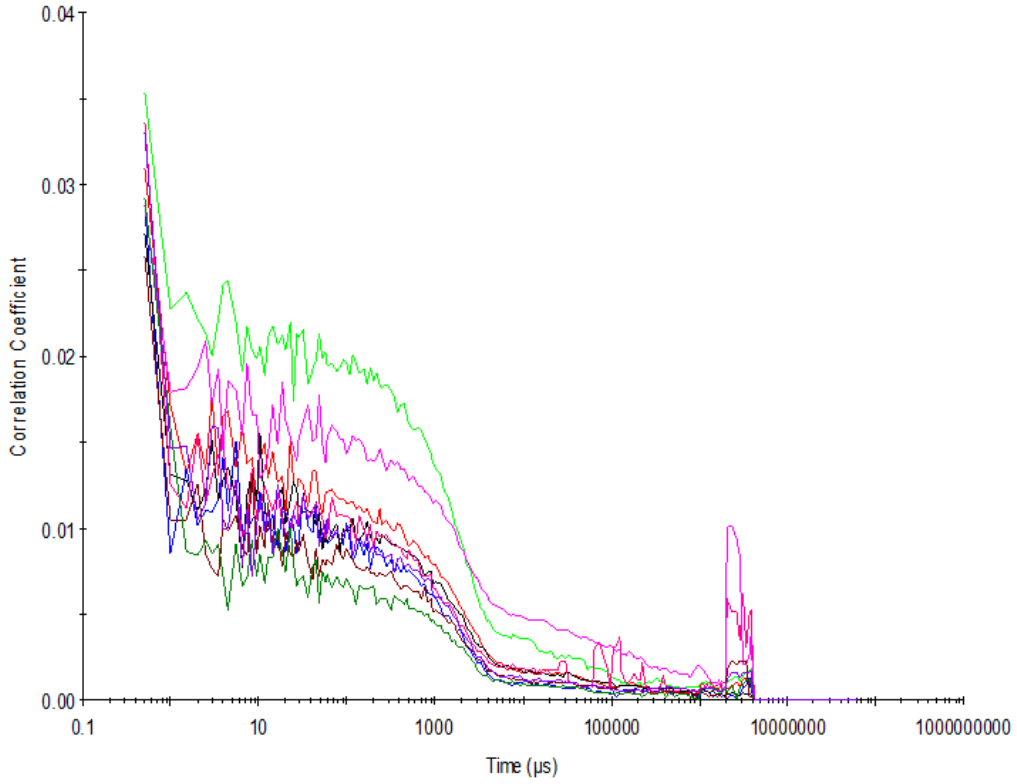

Figure S108 – Raw correlation data for 9 DLS runs at 25 °C before heating to 40 °C with compound **5** at a concentration of 0.56 mM in DMSO.

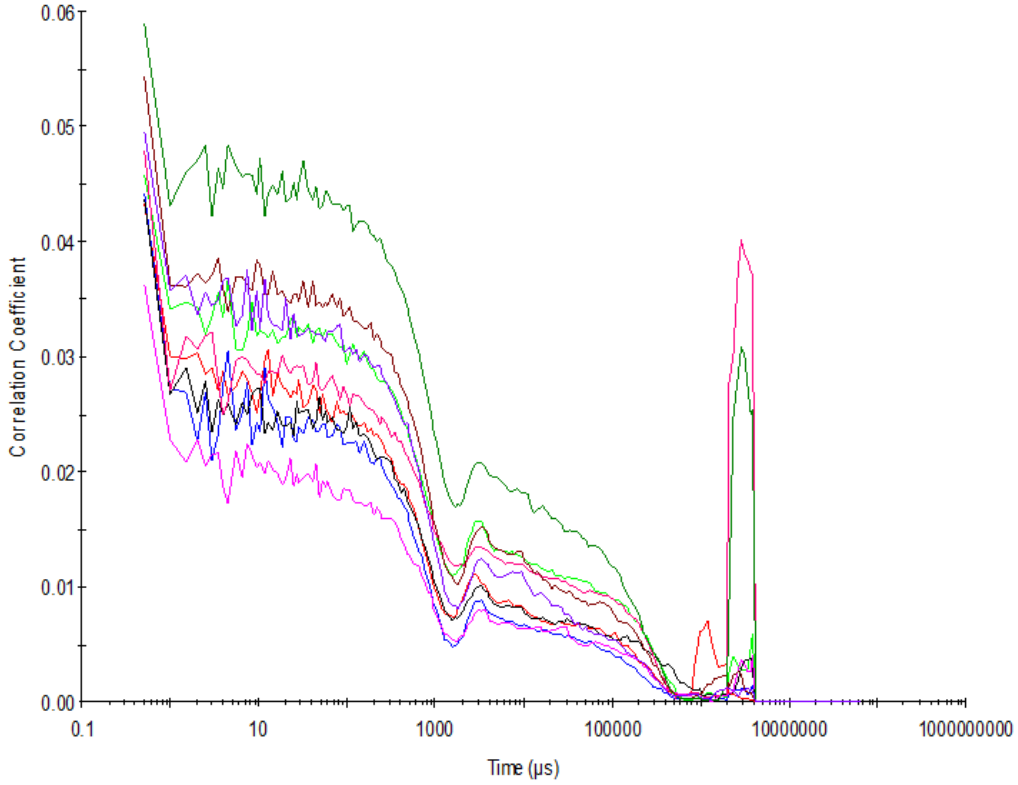

Figure S109 – Raw correlation data for 9 DLS runs at 40 °C with compound **5** at a concentration of 0.56 mM in DMSO.

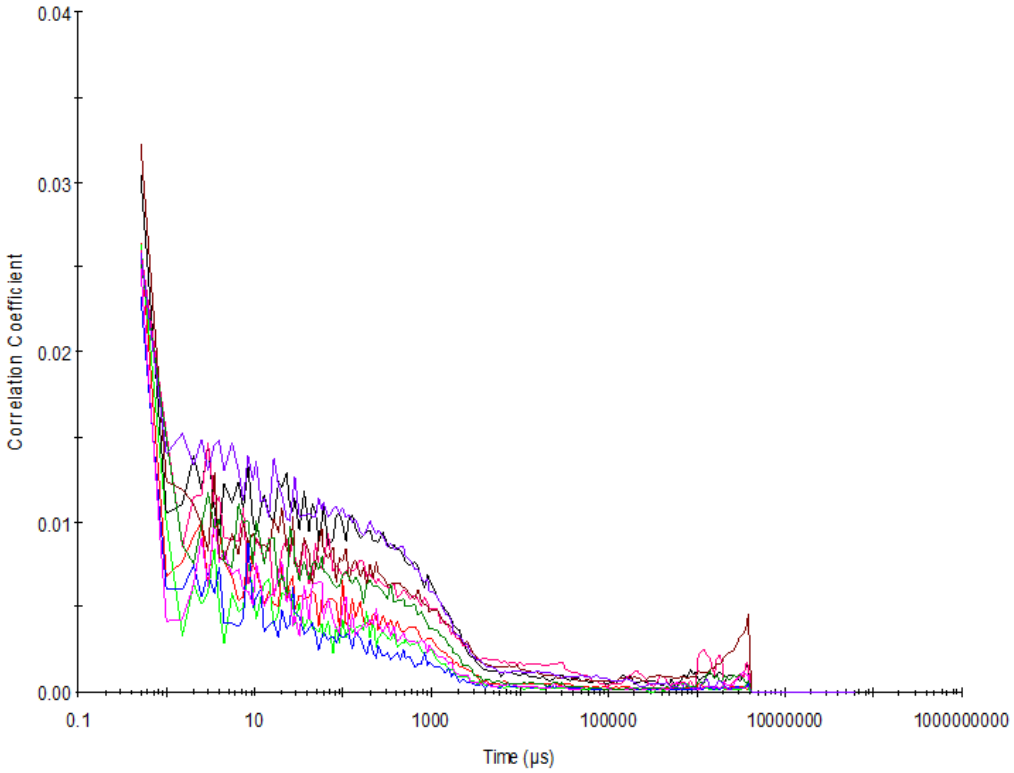

Figure S110 – Raw correlation data for 9 DLS runs at 25 °C after heating to 40 °C with compound **5** at a concentration of 0.56 mM in DMSO.

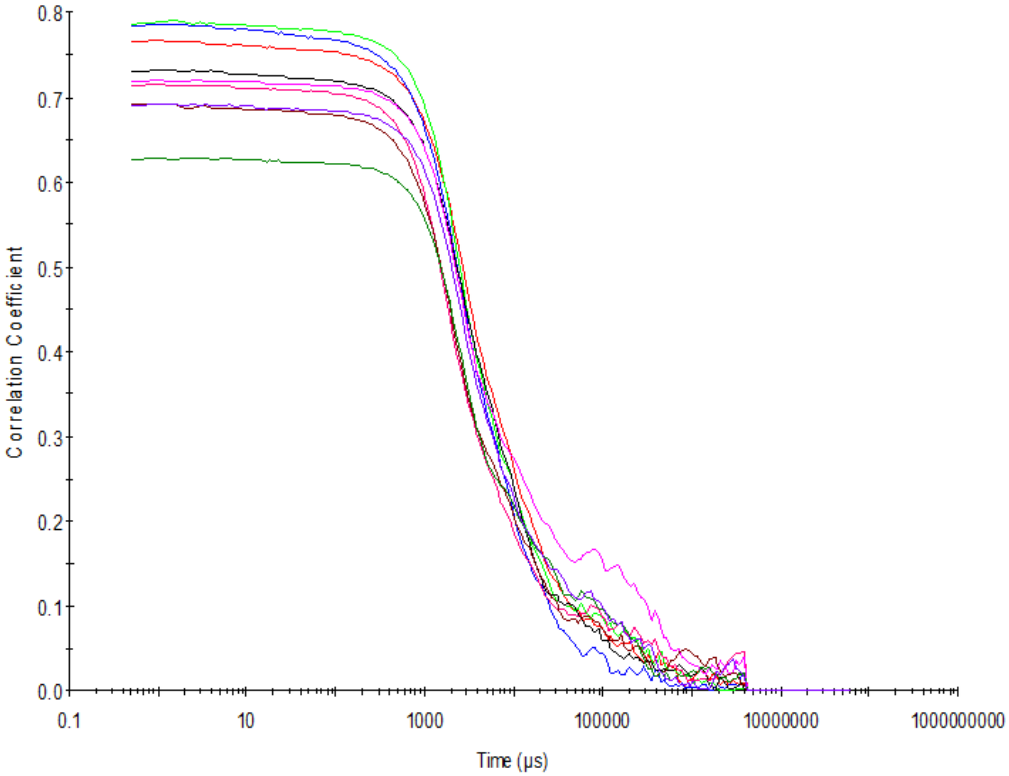

Figure S111 - Raw correlation data for 9 DLS runs at 25 °C after heating to 40 °C with compound **5** at a concentration of 55.56 mM in DMSO: H_2O 1: 1.

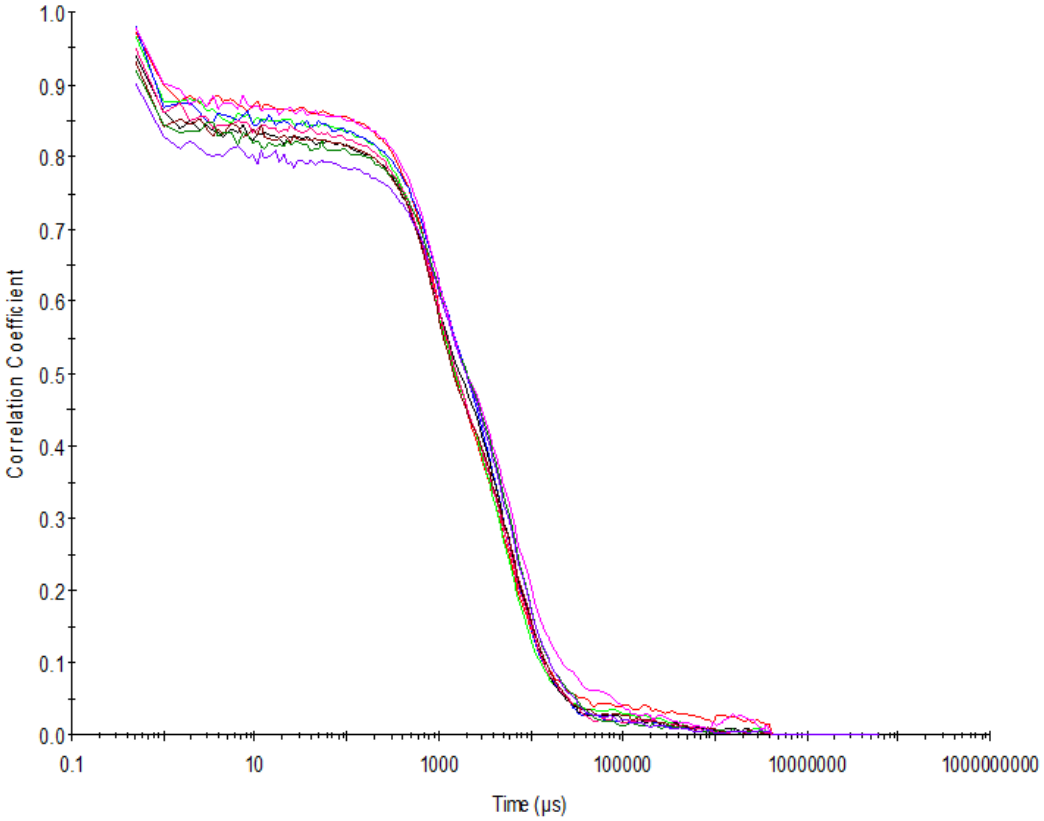

Figure S112 - Raw correlation data for 9 DLS runs at 25 °C after heating to 40 °C with compound **5** at a concentration of 5.56 mM in DMSO: H_2O 1: 1.

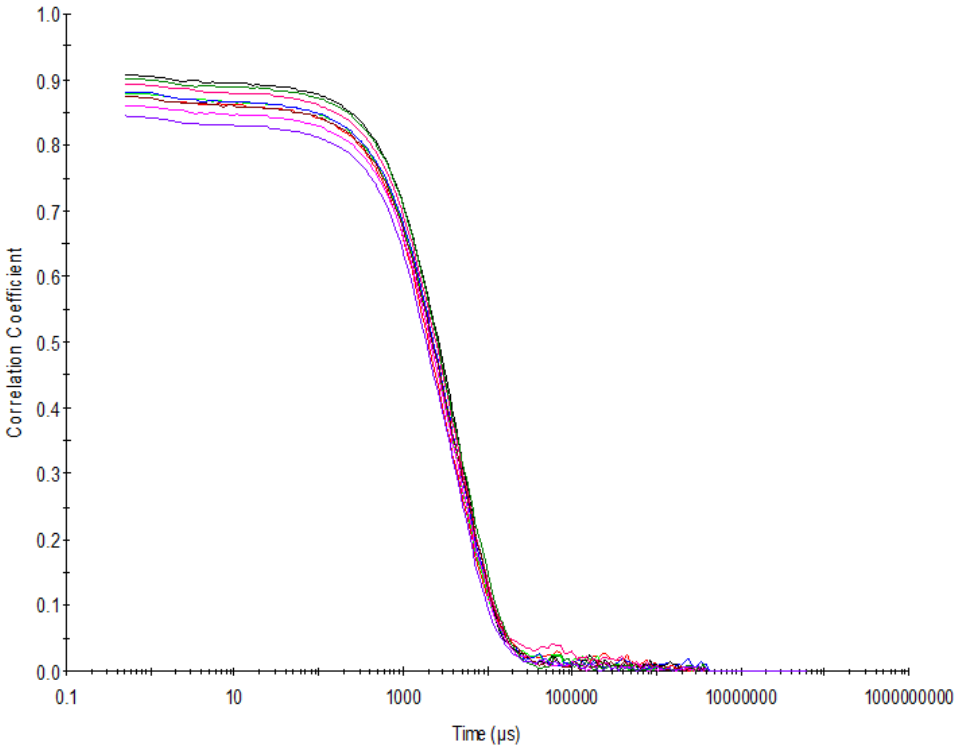

Figure S113 - Raw correlation data for 9 DLS runs at 25 °C after heating to 40 °C with compound **5** at a concentration of 0.56 mM in DMSO: H_2O 1: 1.

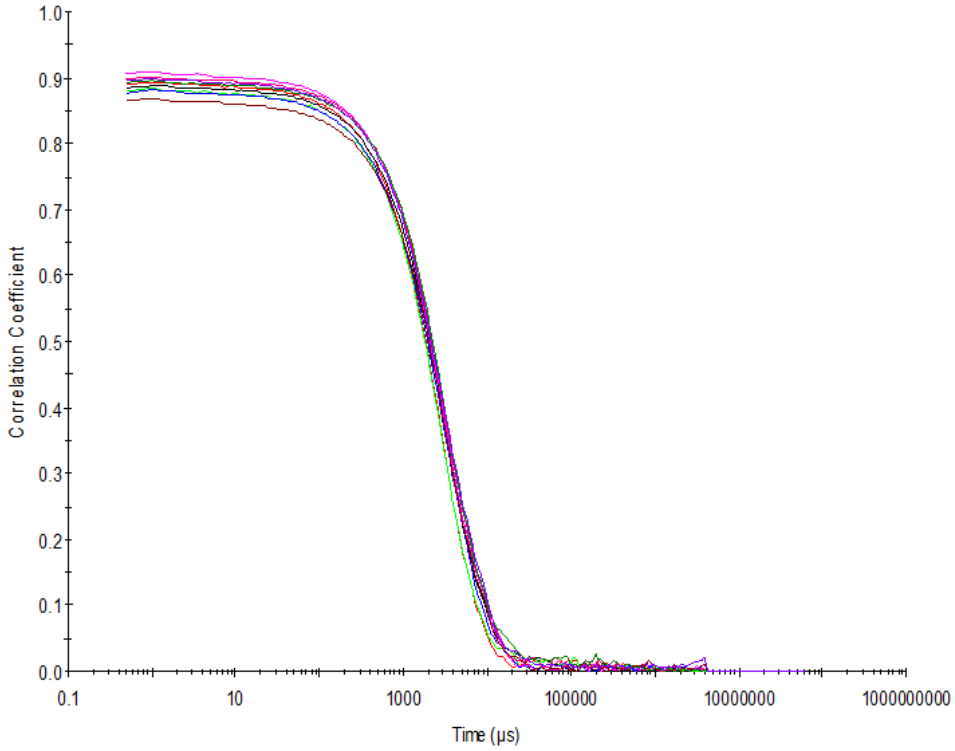

Figure S114 - Raw correlation data for 9 DLS runs at 25 °C after heating to 40 °C with compound **5** at a concentration of 5.56 mM in DMSO: H_2O 3: 7.

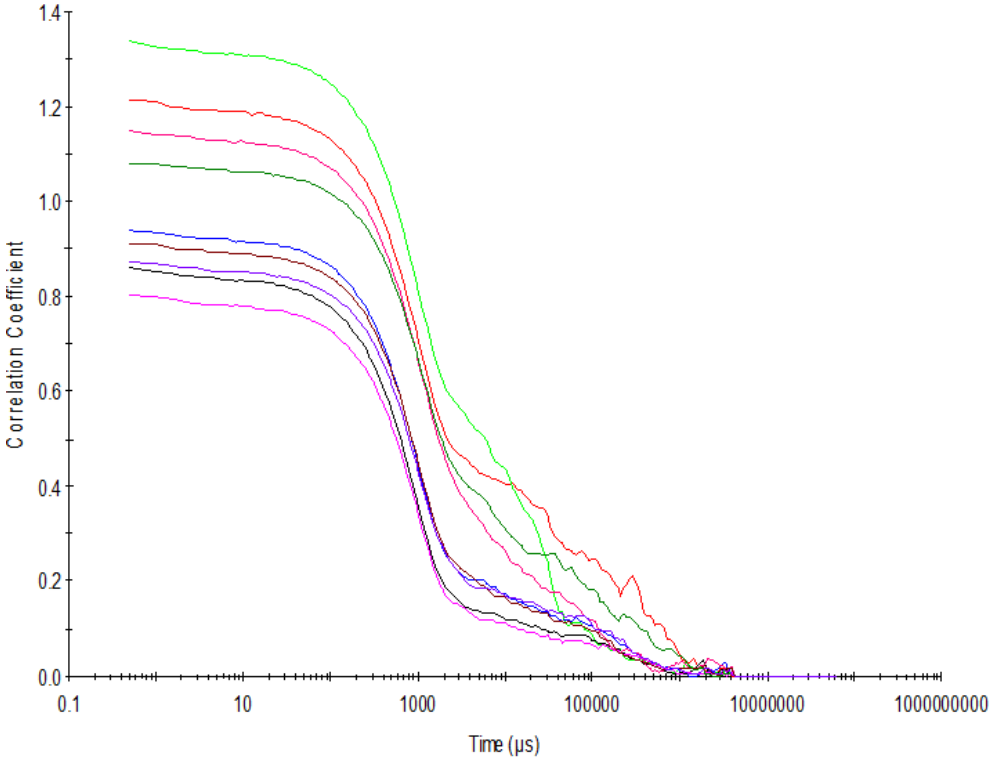

Figure S115 - Raw correlation data for 9 DLS runs at 25 °C after heating to 40 °C with compound **5** at a concentration of 0.56 mM in DMSO: H_2O 3: 7.

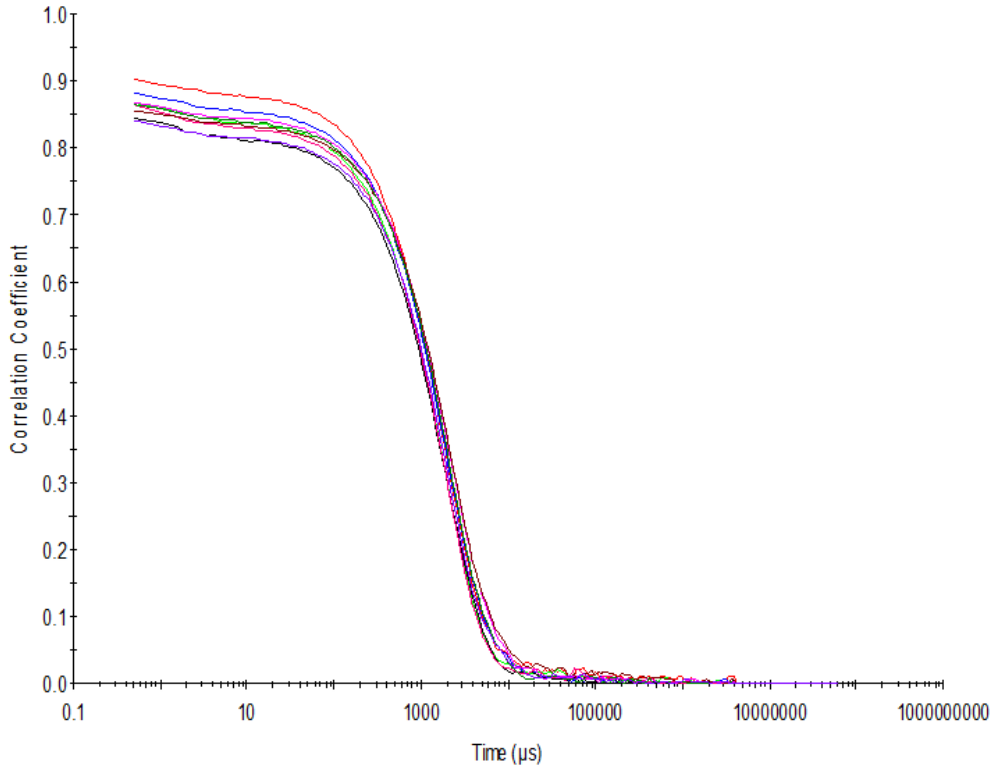

Figure S116 - Raw correlation data for 9 DLS runs at 25 °C after heating to 40 °C with compound **5** at a concentration of 0.56 mM in DMSO: H_2O 1: 4.

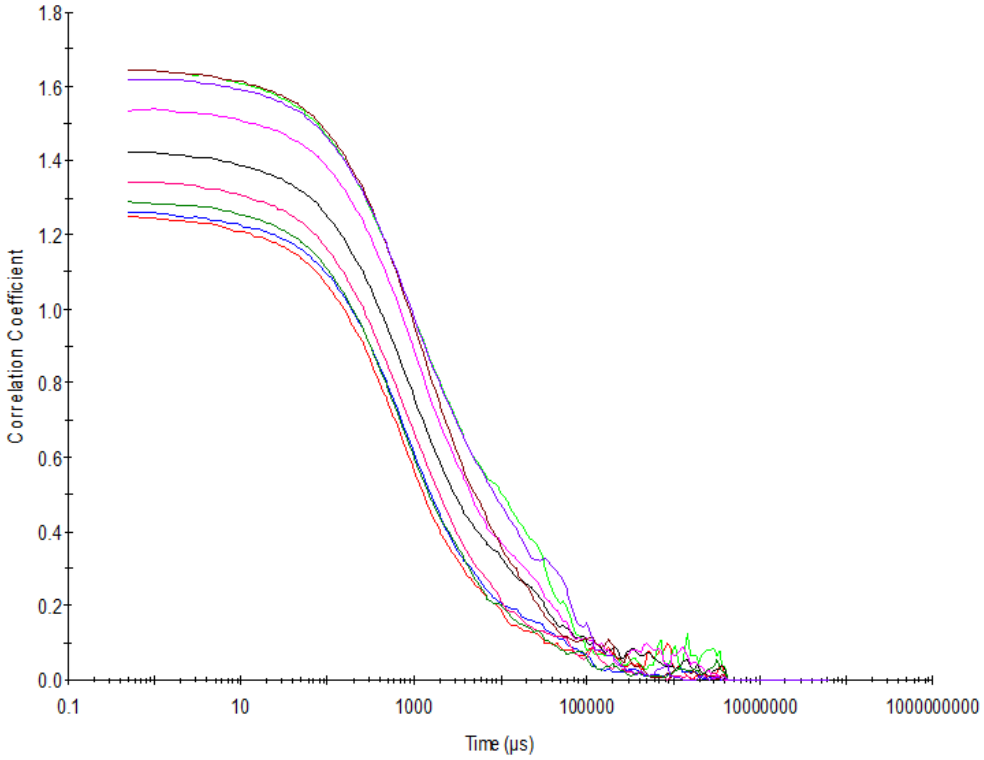

Figure S117 - Raw correlation data for 9 DLS runs at 25 °C after heating to 40 °C with compound **5** at a concentration of 5.56 mM in EtOH: H_2O 1: 19.

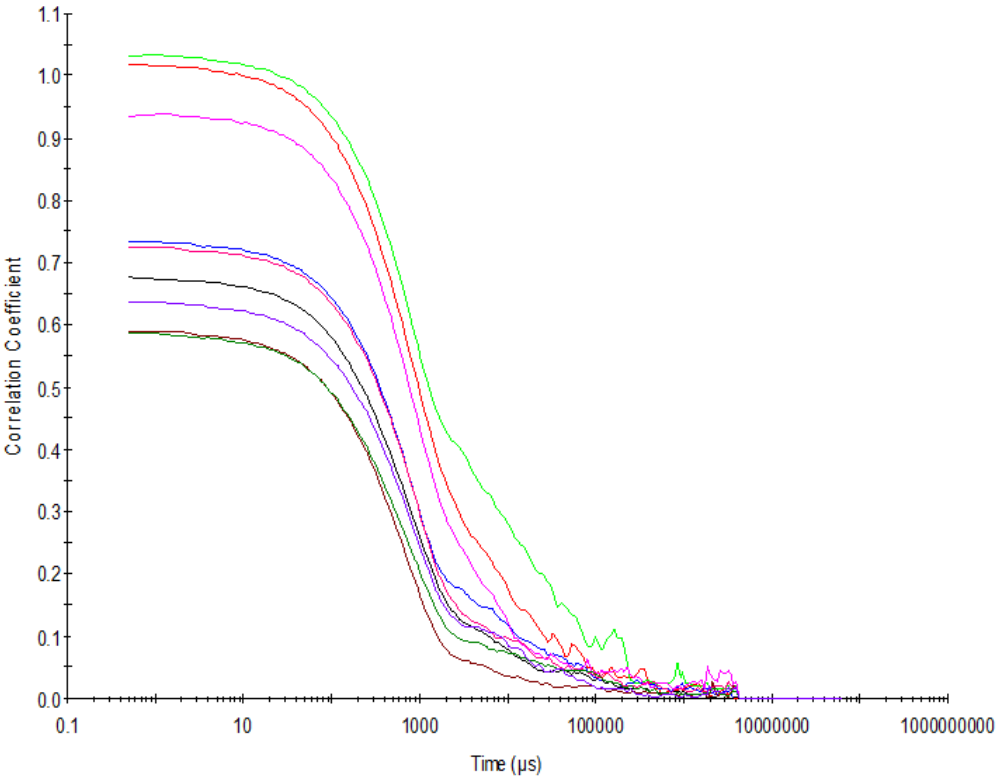

Figure S118 - Raw correlation data for 9 DLS runs at 25 °C after heating to 40 °C with compound **5** at a concentration of 0.56 mM in EtOH: H_2O 1: 19.

Size distribution calculated by DLS

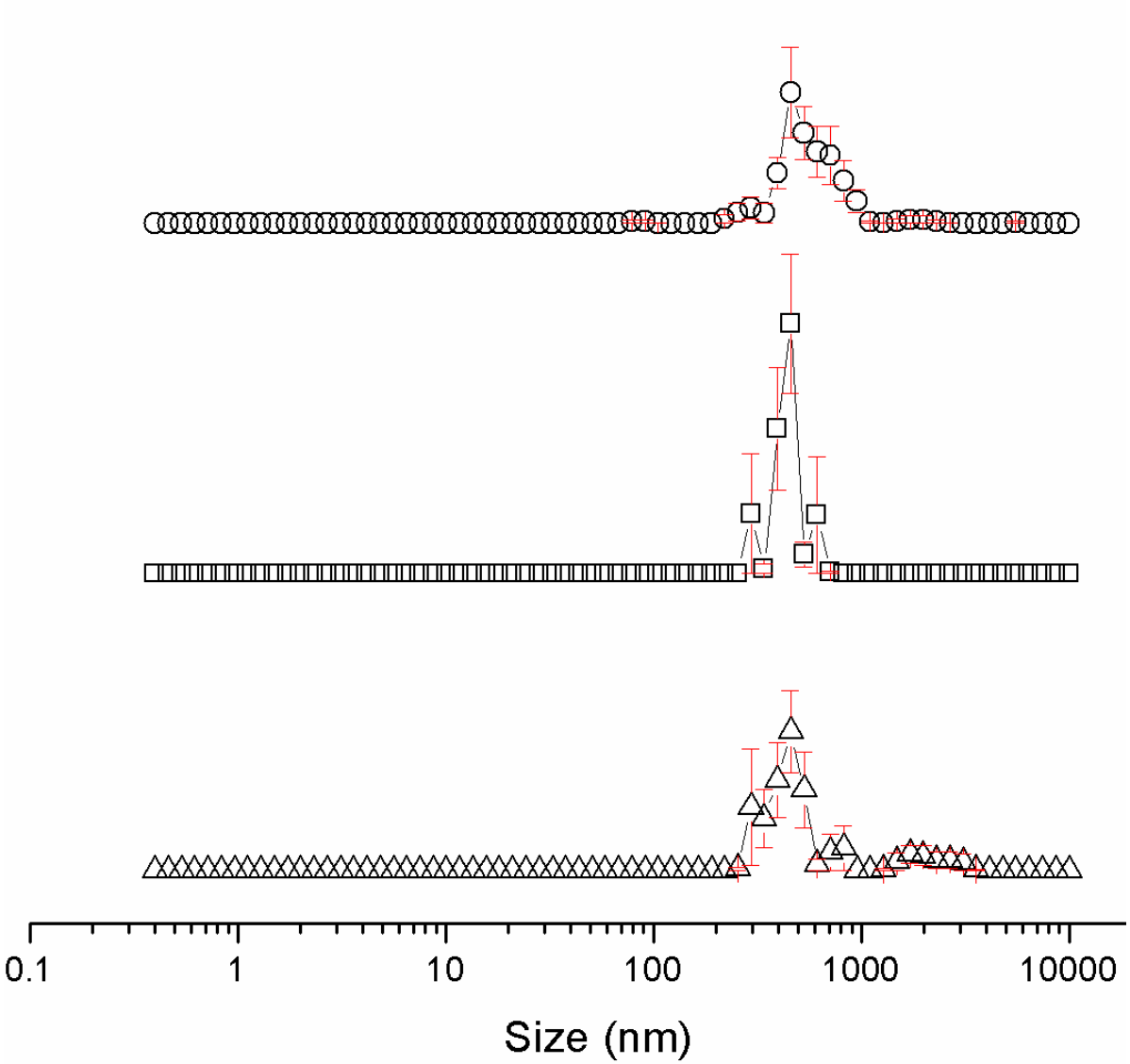

Figure S119 - Average intensity particle size distribution, calculated from 9 DLS runs, of aggregates formed by dissolving compound **1** at a concentration of 111.12 mM in DMSO at Δ) 25 °C, □) heating to 40 °C and ○) cooling to 25 °C. Only 9 of the available 10 DLS runs were used as in some cases, due to the heating and cooling processes there were some obvious temperature equilibration issues for the first run.

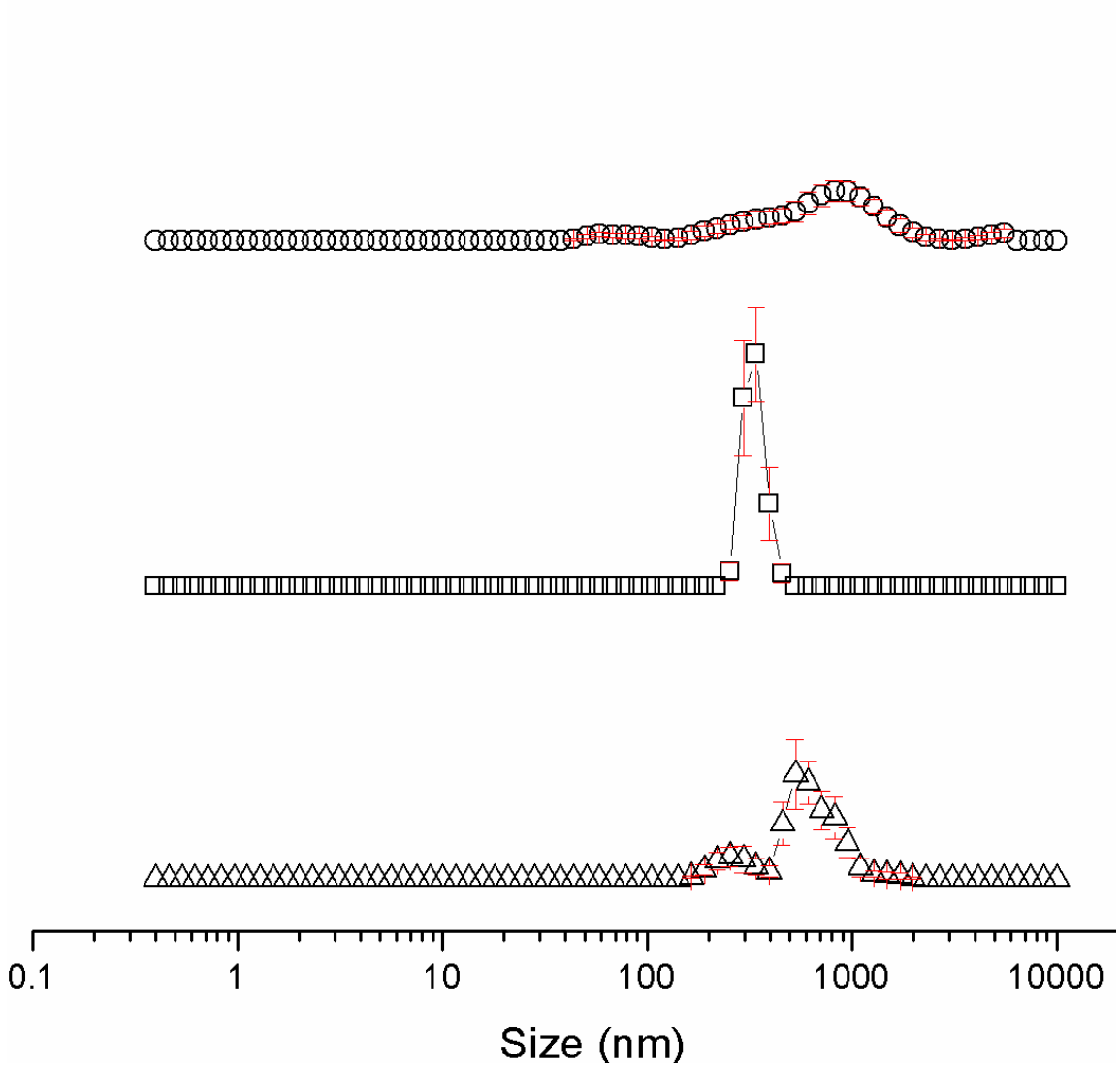

Figure S120 - Average intensity particle size distribution, calculated from 9 DLS runs, of aggregates formed by dissolving compound **1** at a concentration of 55.56 mM in DMSO at Δ) 25 ^{o}C, □) heating to 40 ^{o}C and ○) cooling to 25 ^{o}C. Only 9 of the available 10 DLS runs were used as in some cases, due to the heating and cooling processes there were some obvious temperature equilibration issues for the first run.

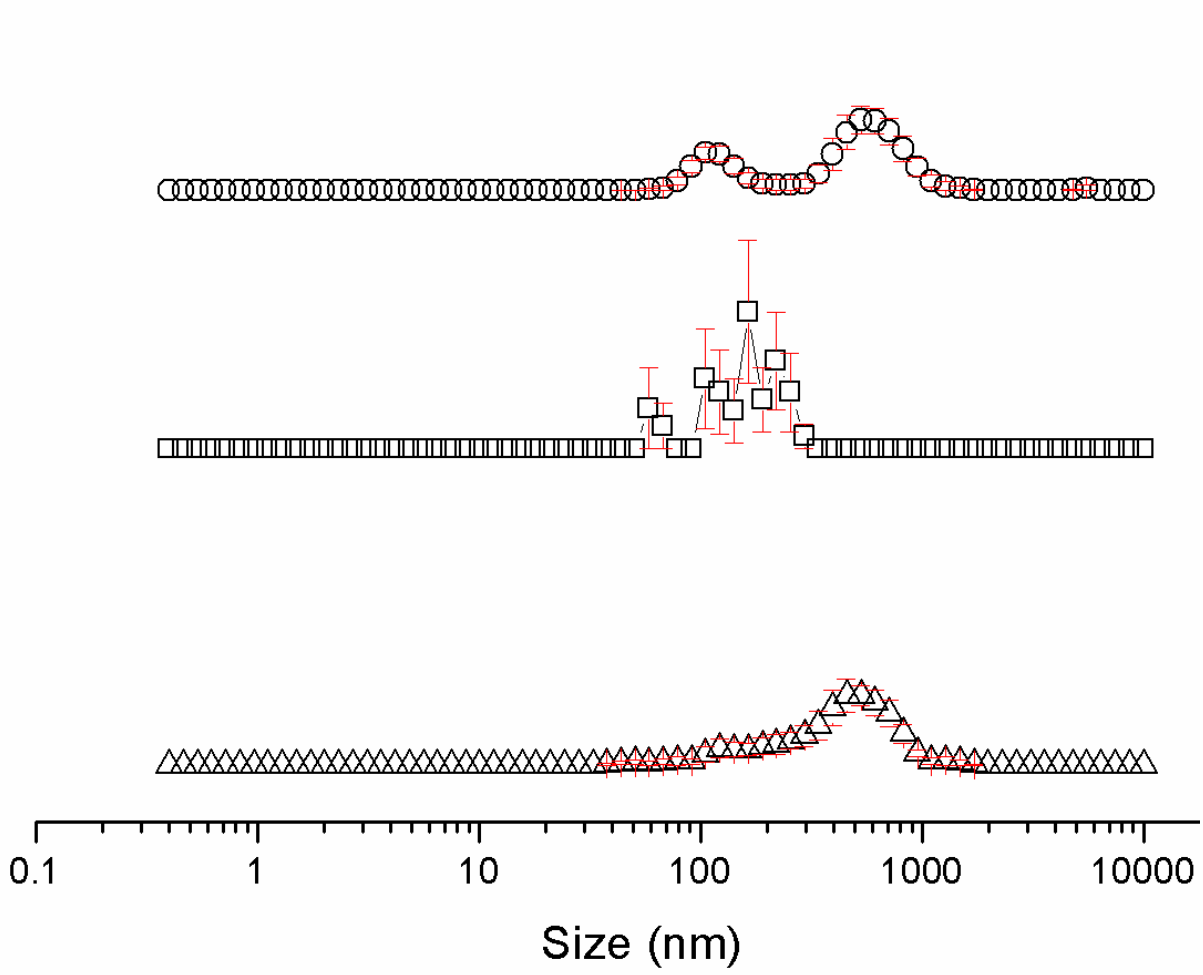

Figure S121 - Average intensity particle size distribution, calculated from 9 DLS runs, of aggregates formed by dissolving compound **1** at a concentration of 5.56 mM in DMSO at Δ) 25 °C, □) heating to 40 °C and ○) cooling to 25 °C. Only 9 of the available 10 DLS runs were used as in some cases, due to the heating and cooling processes there were some obvious temperature equilibration issues for the first run.

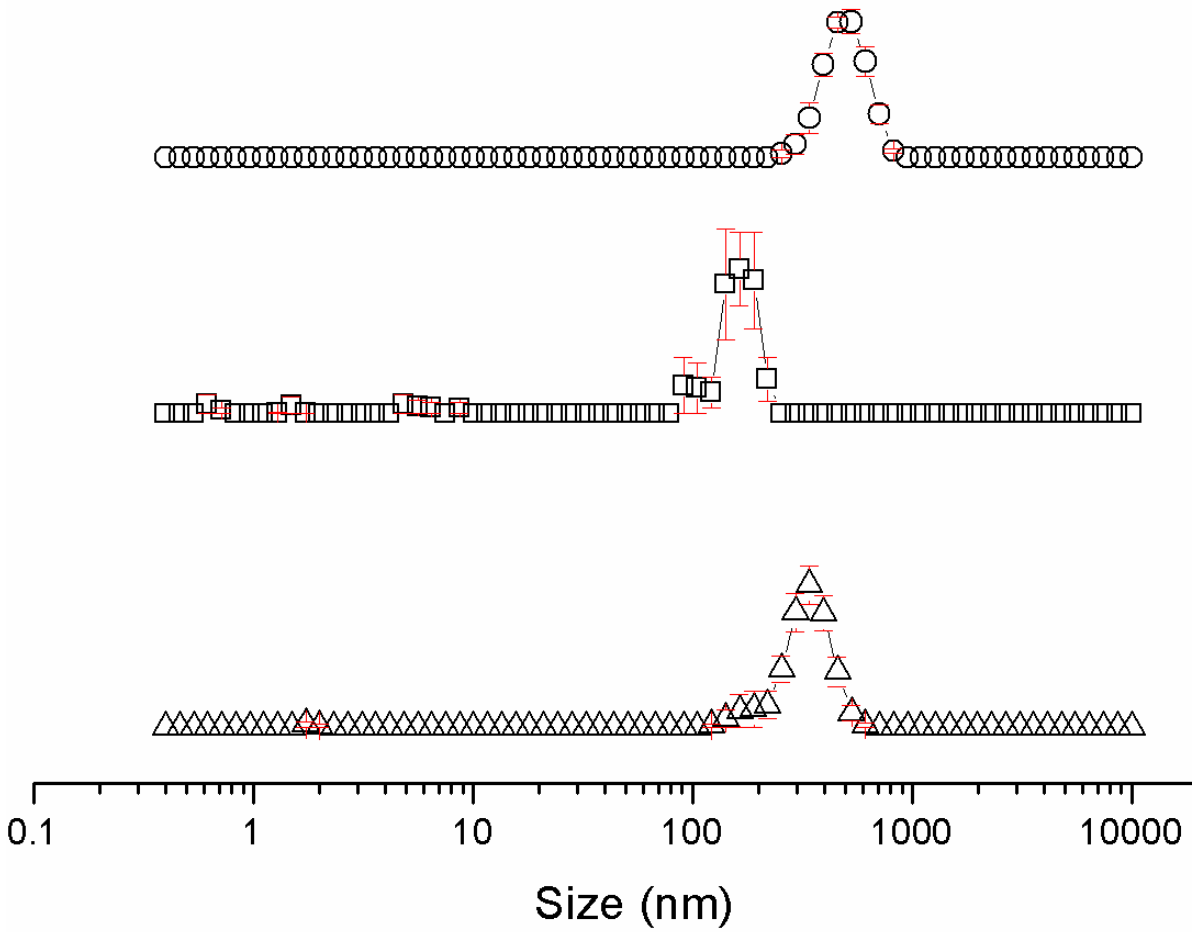

Figure S122 - Average intensity particle size distribution, calculated from 9 DLS runs, of aggregates formed by dissolving compound **1** at a concentration of 0.56 mM in DMSO at Δ) 25 °C, □) heating to 40 °C and ○) cooling to 25 °C. Only 9 of the available 10 DLS runs were used as in some cases, due to the heating and cooling processes there were some obvious temperature equilibration issues for the first run.

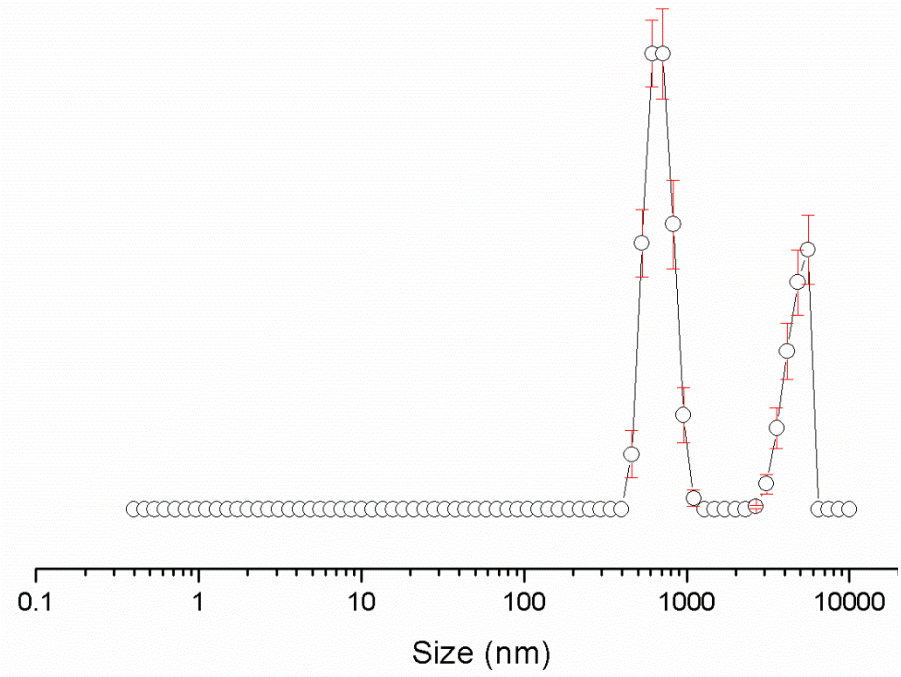

Figure S123 - Average intensity particle size distribution, calculated from 9 DLS runs, of aggregates formed by dissolving compound **1** at a concentration of 55.56 mM in a solution of DMSO: H_2O 1: 1, after heating to 40 ^oC and cooling to 25 ^oC. Only 9 of the available 10 DLS runs were used as in some cases, due to the heating and cooling processes there were some obvious temperature equilibration issues for the first run.

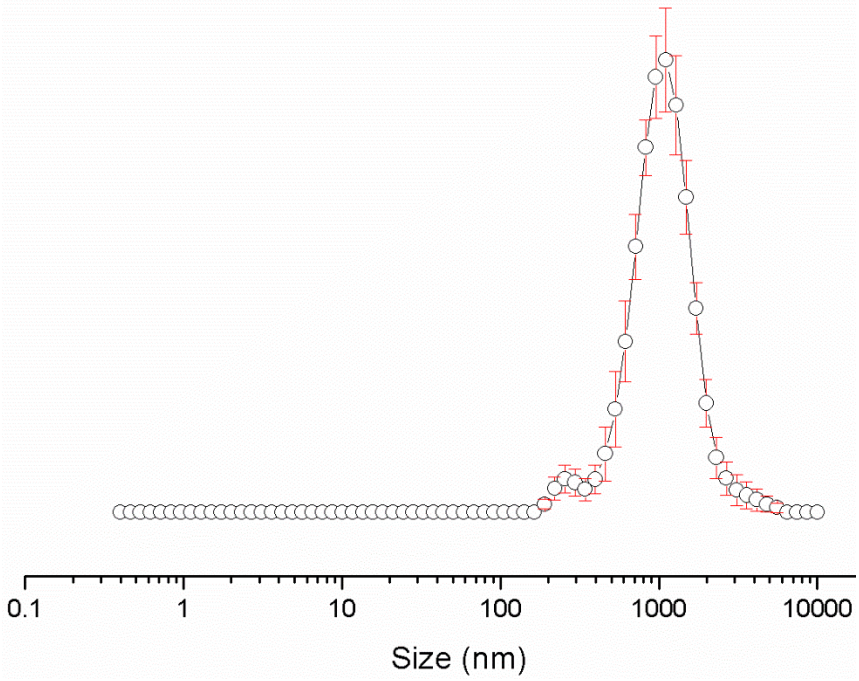

Figure S124 - Average intensity particle size distribution, calculated from 9 DLS runs, of aggregates formed by dissolving compound **1** at a concentration of 5.56 mM in a solution of DMSO: H_2O 1: 1, after heating to 40 ^oC and cooling to 25 ^oC. Only 9 of the available 10 DLS runs were used as in some cases, due to the heating and cooling processes there were some obvious temperature equilibration issues for the first run.

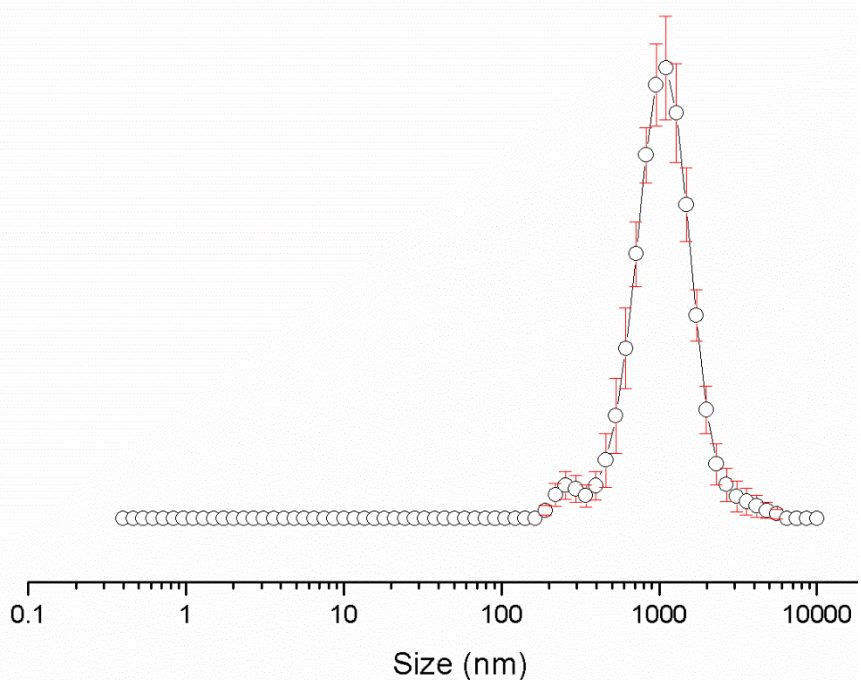

Figure S125 - Average intensity particle size distribution, calculated from 9 DLS runs, of aggregates formed by dissolving compound **1** at a concentration of 0.56 mM in a solution of DMSO: H_2O 1: 1, after heating to 40 ^oC and cooling to 25 ^oC. Only 9 of the available 10 DLS runs were used as in some cases, due to the heating and cooling processes there were some obvious temperature equilibration issues for the first run.

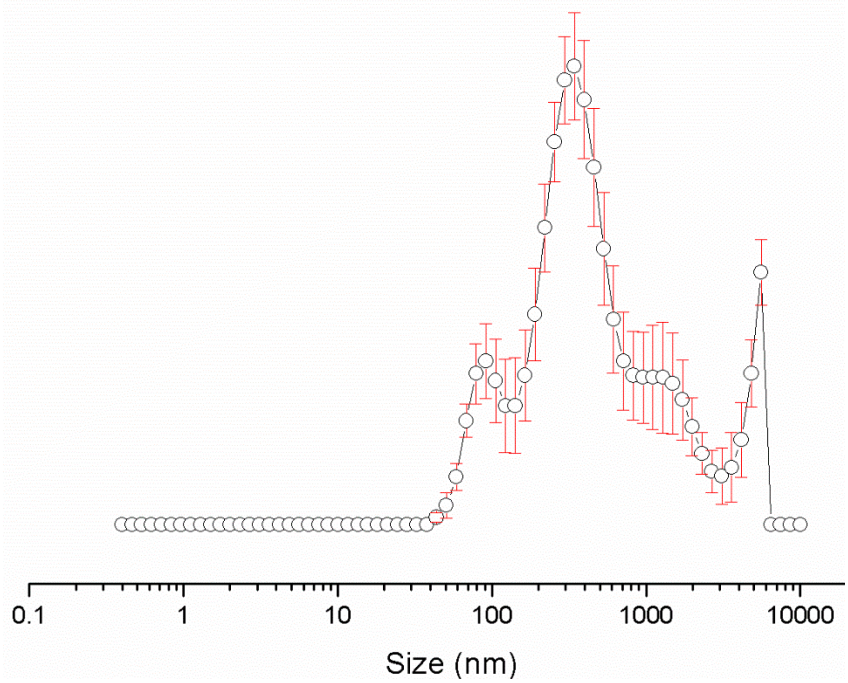

Figure S126 - Average intensity particle size distribution, calculated from 9 DLS runs, of aggregates formed by dissolving compound **1** at a concentration of 5.56 mM in a solution of DMSO: H_2O 3: 7, after heating to 40 ^oC and cooling to 25 ^oC. Only 9 of the available 10 DLS runs were used as in some cases, due to the heating and cooling processes there were some obvious temperature equilibration issues for the first run.

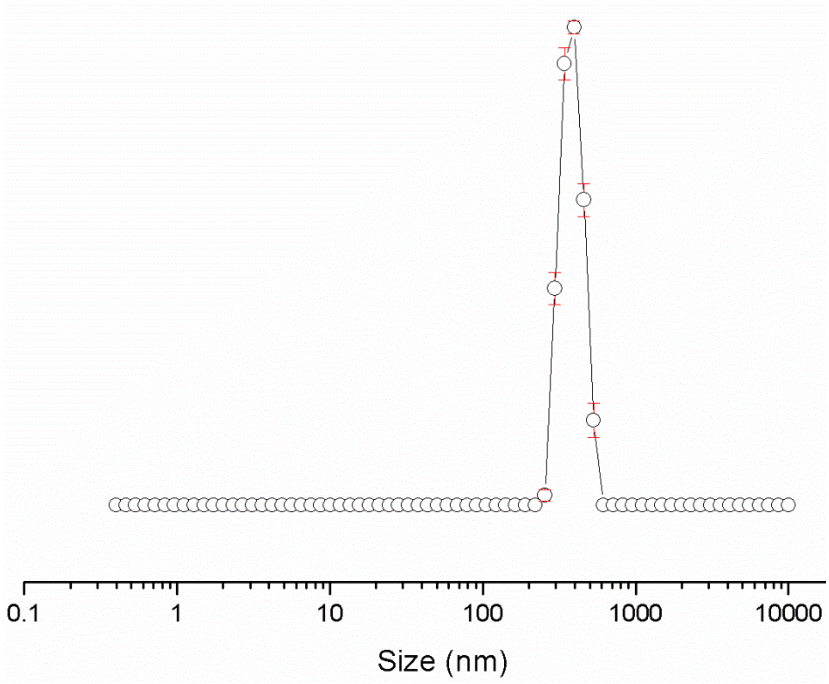

Figure S127 - Average intensity particle size distribution, calculated from 9 DLS runs, of aggregates formed by dissolving compound **1** at a concentration of 0.56 mM in a solution of DMSO: H_2O 3: 7, after heating to 40 ^oC and cooling to 25 ^oC. Only 9 of the available 10 DLS runs were used as in some cases, due to the heating and cooling processes there were some obvious temperature equilibration issues for the first run.

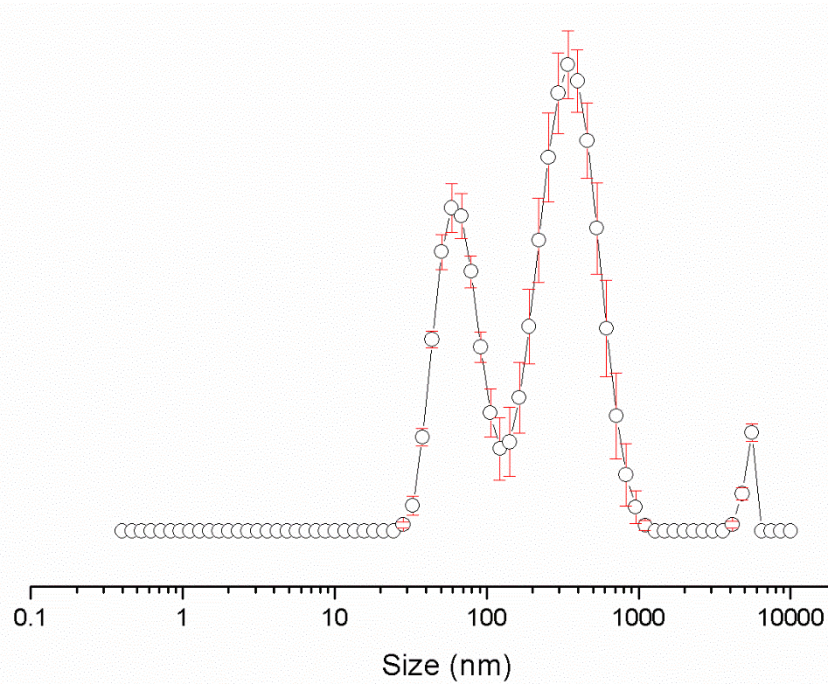

Figure S128 - Average intensity particle size distribution, calculated from 9 DLS runs, of aggregates formed by dissolving compound **1** at a concentration of 0.56 mM in a solution of DMSO: H_2O 1: 4, after heating to 40 ^oC and cooling to 25 ^oC. Only 9 of the available 10 DLS runs were used as in some cases, due to the heating and cooling processes there were some obvious temperature equilibration issues for the first run.

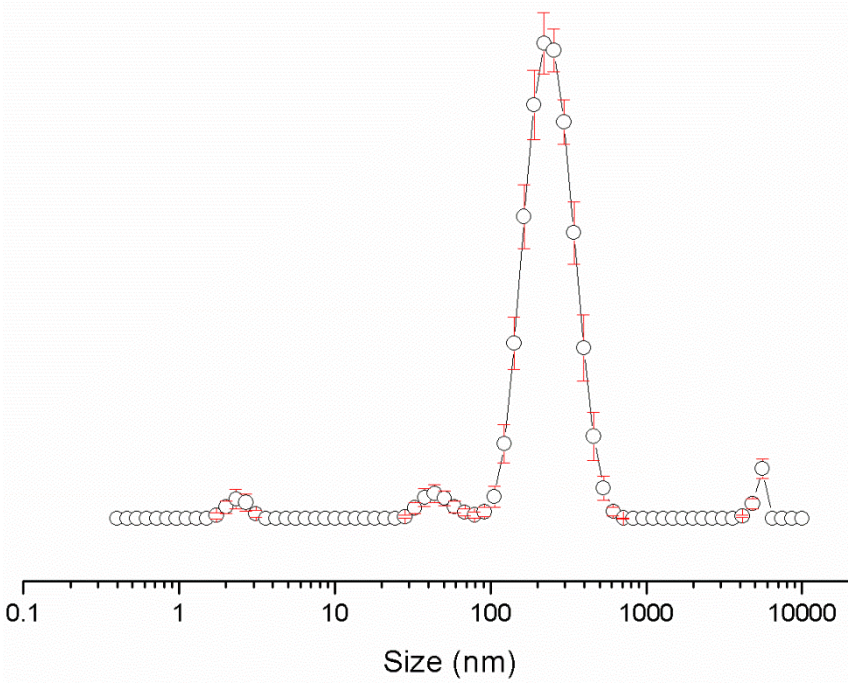

Figure S129 - Average intensity particle size distribution, calculated from 9 DLS runs, of aggregates formed by dissolving compound **1** at a concentration of 5.56 mM in a solution of EtOH: H_2O 1: 19, after heating to 40 ^oC and cooling to 25 ^oC. Only 9 of the available 10 DLS runs were used as in some cases, due to the heating and cooling processes there were some obvious temperature equilibration issues for the first run.

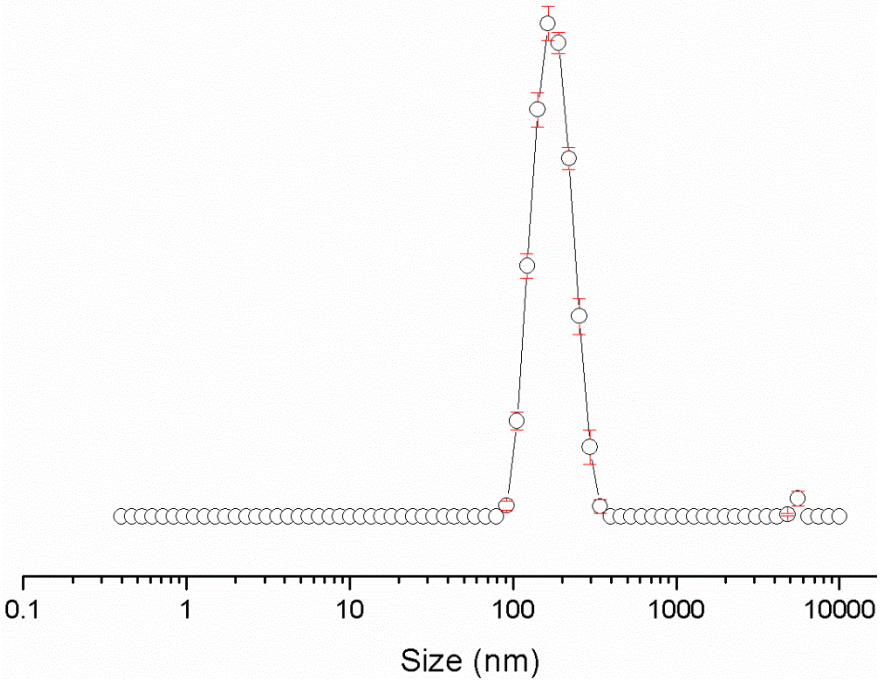

Figure S130 - Average intensity particle size distribution, calculated from 9 DLS runs, of aggregates formed by dissolving compound **1** at a concentration of 0.56 mM in a solution of EtOH: H_2O 1: 19, after heating to 40 ^oC and cooling to 25 ^oC. Only 9 of the available 10 DLS runs were used as in some cases, due to the heating and cooling processes there were some obvious temperature equilibration issues for the first run.

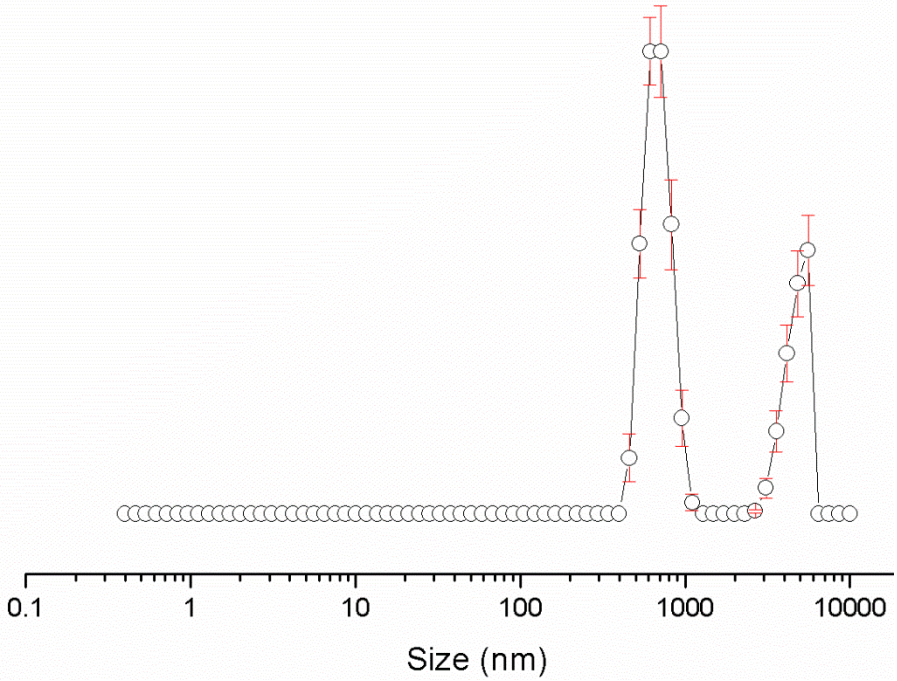

Figure S131 - Average intensity particle size distribution, calculated from 9 DLS runs, of aggregates formed by dissolving compound **2** at a concentration of 55.56 mM in a solution of DMSO: H_2O 1: 1, after heating to 40 ^oC and cooling to 25 ^oC. Only 9 of the available 10 DLS runs were used as in some cases, due to the heating and cooling processes there were some obvious temperature equilibration issues for the first run.

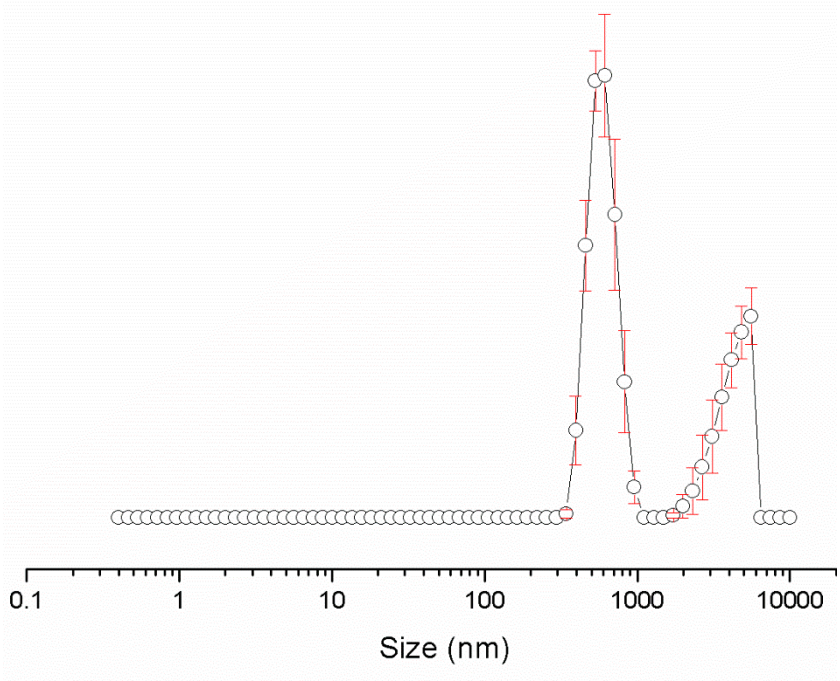

Figure S132 - Average intensity particle size distribution, calculated from 9 DLS runs, of aggregates formed by dissolving compound **2** at a concentration of 5.56 mM in a solution of DMSO: H_2O 1: 1, after heating to 40 ^oC and cooling to 25 ^oC. Only 9 of the available 10 DLS runs were used as in some cases, due to the heating and cooling processes there were some obvious temperature equilibration issues for the first run.

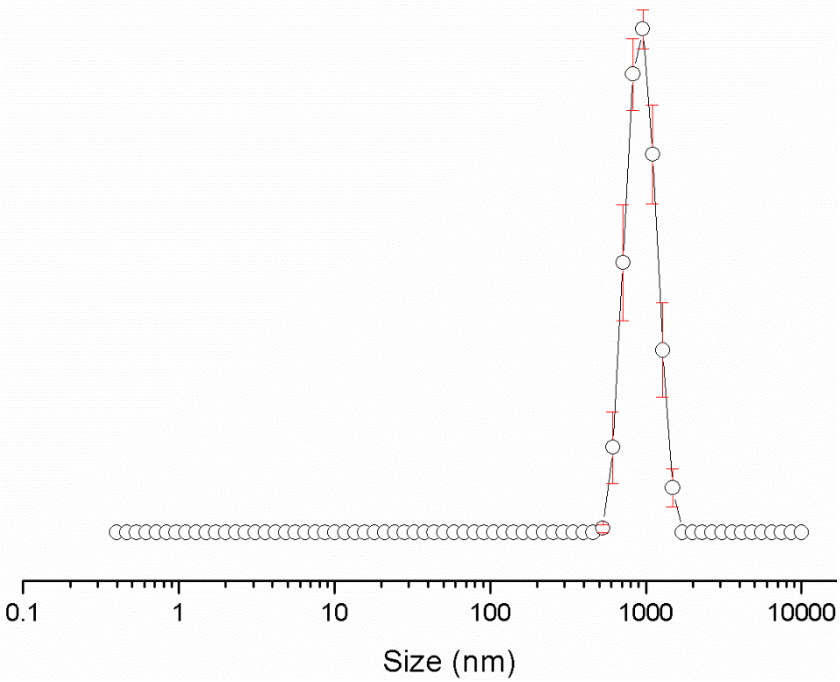

Figure S133 - Average intensity particle size distribution, calculated from 9 DLS runs, of aggregates formed by dissolving compound **2** at a concentration of 0.56 mM in a solution of DMSO: H_2O 1: 1, after heating to 40 ^oC and cooling to 25 ^oC. Only 9 of the available 10 DLS runs were used as in some cases, due to the heating and cooling processes there were some obvious temperature equilibration issues for the first run.

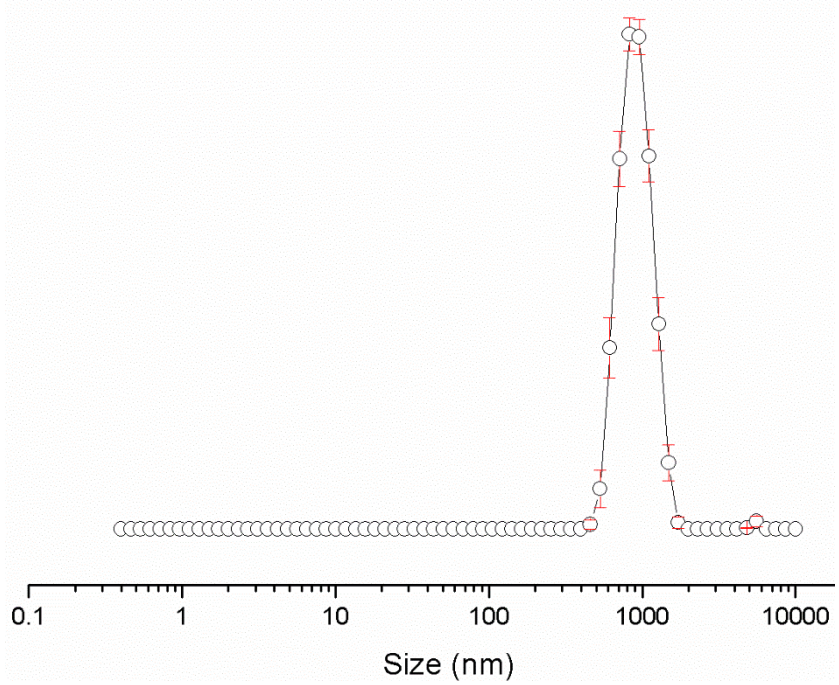

Figure S134 - Average intensity particle size distribution, calculated from 9 DLS runs, of aggregates formed by dissolving compound **2** at a concentration of 5.56 mM in a solution of DMSO: H_2O 3: 7, after heating to 40 ^oC and cooling to 25 ^oC. Only 9 of the available 10 DLS runs were used as in some cases, due to the heating and cooling processes there were some obvious temperature equilibration issues for the first run.

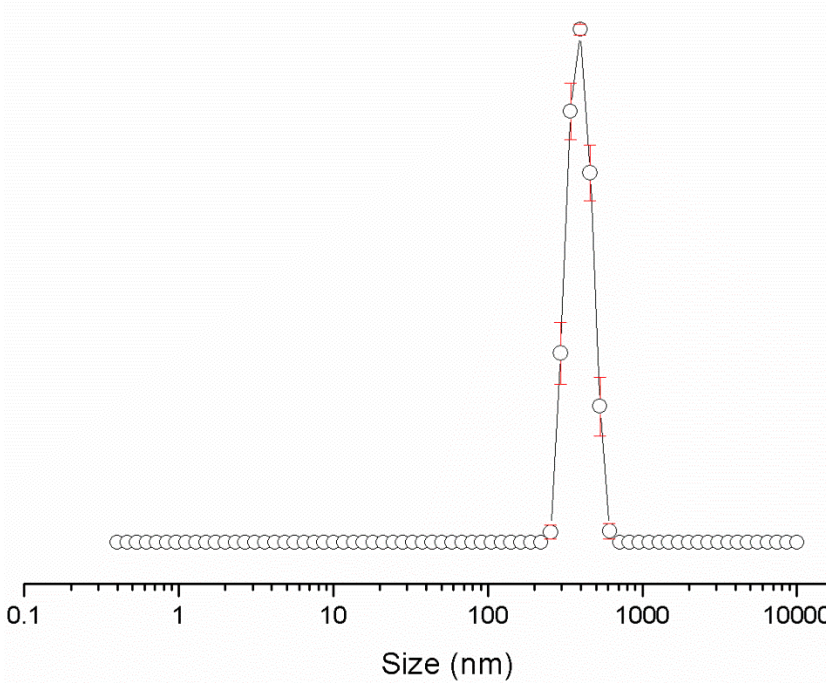

Figure S135 - Average intensity particle size distribution, calculated from 9 DLS runs, of aggregates formed by dissolving compound **2** at a concentration of 0.56 mM in a solution of DMSO: H_2O 3: 7, after heating to 40 ^oC and cooling to 25 ^oC. Only 9 of the available 10 DLS runs were used as in some cases, due to the heating and cooling processes there were some obvious temperature equilibration issues for the first run.

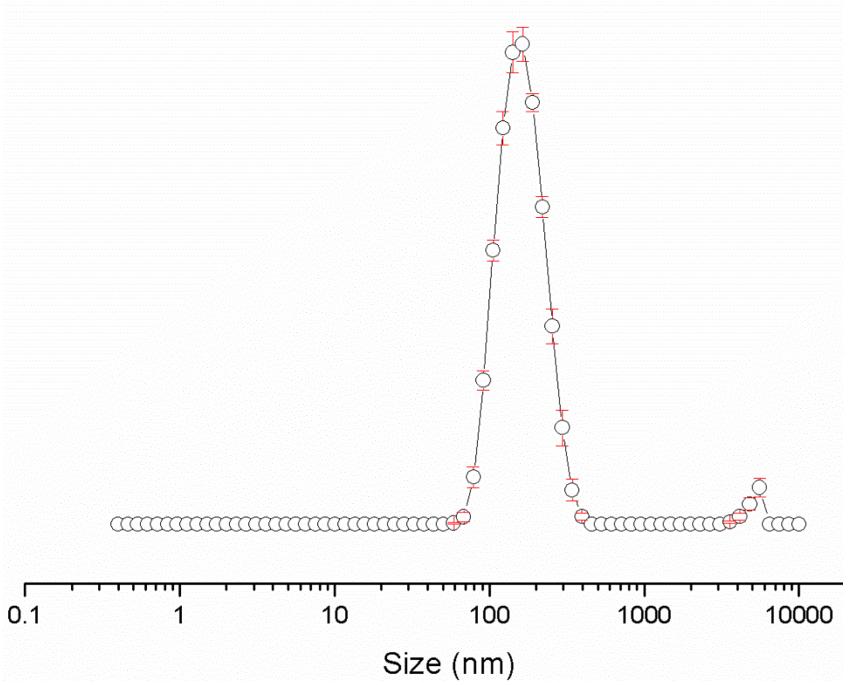

Figure S136 - Average intensity particle size distribution, calculated from 9 DLS runs, of aggregates formed by dissolving compound **2** at a concentration of 0.56 mM in a solution of DMSO: H_2O 1: 4, after heating to 40 ^oC and cooling to 25 ^oC. Only 9 of the available 10 DLS runs were used as in some cases, due to the heating and cooling processes there were some obvious temperature equilibration issues for the first run.

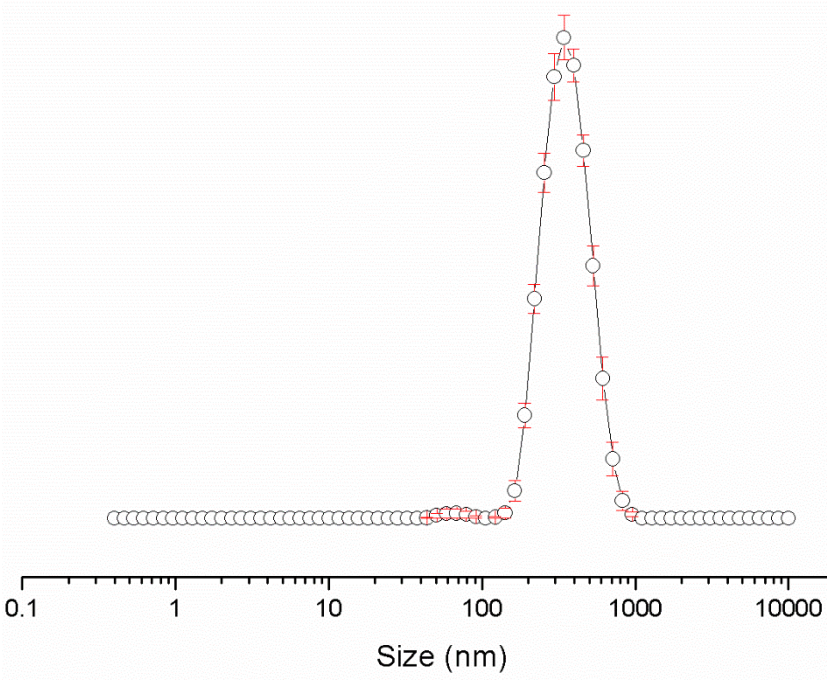

Figure S137 - Average intensity particle size distribution, calculated from 9 DLS runs, of aggregates formed by dissolving compound **2** at a concentration of 5.56 mM in a solution of EtOH: H_2O 1: 19, after heating to 40 ^oC and cooling to 25 ^oC. Only 9 of the available 10 DLS runs were used as in some cases, due to the heating and cooling processes there were some obvious temperature equilibration issues for the first run.

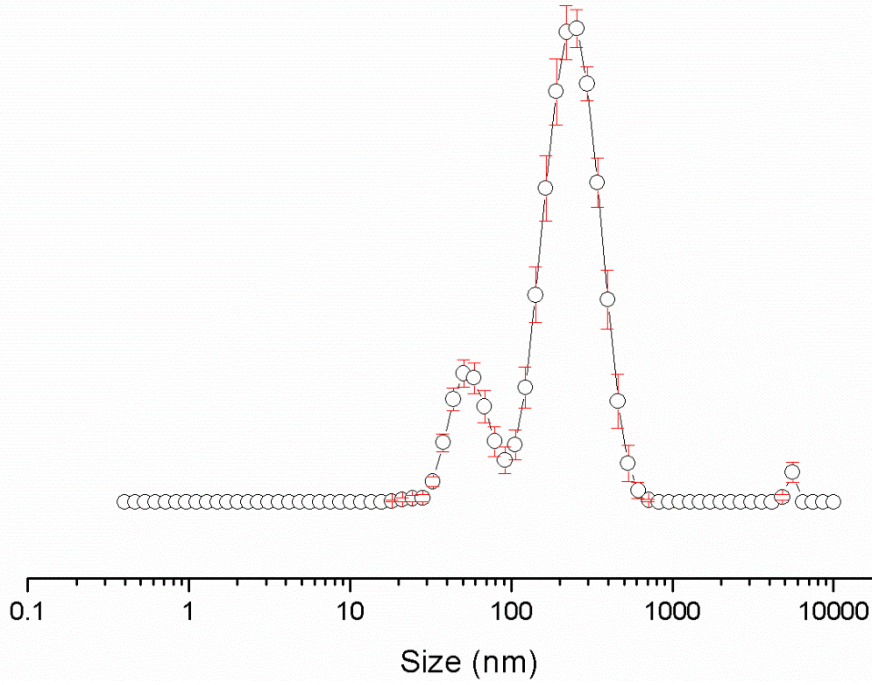

Figure S138 - Average intensity particle size distribution, calculated from 9 DLS runs, of aggregates formed by dissolving compound **2** at a concentration of 0.56 mM in a solution of EtOH: H_2O 1: 19, after heating to 40 ^oC and cooling to 25 ^oC. Only 9 of the available 10 DLS runs were used as in some cases, due to the heating and cooling processes there were some obvious temperature equilibration issues for the first run.

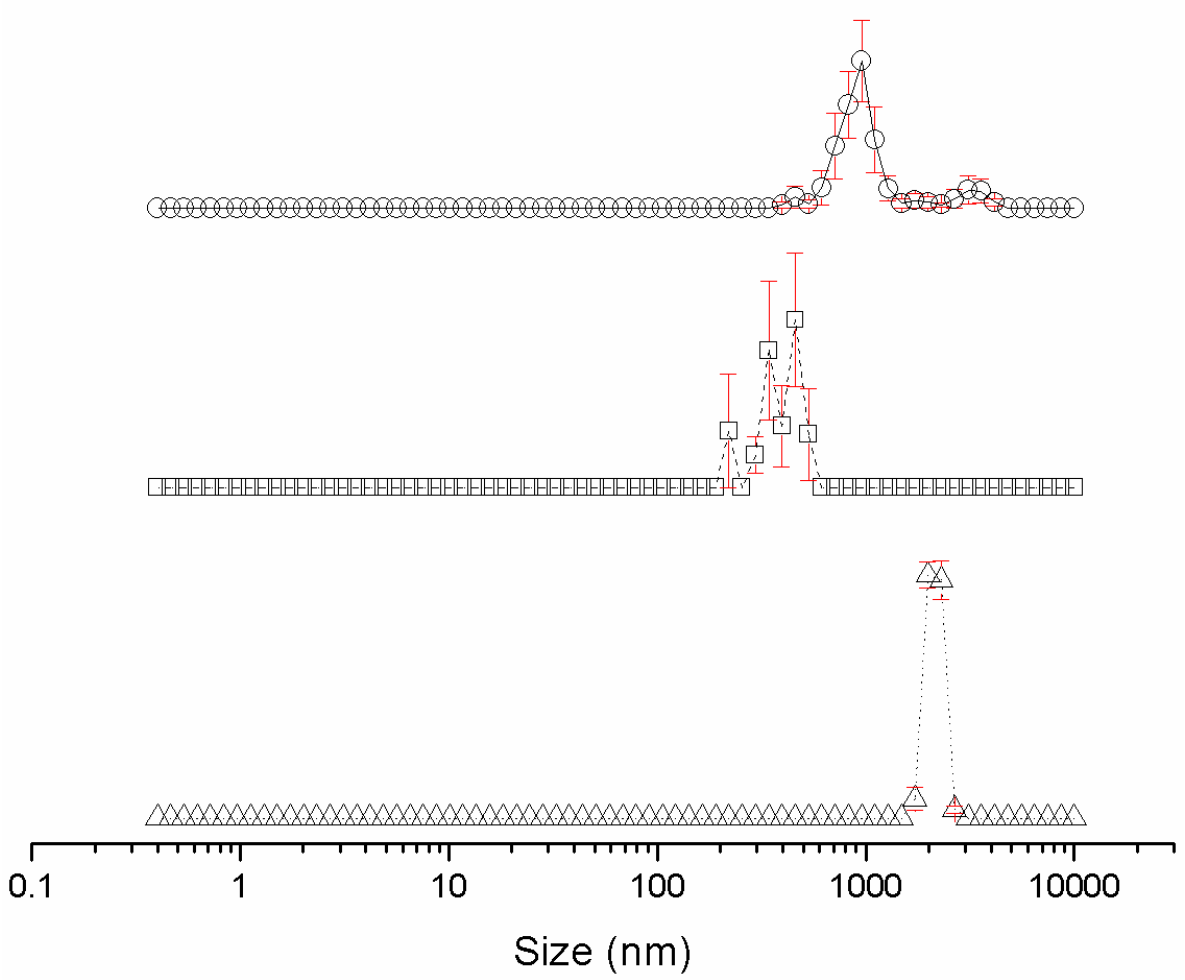

Figure S139 - Average intensity particle size distribution, calculated from 9 DLS runs, of aggregates formed by dissolving compound **3** at a concentration of 111.12 mM in DMSO at Δ) 25 °C, □) heating to 40 °C and ○) cooling to 25 °C. Only 9 of the available 10 DLS runs were used as in some cases, due to the heating and cooling processes there were some obvious temperature equilibration issues for the first run.

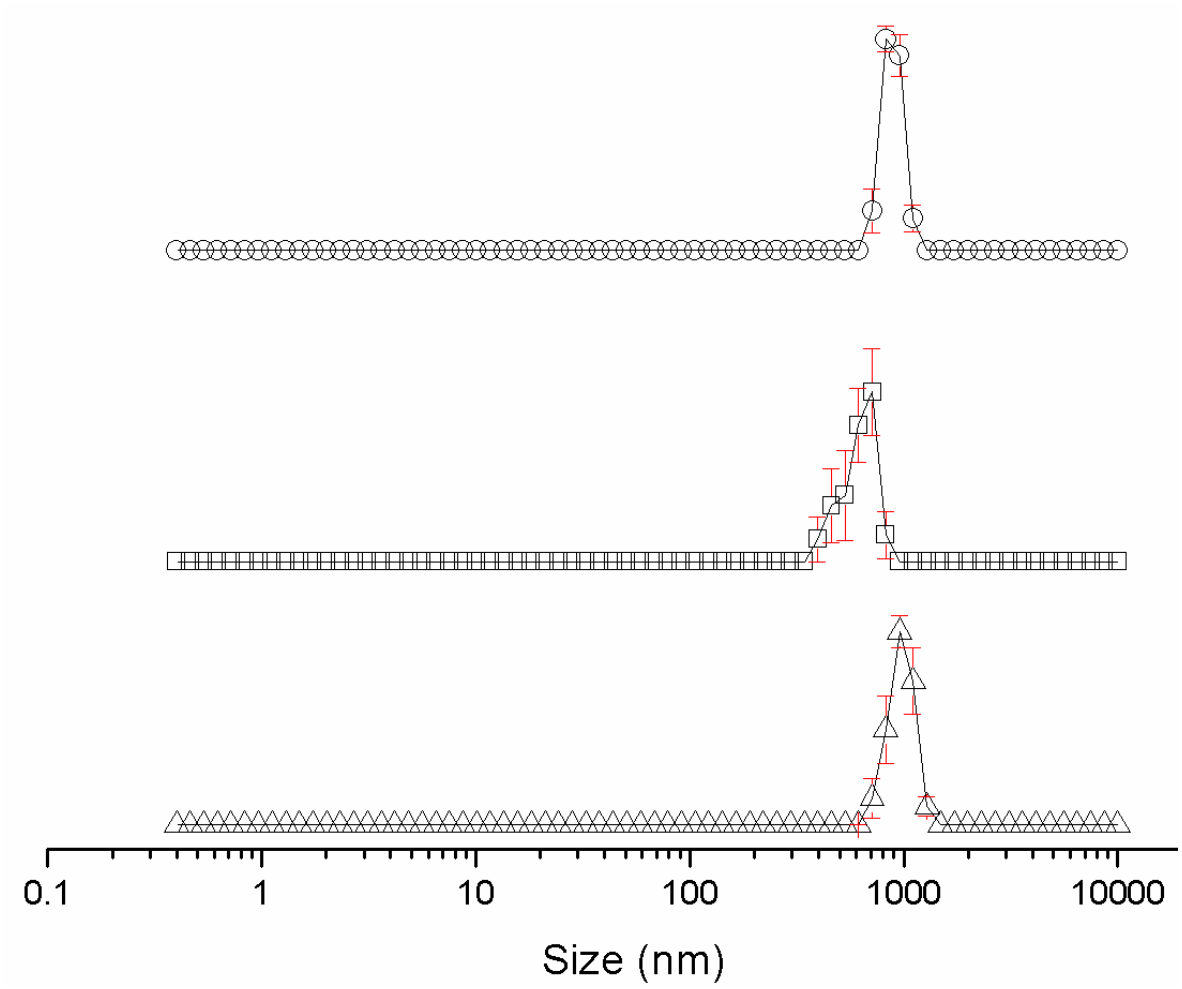

Figure S140 - Average intensity particle size distribution, calculated from 9 DLS runs, of aggregates formed by dissolving compound **3** at a concentration of 55.56 mM in DMSO at Δ) 25 °C, □) heating to 40 °C and ○) cooling to 25 °C. Only 9 of the available 10 DLS runs were used as in some cases, due to the heating and cooling processes there were some obvious temperature equilibration issues for the first run.

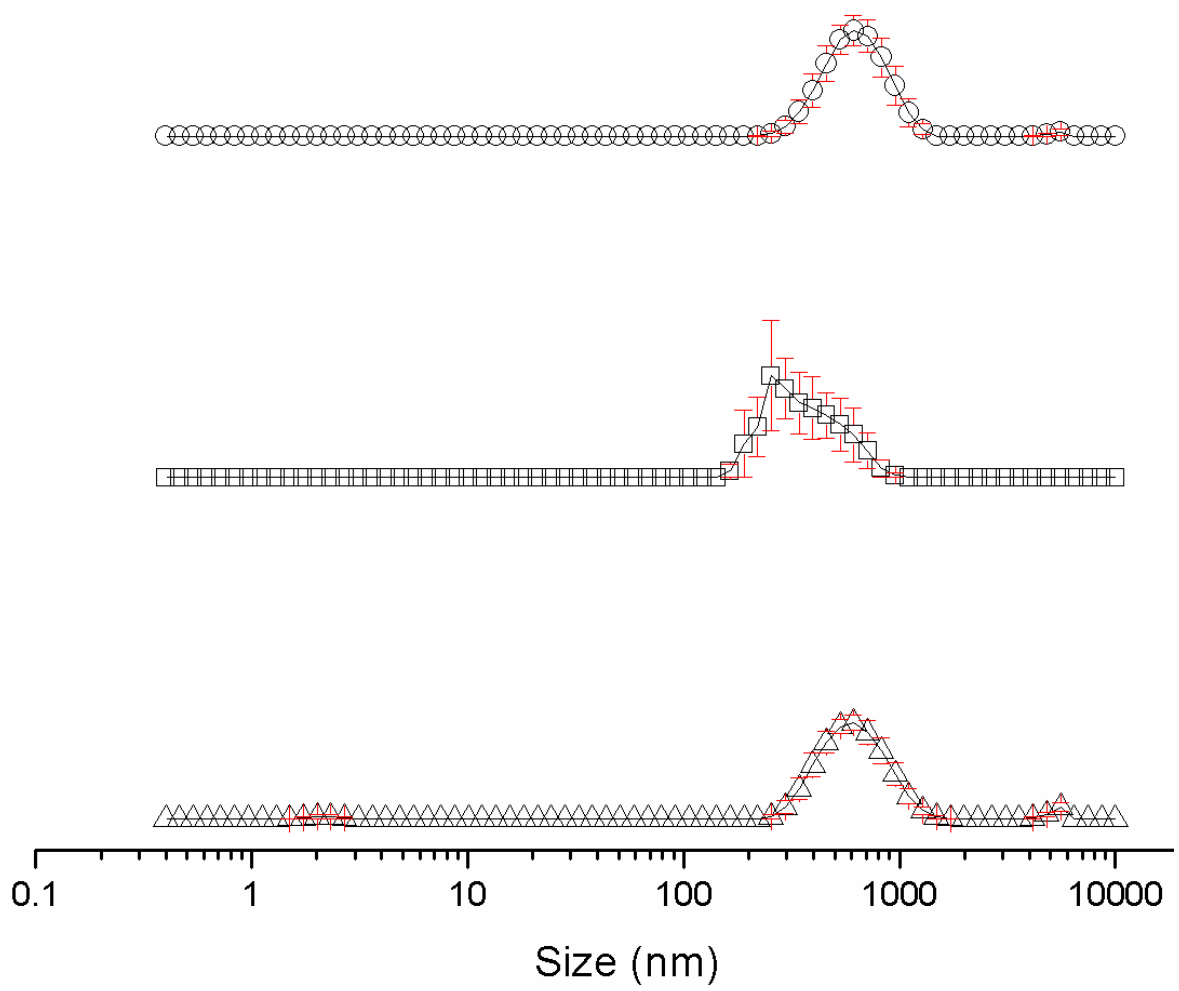

Figure S141 - Average intensity particle size distribution, calculated from 9 DLS runs, of aggregates formed by dissolving compound **3** at a concentration of 5.56 mM in DMSO at Δ) 25 °C, □) heating to 40 °C and ○) cooling to 25 °C. Only 9 of the available 10 DLS runs were used as in some cases, due to the heating and cooling processes there were some obvious temperature equilibration issues for the first run.

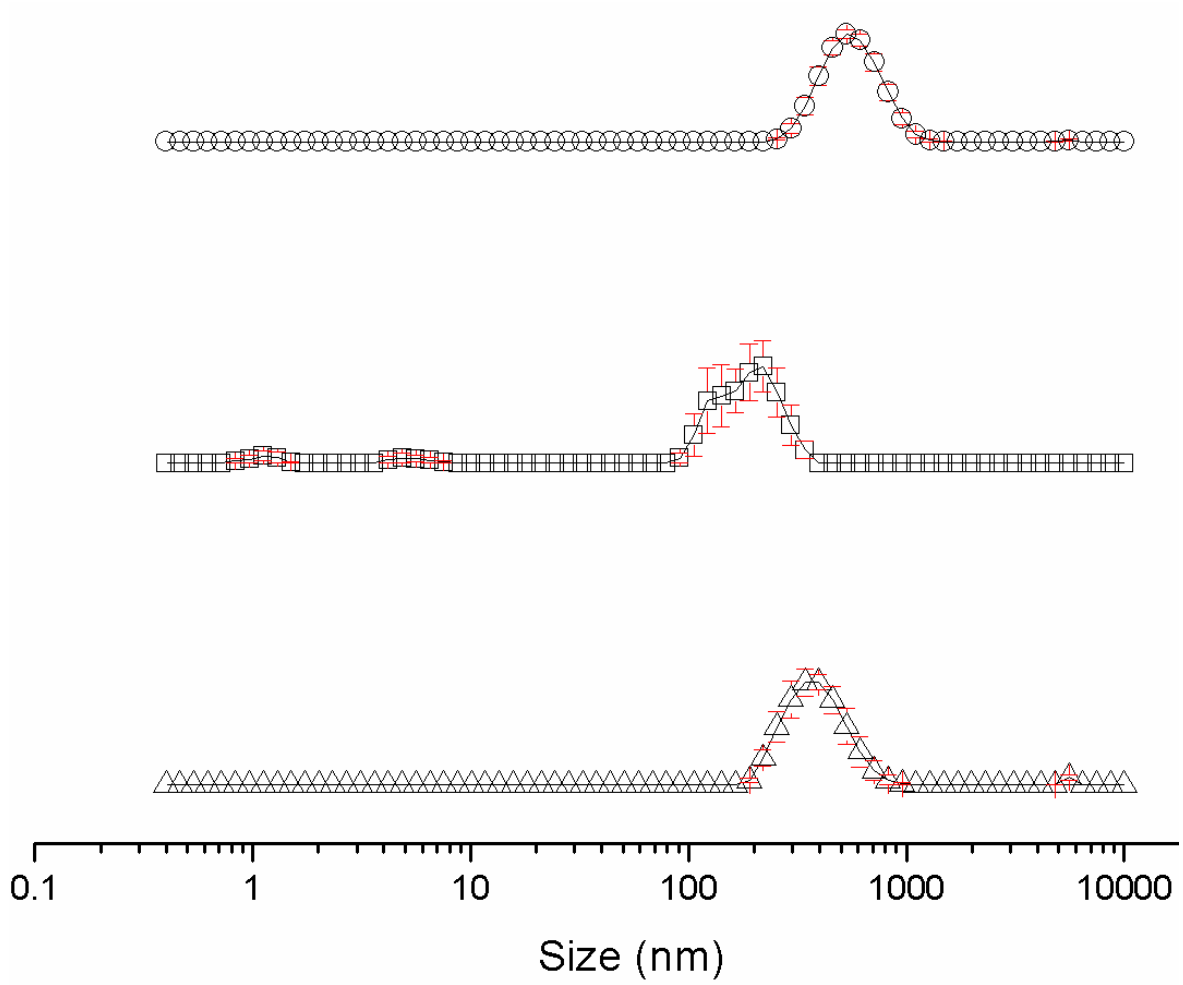

Figure S142 - Average intensity particle size distribution, calculated from 9 DLS runs, of aggregates formed by dissolving compound **3** at a concentration of 0.56 mM in DMSO at Δ) 25 ^{o}C, □) heating to 40 ^{o}C and ○) cooling to 25 ^{o}C. Only 9 of the available 10 DLS runs were used as in some cases, due to the heating and cooling processes there were some obvious temperature equilibration issues for the first run.

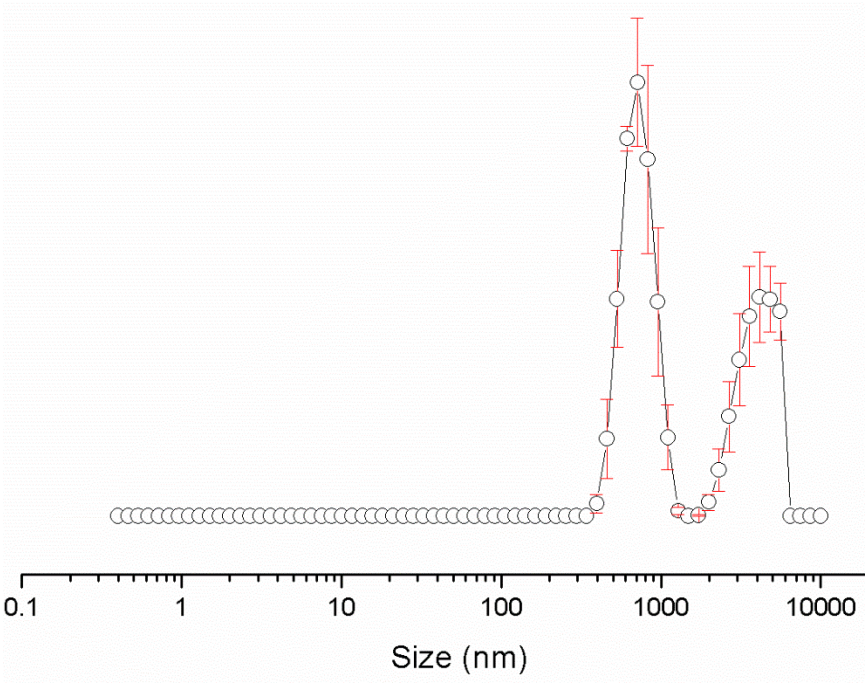

Figure S143 - Average intensity particle size distribution, calculated from 9 DLS runs, of aggregates formed by dissolving compound **3** at a concentration of 55.56 mM in a solution of DMSO: H_2O 1: 1, after heating to 40 ^oC and cooling to 25 ^oC. Only 9 of the available 10 DLS runs were used as in some cases, due to the heating and cooling processes there were some obvious temperature equilibration issues for the first run.

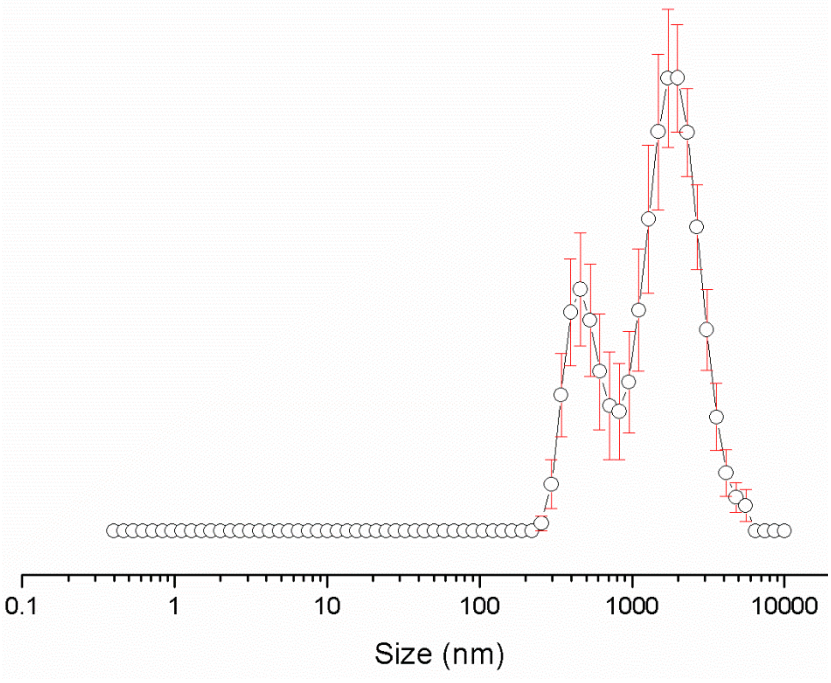

Figure S144 - Average intensity particle size distribution, calculated from 9 DLS runs, of aggregates formed by dissolving compound **3** at a concentration of 5.56 mM in a solution of DMSO: H_2O 1: 1, after heating to 40 ^oC and cooling to 25 ^oC. Only 9 of the available 10 DLS runs were used as in some cases, due to the heating and cooling processes there were some obvious temperature equilibration issues for the first run.

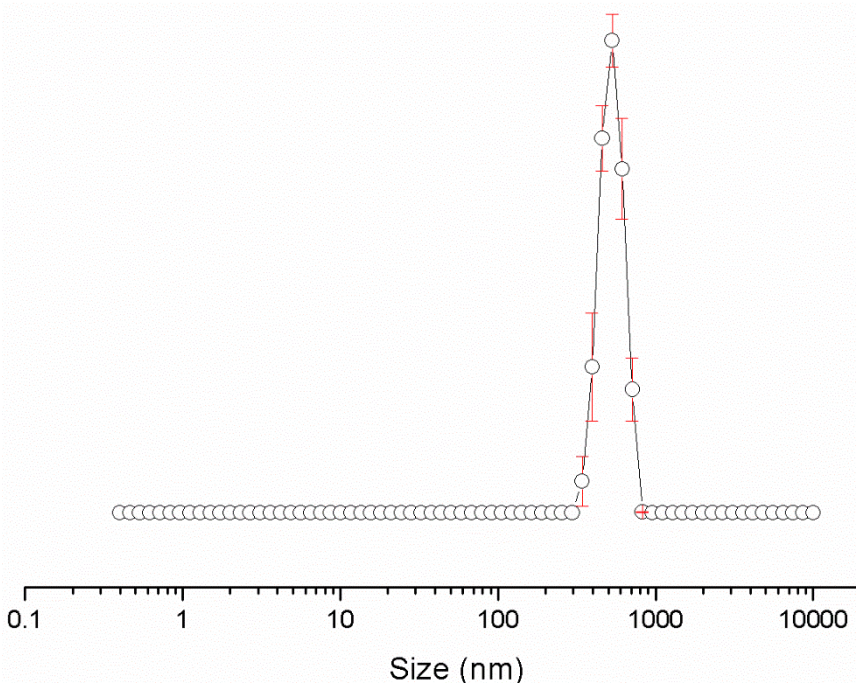

Figure S145 - Average intensity particle size distribution, calculated from 9 DLS runs, of aggregates formed by dissolving compound **3** at a concentration of 0.56 mM in a solution of DMSO: H_2O 1: 1, after heating to 40 ^oC and cooling to 25 ^oC. Only 9 of the available 10 DLS runs were used as in some cases, due to the heating and cooling processes there were some obvious temperature equilibration issues for the first run.

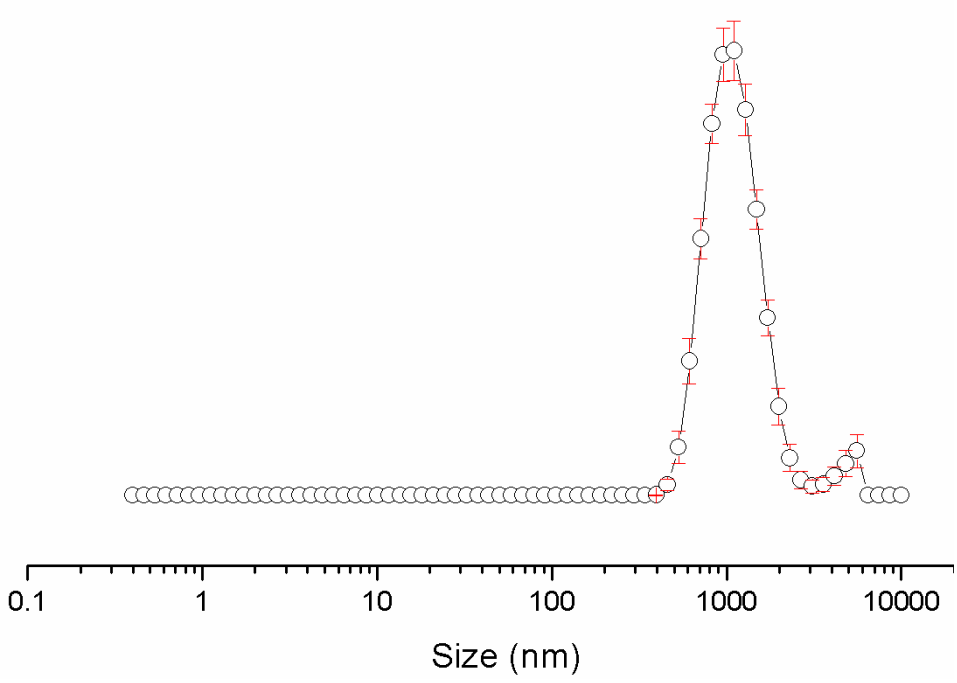

Figure S146 - Average intensity particle size distribution, calculated from 9 DLS runs, of aggregates formed by dissolving compound **3** at a concentration of 5.56 mM in a solution of DMSO: H_2O 3: 7, after heating to 40 ^oC and cooling to 25 ^oC. Only 9 of the available 10 DLS runs were used as in some cases, due to the heating and cooling processes there were some obvious temperature equilibration issues for the first run.

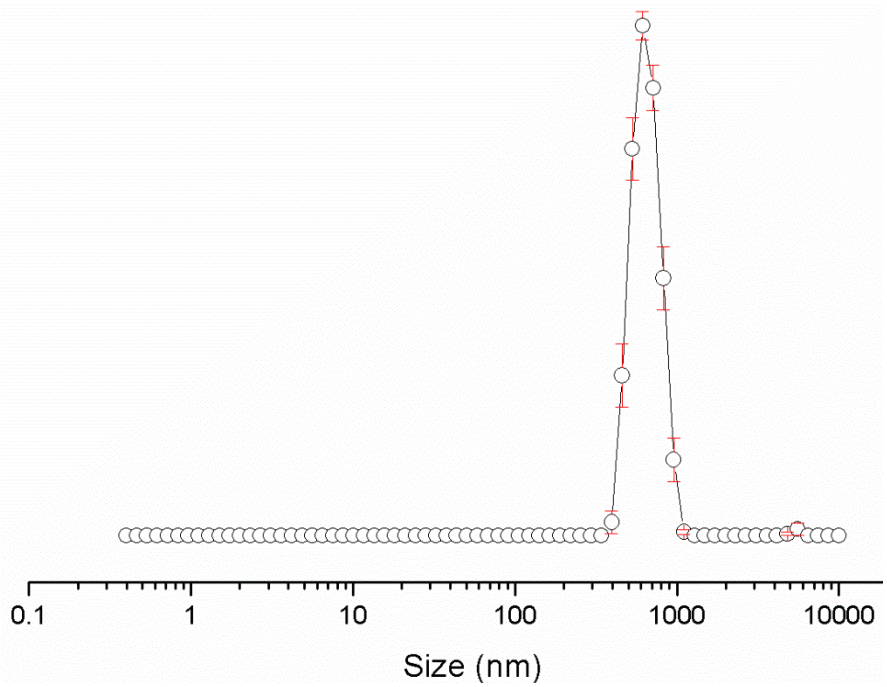

Figure S147 - Average intensity particle size distribution, calculated from 9 DLS runs, of aggregates formed by dissolving compound **3** at a concentration of 0.56 mM in a solution of DMSO: H_2O 3: 7, after heating to 40 ^oC and cooling to 25 ^oC. Only 9 of the available 10 DLS runs were used as in some cases, due to the heating and cooling processes there were some obvious temperature equilibration issues for the first run.

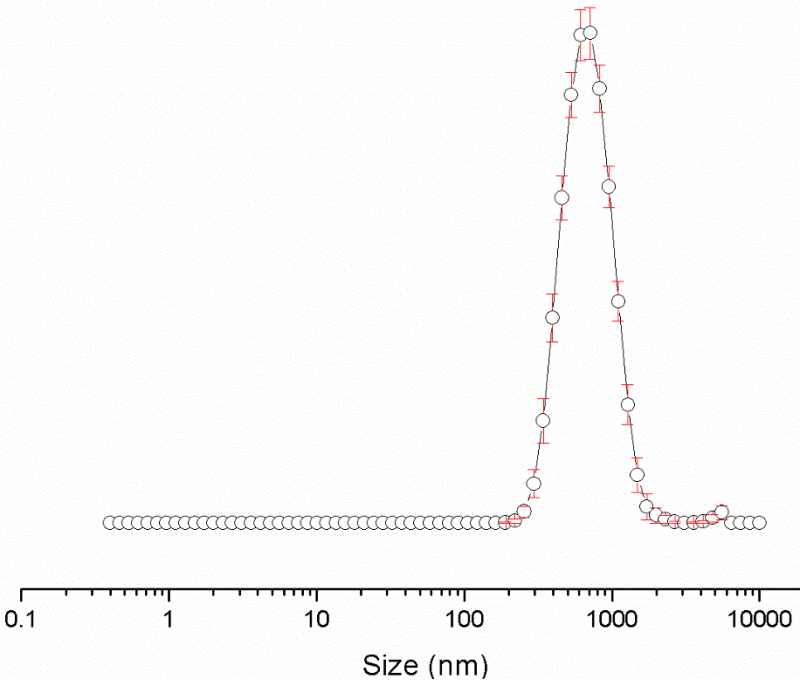

Figure S148 - Average intensity particle size distribution, calculated from 9 DLS runs, of aggregates formed by dissolving compound **3** at a concentration of 0.56 mM in a solution of DMSO: H_2O 1: 4, after heating to 40 ^oC and cooling to 25 ^oC. Only 9 of the available 10 DLS runs were used as in some cases, due to the heating and cooling processes there were some obvious temperature equilibration issues for the first run.

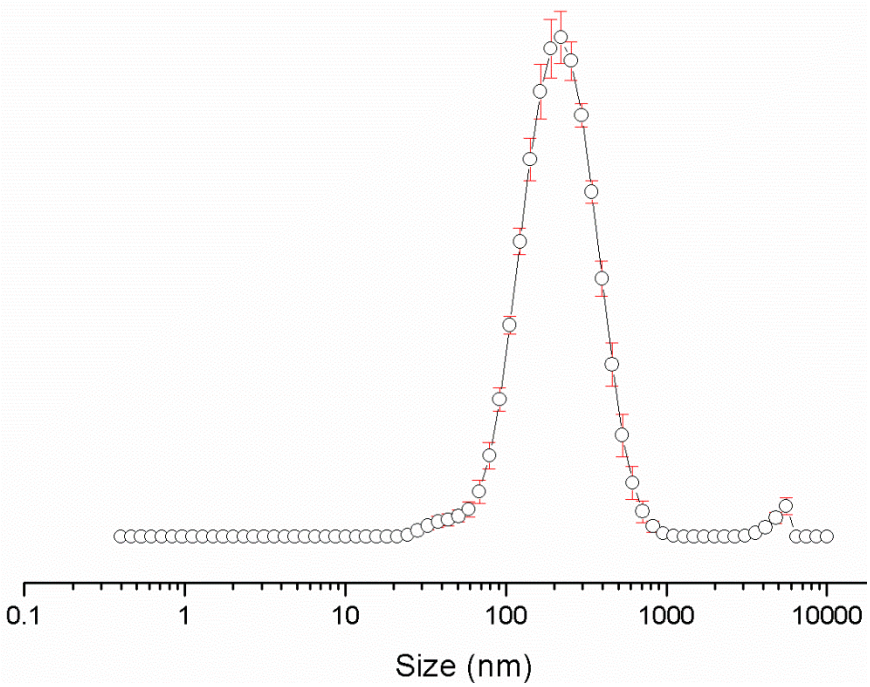

Figure S149 - Average intensity particle size distribution, calculated from 9 DLS runs, of aggregates formed by dissolving compound **3** at a concentration of 5.56 mM in a solution of EtOH: H_2O 1: 19 after heating to 40 ^oC and cooling to 25 ^oC. Only 9 of the available 10 DLS runs were used as in some cases, due to the heating and cooling processes there were some obvious temperature equilibration issues for the first run.

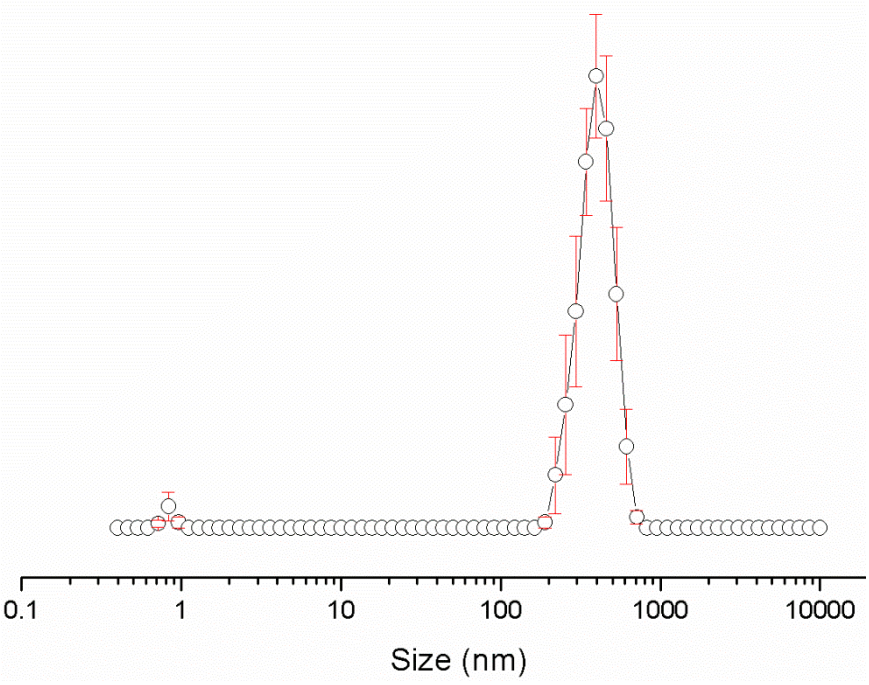

Figure S150 - Average intensity particle size distribution, calculated from 9 DLS runs, of aggregates formed by dissolving compound **3** at a concentration of 0.56 mM in a solution of EtOH: H_2O 1: 19, after heating to 40 ^oC and cooling to 25 ^oC. Only 9 of the available 10 DLS runs were used as in some cases, due to the heating and cooling processes there were some obvious temperature equilibration issues for the first run.

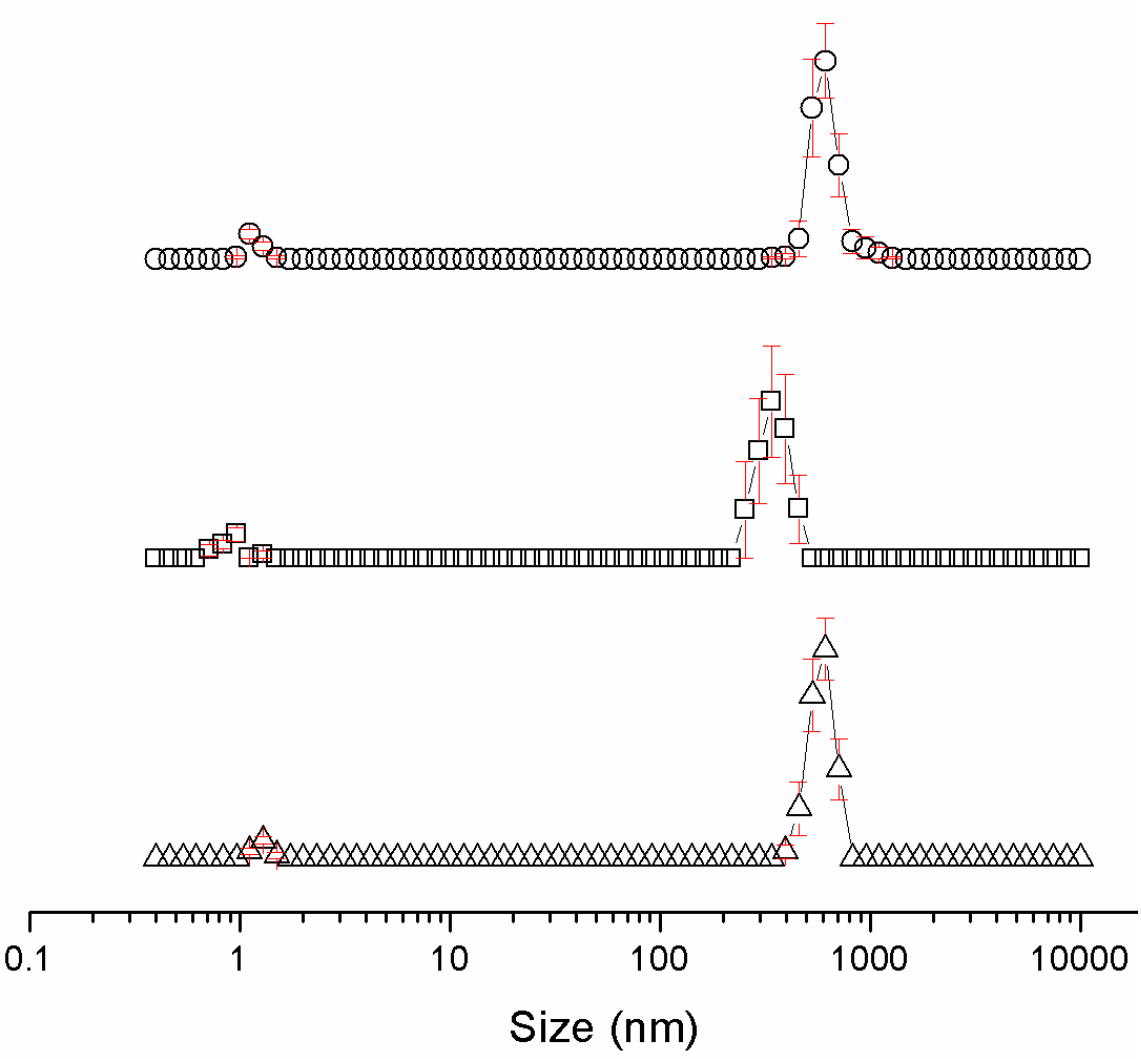

Figure S151 - Average intensity particle size distribution, calculated from 9 DLS runs, of aggregates formed by dissolving compound **4** at a concentration of 111.12 mM in DMSO (1 mL) at Δ) 25 °C, □) heating to 40 °C and ○) cooling to 25 °C. Only 9 of the available 10 DLS runs were used as in some cases, due to the heating and cooling processes there were some obvious temperature equilibration issues for the first run.

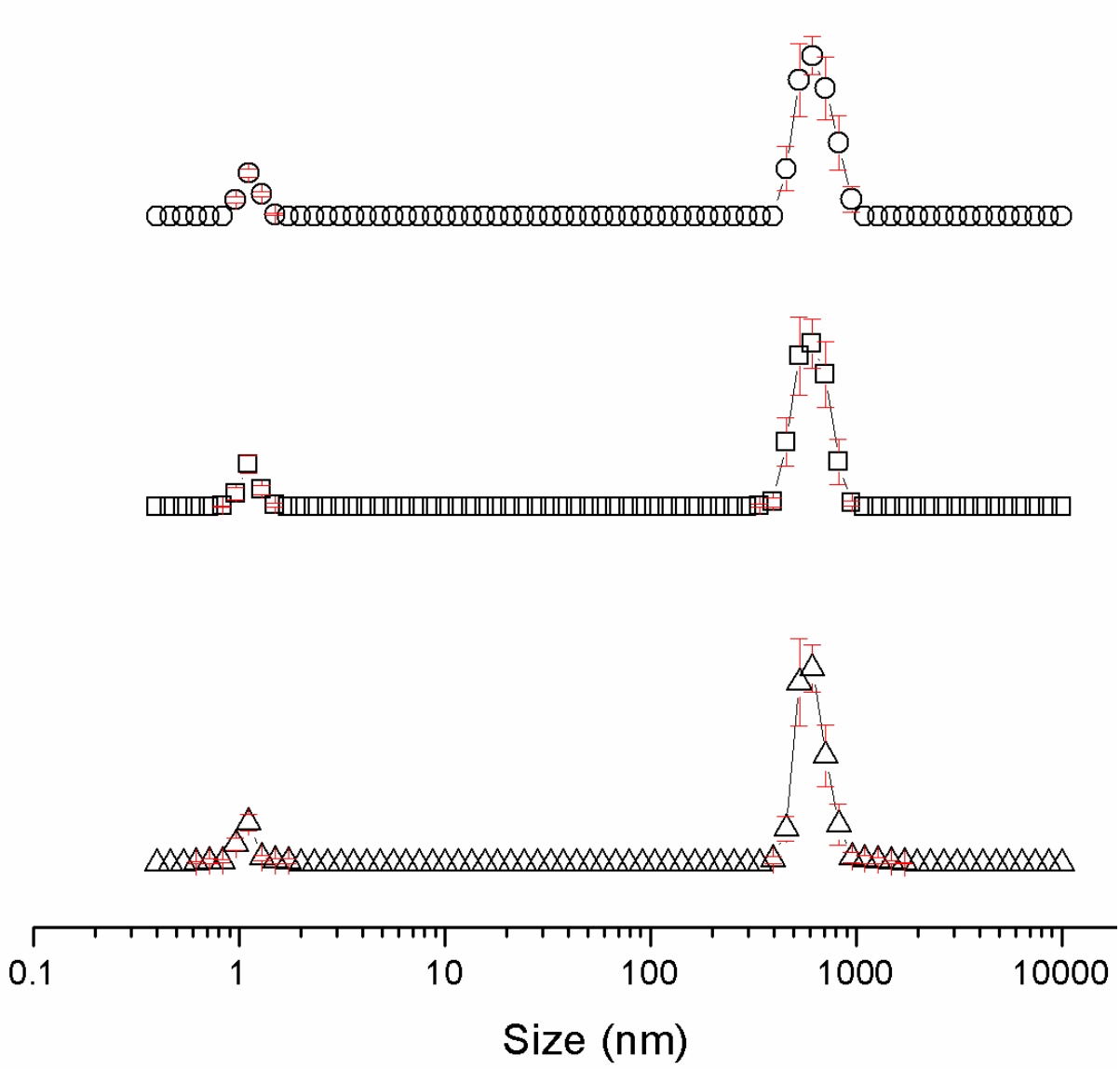

Figure S152 - Average intensity particle size distribution, calculated from 9 DLS runs, of aggregates formed by dissolving compound **4** at a concentration of 55.56 mM in DMSO at Δ) 25 °C, □) heating to 40 °C and ○) cooling to 25 °C. Only 9 of the available 10 DLS runs were used as in some cases, due to the heating and cooling processes there were some obvious temperature equilibration issues for the first run.

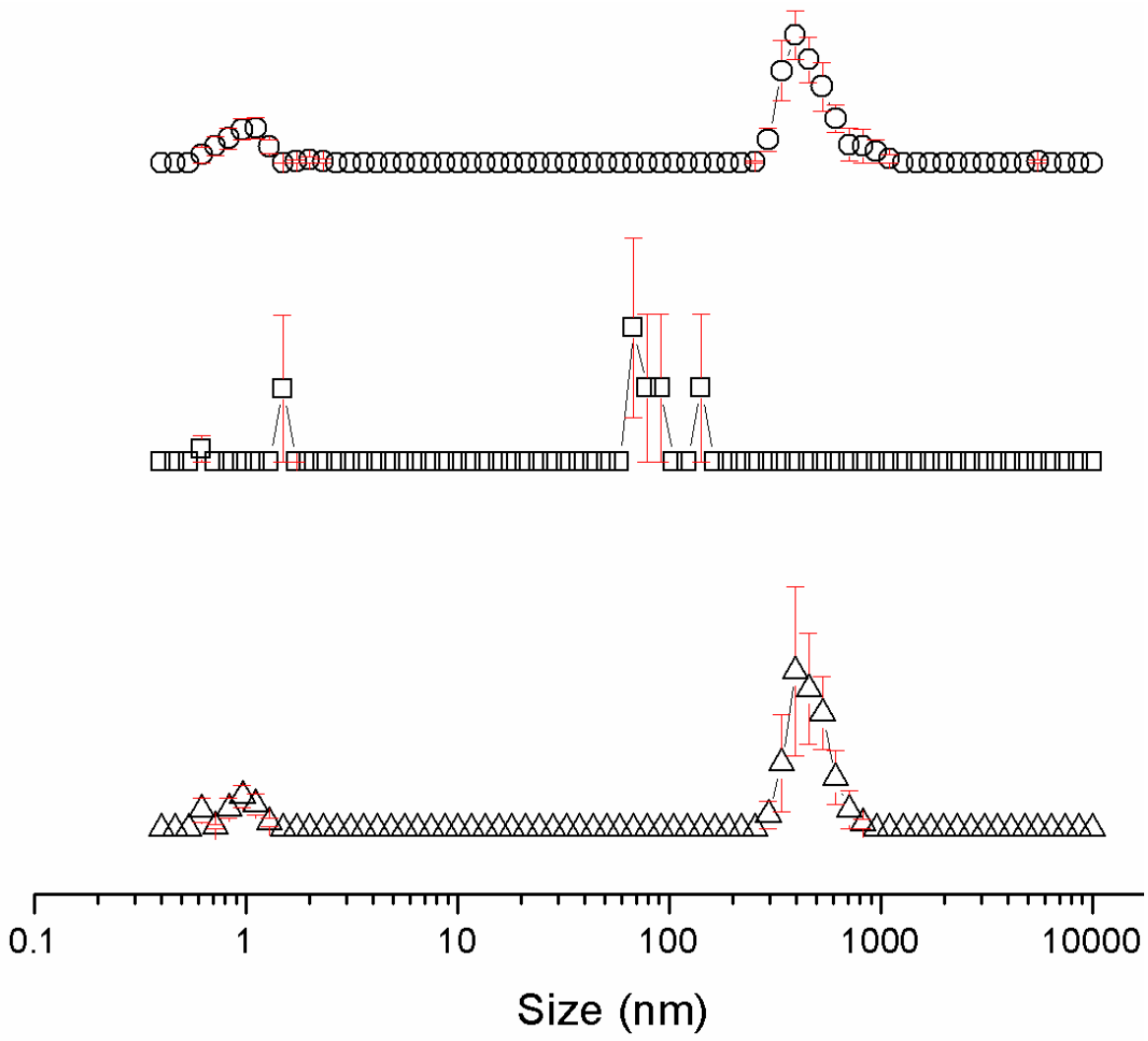

Figure S153 - Average intensity particle size distribution, calculated from 9 DLS runs, of aggregates formed by dissolving compound **4** at a concentration of 5.56 mM in DMSO at Δ) 25 °C, □) heating to 40 °C and ○) cooling to 25 °C. Only 9 of the available 10 DLS runs were used as in some cases, due to the heating and cooling processes there were some obvious temperature equilibration issues for the first run.

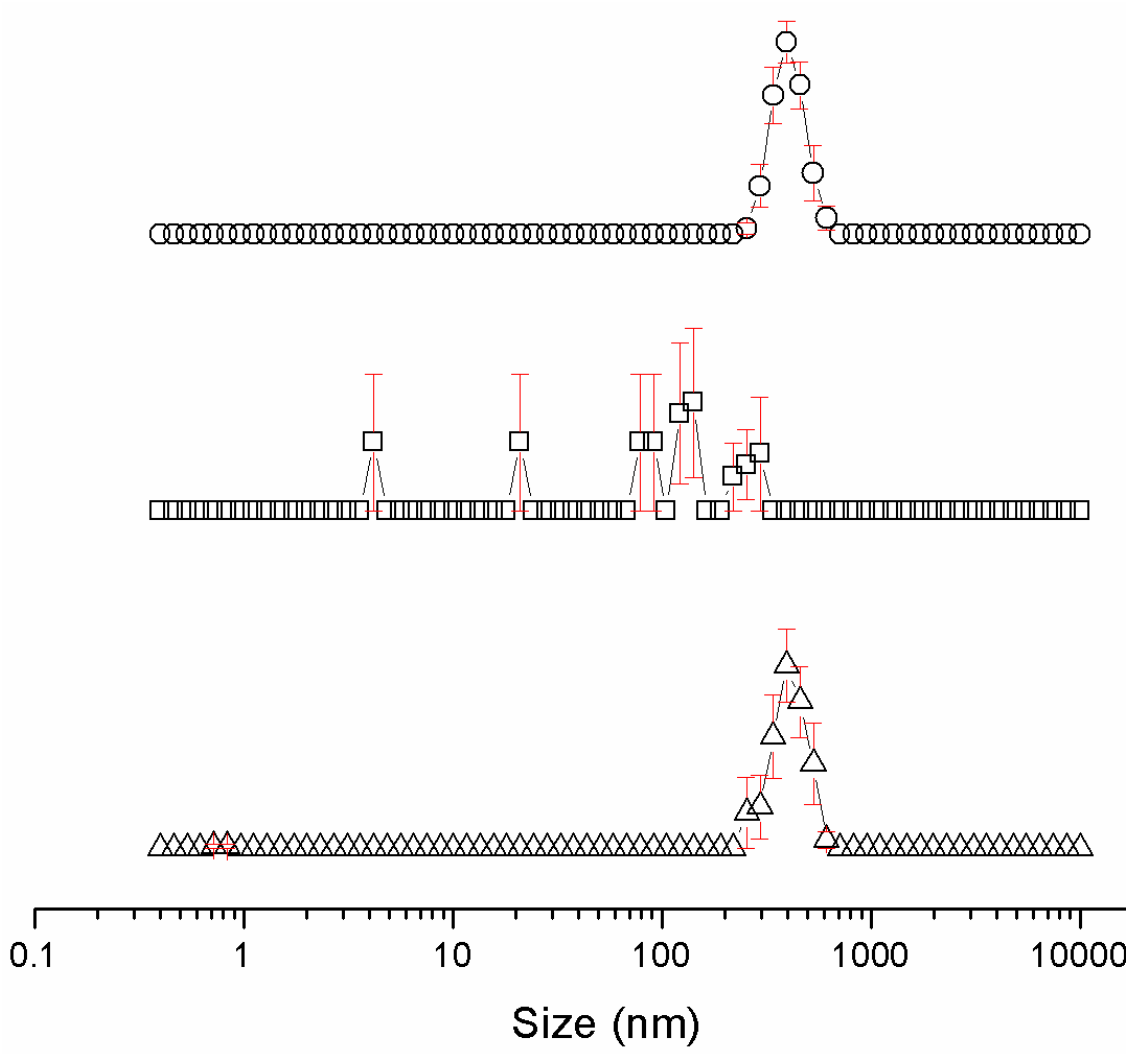

Figure S154 - Average intensity particle size distribution, calculated from 9 DLS runs, of aggregates formed by dissolving compound **4** at a concentration of O.56 mM in DMSO at Δ) 25 °C, □) heating to 40 °C and ○) cooling to 25 °C. Only 9 of the available 10 DLS runs were used as in some cases, due to the heating and cooling processes there were some obvious temperature equilibration issues for the first run.

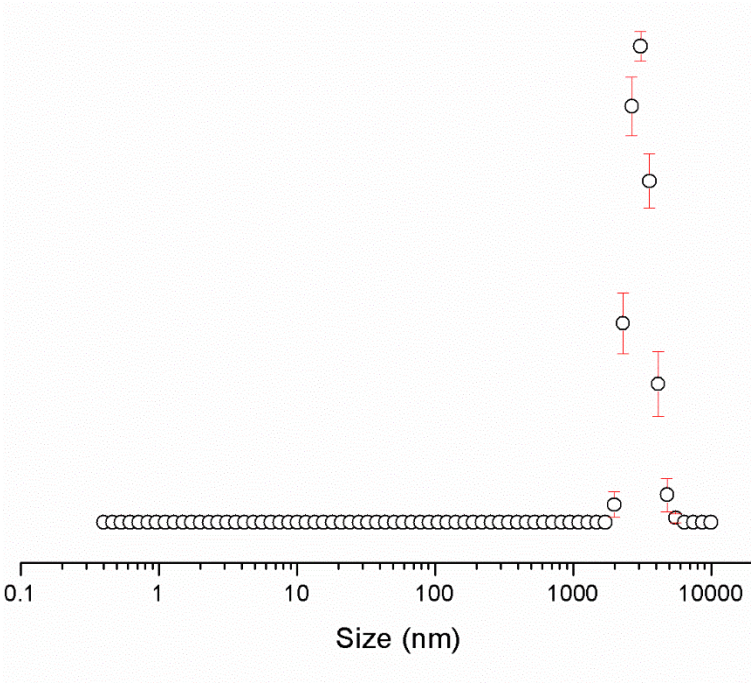

Figure S155 - Average intensity particle size distribution, calculated from 9 DLS runs, of aggregates formed by dissolving compound **4** at a concentration of 55.56 mM in a solution of DMSO 1: 1 H_2O, after heating to 40 ^oC and cooling to 25 ^oC. Only 9 of the available 10 DLS runs were used as in some cases, due to the heating and cooling processes there were some obvious temperature equilibration issues for the first run.

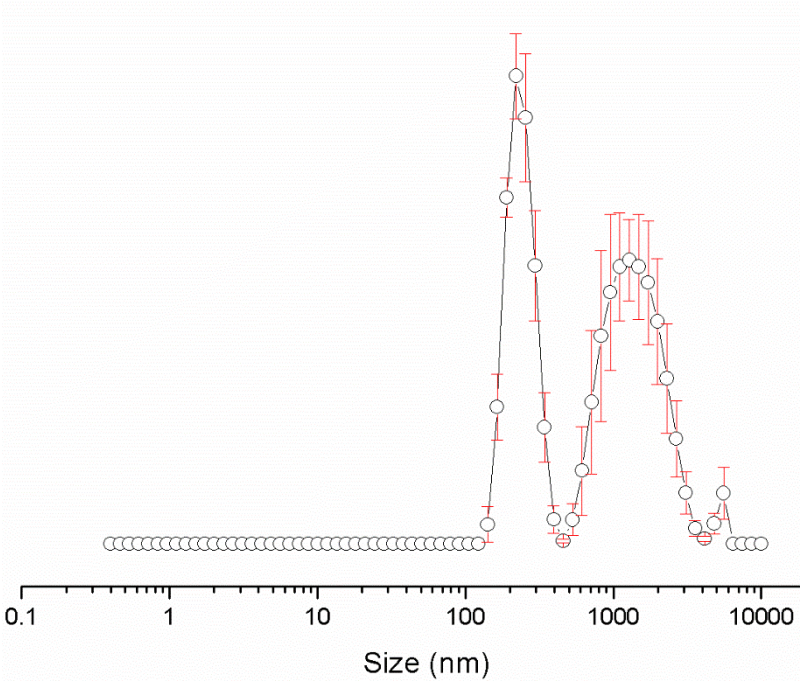

Figure S156 - Average intensity particle size distribution, calculated from 9 DLS runs, of aggregates formed by dissolving compound **4** at a concentration of 5.56 mM in a solution of DMSO: H_2O 1: 1, after heating to 40 ^oC and cooling to 25 ^oC. Only 9 of the available 10 DLS runs were used as in some cases, due to the heating and cooling processes there were some obvious temperature equilibration issues for the first run.

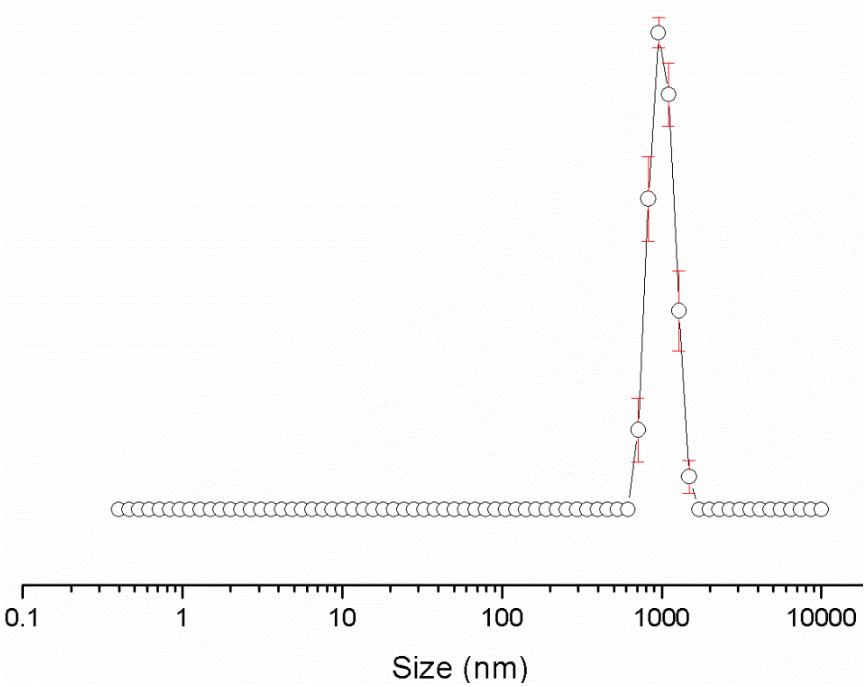

Figure S157 - Average intensity particle size distribution, calculated from 9 DLS runs, of aggregates formed by dissolving compound **4** at a concentration of 0.56 mM in a solution of DMSO: H_2O 1: 1, after heating to 40 ^oC and cooling to 25 ^oC. Only 9 of the available 10 DLS runs were used as in some cases, due to the heating and cooling processes there were some obvious temperature equilibration issues for the first run.

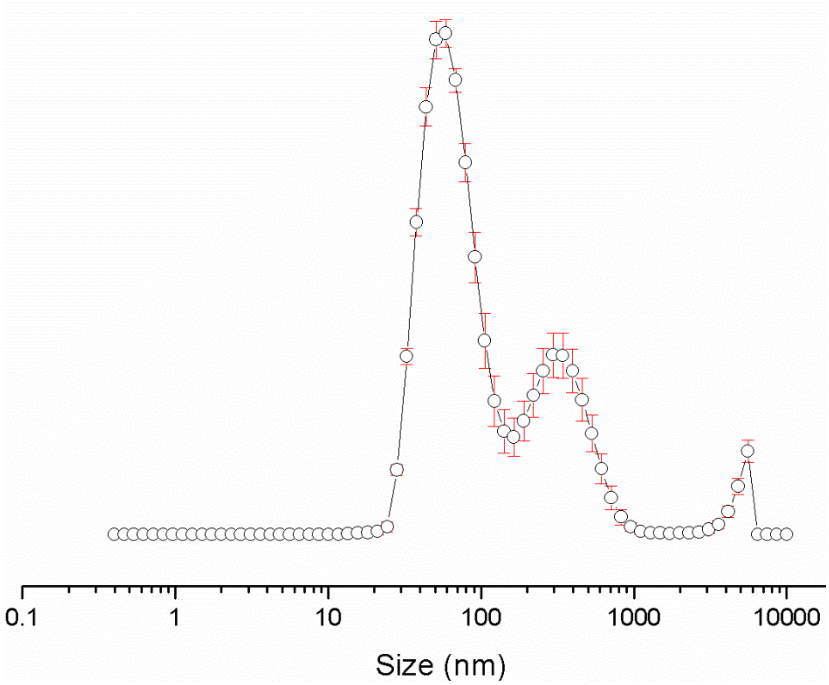

Figure S158 - Average intensity particle size distribution, calculated from 9 DLS runs, of aggregates formed by dissolving compound **4** at a concentration of 5.56 mM in a solution of DMSO: H_2O 3: 7, after heating to 40 ^oC and cooling to 25 ^oC. Only 9 of the available 10 DLS runs were used as in some cases, due to the heating and cooling processes there were some obvious temperature equilibration issues for the first run.

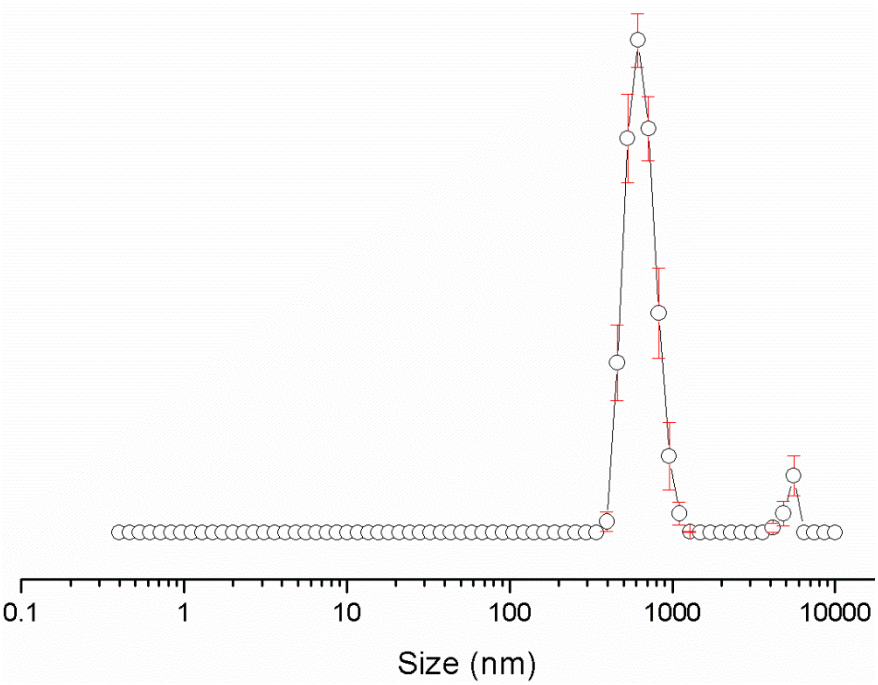

Figure S159 - Average intensity particle size distribution, calculated from 9 DLS runs, of aggregates formed by dissolving compound **4** at a concentration of 0.56 mM in a solution of DMSO: H_2O 3: 7, after heating to 40 ^oC and cooling to 25 ^oC. Only 9 of the available 10 DLS runs were used as in some cases, due to the heating and cooling processes there were some obvious temperature equilibration issues for the first run.

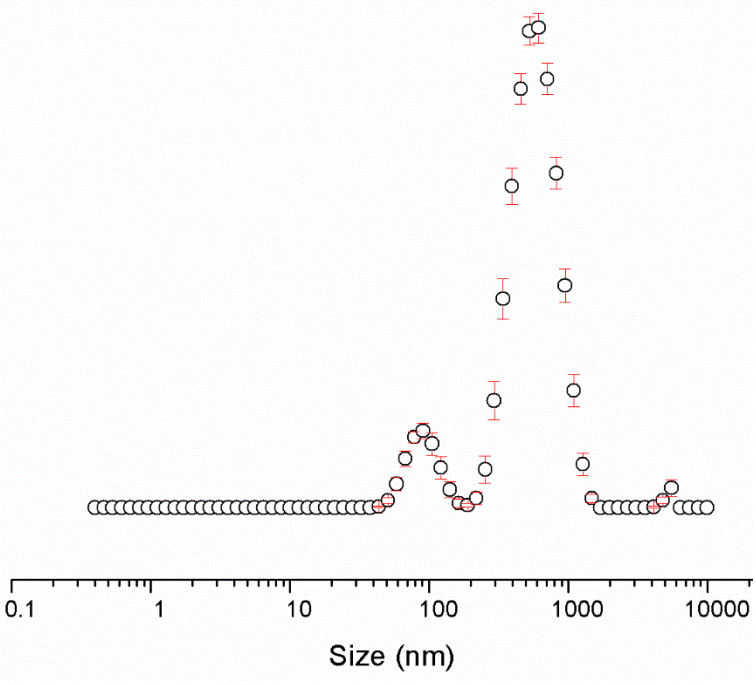

Figure S160 - Average intensity particle size distribution, calculated from 9 DLS runs, of aggregates formed by dissolving compound **4** at a concentration of 0.56 mM in a solution of DMSO: H_2O 1: 4, after heating to 40 ^oC and cooling to 25 ^oC. Only 9 of the available 10 DLS runs were used as in some cases, due to the heating and cooling processes there were some obvious temperature equilibration issues for the first run.

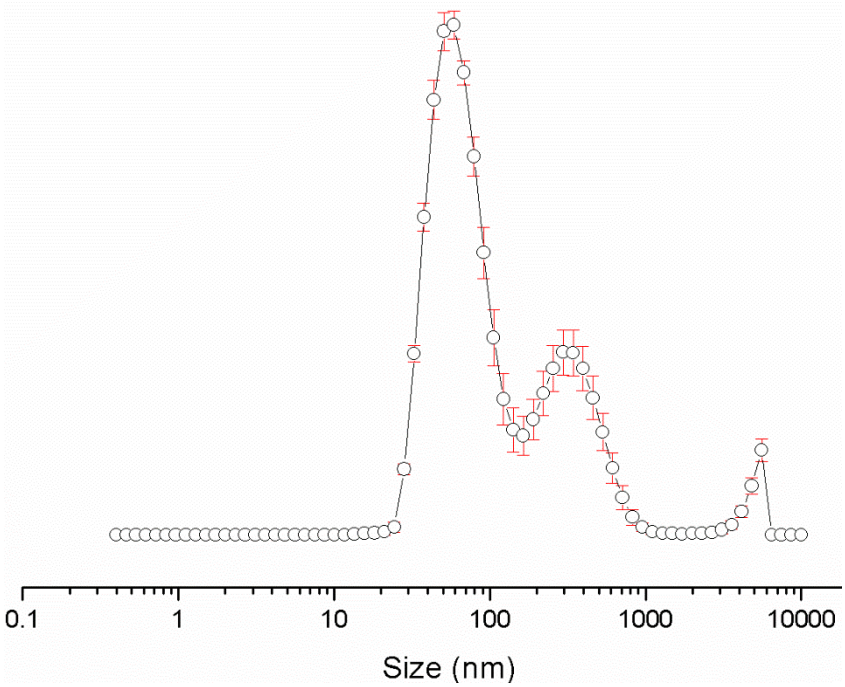

Figure S161 - Average intensity particle size distribution, calculated from 9 DLS runs, of aggregates formed by dissolving compound **4** at a concentration of 5.56 mM in a solution of EtOH: H_2O 1: 19, after heating to 40 ^oC and cooling to 25 ^oC. Only 9 of the available 10 DLS runs were used as in some cases, due to the heating and cooling processes there were some obvious temperature equilibration issues for the first run.

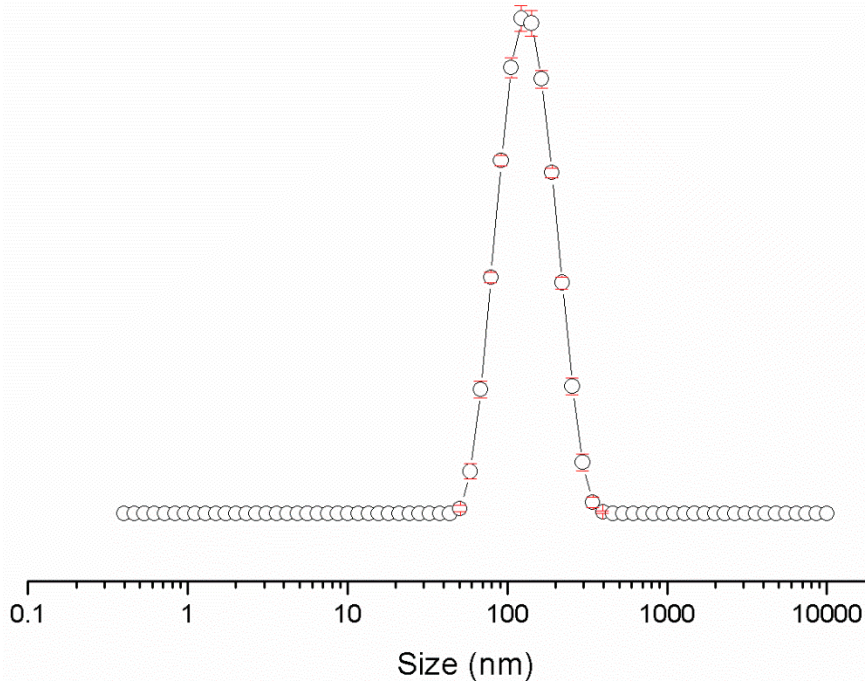

Figure S162 - Average intensity particle size distribution, calculated from 9 DLS runs, of aggregates formed by dissolving compound **4** at a concentration of 0.56 mM in a solution of EtOH: H_2O 1: 19, after heating to 40 ^oC and cooling to 25 ^oC. Only 9 of the available 10 DLS runs were used as in some cases, due to the heating and cooling processes there were some obvious temperature equilibration issues for the first run.

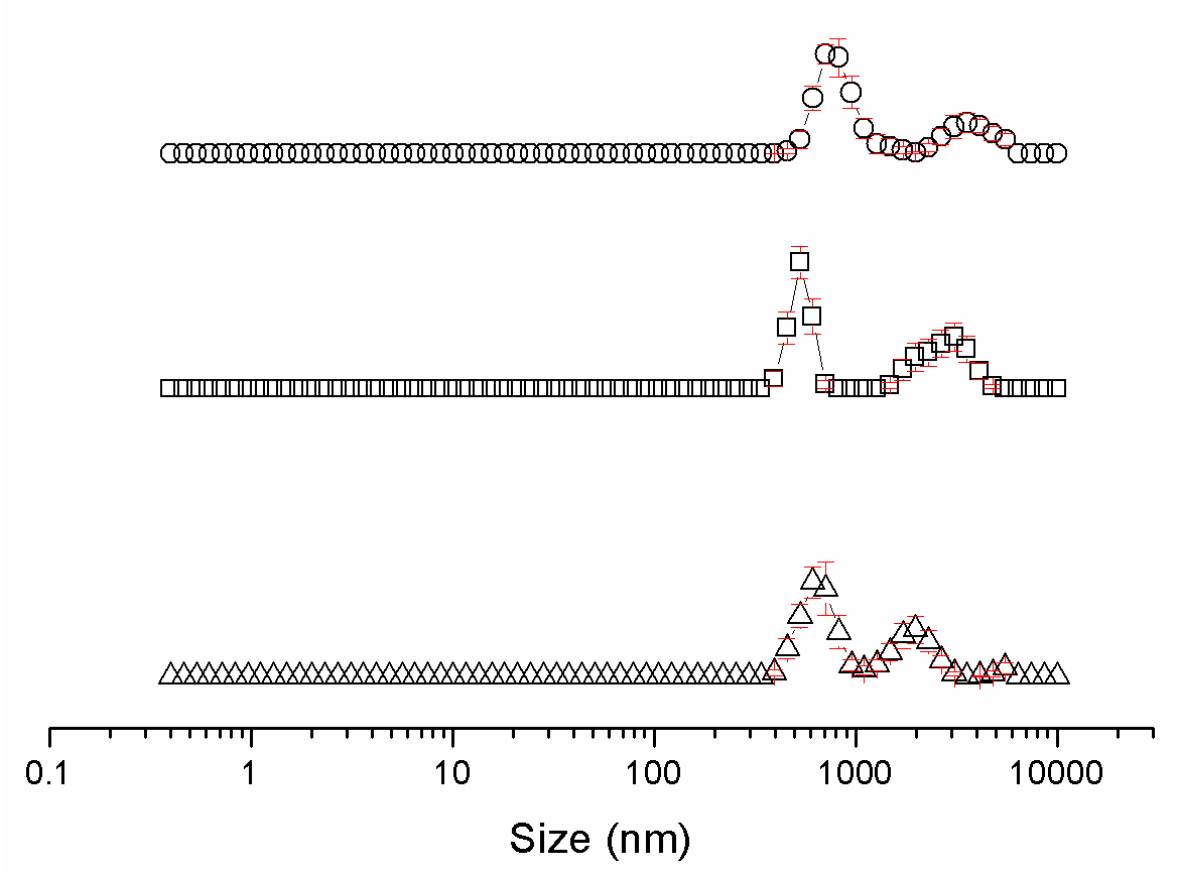

Figure S163 - Average intensity particle size distribution, calculated from 9 DLS runs, of aggregates formed by dissolving compound **5** at a concentration of 111.12 mM in DMSO at Δ) 25 °C, □) heating to 40 °C and ○) cooling to 25 °C. Only 9 of the available 10 DLS runs were used as in some cases, due to the heating and cooling processes there were some obvious temperature equilibration issues for the first run.

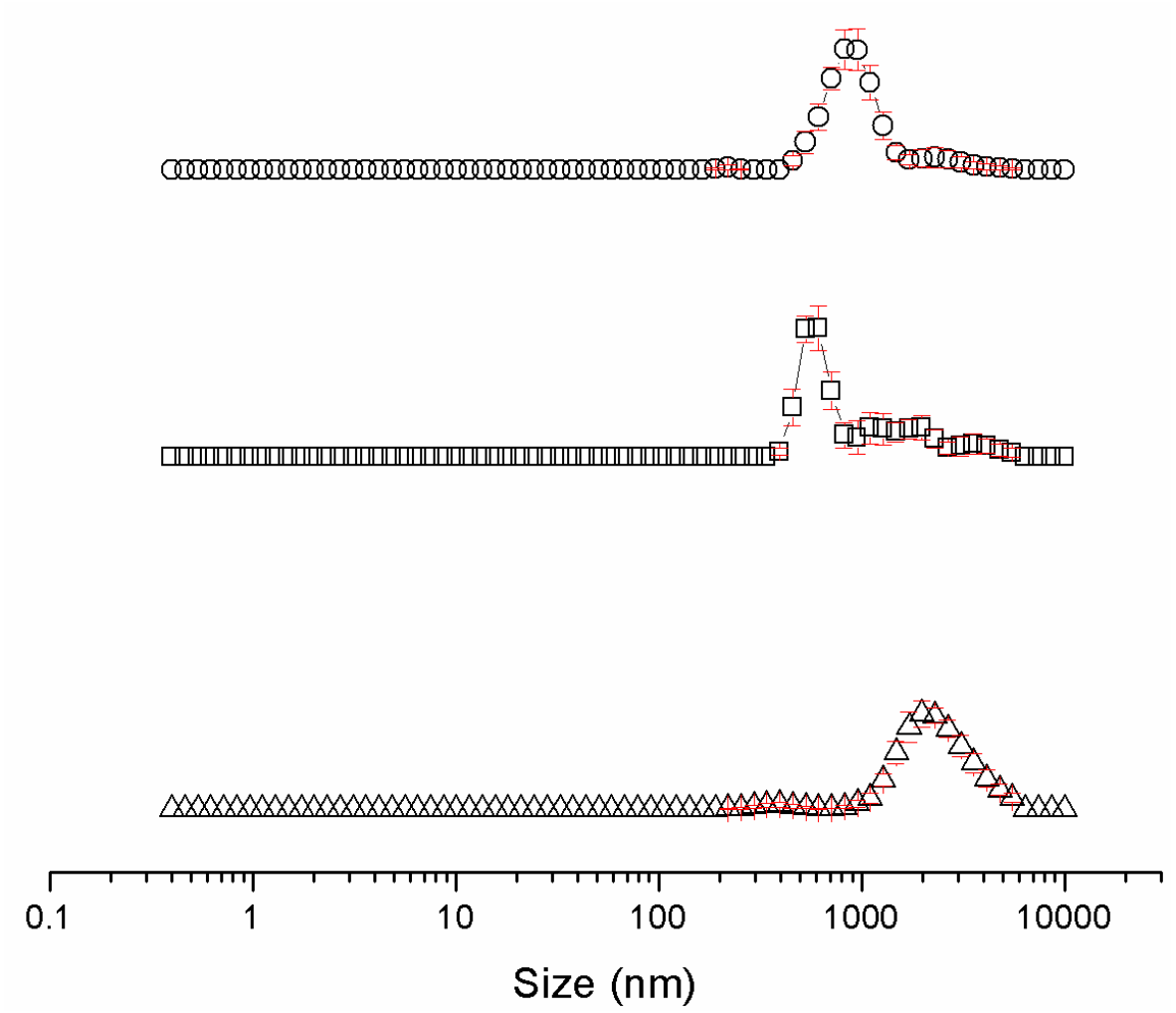

Figure S164 - Average intensity particle size distribution, calculated from 9 DLS runs, of aggregates formed by dissolving compound **5** at a concentration of 55.56 mM in DMSO at Δ) 25 °C, □) heating to 40 °C and ○) cooling to 25 °C. Only 9 of the available 10 DLS runs were used as in some cases, due to the heating and cooling processes there were some obvious temperature equilibration issues for the first run.

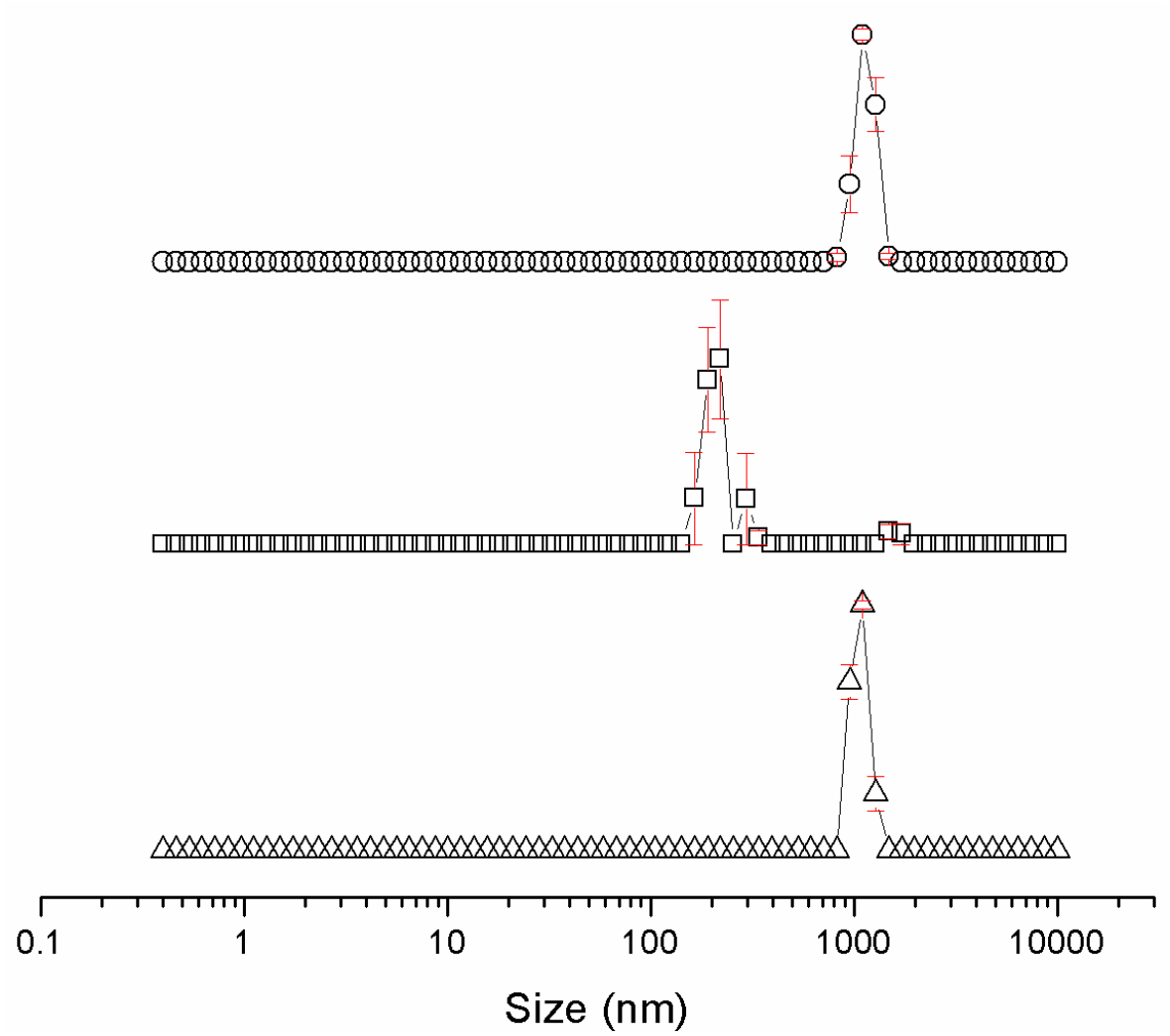

Figure S165 - Average intensity particle size distribution, calculated from 9 DLS runs, of aggregates formed by dissolving compound **5** at a concentration of 5.56 mM in DMSO at Δ) 25 °C, □) heating to 40 °C and ○) cooling to 25 °C. Only 9 of the available 10 DLS runs were used as in some cases, due to the heating and cooling processes there were some obvious temperature equilibration issues for the first run.

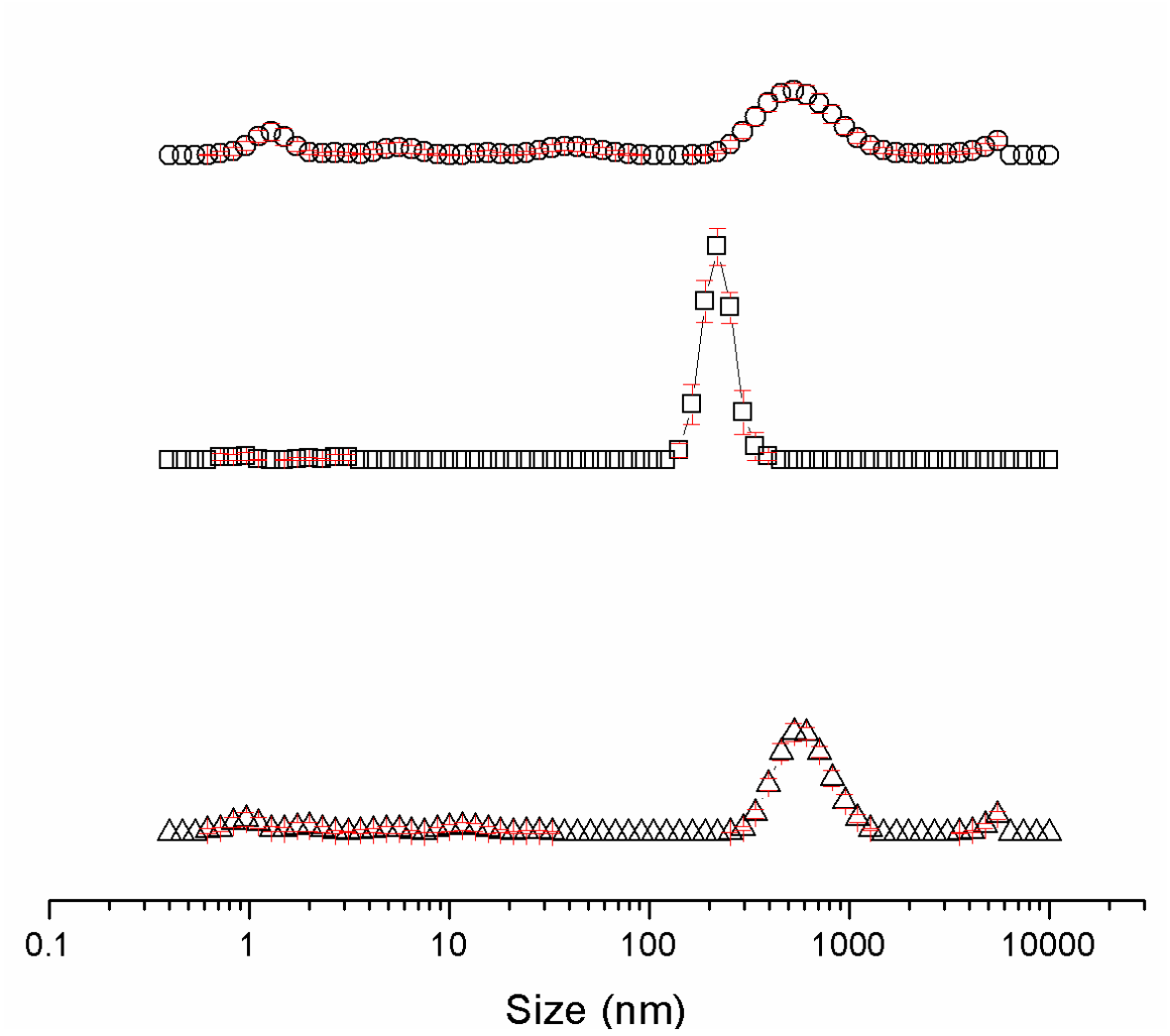

Figure S166 - Average intensity particle size distribution, calculated from 9 DLS runs, of aggregates formed by dissolving compound **5** at a concentration of 0.56 mM in DMSO at Δ) 25 °C, □) heating to 40 °C and ○) cooling to 25 °C. Only 9 of the available 10 DLS runs were used as in some cases, due to the heating and cooling processes there were some obvious temperature equilibration issues for the first run.

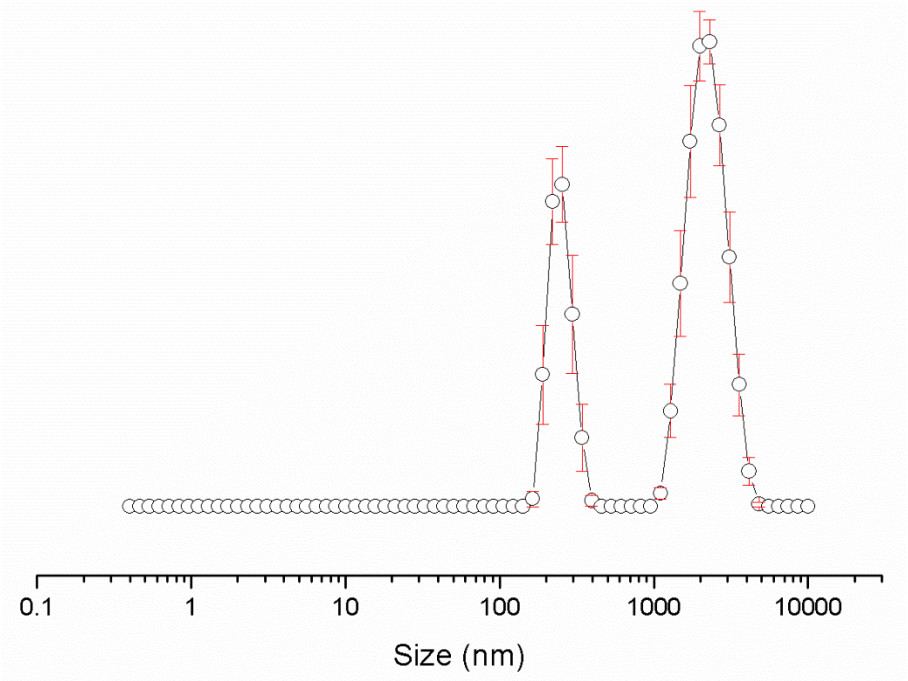

Figure S167 - Average intensity particle size distribution, calculated from 9 DLS runs, of aggregates formed by dissolving compound **5** at a concentration of 55.56 mM in a solution of DMSO: H_2O 1: 1, after heating to 40 ^oC and cooling to 25 ^oC. Only 9 of the available 10 DLS runs were used as in some cases, due to the heating and cooling processes there were some obvious temperature equilibration issues for the first run.

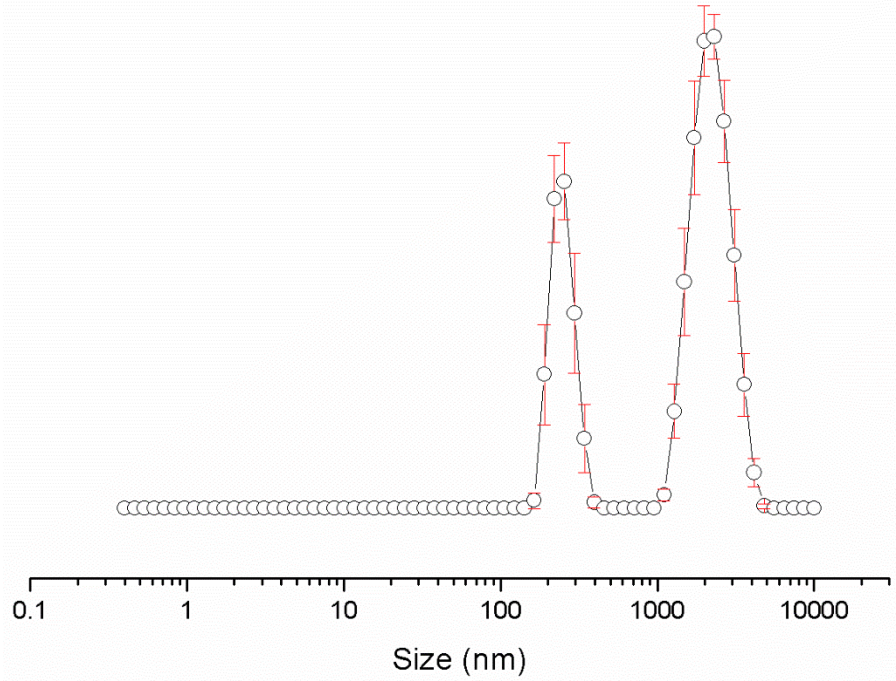

Figure S168 - Average intensity particle size distribution, calculated from 9 DLS runs, of aggregates formed by dissolving compound **5** at a concentration of 5.56 mM in a solution of DMSO: H_2O 1: 1, after heating to 40 ^oC and cooling to 25 ^oC. Only 9 of the available 10 DLS runs were used as in some cases, due to the heating and cooling processes there were some obvious temperature equilibration issues for the first run.

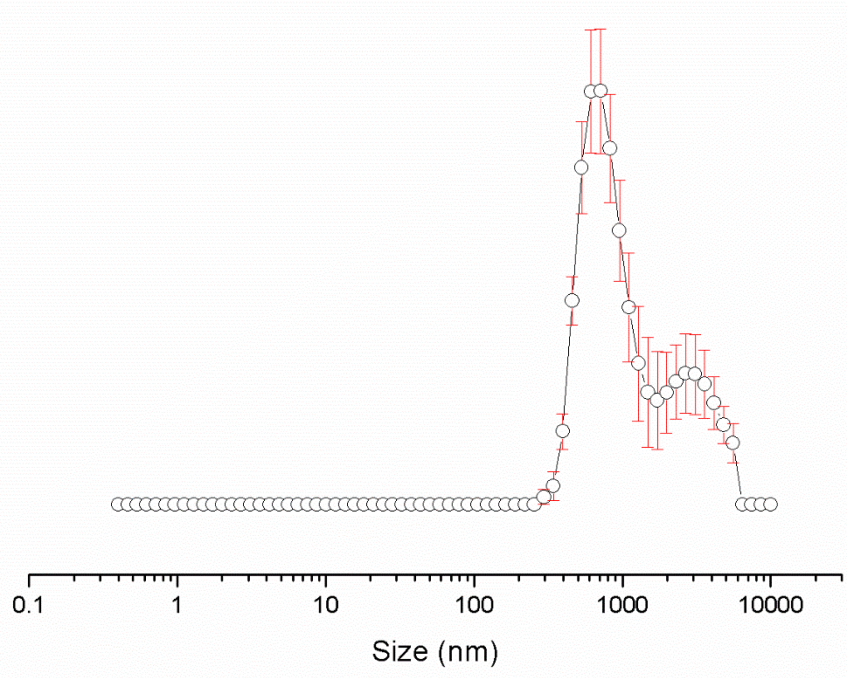

Figure S169 - Average intensity particle size distribution, calculated from 9 DLS runs, of aggregates formed by dissolving compound **5** at a concentration of 0.56 mM in a solution of DMSO: H_2O 1: 1, after heating to 40 ^oC and cooling to 25 ^oC. Only 9 of the available 10 DLS runs were used as in some cases, due to the heating and cooling processes there were some obvious temperature equilibration issues for the first run.

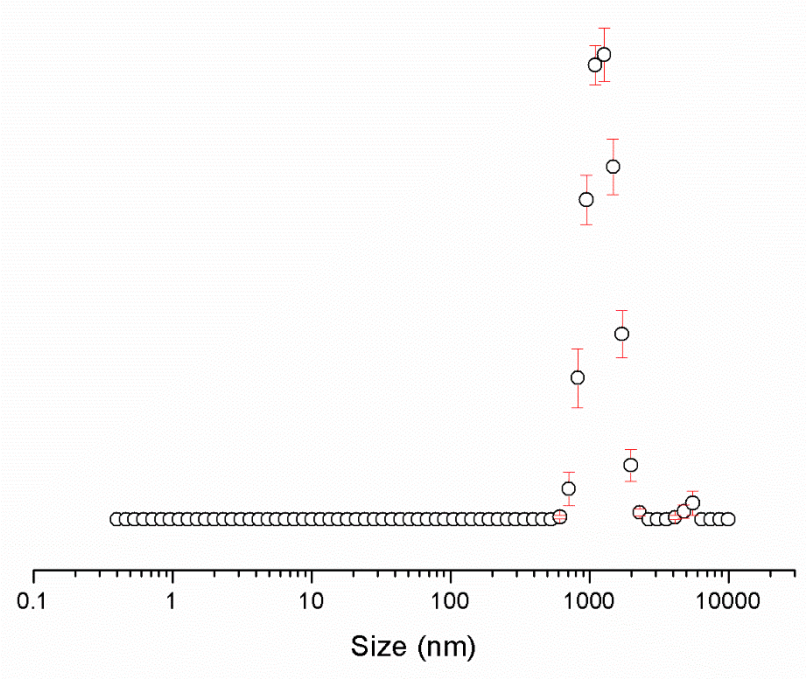

Figure S170 - Average intensity particle size distribution, calculated from 9 DLS runs, of aggregates formed by dissolving compound **5** at a concentration of 5.56 mM in a solution of DMSO: H_2O 3: 7, after heating to 40 ^oC and cooling to 25 ^oC. Only 9 of the available 10 DLS runs were used as in some cases, due to the heating and cooling processes there were some obvious temperature equilibration issues for the first run.

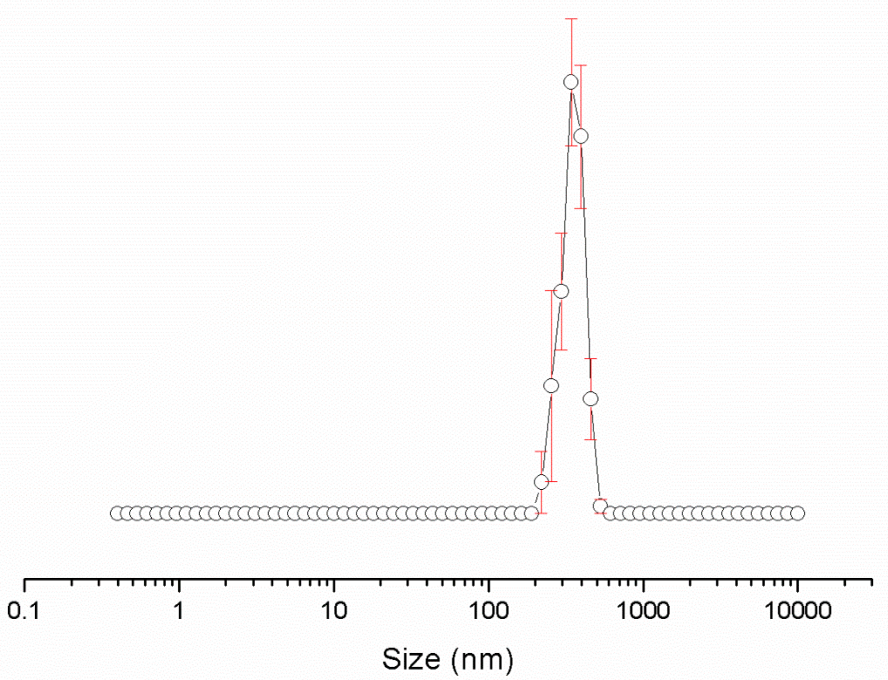

Figure S171 - Average intensity particle size distribution, calculated from 9 DLS runs, of aggregates formed by dissolving compound **5** at a concentration of 0.56 mM in a solution of DMSO: H_2O 3: 7, after heating to 40 ^oC and cooling to 25 ^oC. Only 9 of the available 10 DLS runs were used as in some cases, due to the heating and cooling processes there were some obvious temperature equilibration issues for the first run.

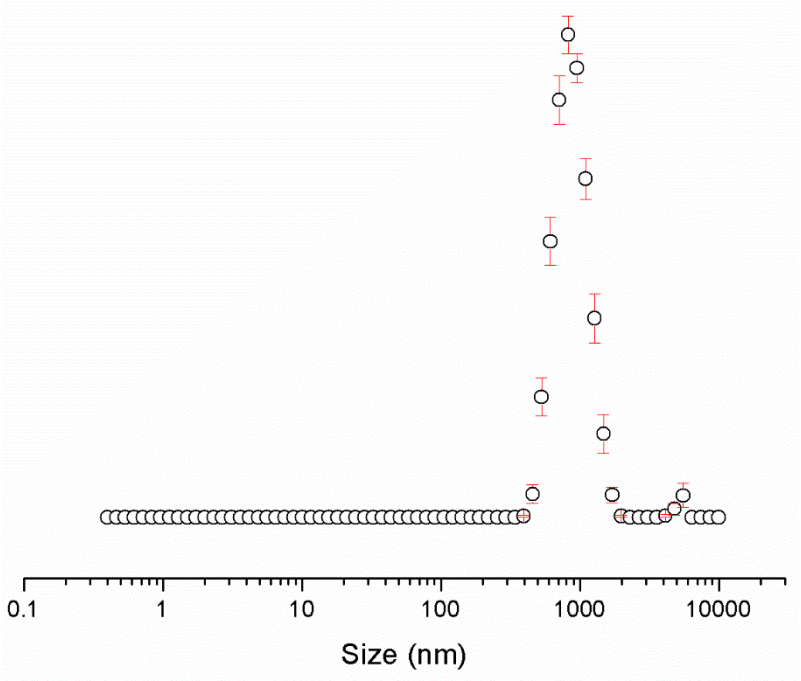

Figure S172 - Average intensity particle size distribution, calculated from 9 DLS runs, of aggregates formed by dissolving compound **5** at a concentration of 0.56 mM in a solution of DMSO: H_2O 1: 4, after heating to 40 ^oC and cooling to 25 ^oC. Only 9 of the available 10 DLS runs were used as in some cases, due to the heating and cooling processes there were some obvious temperature equilibration issues for the first run.

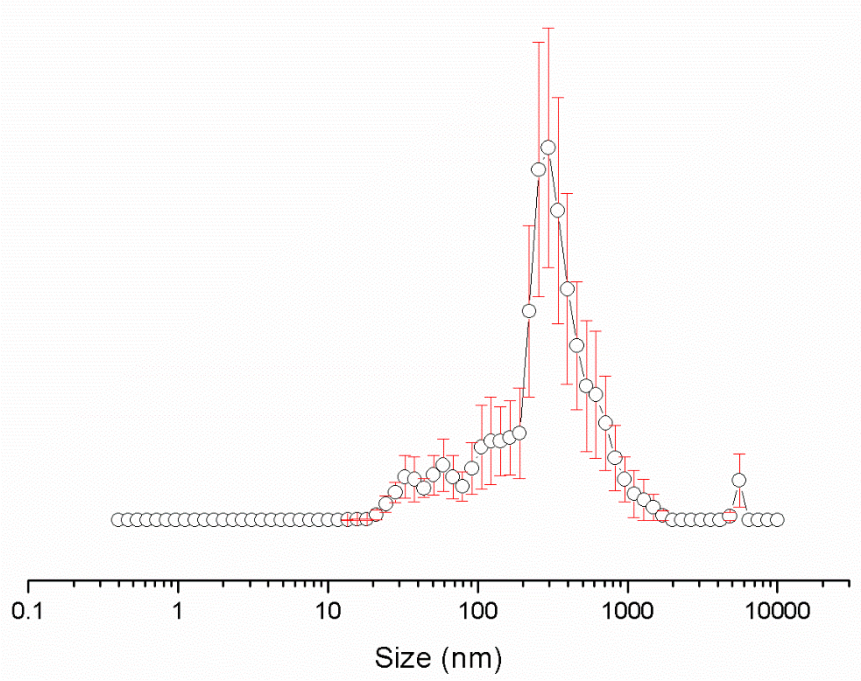

Figure S173 - Average intensity particle size distribution, calculated from 9 DLS runs, of aggregates formed by dissolving compound **5** at a concentration of 5.56 mM in a solution of EtOH: H_2O 1: 19, after heating to 40 ^oC and cooling to 25 ^oC. Only 9 of the available 10 DLS runs were used as in some cases, due to the heating and cooling processes there were some obvious temperature equilibration issues for the first run.

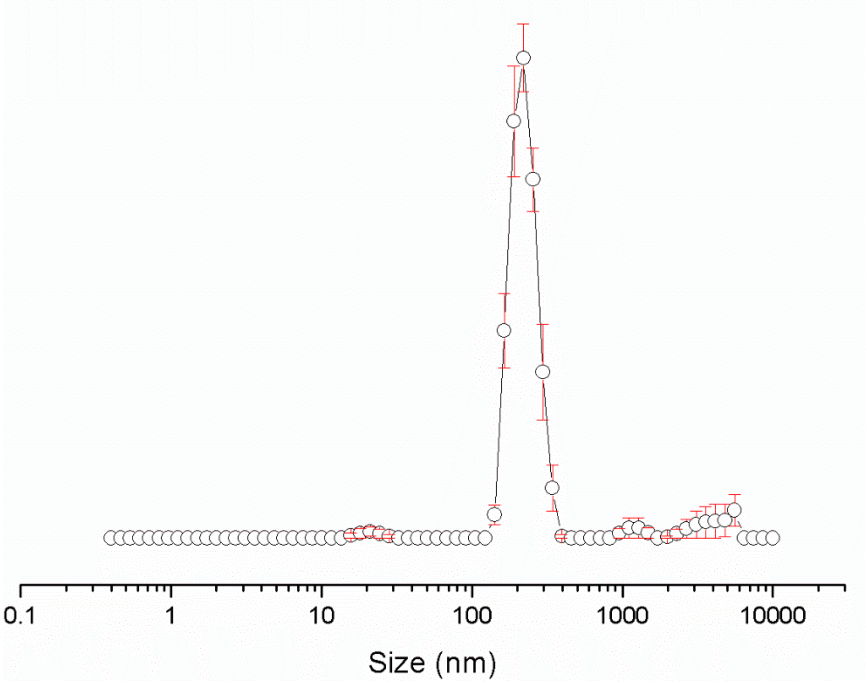

Figure S174 - Average intensity particle size distribution, calculated from 9 DLS runs, of aggregates formed by dissolving compound **5** at a concentration of 0.56 mM in a solution of EtOH: H_2O 1: 19, after heating to 40 ^oC and cooling to 25 ^oC. Only 9 of the available 10 DLS runs were used as in some cases, due to the heating and cooling processes there were some obvious temperature equilibration issues for the first run.

Count Rate

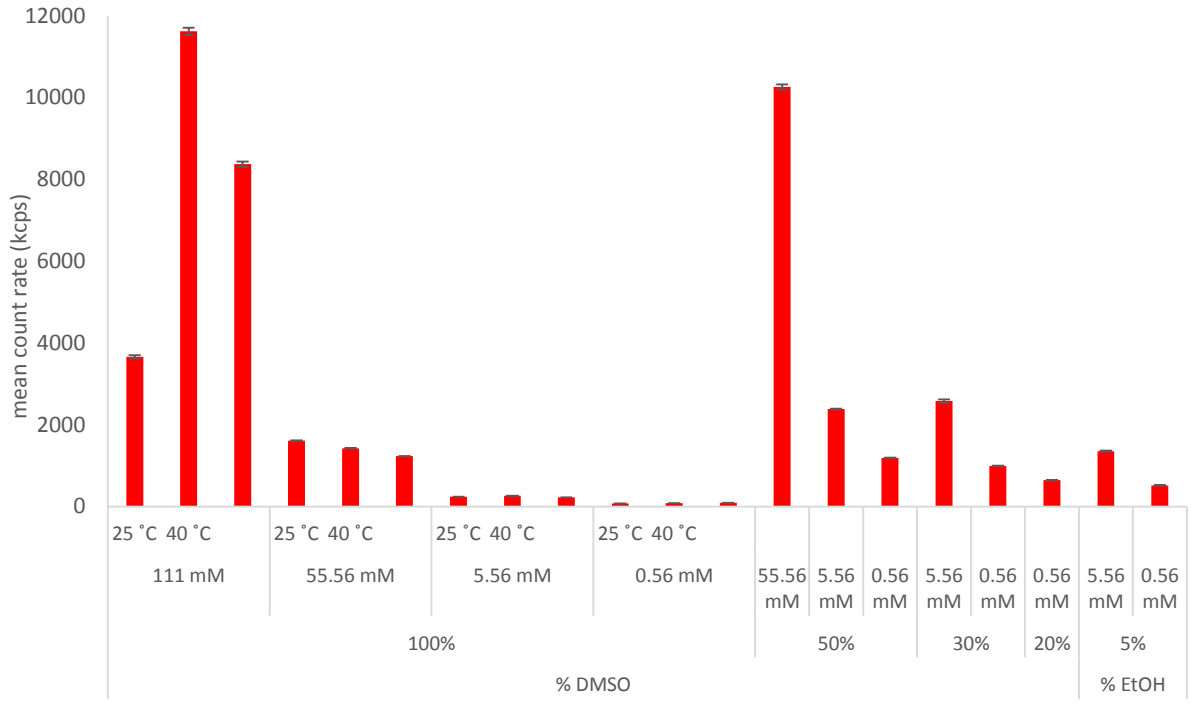

Figure S175 - Graph illustrating the average count rate from 9 DLS runs of compound **1** in aqueous DMSO/EtOH solvent mixtures at a temperature of 25°C, after heating to 40°C unless stated otherwise.

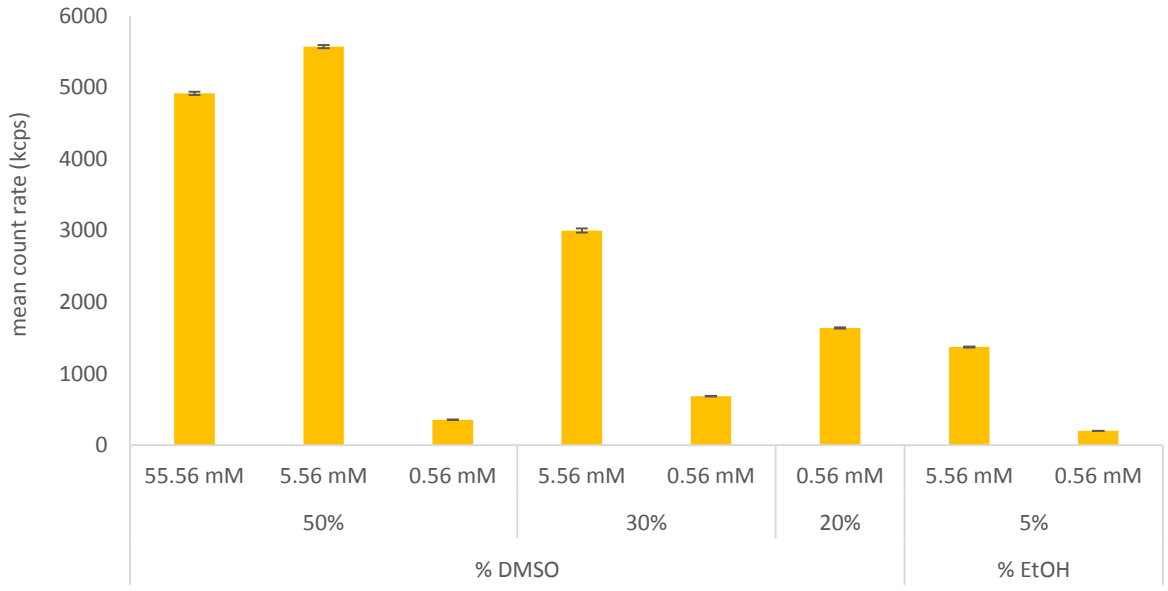

Figure S176 - Graph illustrating the average count rate for 9 DLS runs of compound **2** in aqueous DMSO/EtOH solvent mixtures at a temperature of 25°C, after heating to 40°C.

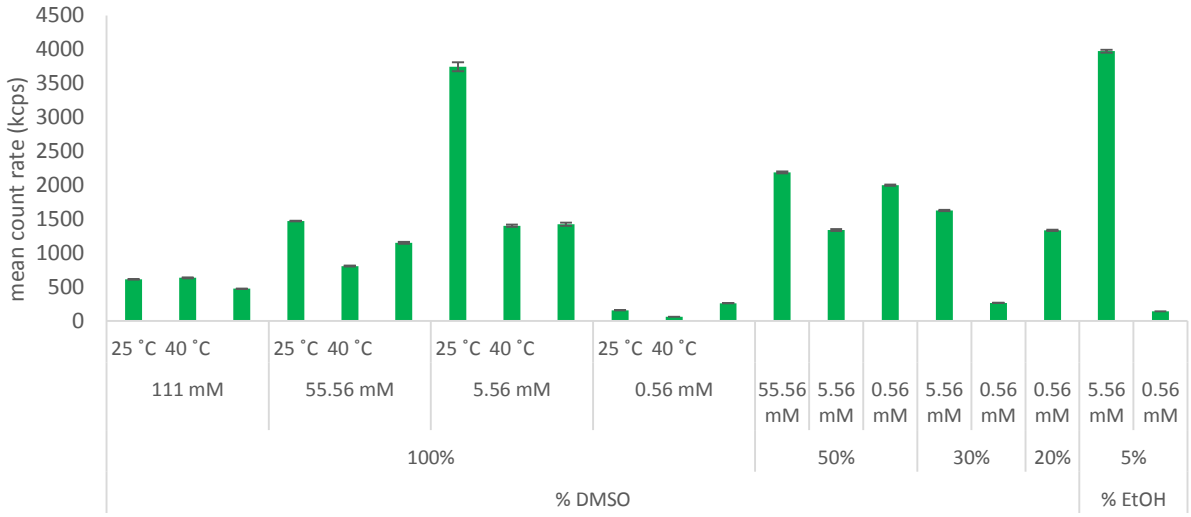

Figure S177- Graph illustrating the average count rate for 9 DLS runs of compound **3** in aqueous DMSO/EtOH solvent mixtures at a temperature of 25°C, after heating to 40°C unless stated otherwise.

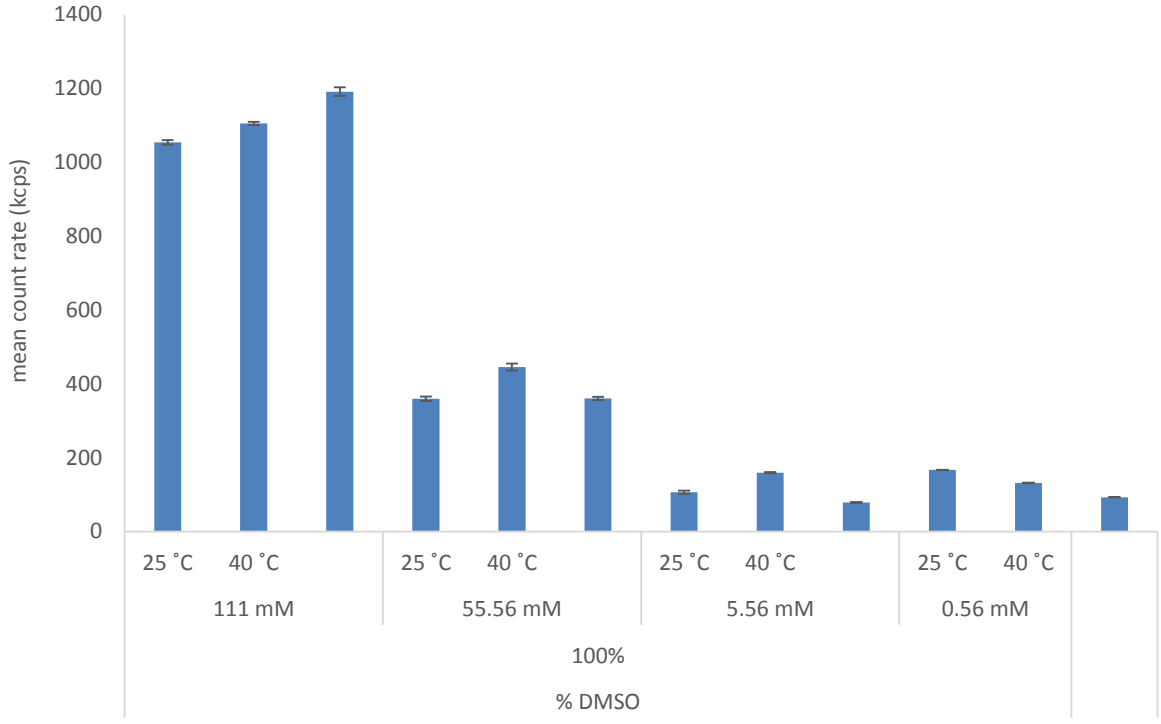

Figure S178- Graph illustrating the average count rate for 9 DLS runs of compound **4** in DMSO at a temperature of 25°C, after heating to 40°C unless stated otherwise.

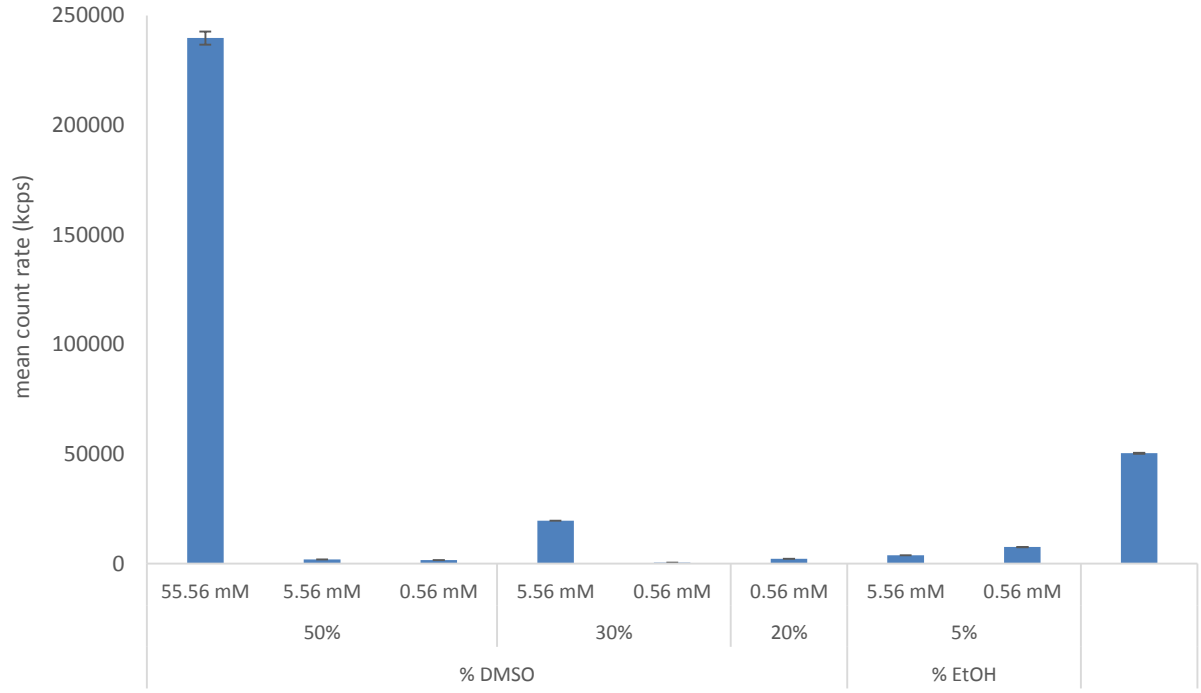

Figure S179- Graph illustrating the average count rate for 9 DLS runs of compound **4** in aqueous DMSO/EtOH solvent mixtures, at a temperature of 25°C, after heating to 40°C.

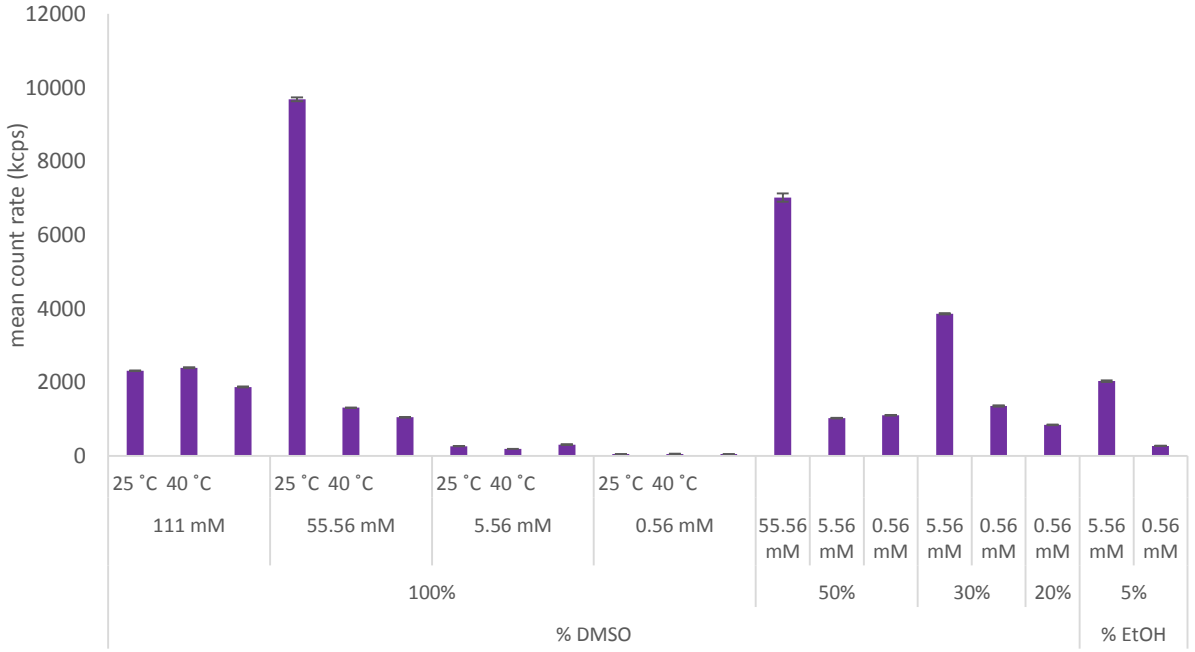

Figure S180 - Graph illustrating the average count rate for 9 DLS runs of compound **5** in aqueous DMSO/EtOH solvent mixtures, at a temperature of 25°C, after heating to 40°C unless stated otherwise.

Comparative overview of DLS results

Table S1 – Average intensity particle size distributions for compounds **1, 3, 4** and **5**, calculated from 9 DLS runs. Samples were prepared in series, with an aliquot of the most concentrated solution undergoing serial dilution and measured at 25 ^{o}C after heating to 40 ^{o}C and cooling to 25 ^{o}C.

Solvent	Conc. (mM)	**1**		**2**	**3**		**4**		**5**	
		peak maxima		peak maxima	peak maxima		peak maxima		peak maxima	
DMSO	111.12	458.7	1718	*a**	955.4	3091	615.1	1.11	712.4	3580
	55.56	825	58.77	*a**	825		615.1	1.11	825	220.2
	5. 56	531.2	105.7	*a**	615.1**		396.1	1.11	1106	
	0.56	531.2		*a**	531.2		396.1		531.2	0.72

*a** - DLS Size distribution in a solution of DMSO for compound **2** could not be gathered due to the inherent absorbance and fluorescent characteristics of this compound.

Table S2 – Average intensity particle size distribution of compounds **1**, **3**, **4** and **5**, calculated from 9 DLS runs in different solvent conditions at concentrations of 5.56 Mm and 0.56 mM. Samples were prepared in series, with an aliquot of the most concentrated solution undergoing serial dilution and measured after heating to 40 ^{o}C and cooling to 25 ^{o}C.

Solvent conditions		Conc. (mM)	**1**		**2**		**3**		**4**		**5**	
			peak maxima		peak maxima		peak maxima		peak maxima		peak maxima	
DMSO		5. 56	531.2	106	*a**		615.1		396.1	1.11	1106	
		0.56	531.2		*a**		531.2		396.1		531.2	0.72
DMSO : H_2O	1 : 1	5. 56	1990		615.1		1990	458.7	220.2	1281	2305	255
		0.56	1106		955		531.2		955		712.4	2669
	3 : 7	5. 56	342		825		1106		458.7	78.82	1281	
		0.56	396.1		396.1		615.1		615.1		342	
	1 : 4	0.56	58.77	342	342	68	712.4		91.28	615.1	825	
EtOH : H_2O	1 : 19	5. 56	220.2		164.2		220.2		58.77	295.3	295.3	
		0.56	164.2		255		396.1	0.83	122		220.2	

*a** - DLS Size distribution in a solution of DMSO for compound **2** could not be gathered due to the inherent absorbance and fluorescent characteristics of this compound.

Zeta potential

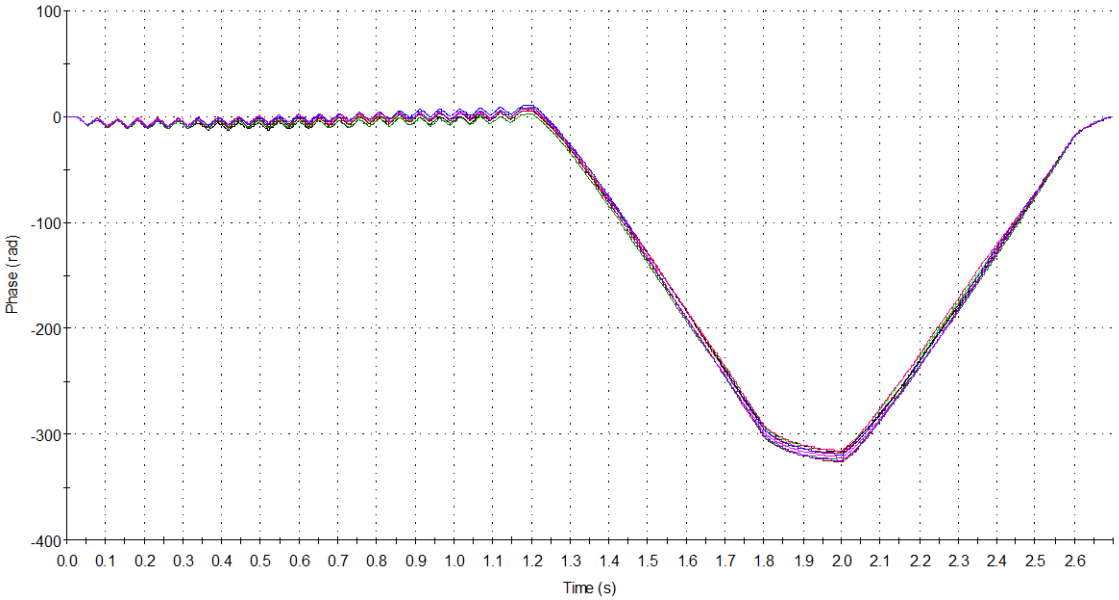

Figure S181 - Phase plot taken during the measurement of 9 Zeta Potential Transfer Standard (PTS) runs of compound **1** at a concentration of 5.56 mM in a solution of EtOH: H_2O 1: 19. Average measurement value = -81.5 mV.

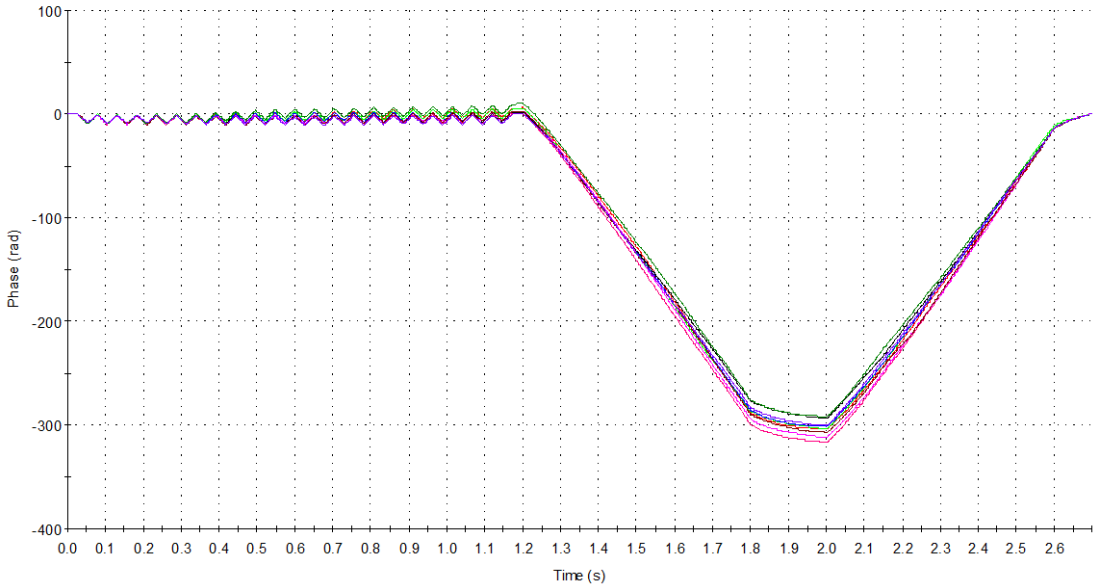

Figure S182 - Phase plot taken during the measurement of 9 Zeta Potential Transfer Standard (PTS) runs of compound **2** at a concentration of 5.56 mM in a solution EtOH: H_2O 1: 19. Average measurement value -96.2 mV.

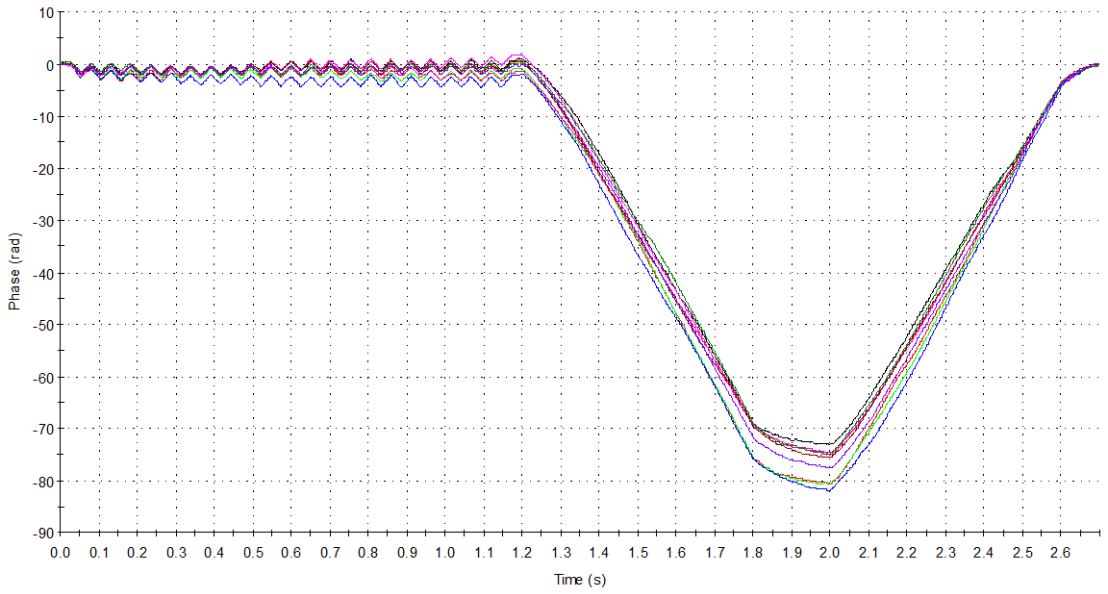

Figure S183 - Phase plot taken during the measurement of 9 Zeta Potential Transfer Standard (PTS) runs of compound **3** at a concentration of 5.56 mM in a solution EtOH: H_2O 1: 19. Average measurement value **-**18.5 mV.

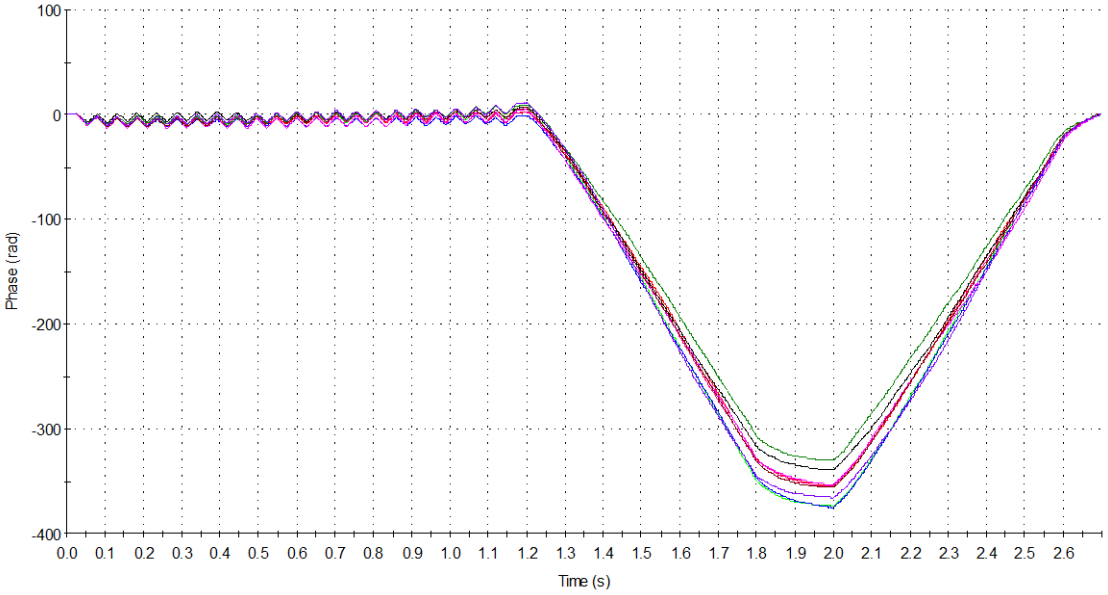

Figure S184 - Phase plot taken during the measurement of 9 Zeta Potential Transfer Standard (PTS) runs of compound **4** at a concentration of 5.56 mM in a solution EtOH: H_2O 1: 19. Average measurement value **-**101 mV.

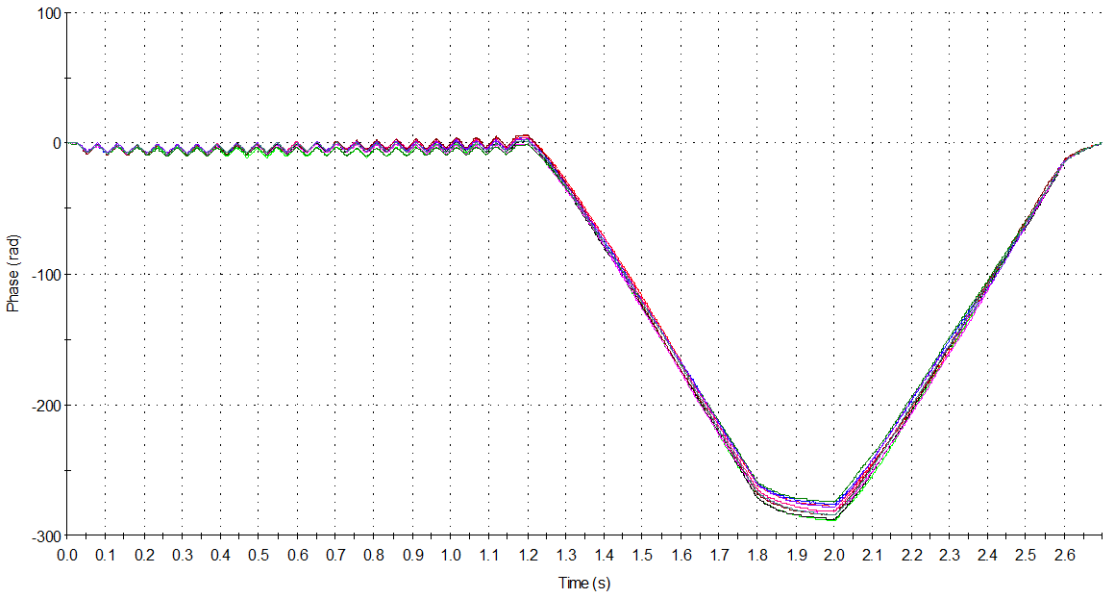

Figure S185 - Phase plot taken during the measurement of 9 Zeta Potential Transfer Standard (PTS) runs of compound **5** at a concentration of 5.56 mM in a solution EtOH: H_2O 1: 19. Average measurement value **-**79.3 mV.

UV-Vis spectra

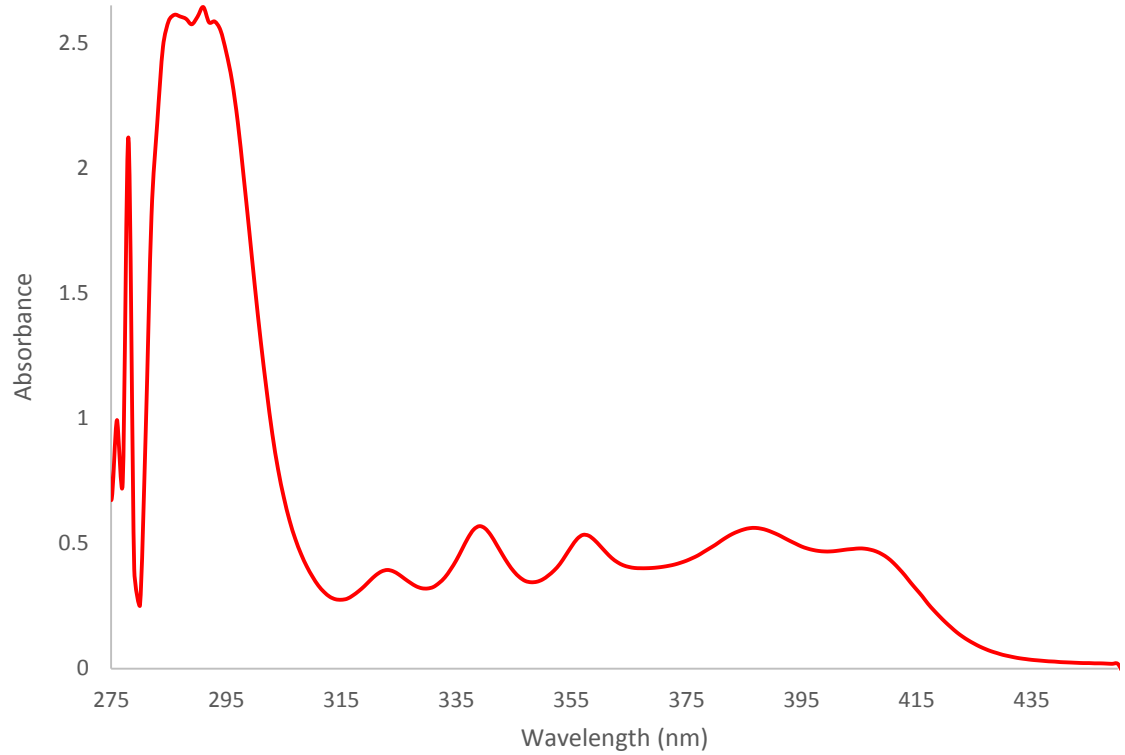

Figure S186 - UV-Vis spectra of compound **1** (0.30 mM) in DMSO.

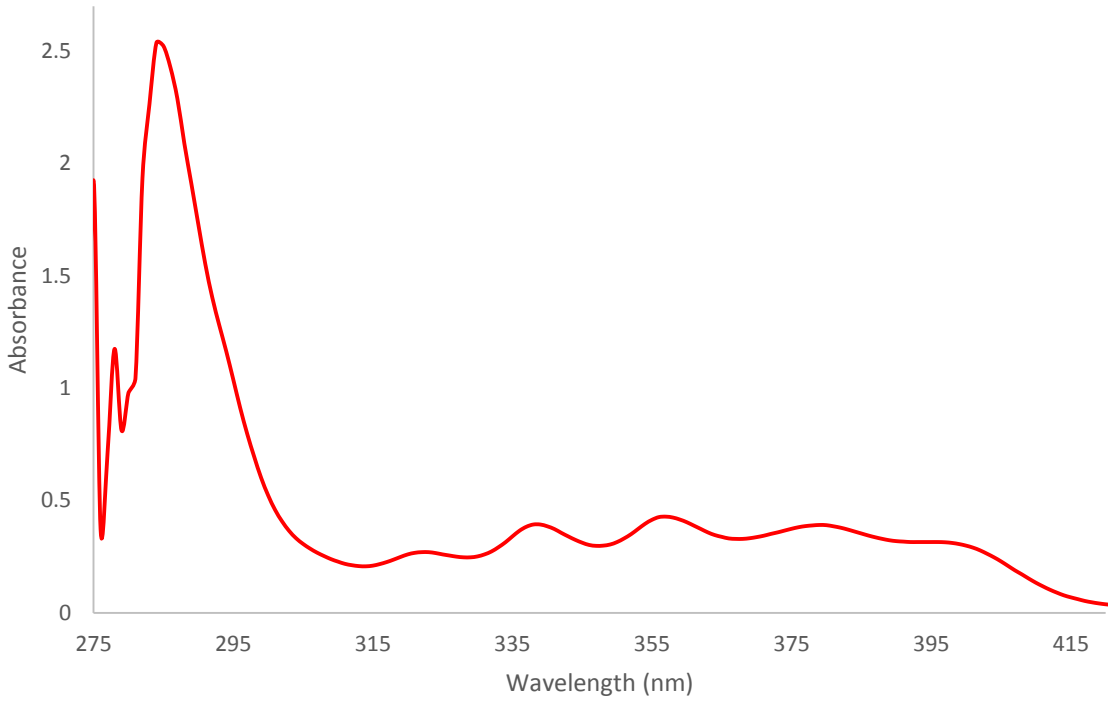

Figure S187 - UV-Vis spectra of compound **1** (0.30 mM) in a solution of DMSO: H_2O 1: 1.

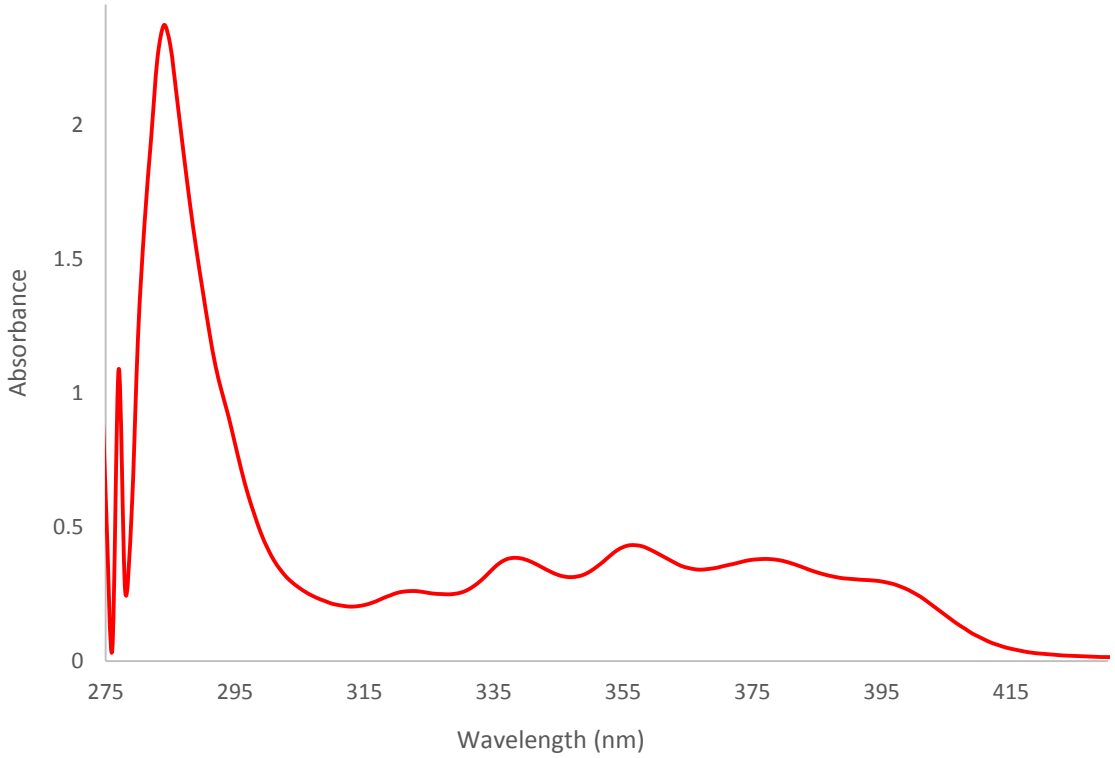

Figure S188 - UV-Vis spectra of compound **1** (0.30 mM) in a solution of DMSO: H_2O 2: 7.

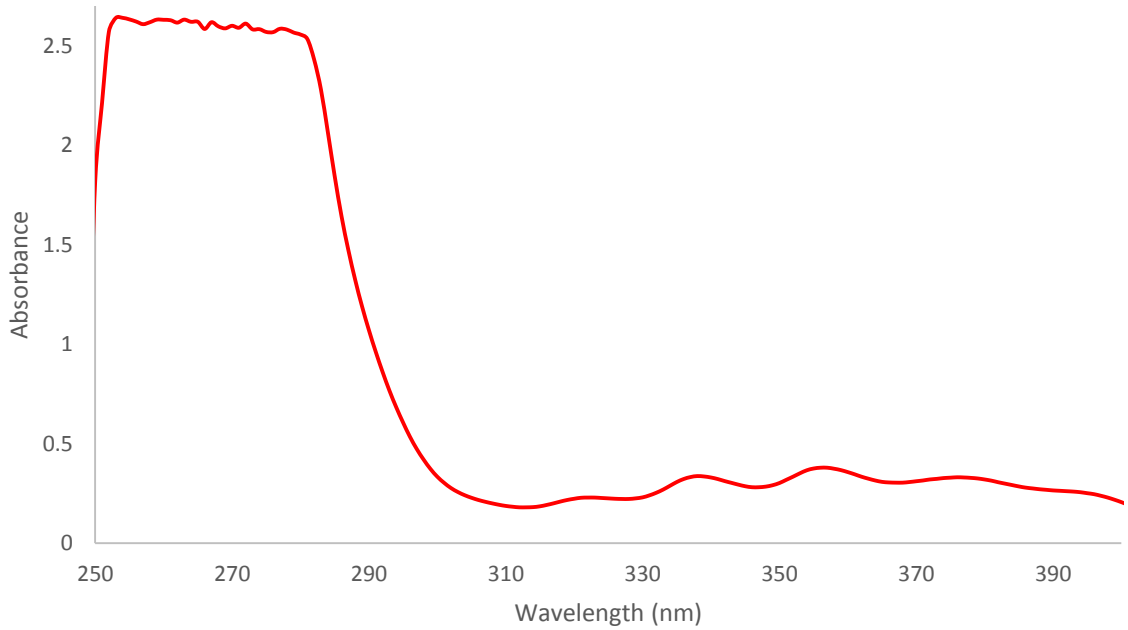

Figure S189- UV-Vis spectra of compound **1** (0.30 mM) in a solution of DMSO: H_2O 1: 4.

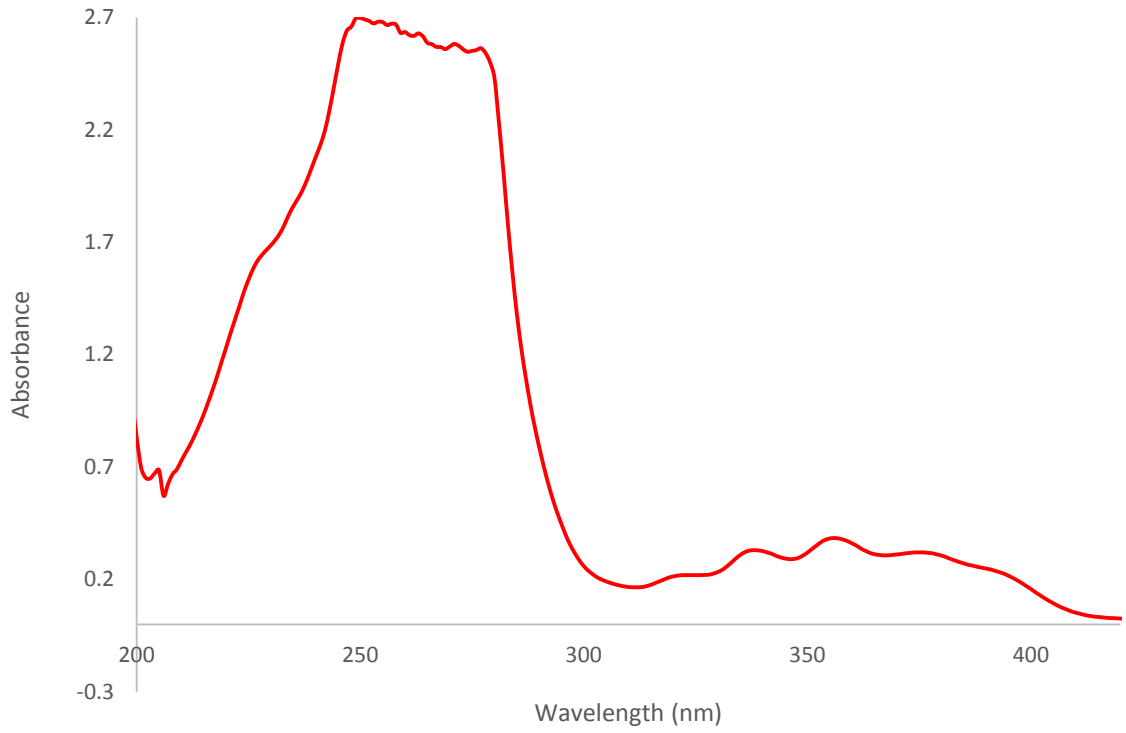

Figure S190- UV-Vis spectra of compound **1** (0.30 mM) in a solution of EtOH: H_2O 1: 19.

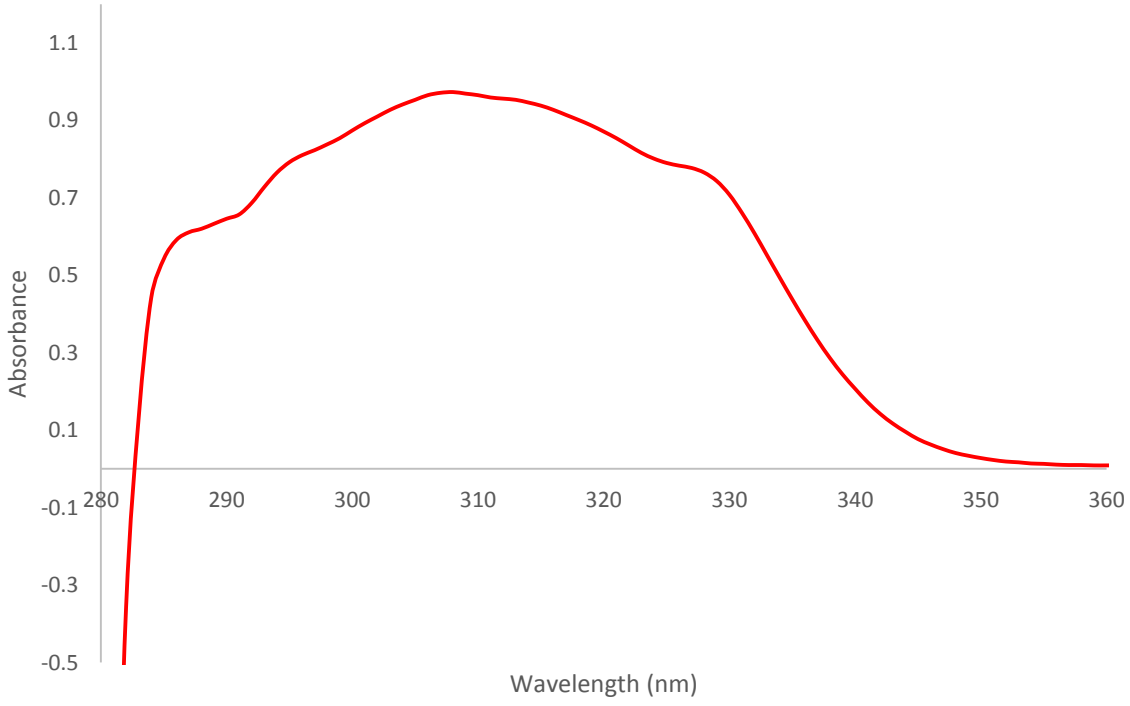

Figure S191 - UV-Vis spectra of compound **2** (0.30 mM) in a solution of DMSO.

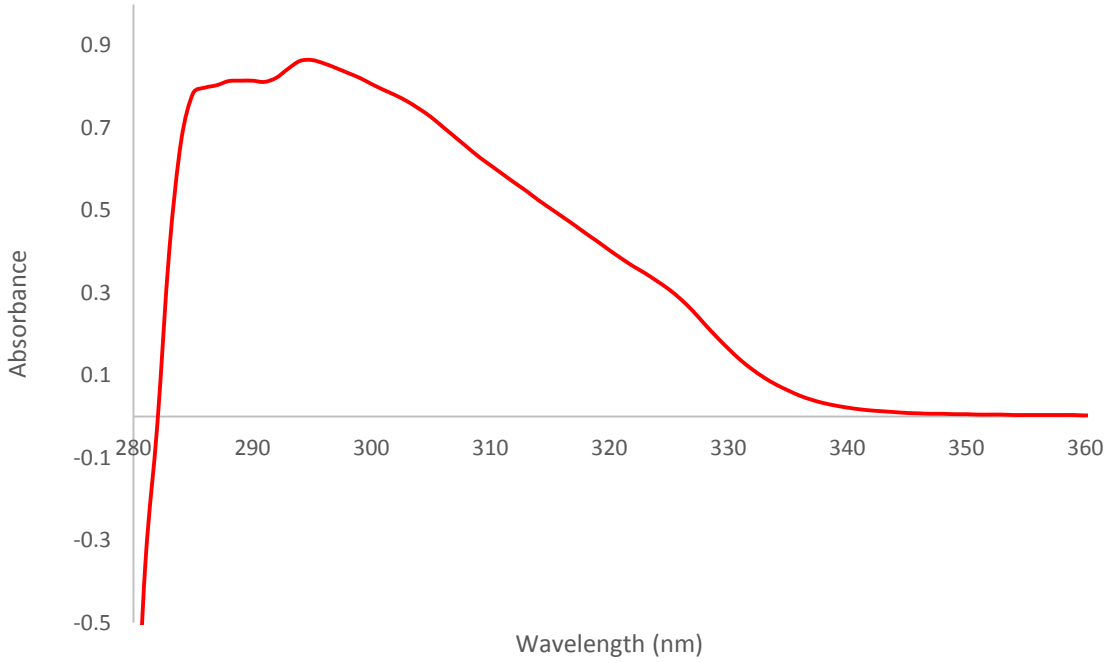

Figure S192 - UV-Vis spectra of compound **2** (0.30 mM) in a solution of DMSO: H_2O 1: 1.

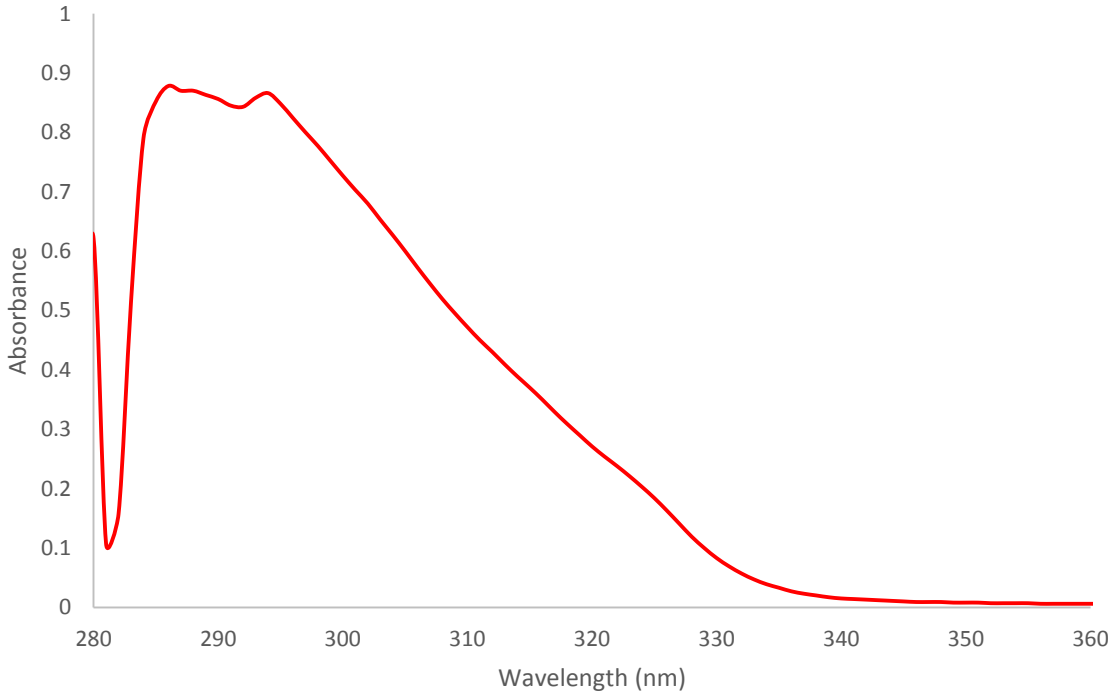

Figure S193 - UV-Vis spectra of compound **2** (0.30 mM) in a solution of DMSO: H_2O 3: 7.

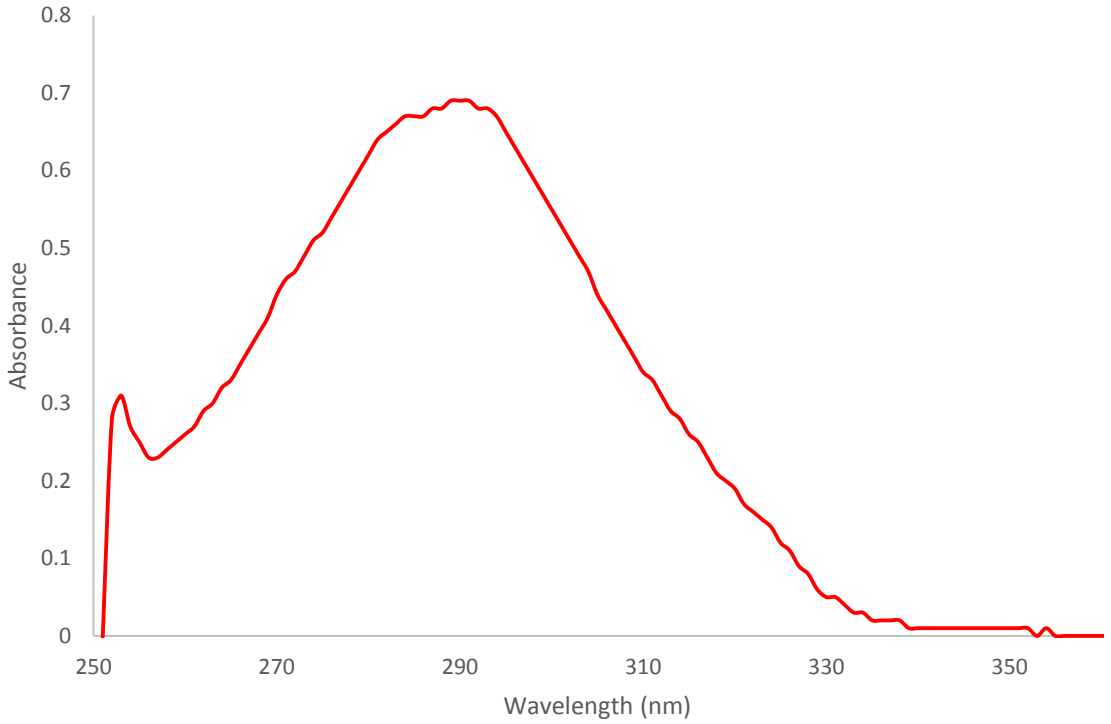

Figure S194 - UV-Vis spectra of compound **2** (0.30 mM) in a solution of DMSO: H_2O 1: 4.

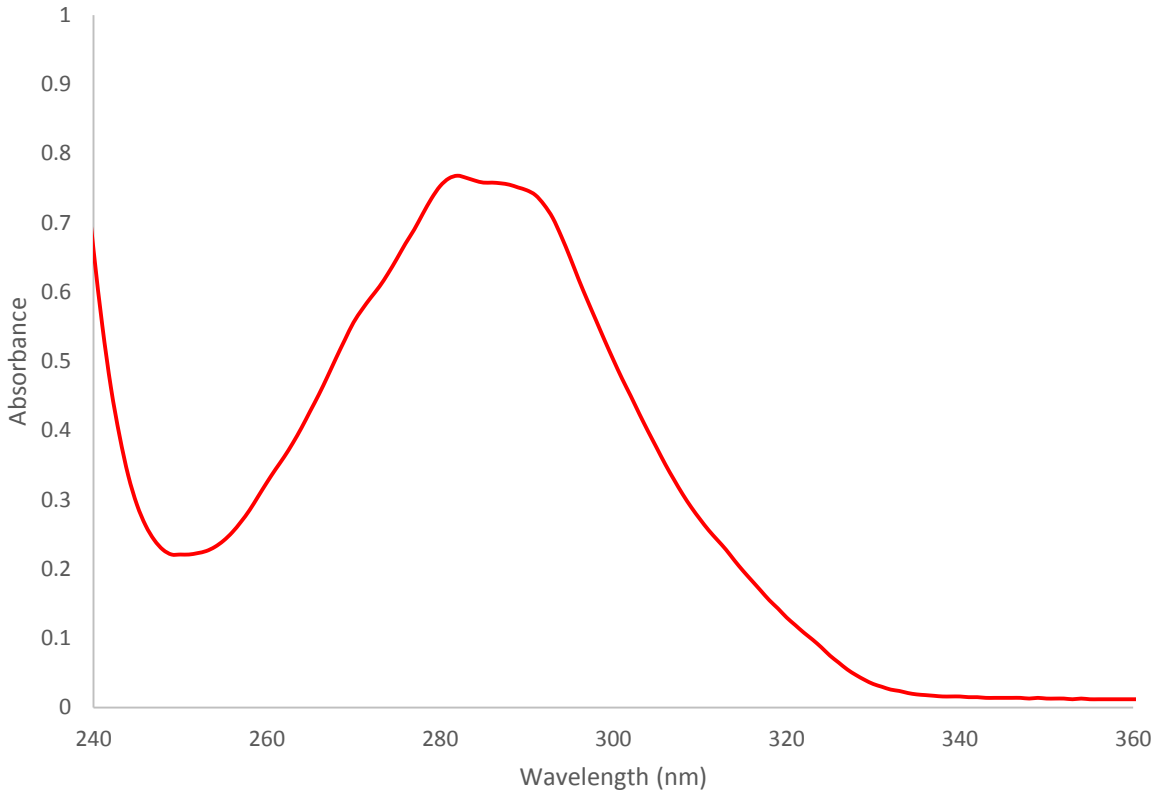

Figure S195 - UV-Vis spectra of compound **2** (0.30 mM) in a solution of EtOH: H_2O 1: 19.

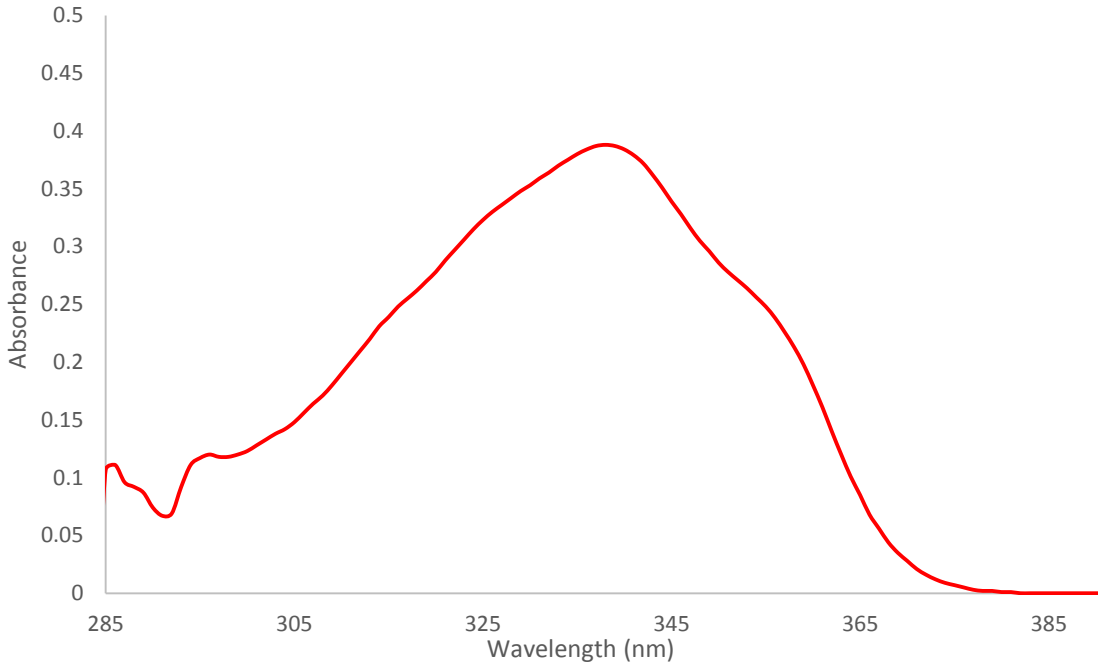

Figure S196 - UV-Vis spectra of compound **4** (0.08 mM) in a DMSO.

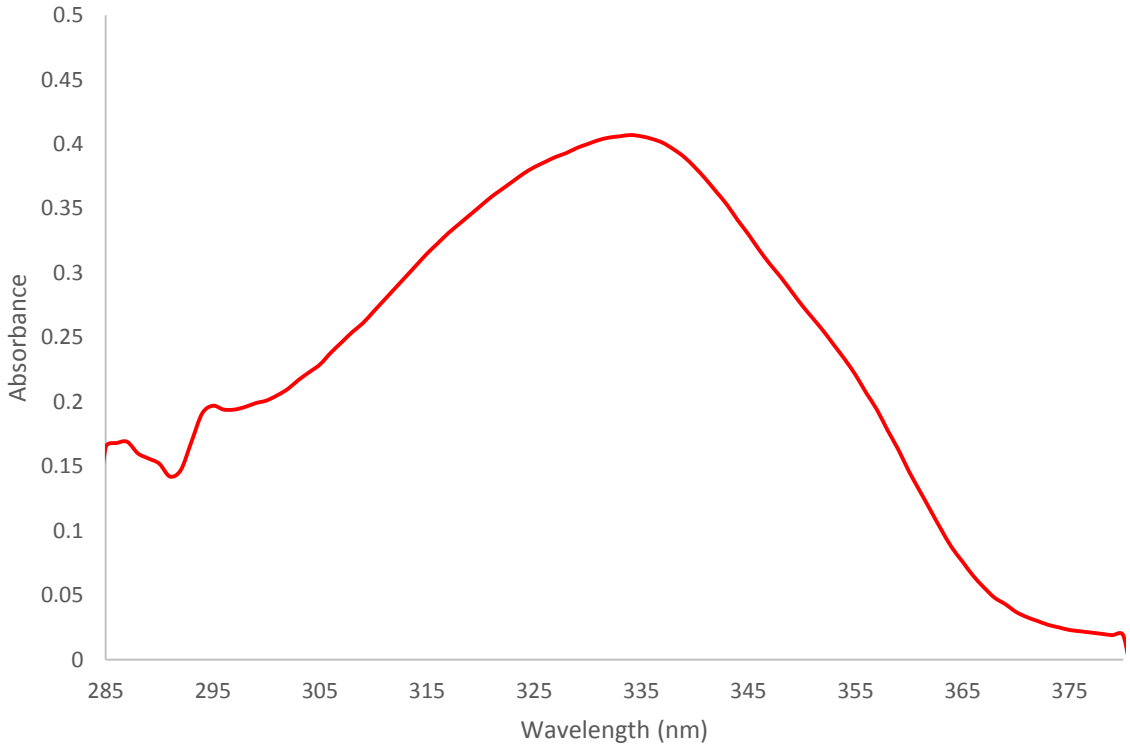

Figure S197 - UV-Vis spectra of compound **4** (0.08 mM) in a solution of DMSO: H_2O 1: 1.

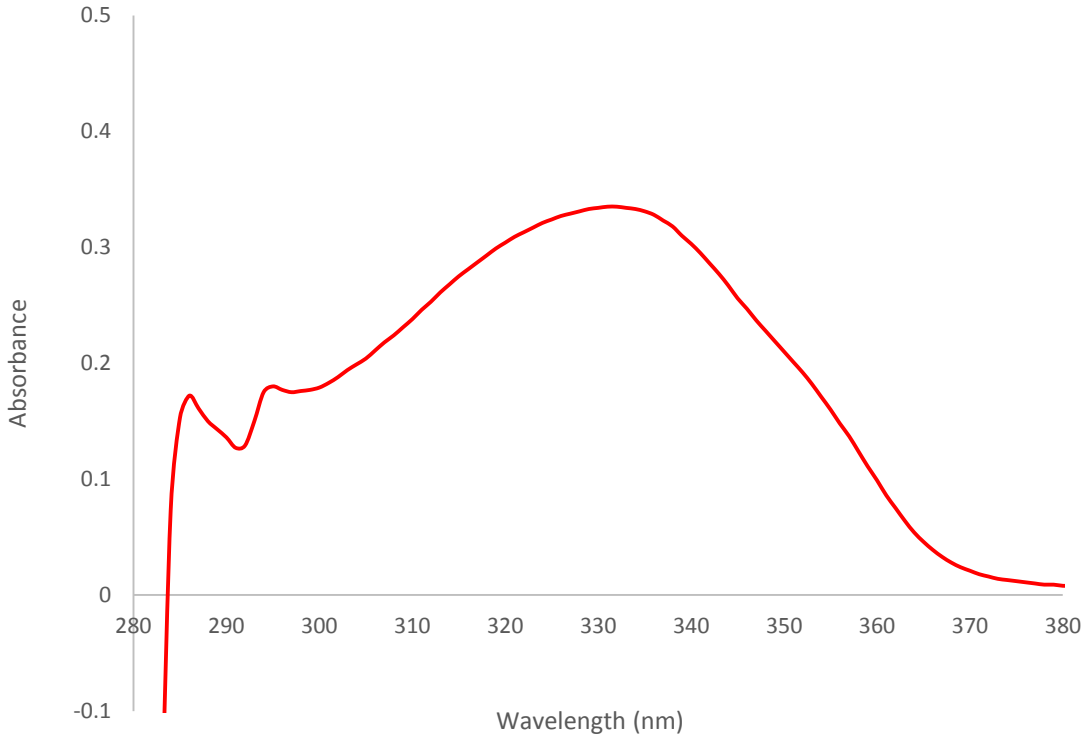

Figure S198 - UV-Vis spectra of compound **4** (0.08 mM) in a solution of DMSO: H_2O 2: 7.

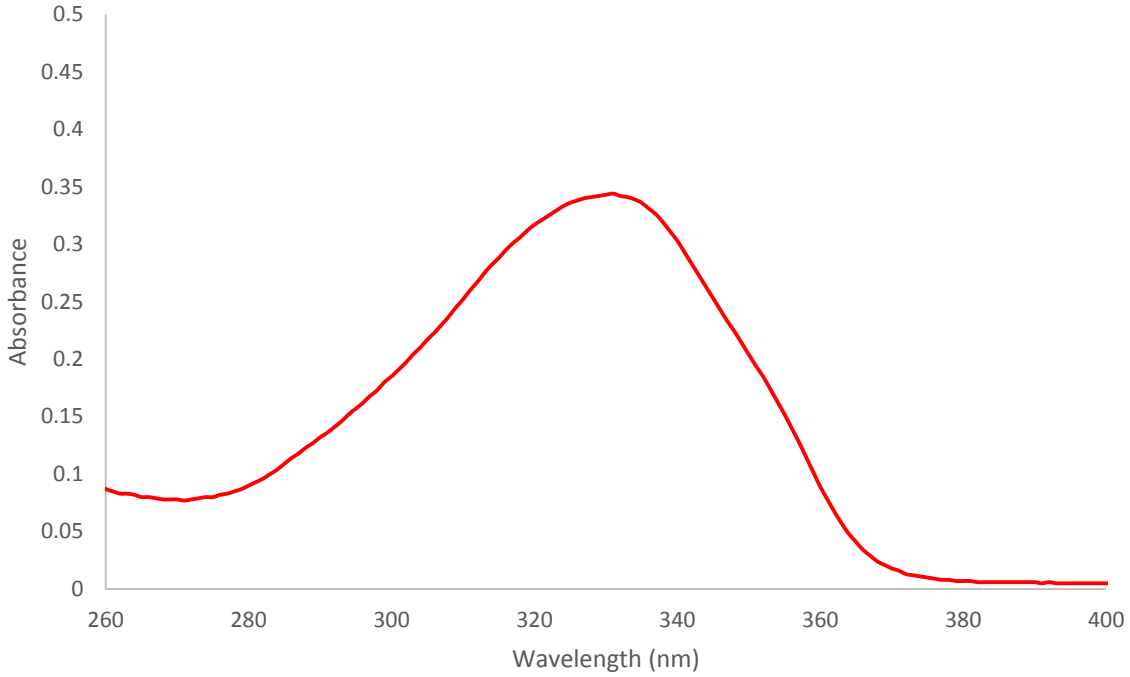

Figure S199 - UV-Vis spectra of compound **4** (0.08 mM) in a solution of DMSO: H_2O 1: 4.

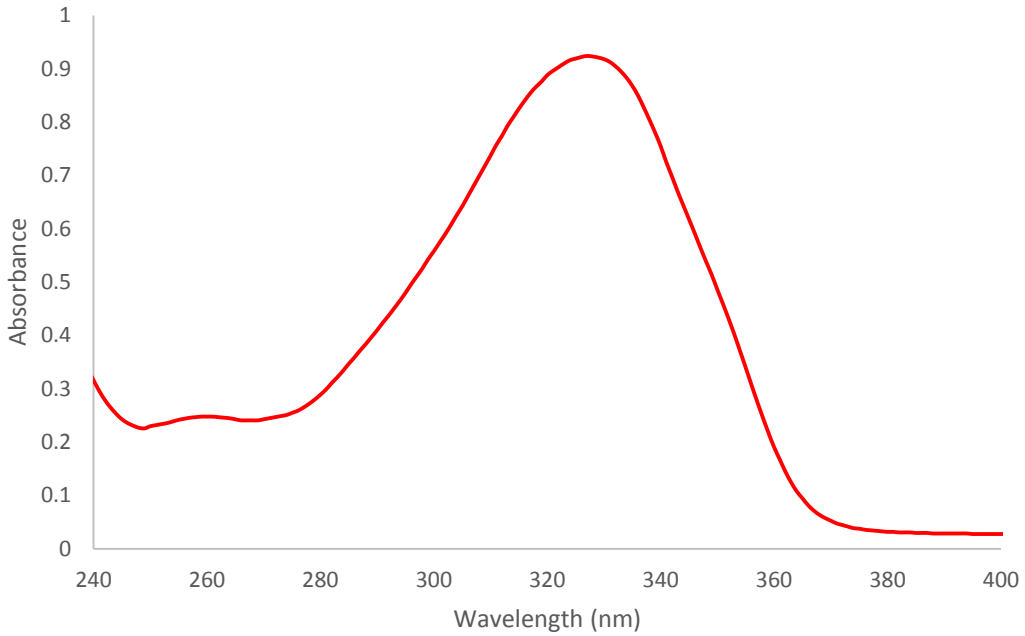

Figure S200 - UV-Vis spectra of compound **4** (0.08 mM) in a solution of EtOH: H_2O 1: 19.

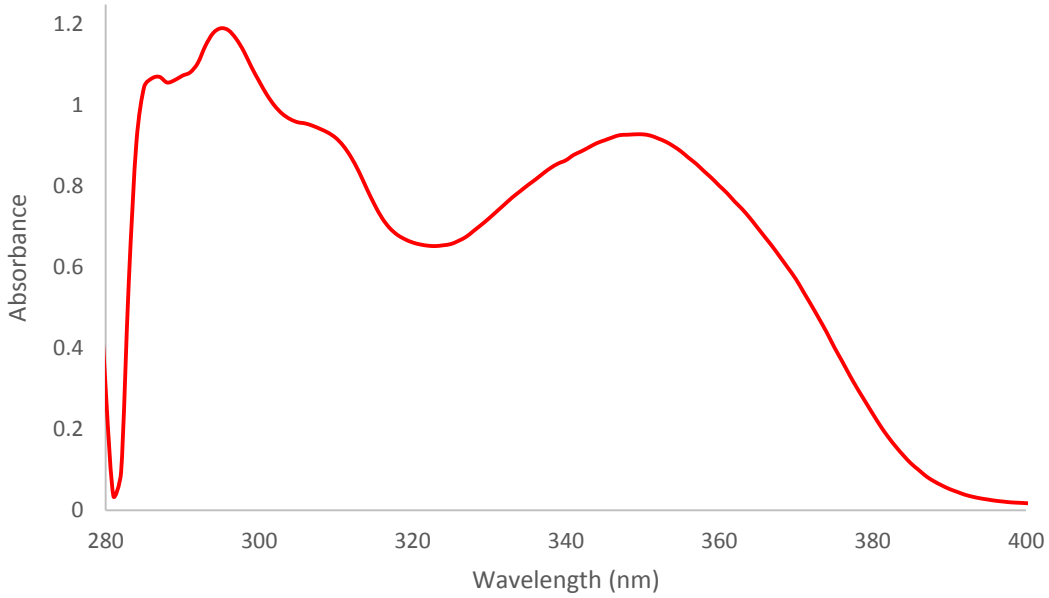

Figure S201 - UV-Vis spectra of compound **5** (0.30 mM) in DMSO.

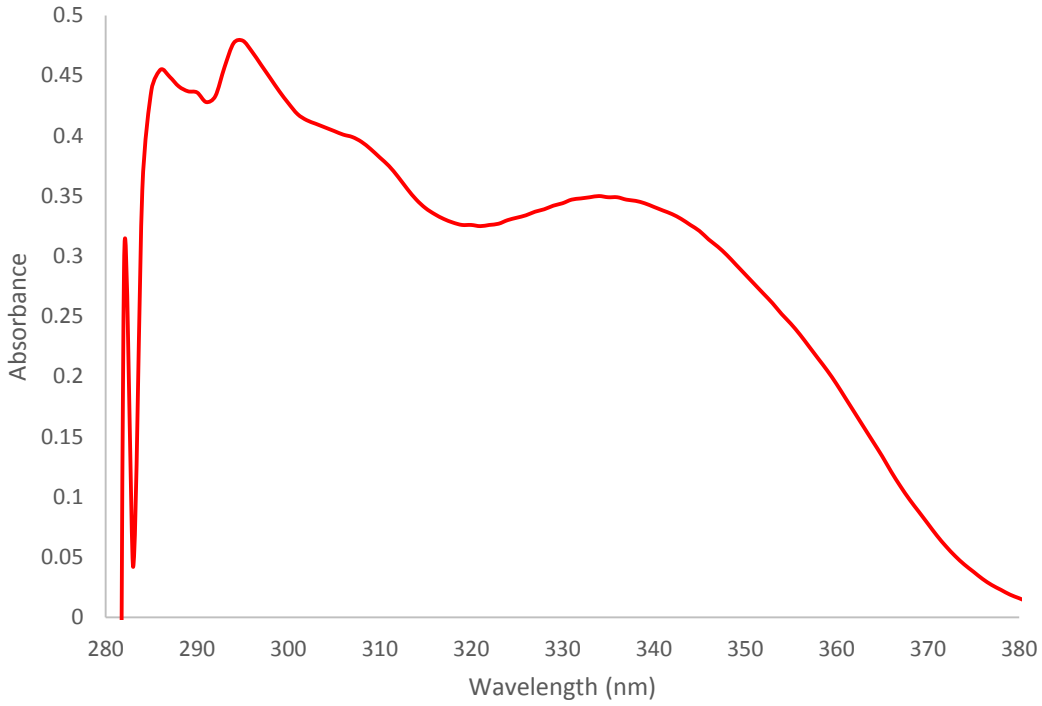

Figure S202 - UV-Vis spectra of compound **5** (0.10 mM) in a solution of DMSO: H_2O 1: 1.

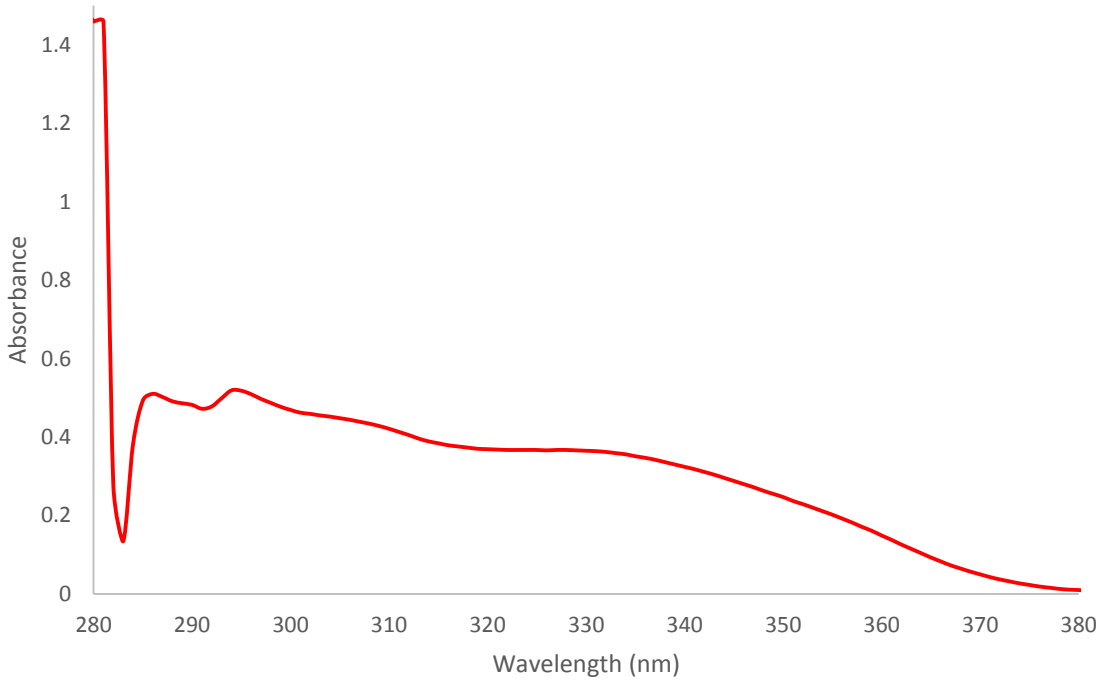

Figure S203 - UV-Vis spectra of compound **5** (0.10 mM) in a solution of DMSO: H_2O 3: 7.

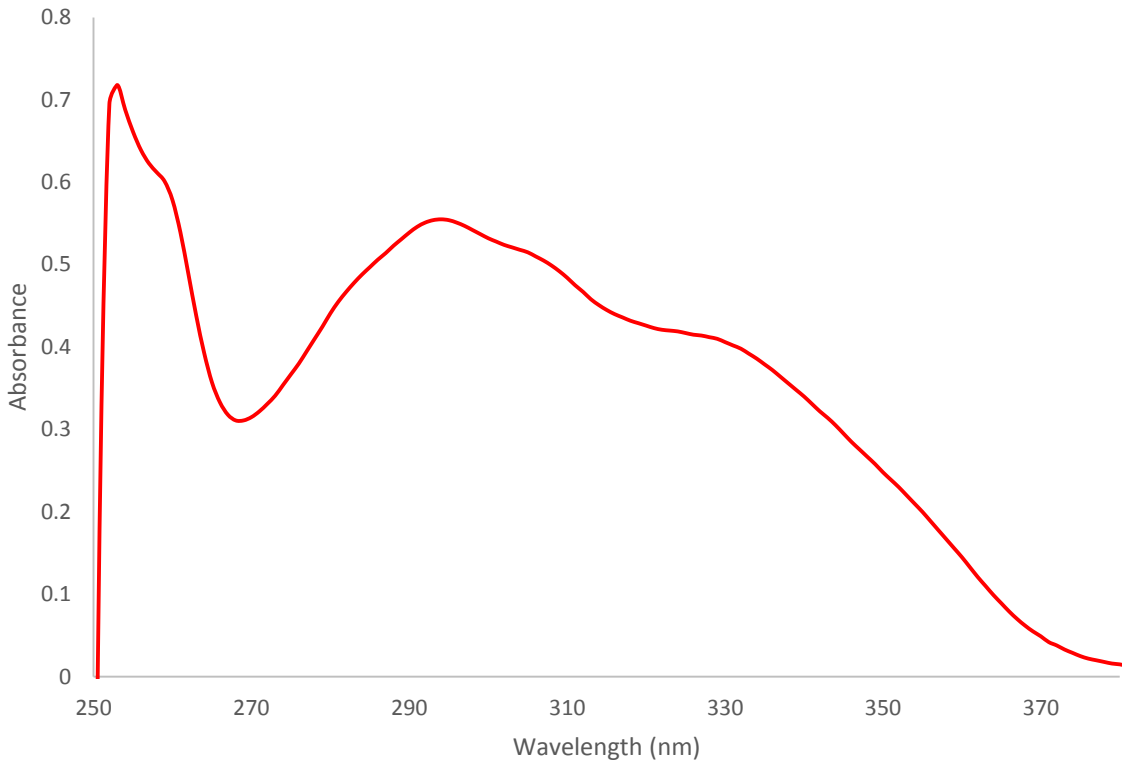

Figure S204 - UV-Vis spectra of compound **5** (0.10 mM) in a solution of DMSO: H_2O 1: 4.

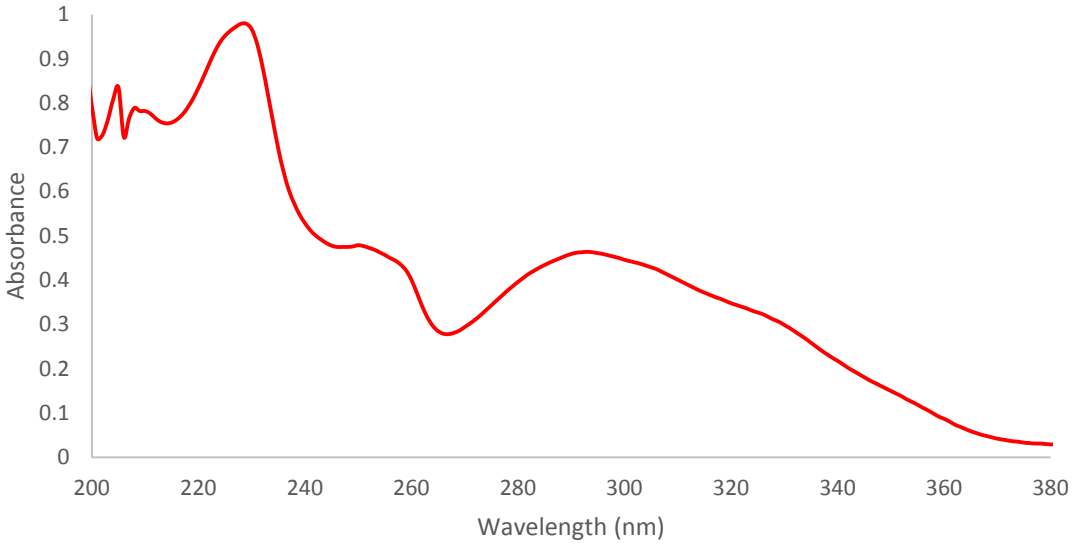

Figure S205 - UV-Vis spectra of compound **5** (0.10 mM) in a solution of EtOH: H_2O 1: 19.

Fluorescence spectra

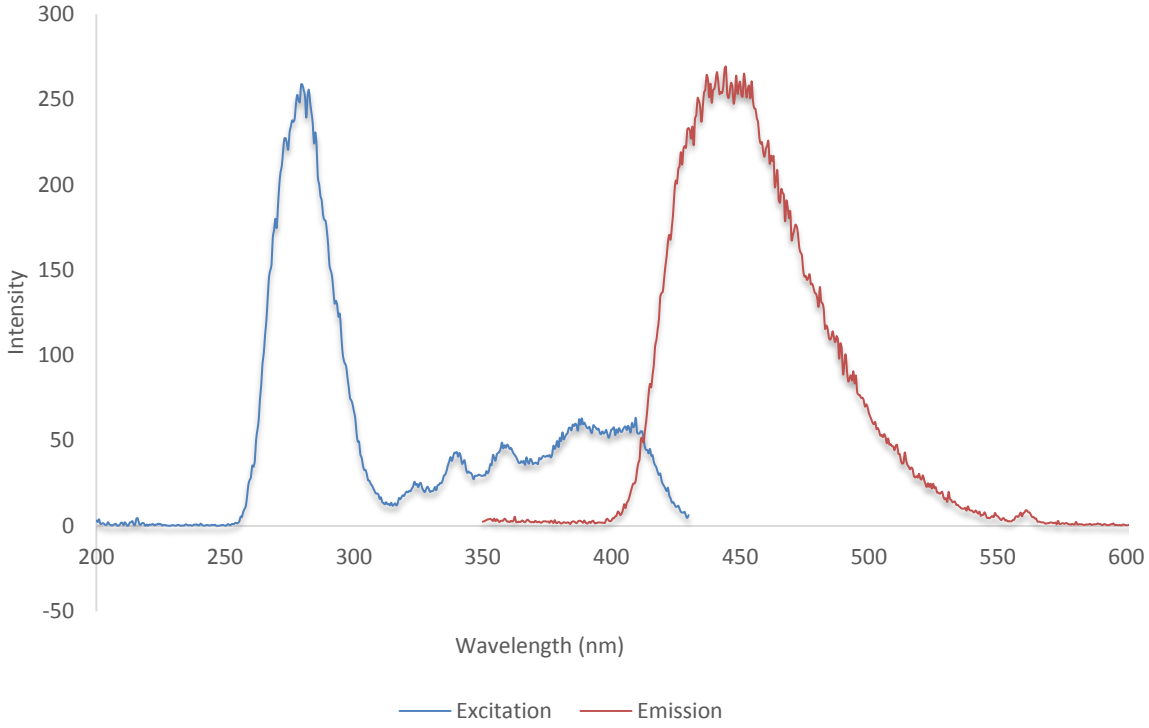

Figure S206 - Fluorescence spectra of compound **1** (0.003 mM) in a solution of DMSO.

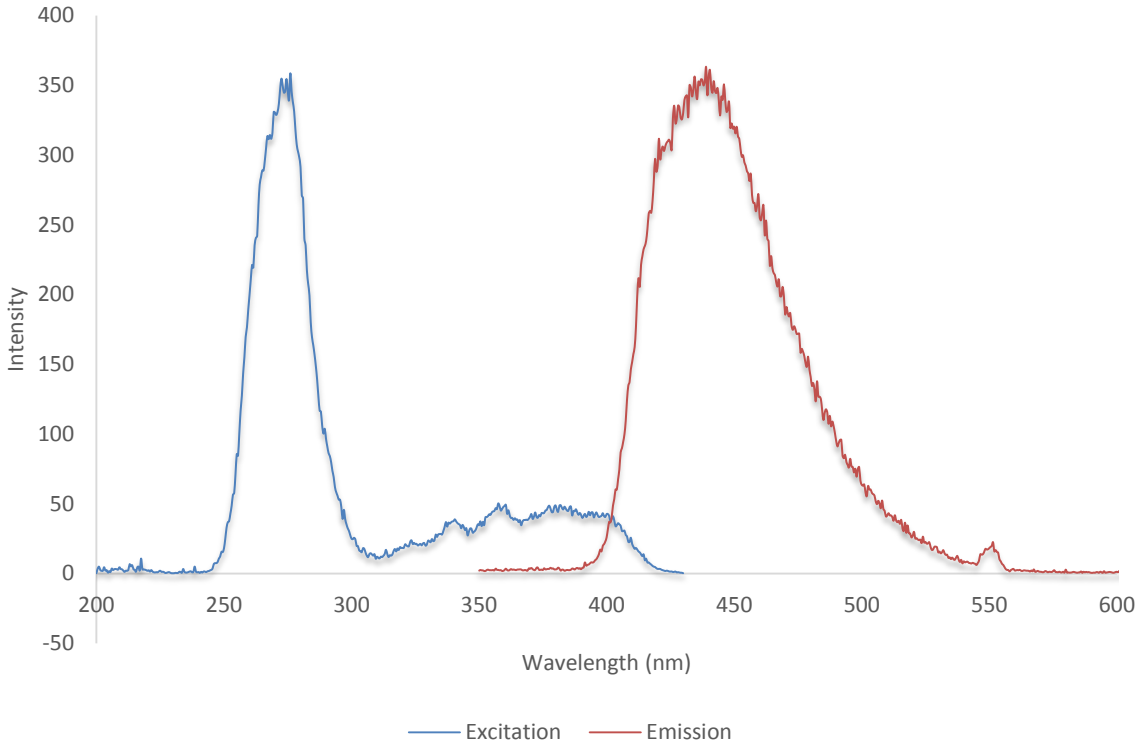

Figure S207 - Fluorescence spectra of compound **1** (0.003 mM) in a solution of DMSO: H_2O 1: 1.

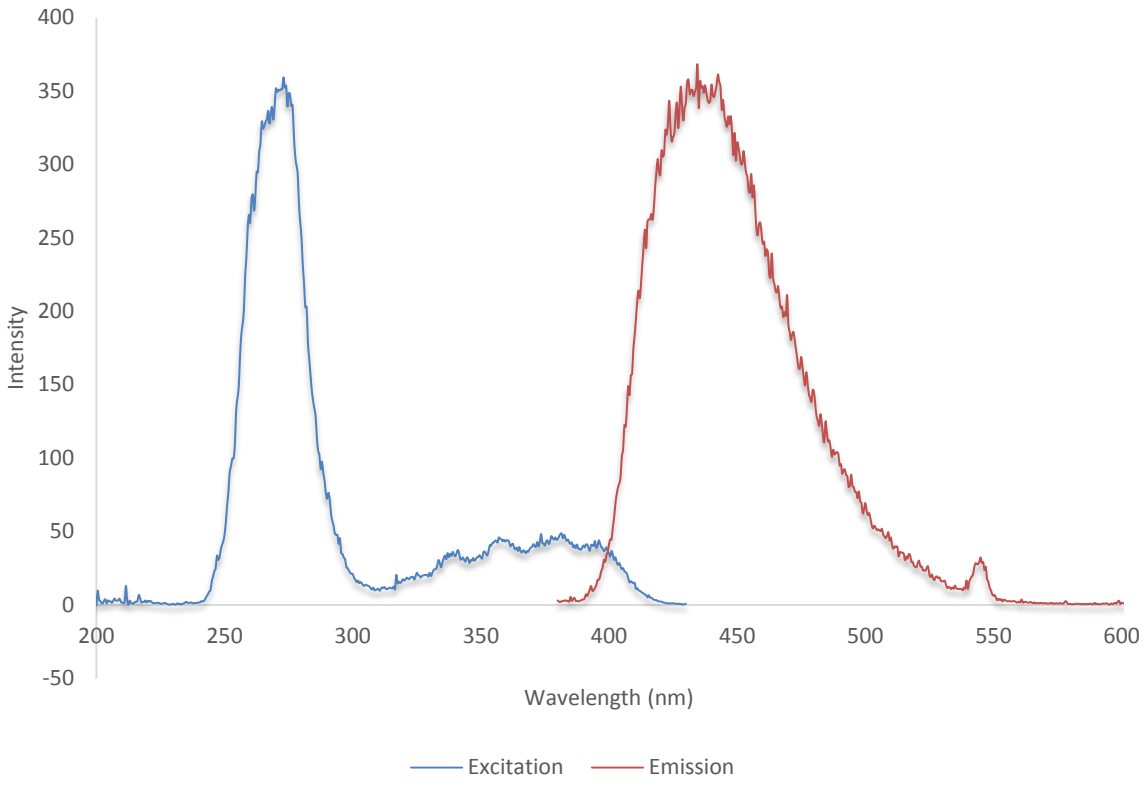

Figure S208 - Fluorescence spectra of compound **1** (0.003 mM) in a solution of DMSO: H_2O 3: 7.

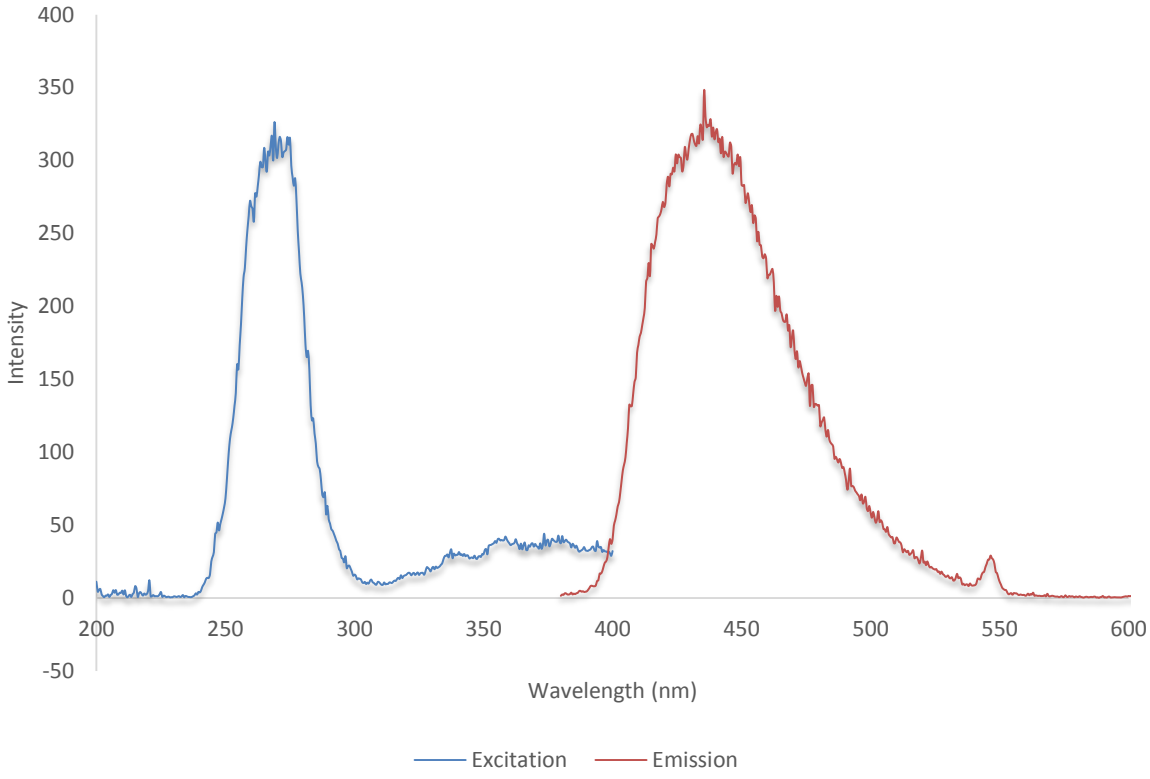

Figure S209 - Fluorescence spectra of compound **1** (0.003 mM) in a solution of DMSO: H_2O 1: 4.

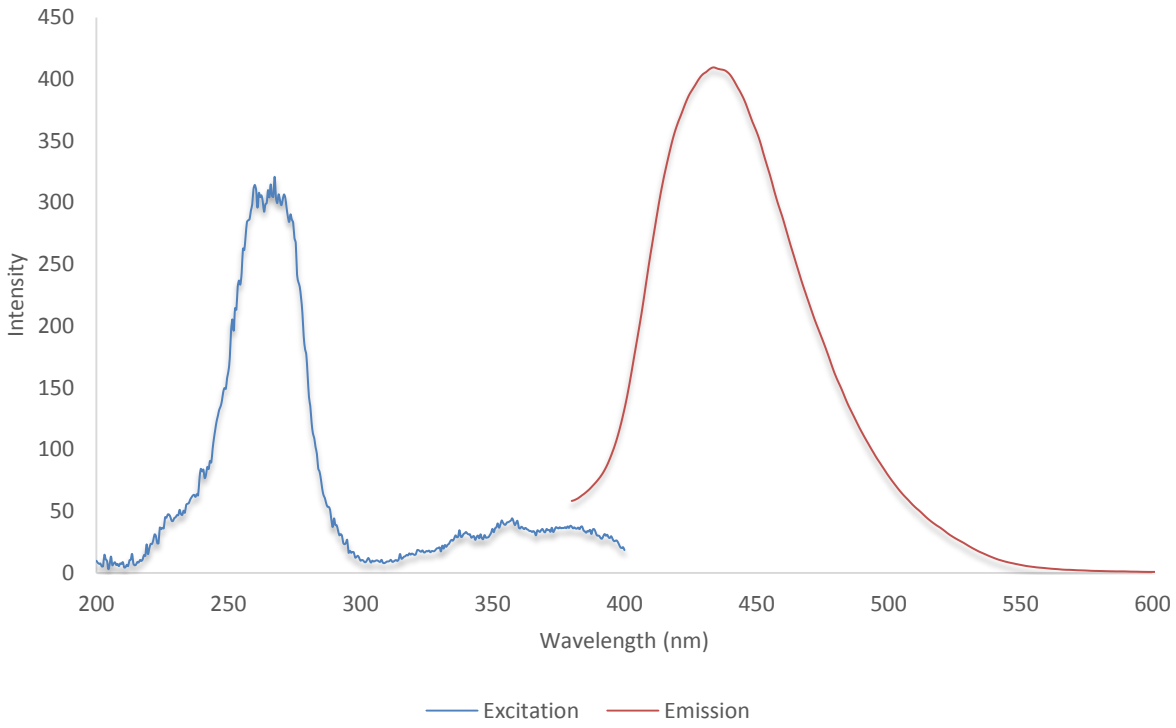

Figure S210 - Fluorescence spectra of compound **1** (0.003 mM) in a solution of EtOH: H_2O 1: 19.

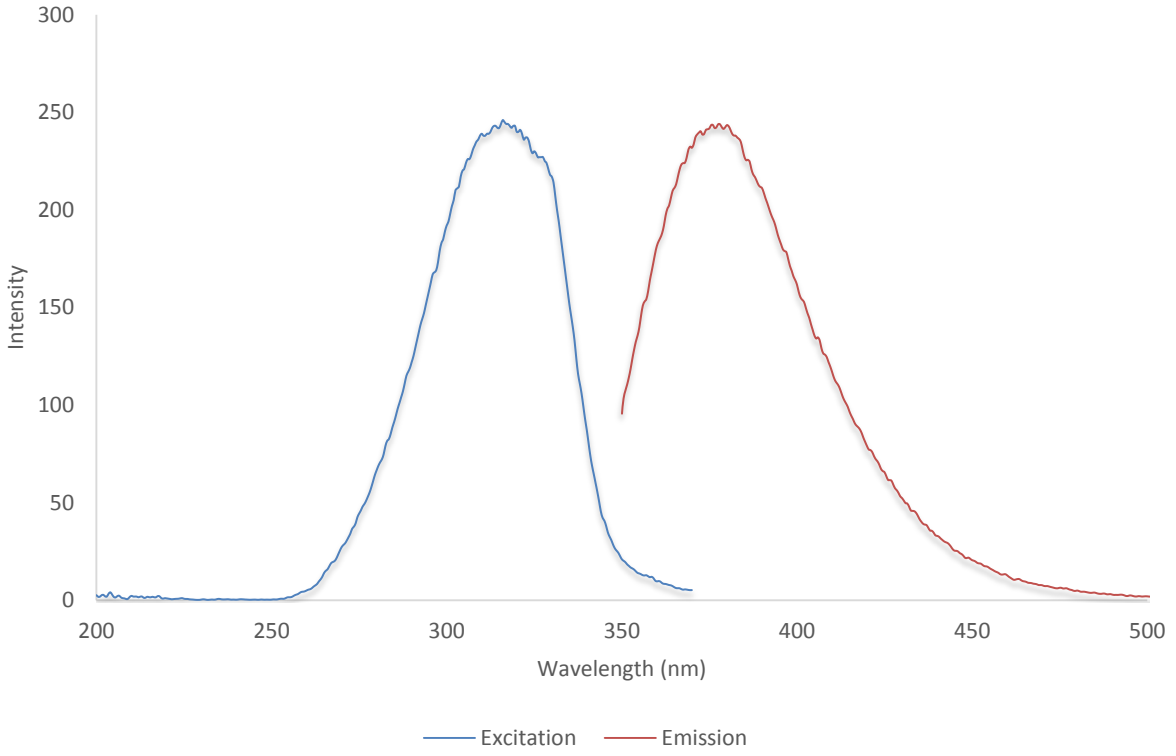

Figure S211 - Fluorescence spectra of compound **2** (0.003 mM) in DMSO.

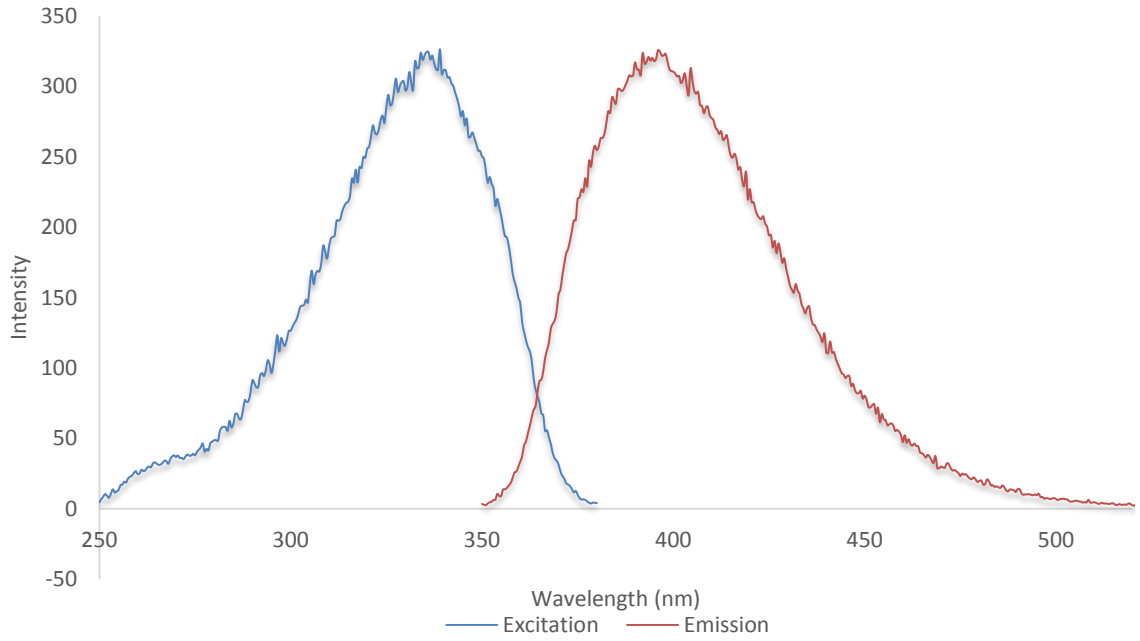

Figure S212 - Fluorescence spectra of compound **2** (0.003 mM) in a solution of DMSO: H_2O 1: 1.

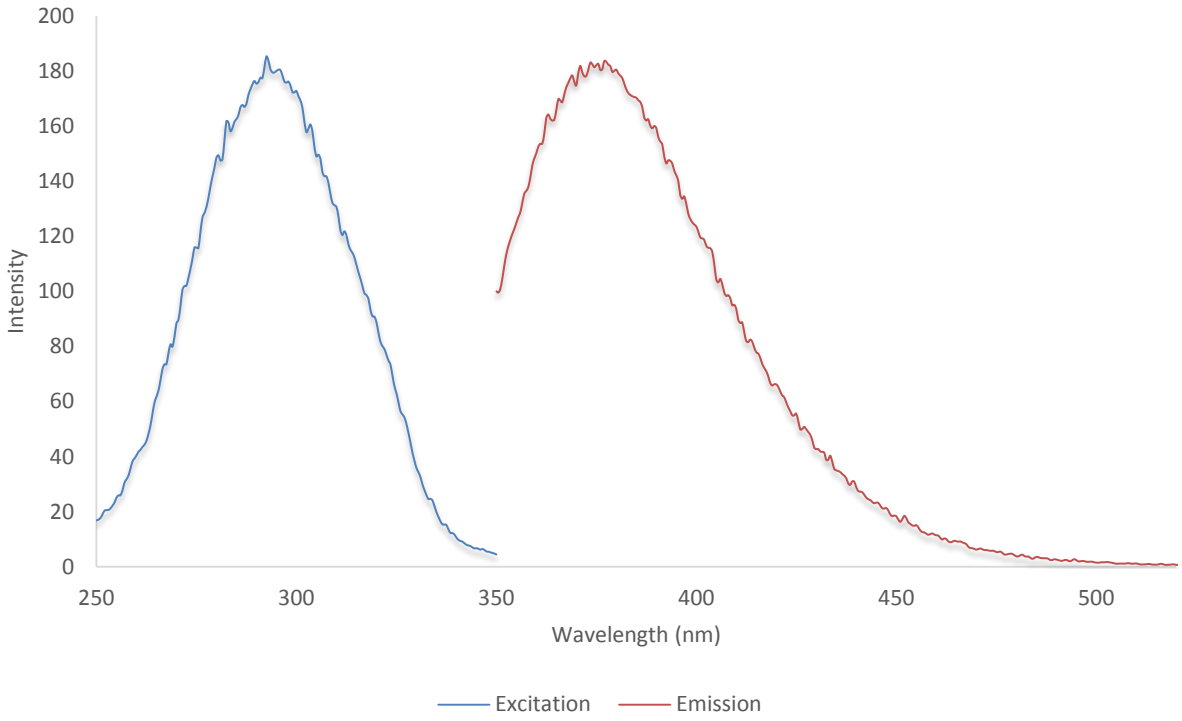

Figure S213 - Fluorescence spectra of compound **2** (0.003 mM) in a solution of DMSO: H_2O 3: 7.

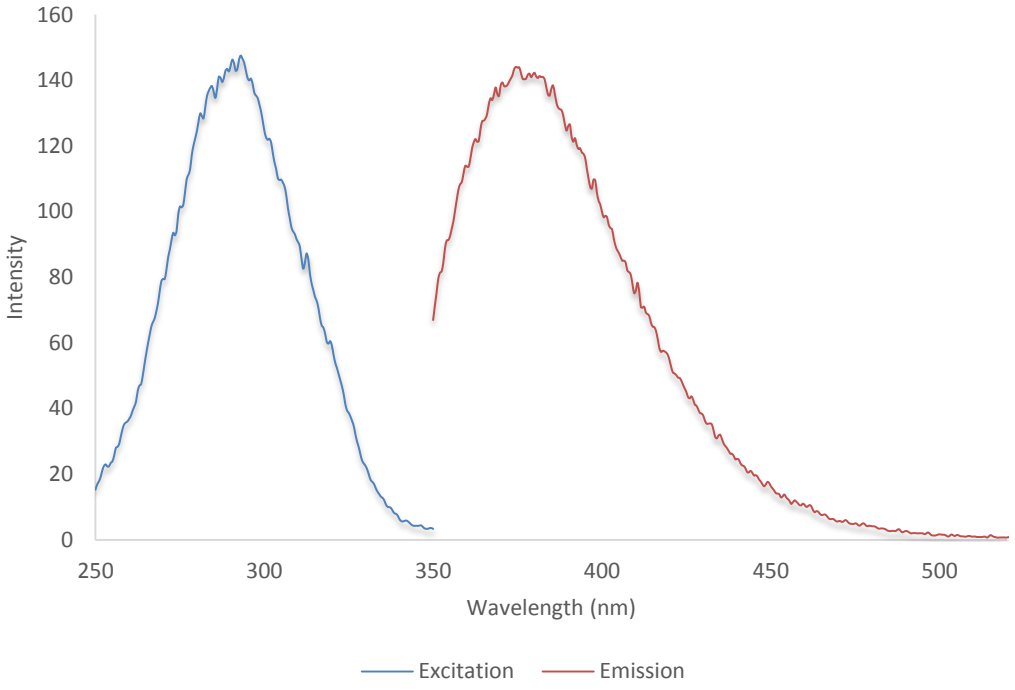

Figure S214 - Fluorescence spectra of compound **2** (0.003 mM) in a solution of DMSO: H_2O 1: 4.

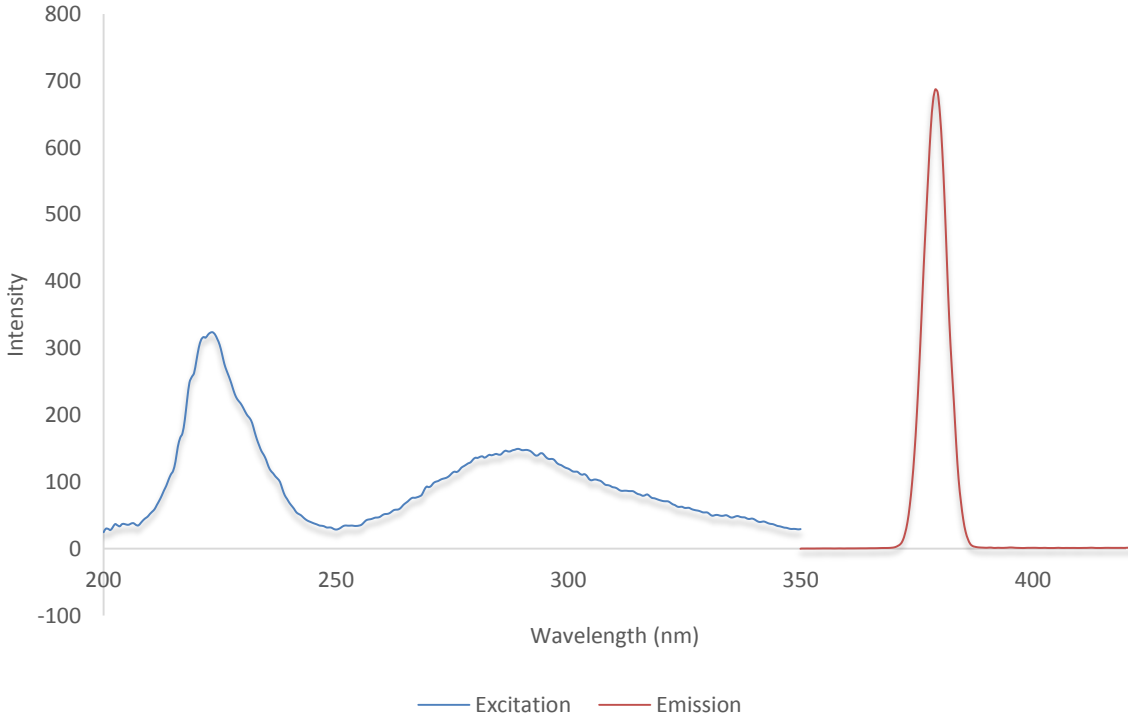

Figure S215 - Fluorescence spectra of compound **2** (0.003 mM) in a solution of EtOH: H_2O 1: 19.

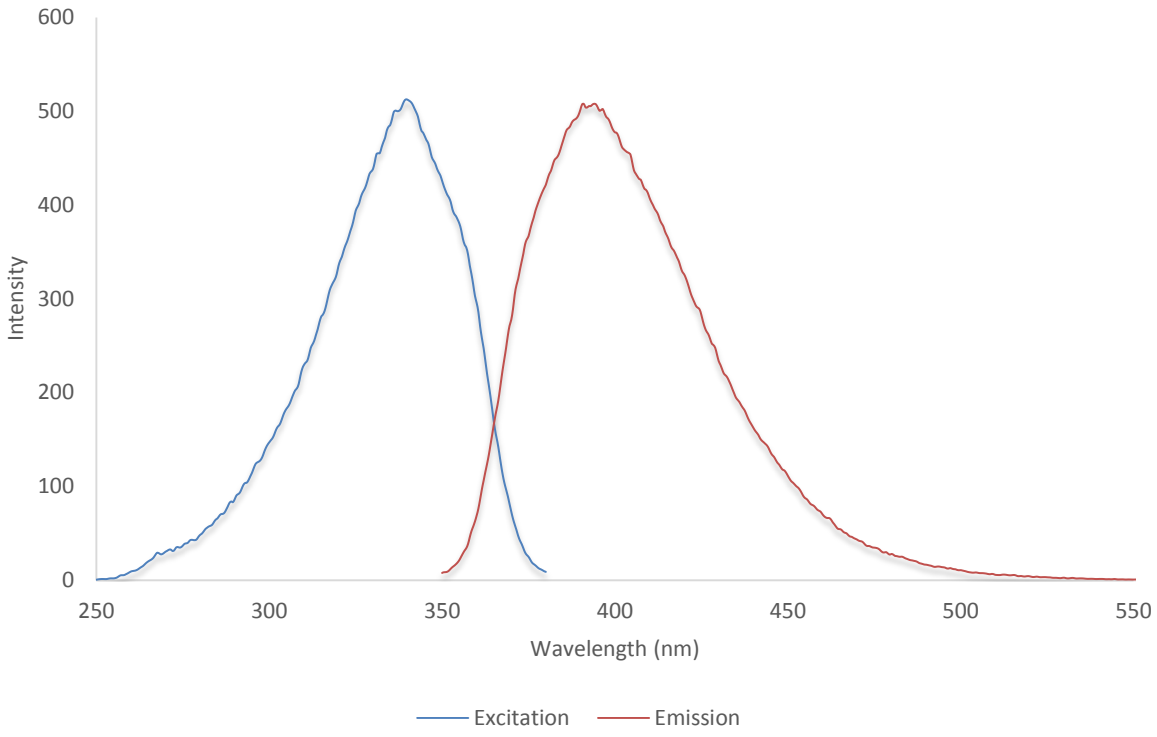

Figure S216 - Fluorescence spectra of compound **4** (0.003 mM) in DMSO.

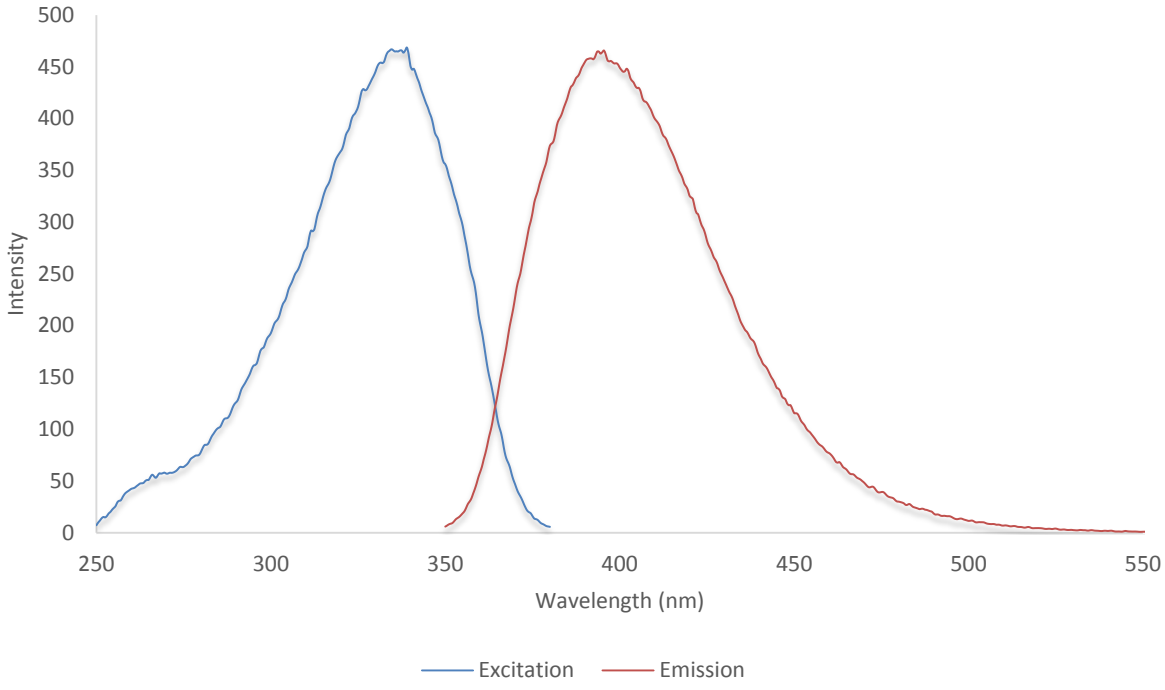

Figure S217 - Fluorescence spectra of compound **4** (0.003 mM) in a solution of DMSO: H_2O 1: 1.

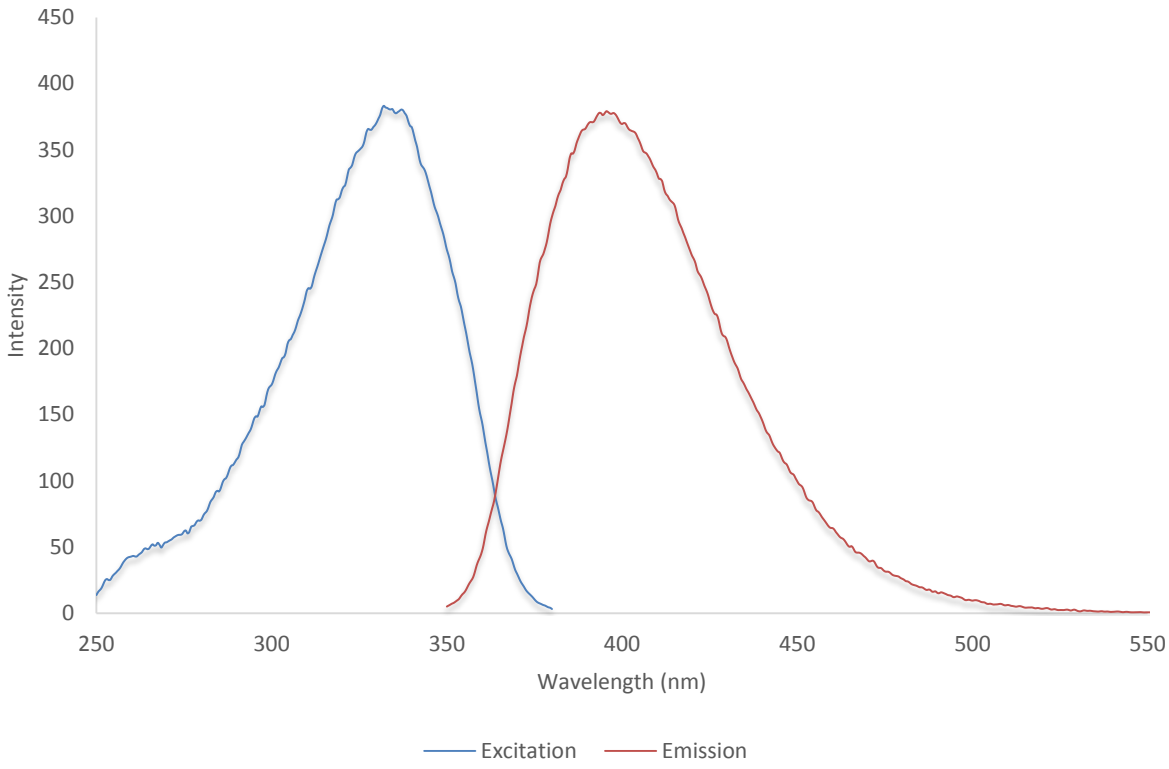

Figure S218 - Fluorescence spectra of compound **4** (0.003 mM) in a solution of DMSO: H_2O 3: 7.

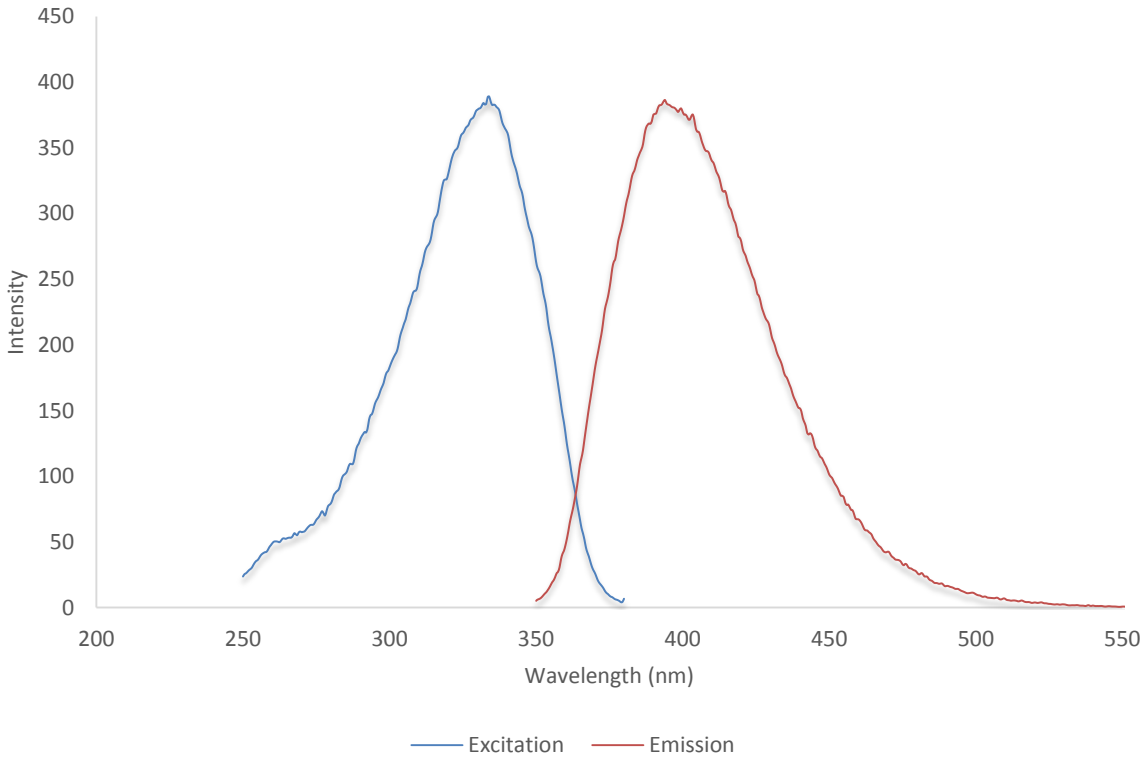

Figure S219 - Fluorescence spectra of compound **4** (0.003 mM) in a solution of DMSO: H_2O 1: 4.

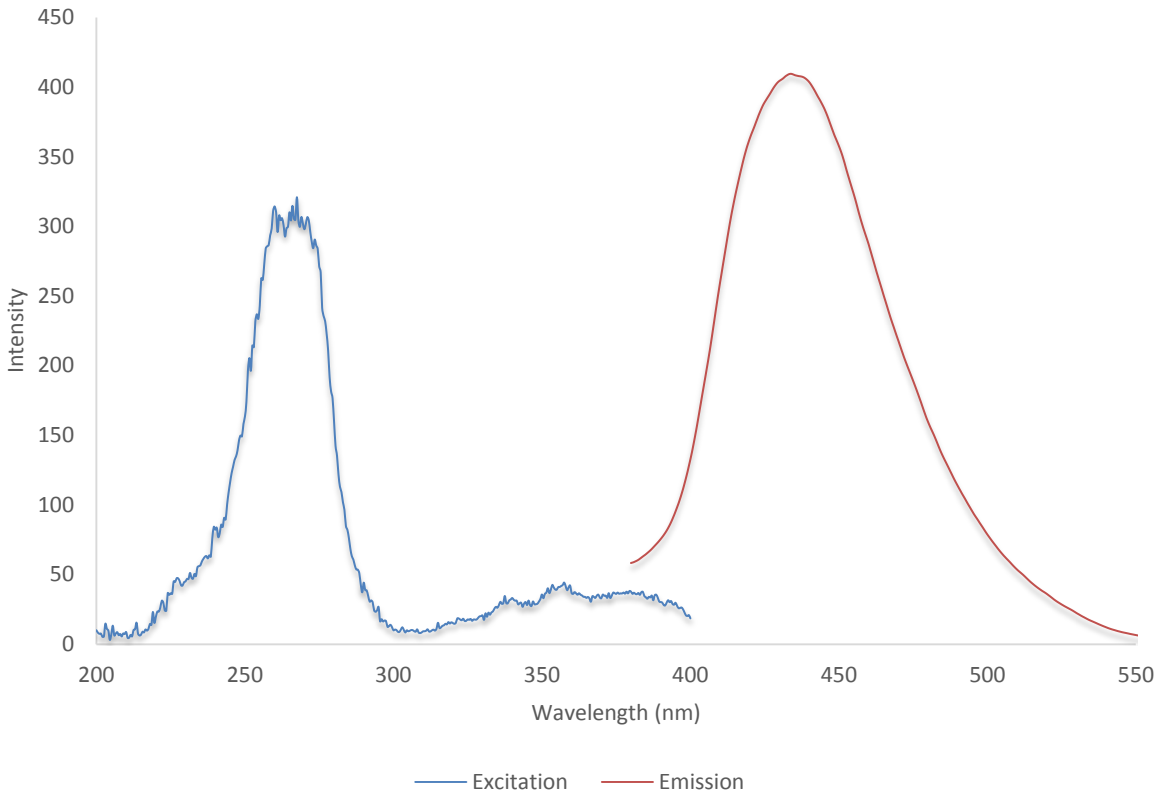

Figure S220 - Fluorescence spectra of compound **4** (0.003 mM) in a solution of EtOH: H_2O 1: 19.

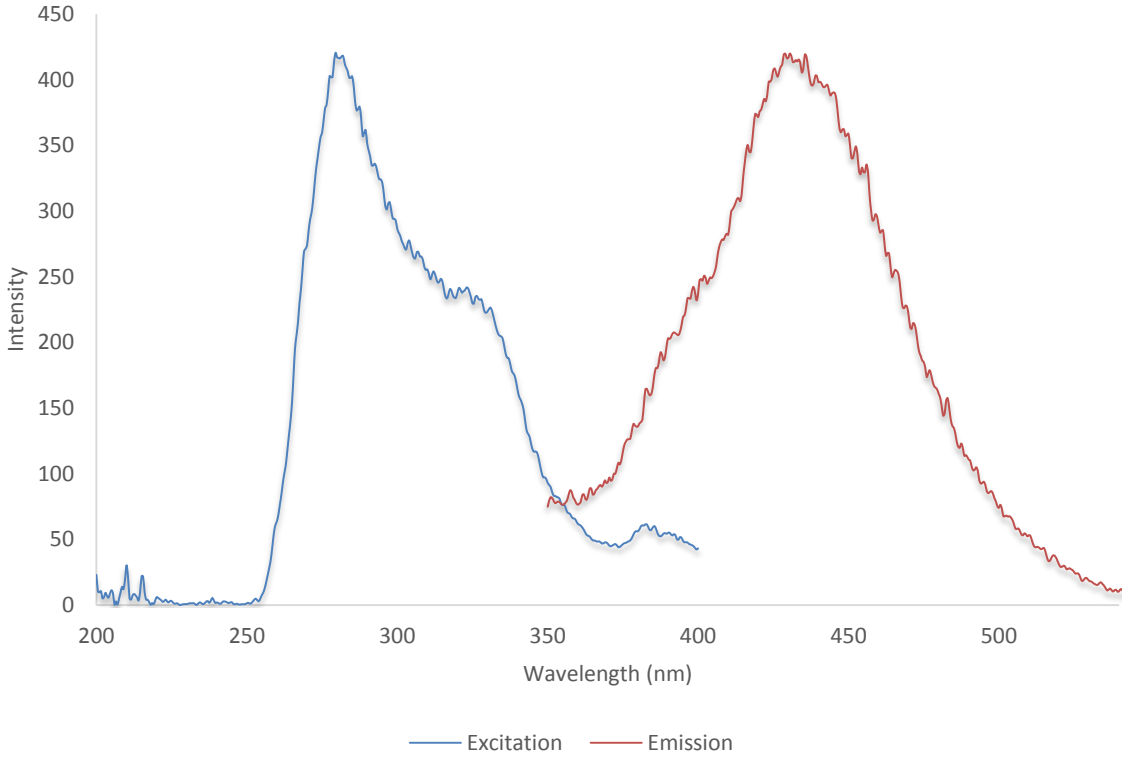

Figure S221 - Fluorescence spectra of compound **5** (0.03 mM) in DMSO.

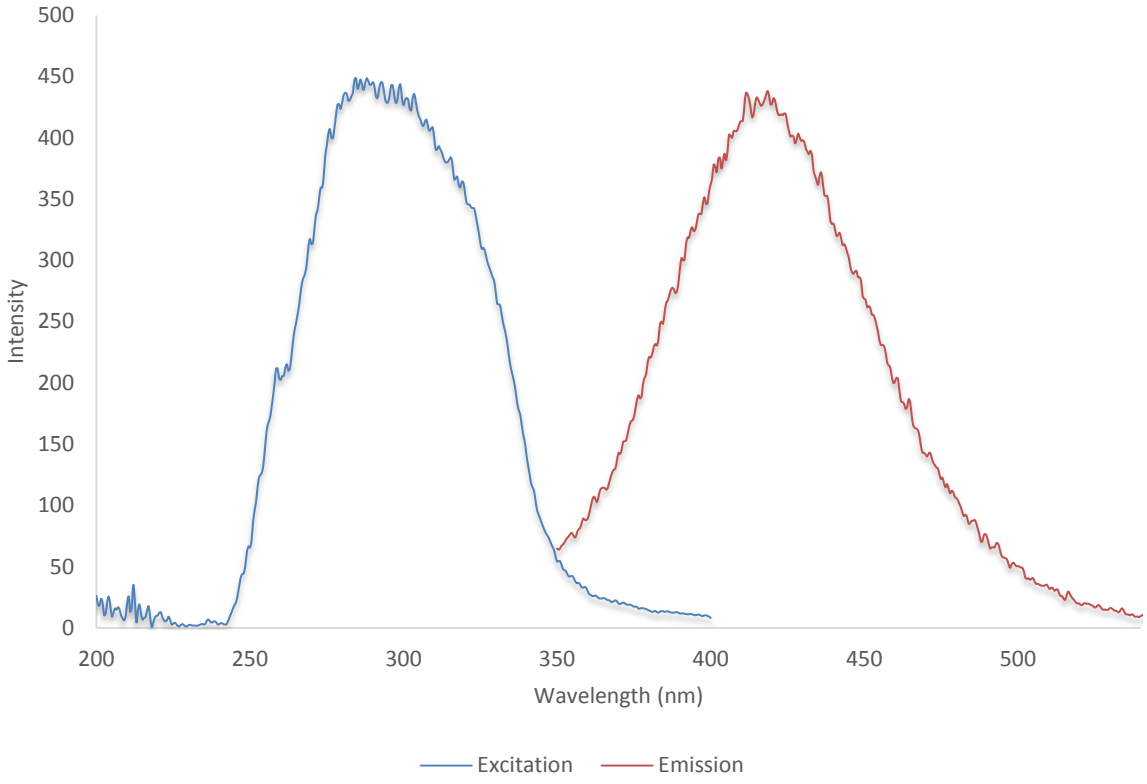

Figure S222 - Fluorescence spectra of compound **5** (0.03 mM) in a solution of DMSO: H_2O 1: 1.

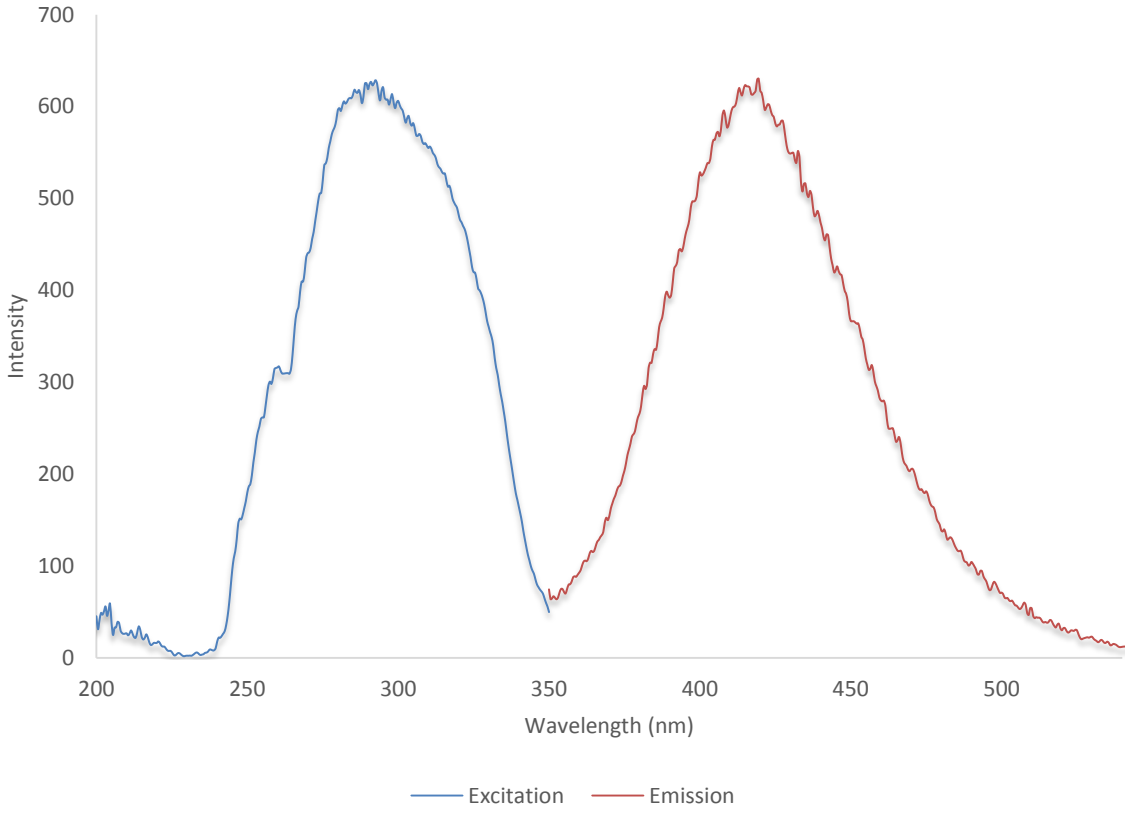

Figure S223 - Fluorescence spectra of compound **5** (0.03 mM) in a solution of DMSO: H_2O 3: 7.

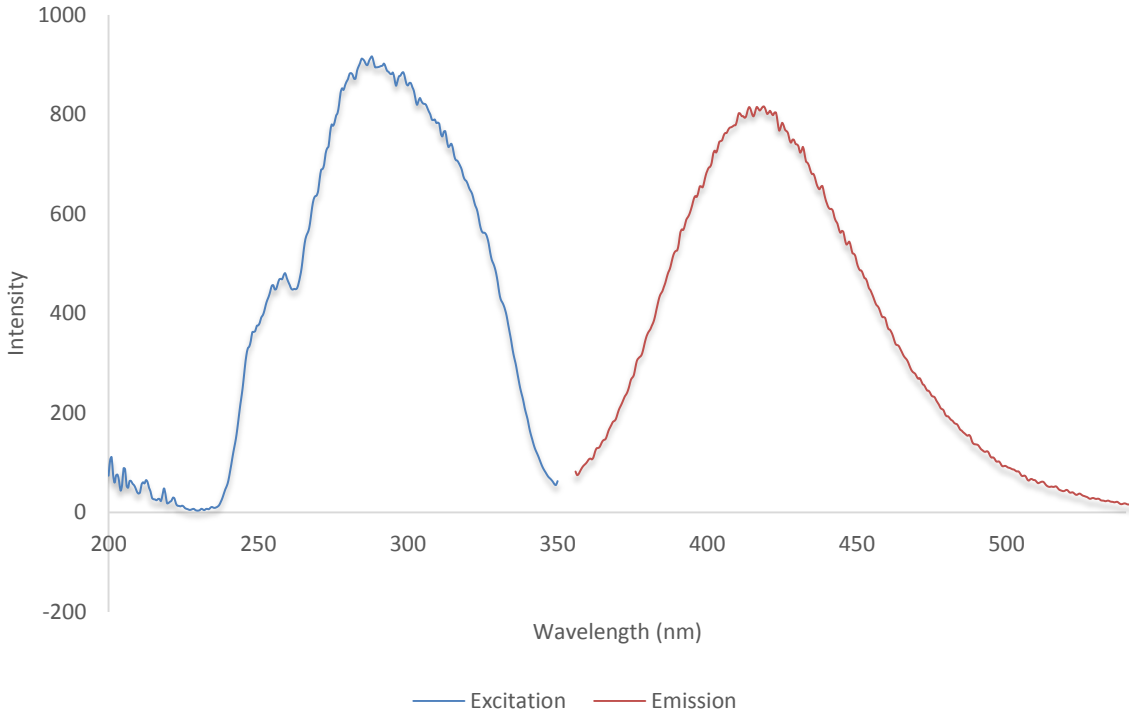

Figure S224 - Fluorescence spectra of compound **5** (0.03 mM) in a solution of DMSO: H_2O 1: 4.

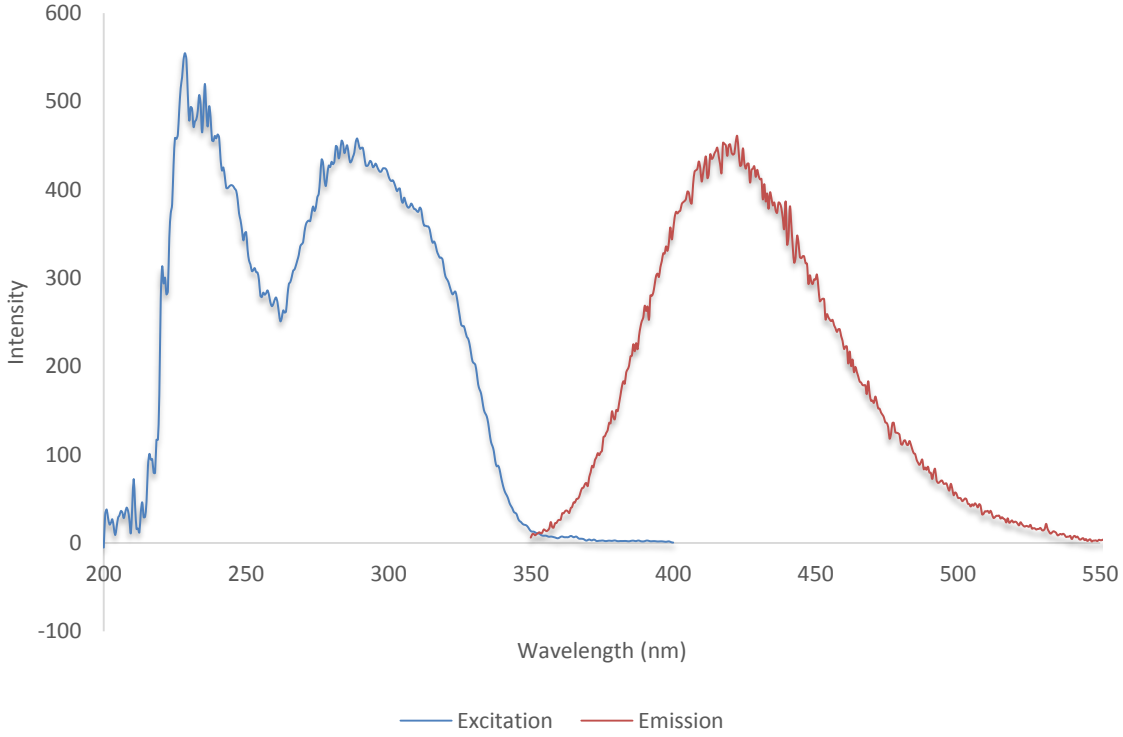

Figure S225 - Fluorescence spectra of compound **5** (0.03 mM) in a solution of EtOH: H_2O 1: 19.

Single crystal X-ray structures

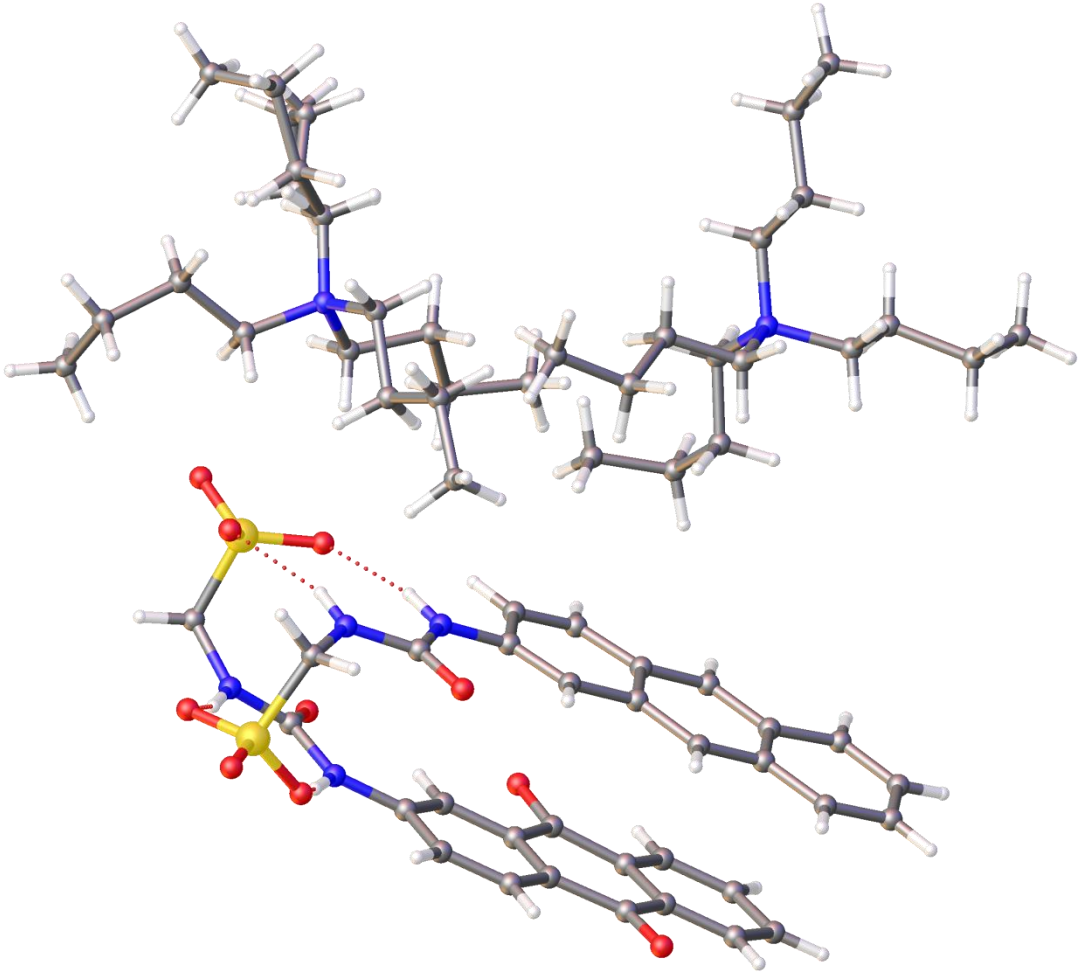

Figure S226 - Crystal data for compound **1**: red = oxygen; yellow = sulfur; blue = nitrogen; white = hydrogen; grey = carbon. CCDC 1562758, $C_{64}H_{95}N_6O_{10}S_2$ (M =1172.57): triclinic, space group P -1, a = 11.2916(13) Å, b = 12.5010(13) Å, c = 23.9203(16) Å, α = 88.359(8)°, β = 86.588(8)°, γ = 76.689(10)°, V = 3276.6(6) $Å^3$, Z = 2, T = 100(1) K, CuK\α = 1.5418 Å, Dcalc = 1.188 g/cm^3, 37401 reflections measured (7.268 ≤ 2Θ ≤ 100.870), 6864 unique (R_{int} = 0.1754, R_{sigma} = 0.1246) which were used in all calculations. The final R_1 was 0.1405 (I > 2σ(I)) and wR_2 was 0.3767 (all data).

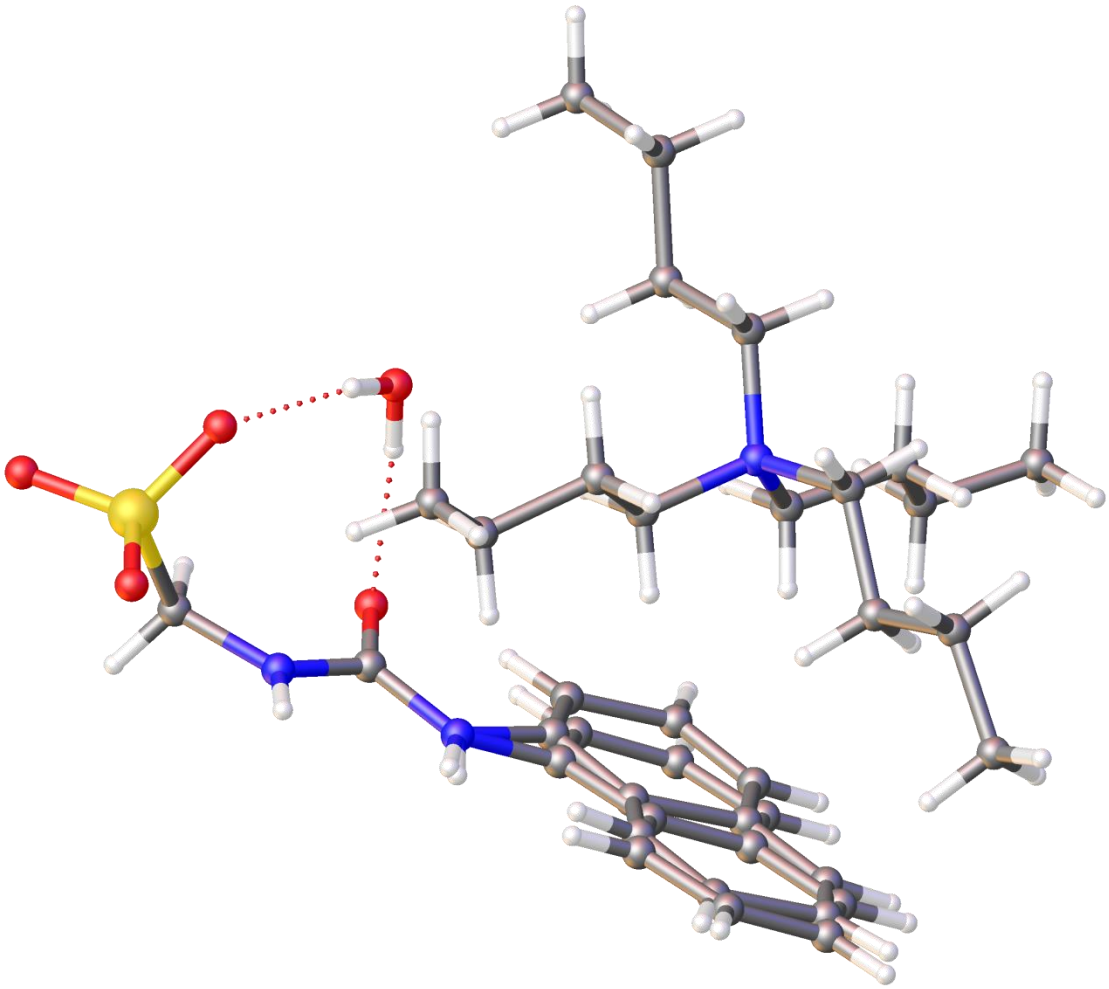

Figure S227 - Crystal data for compound **2**: red = oxygen; yellow = sulfur; blue = nitrogen; white = hydrogen; grey = carbon. CCDC 1562761, $C_{28}H_{49}N_3O_5S_2$ (M =539.76): monoclinic, space group P 1 21/n 1, a = 13.1121(18) Å, b = 16.3159(14) Å, c = 13.6871(16) Å, α = 90°, β = 900.27(11)°, γ = 90°, V = 2928.2(6) $Å^3$, Z = 4, T = 100(1) K, CuK\α = 1.5418 Å, Dcalc = 1.224 g/cm^3, 20834 reflections measured (8.252 ≤ 2Θ ≤ 146.390), 4527 unique (R_{int} = 0.0610 R_{sigma} = 0.0534) which were used in all calculations. The final R_1 was 0.0504 (I > 2σ(I)) and wR_2 was 0.1479 (all data).

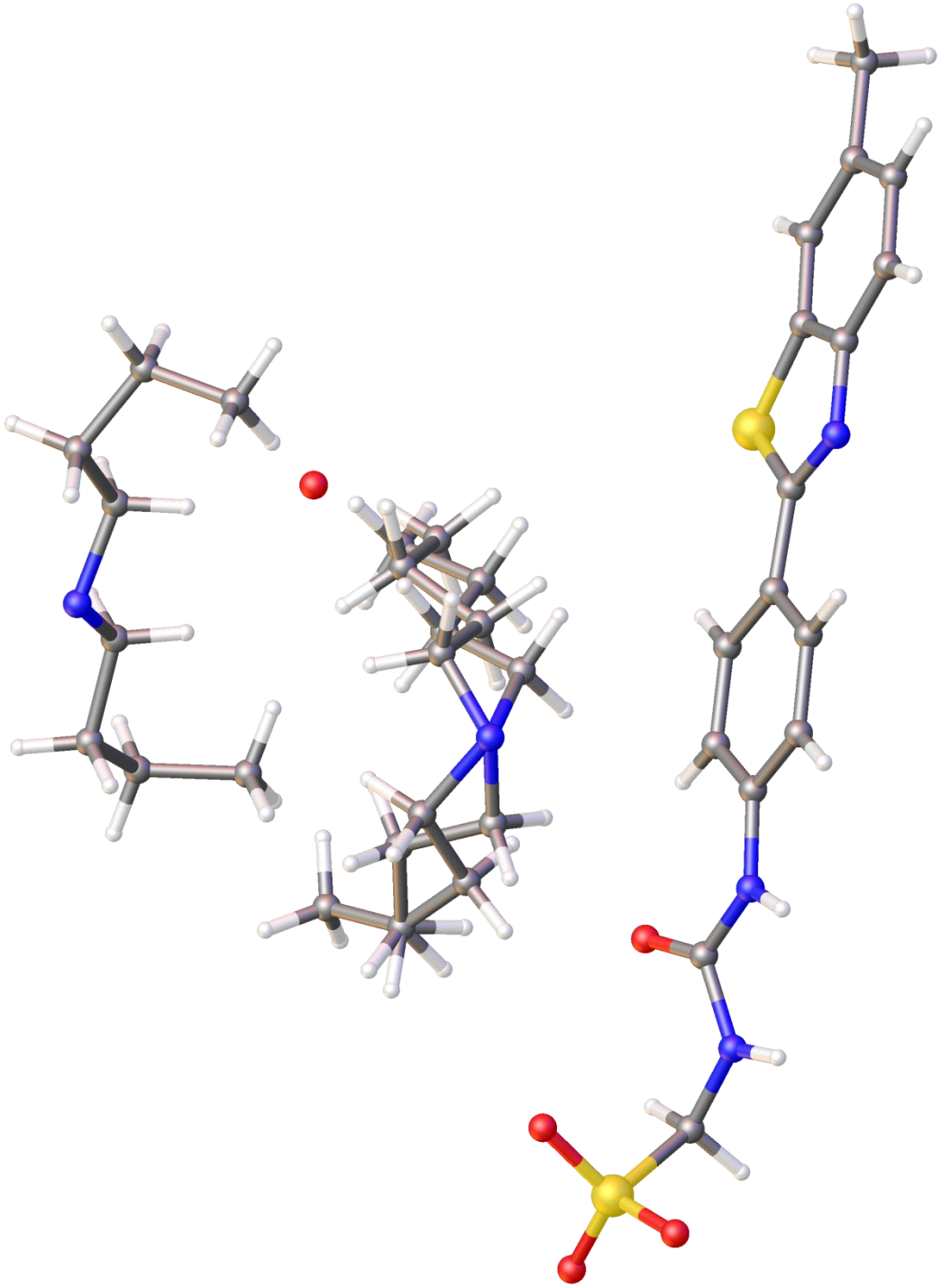

Figure S228 - Crystal data for compound **4**: red = oxygen; yellow = sulfur; blue = nitrogen; white = hydrogen; grey = carbon. CCDC 1562759, $C_{32}H_{50}N_4O_{4.5}S_2$ (M =626.88): monoclinic, space group P 1 2/n 1, a = 12.706(3) Å, b = 13.689(4) Å, c = 19.969(4) Å, α = 90°, β = 107.12(3)°, γ = 90°, V = 3319.3(16) $Å^3$, Z = 4, T = 100(1) K, CuK\α = 1.5418 Å, Dcalc = 1.254 g/cm^3, 12807 reflections measured (7.390 ≤ 2Θ ≤ 133.20), 5872 unique (R_{int} = 0.1197, R_{sigma} = 0.1660) which were used in all calculations. The final R_1 was 0.0673 (I > 2σ(I)) and wR_2 was 0.1610 (all data).

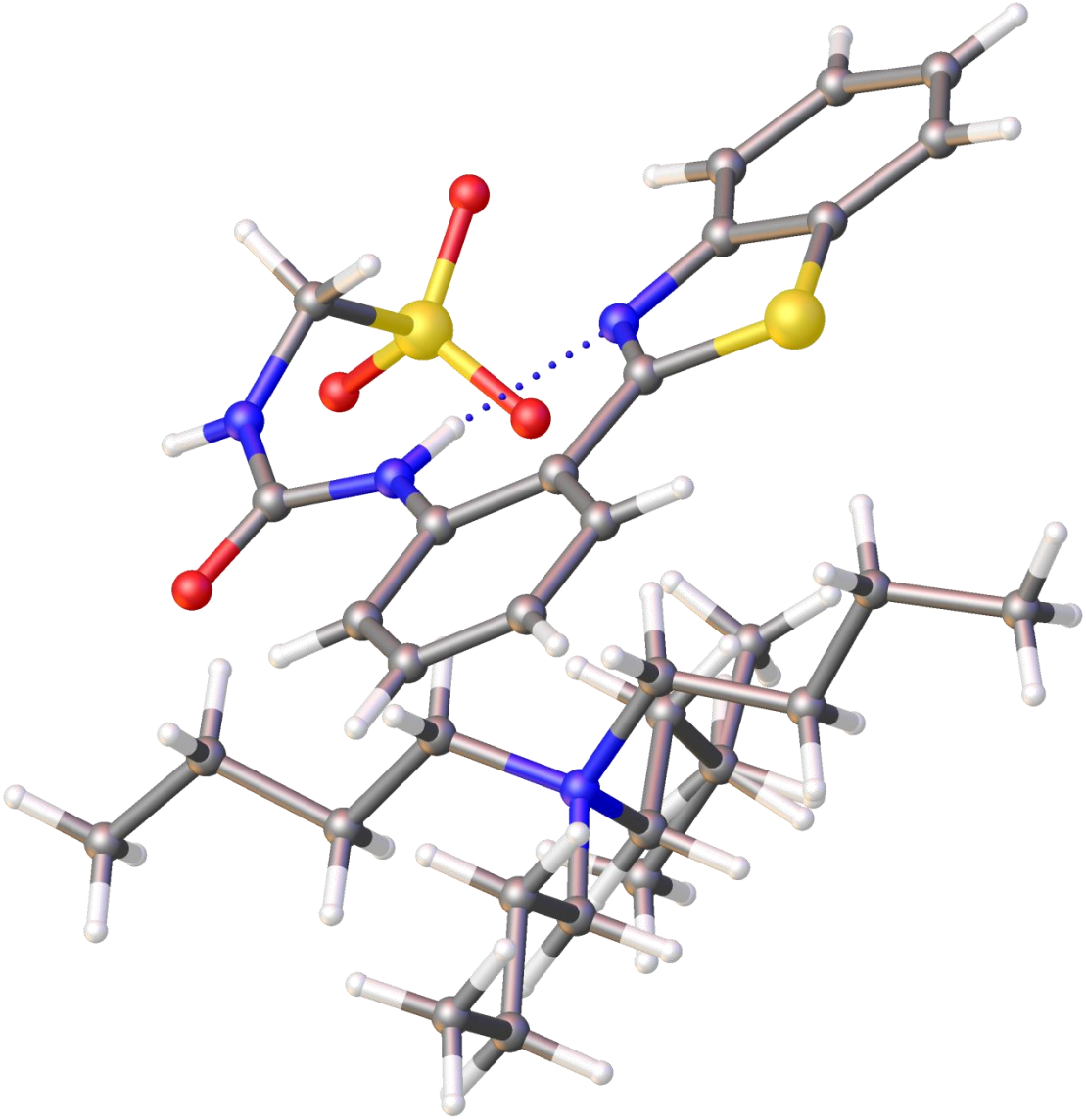

Figure S229 - Crystal data for compound **5**: red = oxygen; yellow = sulfur; blue = nitrogen; white = hydrogen; grey = carbon. CCDC 1562760, $C_{31}H_{48}N_4O_4S_2$ (M =604.85): monoclinic, space group P 1 21/c 1, a = 13.8269(16) Å, b = 14.5451(15) Å, c = 16.5512(16) Å, α = 90°, β = 103.927(11)°, γ = 90°, V = 3230.8(6) $Å^3$, Z = 4, T = 100(1) K, CuK\α = 1.5418 Å, Dcalc = 1.244 g/cm^3, 12954 reflections measured (8.200 ≤ 2Θ ≤ 133.202), 5716 unique (R_{int} = 0.0436, R_{sigma} = 0.0508) which were used in all calculations. The final R_1 was 0.0463 (I > 2σ(I)) and wR_2 was 0.1308 (all data).

Hydrogen bonding tables from single crystal X-ray structures

Table S3: Hydrogen bond distances and angles involved in dimer formation, calculated from single crystal X-ray structures.

Compound	Hydrogen bond donor	Hydrogen atom	Hydrogen bond acceptor	Hydrogen bond length (D•••A) (Å)	Hydrogen bond angle (D-H•••A) (°)
1	N1	H1	O8	2.950 (13)	162.8 (7)
1	N2	H2	O10	2.936 (13)	167.0 (6)
1	N3	H3	O6	2.963 (15)	158.0 (7)
1	N4	H4	O5	2.843 (14)	158.8 (6)
2	N2	H2	O3	2.864 (3)	151.88 (13)
2	N1	H1a	O3	2.858 (3)	155.21 (13)
2	O5	H5b	O1	2.821 (3)	170.08 (17)
2	O5	H5c	O2	2.813 (3)	160.56 (16)
4	N2	H2	O2	2.862 (5)	170.9 (3)
4	N3	H3	O4	2.898 (5)	171.6 (3)
4	O5	-	O4	2.826 (6)	-
5	N3	H3	O4	2.853 (2)	140.47 (13)
5	N2	H2	N1	2.697 (3)	137.56 (12)
5	N2	H2	O2	3.410 (2)	133.09 (12)
5	C12	H12	O1	2.836 (3)	123.43 (14)
5	C2	H2a	O3	3.383 (3)	178.10 (16)

Surface tension measurements

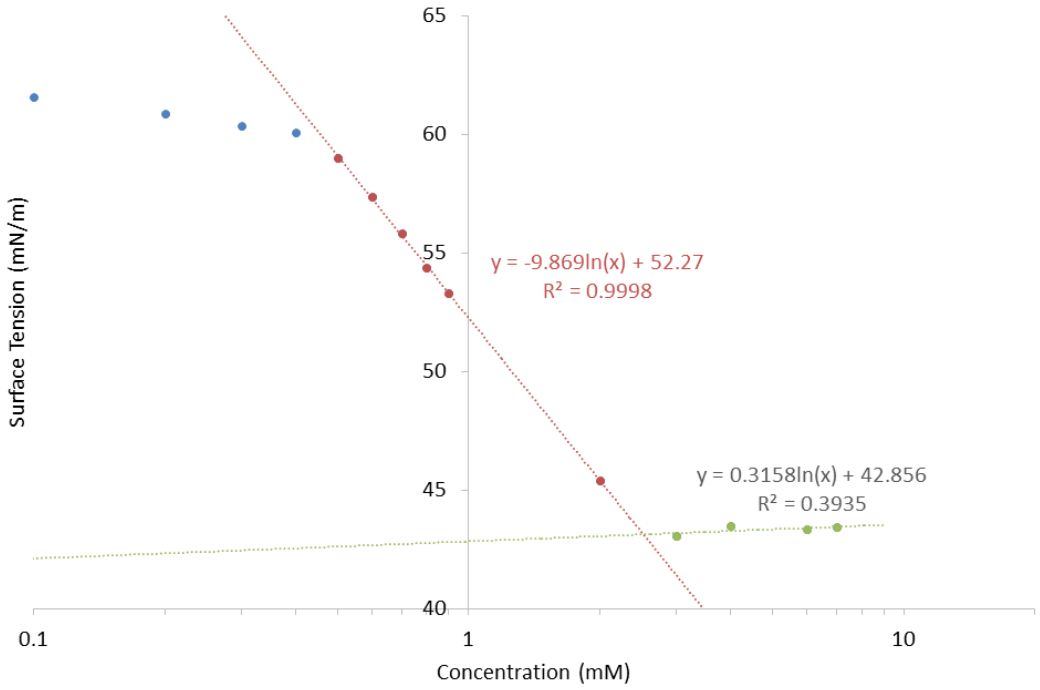

Figure S230 - Calculation of CMC for compound **1** in an EtOH: H_2O 1: 19 mixture using surface tension measurements.

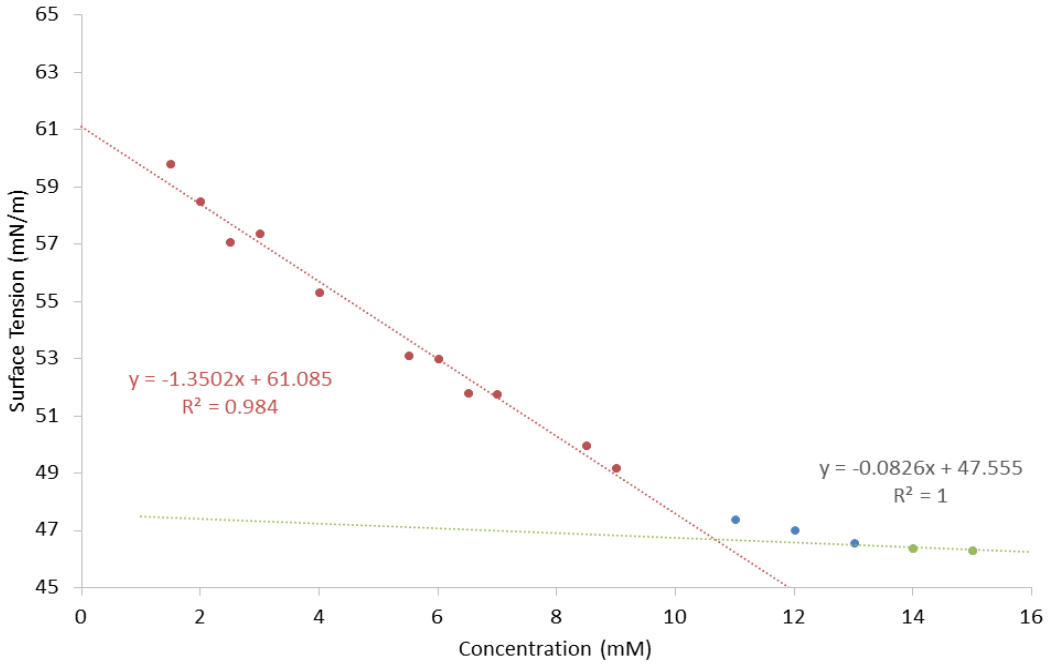

Figure S231 - Calculation of CMC for compound **2** in an EtOH: H_2O 1: 19 mixture using surface tension measurements.

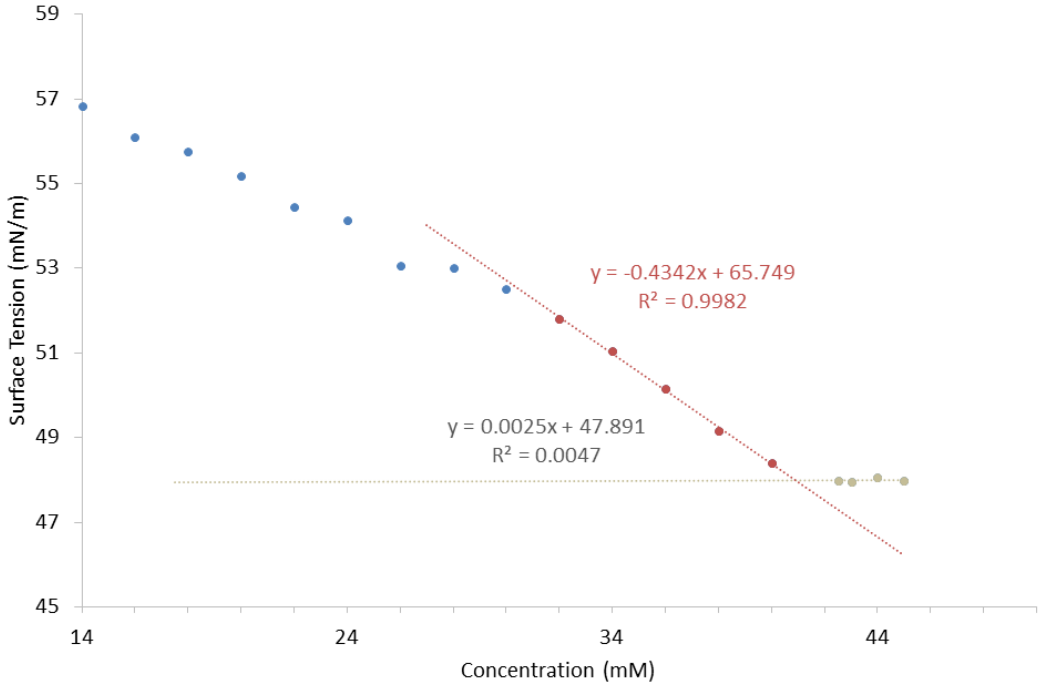

Figure S232 - Calculation of CMC for compound **3** in an EtOH: H_2O 1: 19 mixture using surface tension measurements.

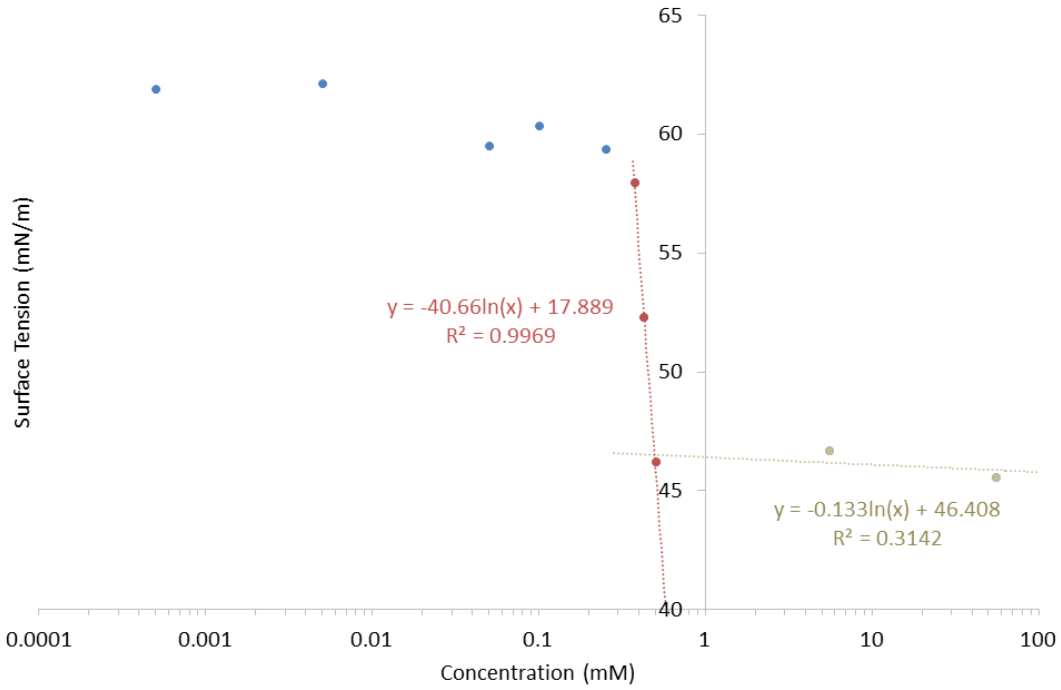

Figure S233 - Calculation of CMC for compound **4** in an EtOH: H_2O 1: 19 mixture using surface tension measurements.

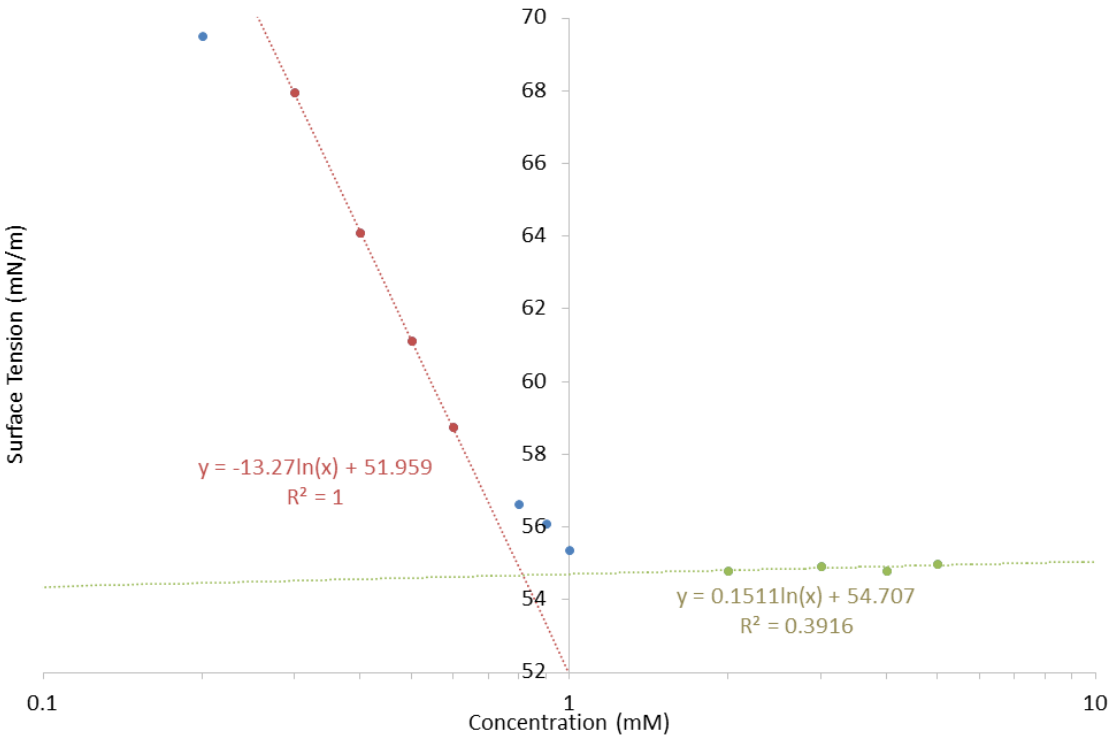

Figure S234 - Calculation of CMC for compound **4** in H_2O using surface tension measurements.

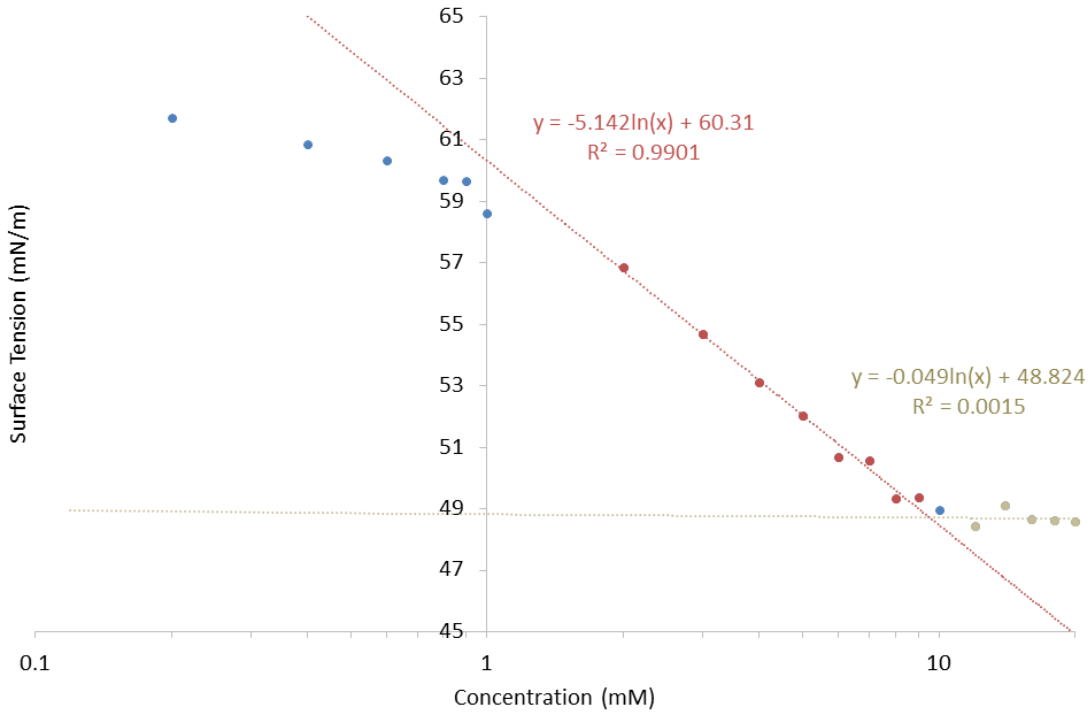

Figure S235 - Calculation of CMC for compound **5** in an EtOH: H_2O 1: 19 mixture using surface tension measurements.

Microscopy images

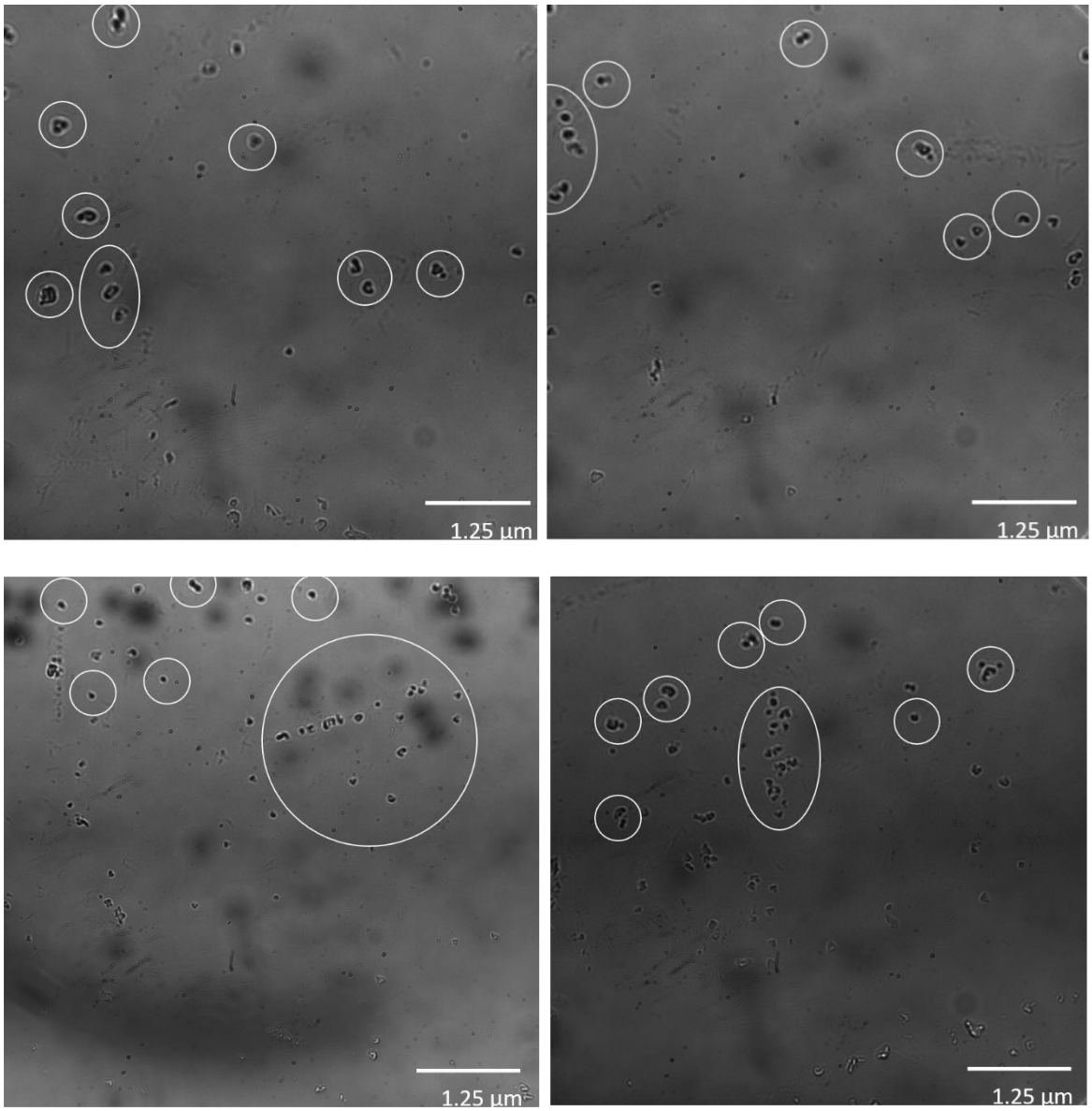

Figure S236 - A selection of transmitted light microscope images of compound **4** (0.50 mM) in an EtOH: H_2O 1: 19 solution. Examples of the aggregate formations have been circled for clarity.

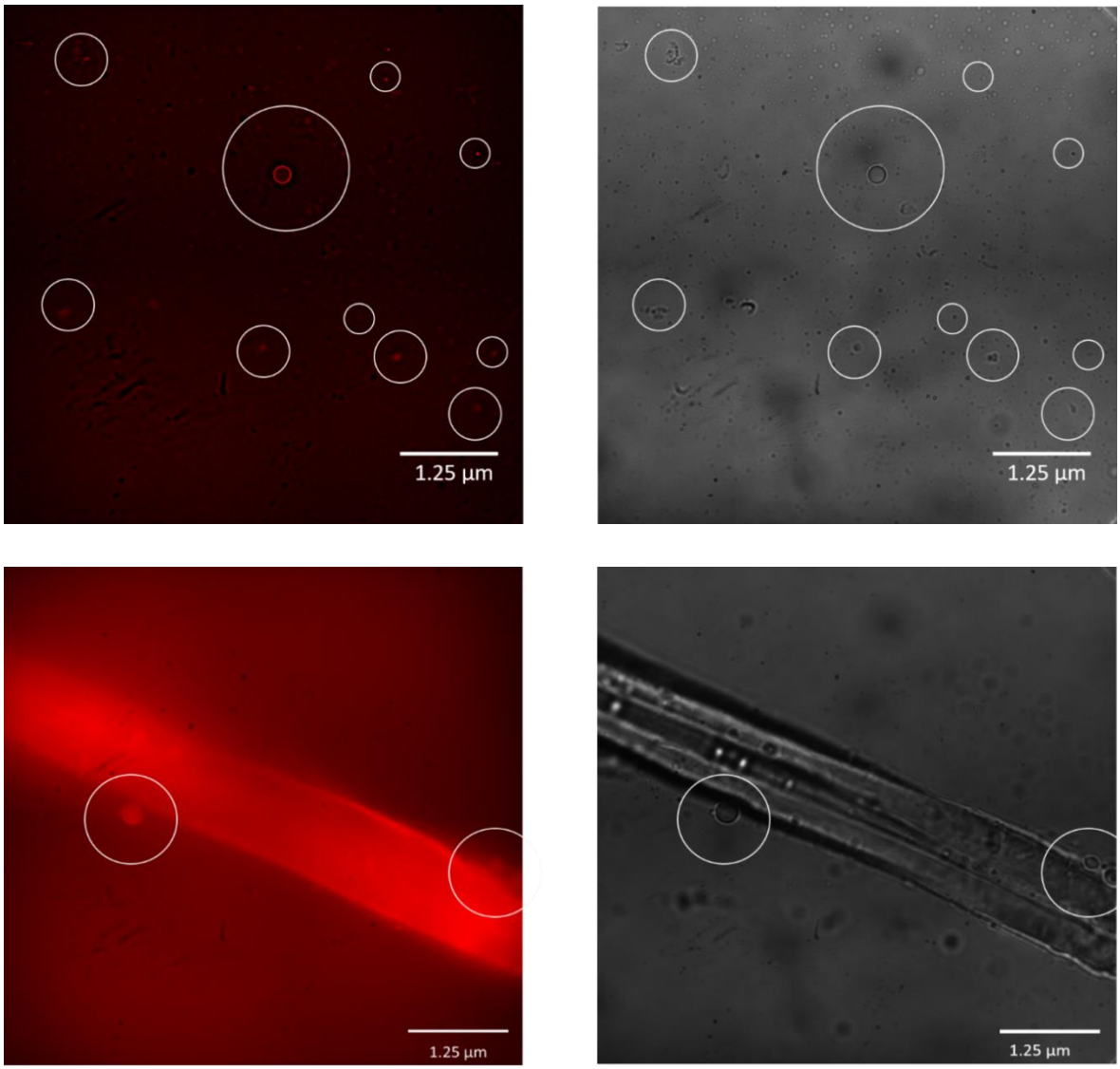

Figure S237 – A selection of DAPI filter composite images (left) and transmitted light images (right) of compound **4** at a concentration of 0.50 mM in a solution of DMSO: H_2O 1: 19. Evidence of aggregate formations are circled for clarity. Photo bleaching during the imagery lead to a loss of fluorescence emission intensity, therefore some compound aggregates could not be successfully captured in one (or both images).

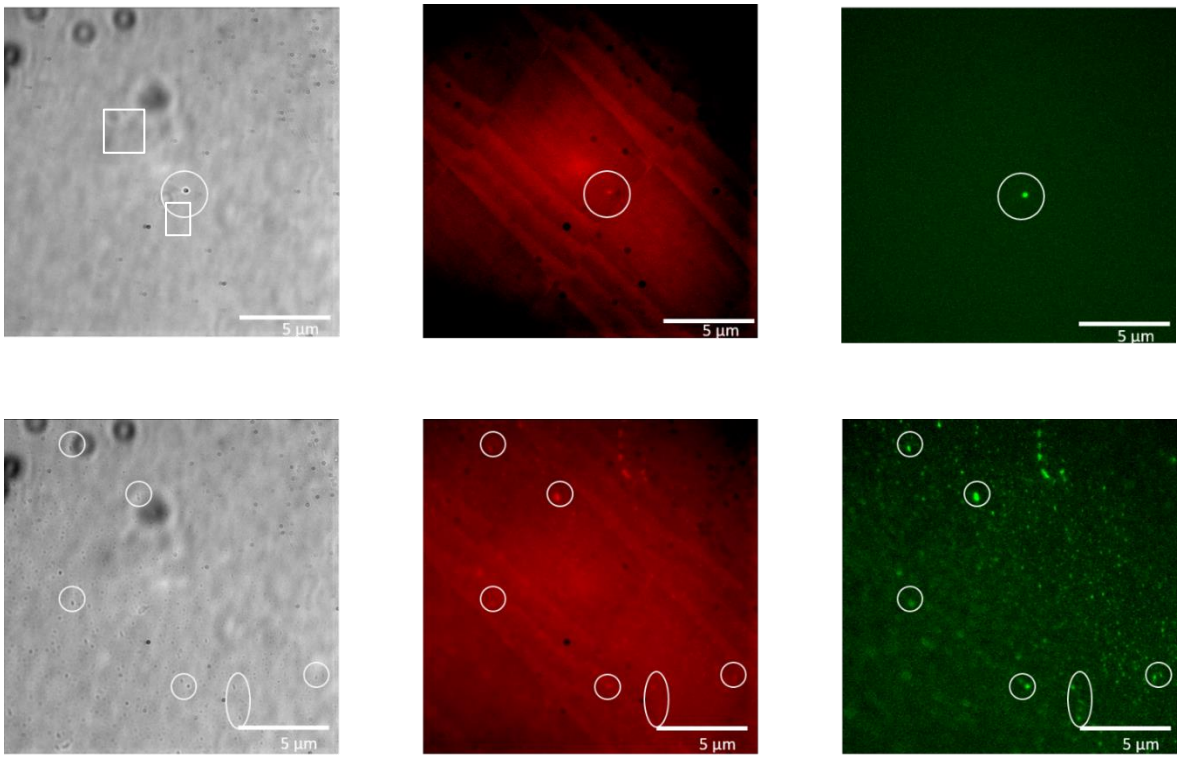

Figure S238 – A selection transmitted light images (left) DAPI filter composite images (centre) and GFP filter image (right) of compound **4** at a concentration of 0.50 mM in a solution of DMSO: H_2O 3: 7. Evidence of aggregate formations of varying sizes are circled for clarity. Photo bleaching during the imagery lead to a loss of fluorescence emission intensity, therefore some compound aggregates could not be successfully captured in one (both or all images).

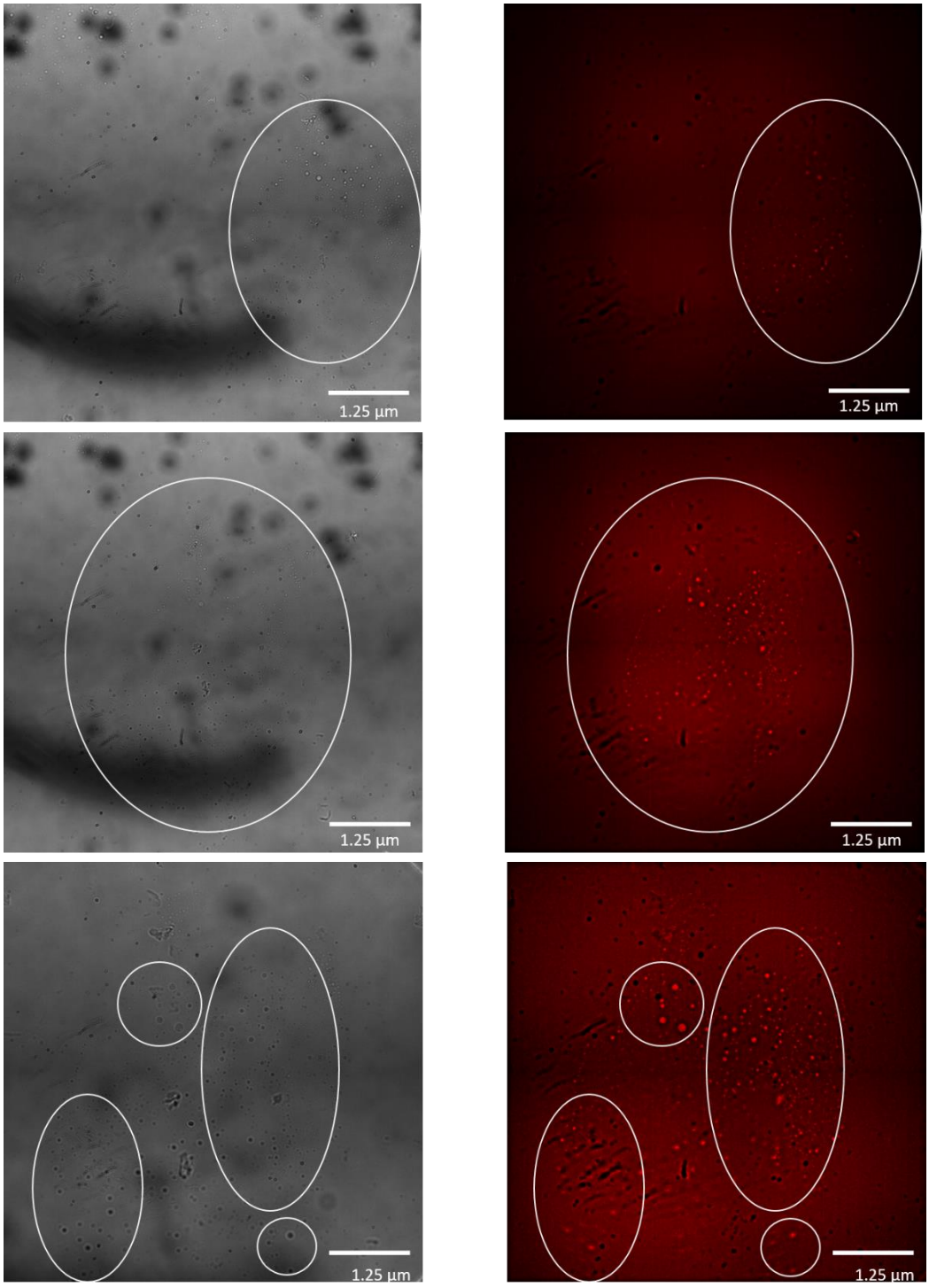

Figure S239 - A selection transmitted light images (left) and DAPI filter composite images (right) of compound **4** at a concentration of 0.50 mM in DMSO. Evidence of aggregate formations are circled for clarity. Photo bleaching during the imagery lead to a loss of fluorescence emission intensity, therefore some compound aggregates could not be successfully captured in one (or both images).

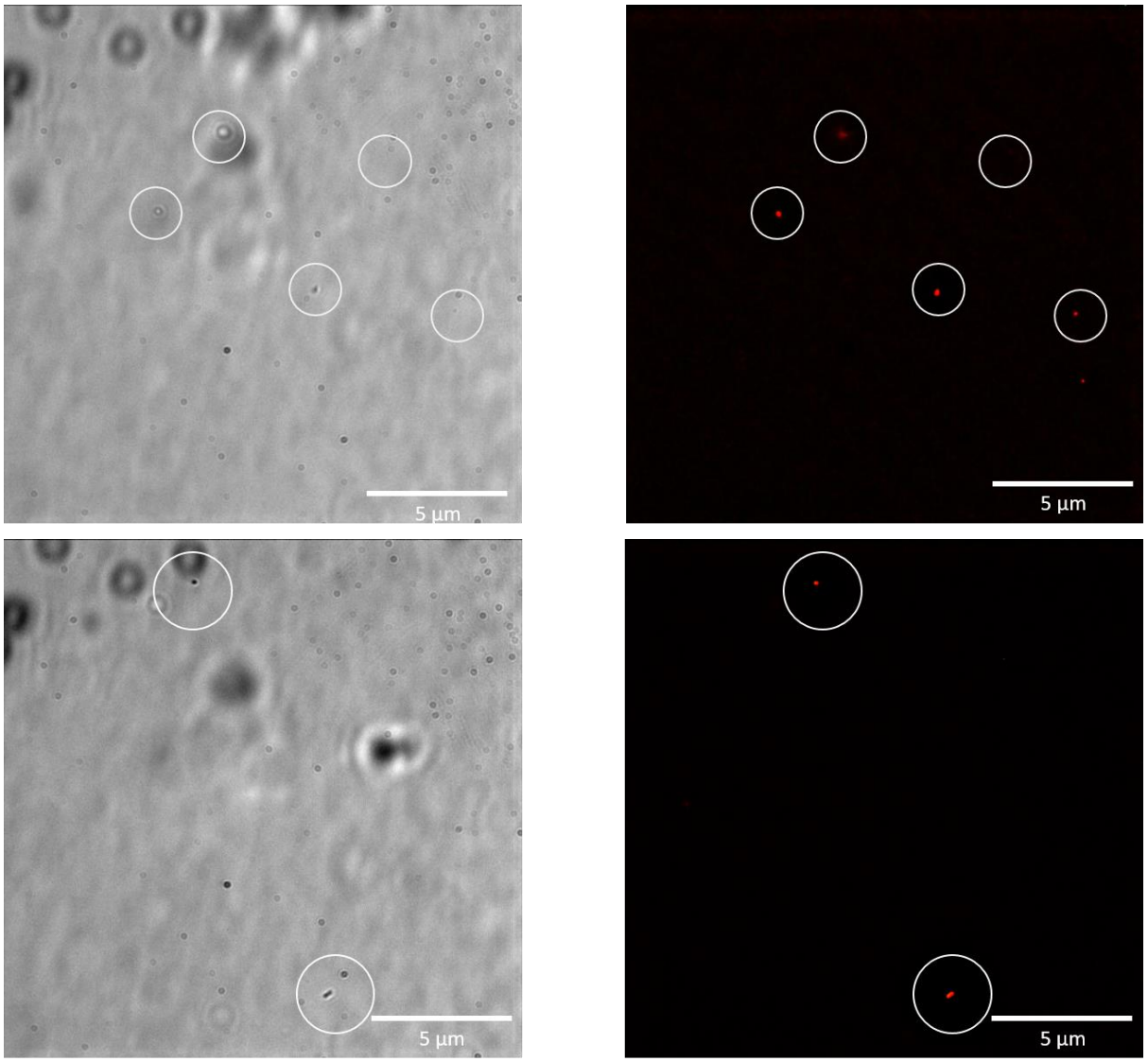

Figure S240 - A selection of transmitted light images (left) and DAPI filter composite images (right) of compound **5** at a concentration of 0.50 mM in a solution of EtOH: H_2O 1: 19. Evidence of aggregate formations are circled for clarity. Photo bleaching during the imagery lead to a loss of fluorescence emission intensity, therefore some compound aggregates could not be successfully captured in one (or both images).

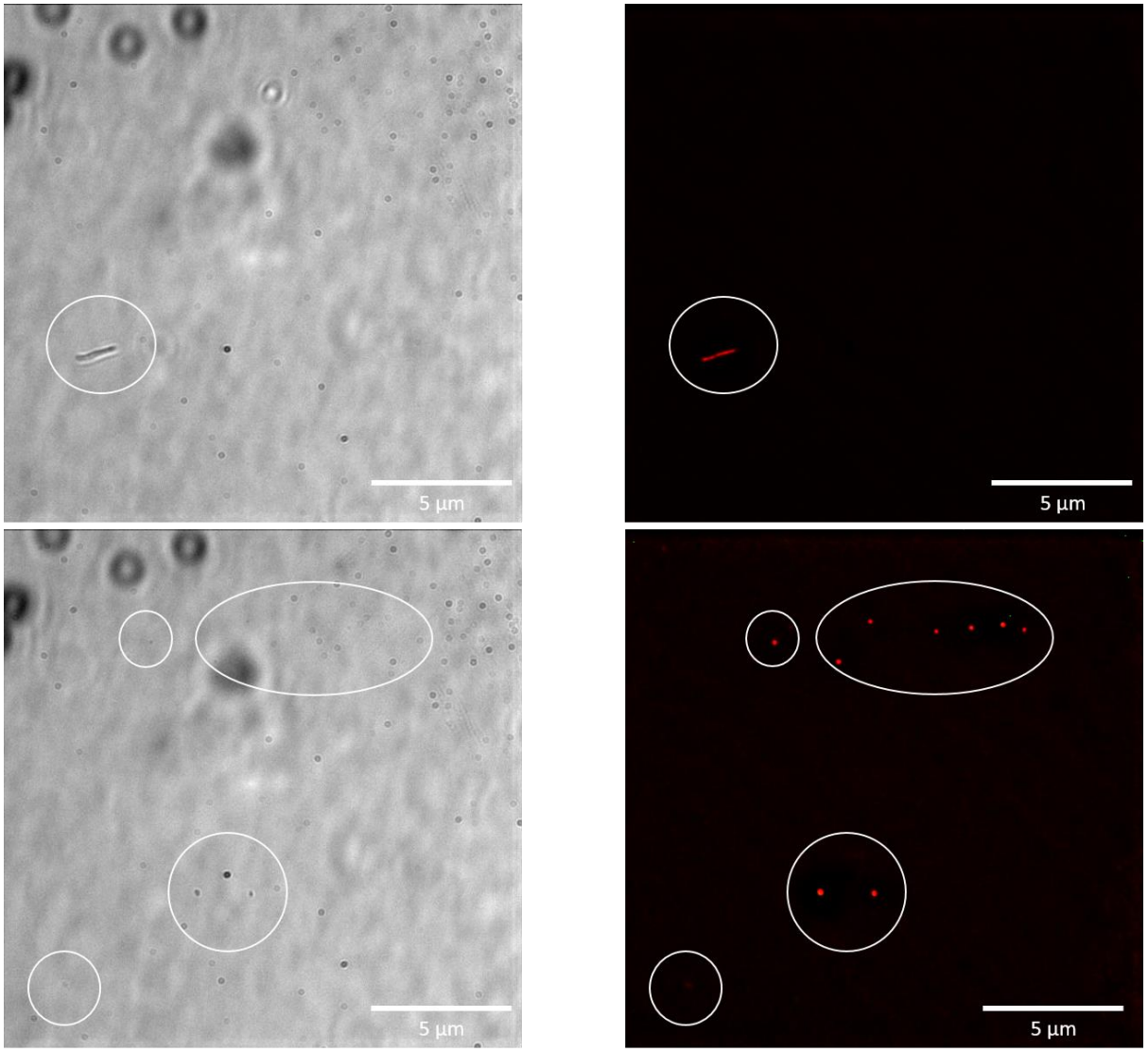

Figure S241 - A selection of transmitted light images (left) and DAPI filter composite images (right) of compound **5** at a concentration of 0.50 mM in a solution of DMSO: H_2O 1: 1. Evidence of aggregate formation are circled for clarity. Photo bleaching during the imagery lead to a loss of fluorescence emission intensity, therefore some compound aggregates could not be successfully captured in one (or both images).

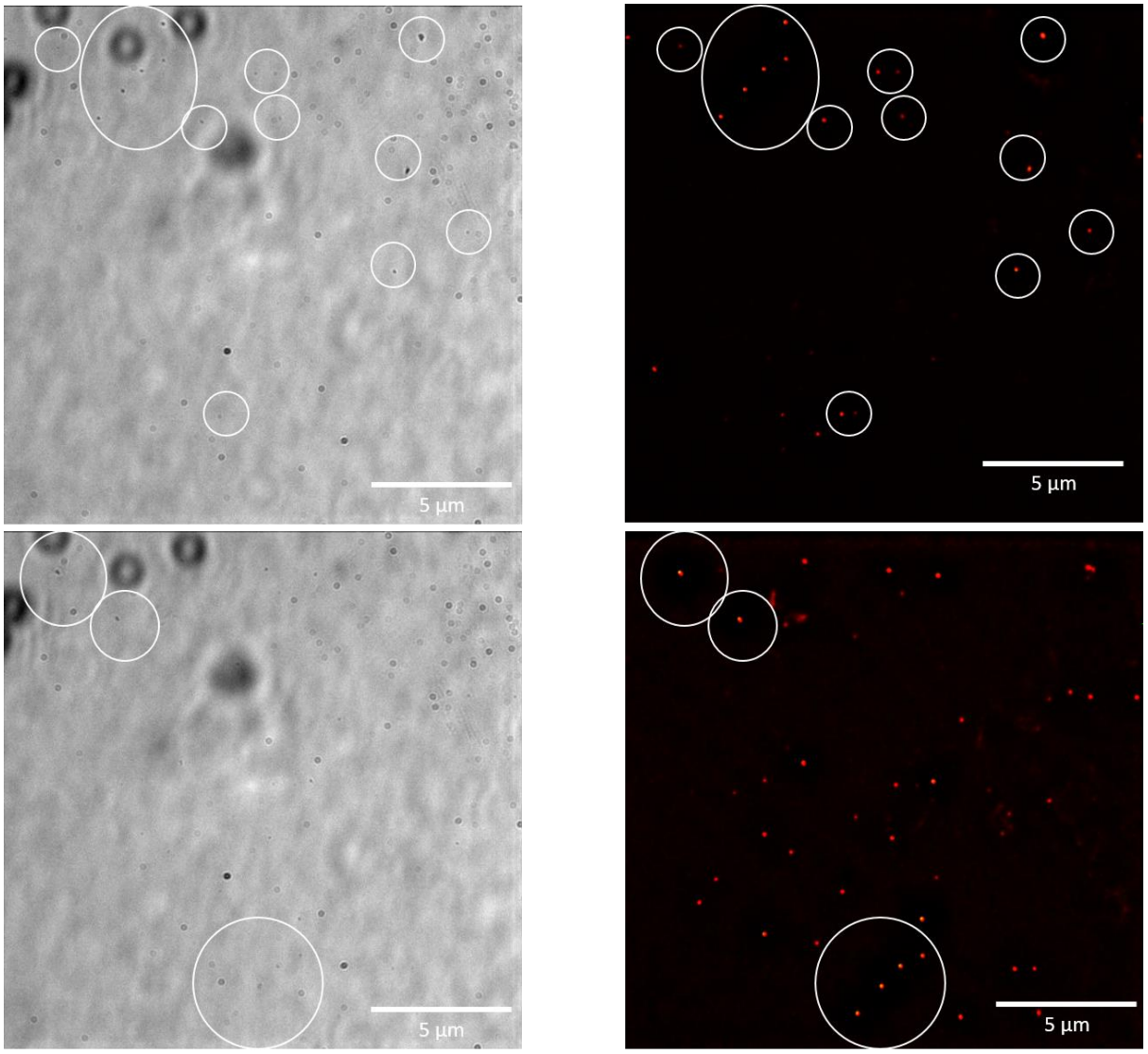

Figure S242 - A selection of transmitted light images (left) and DAPI/ GFP filter overlay images (right) of compound **5** at a concentration of 0.50 mM in a solution of DMSO: H_2O 3: 7. Evidence of aggregate formations are circled for clarity. Photo bleaching during the imagery lead to a loss of fluorescence emission intensity, therefore some compound aggregates could not be successfully captured in one (or both images).

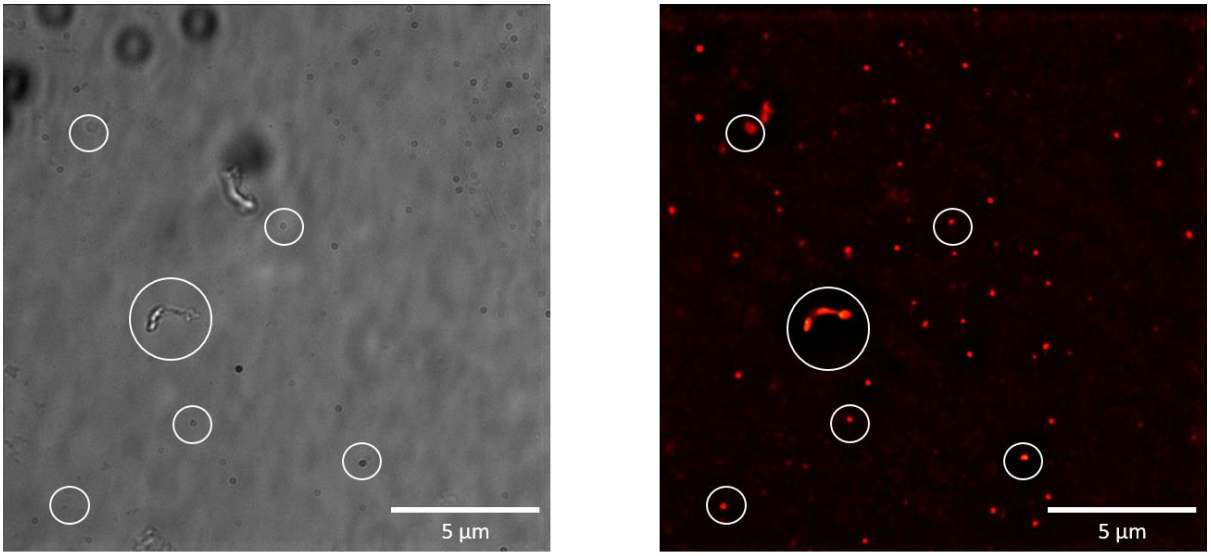

Figure S243 - A selection from transmitted light images (left) and comparison DAPI/ GFP filter overlay images (right) of compound **5** at a concentration of 0.50 mM in a solution of DMSO 1: 4 H_2O Evidence of aggregate formations are circled for clarity. Photo bleaching during the imagery lead to a loss of fluorescence emission intensity, therefore some compound aggregates could not be successfully captured in one (or both images).

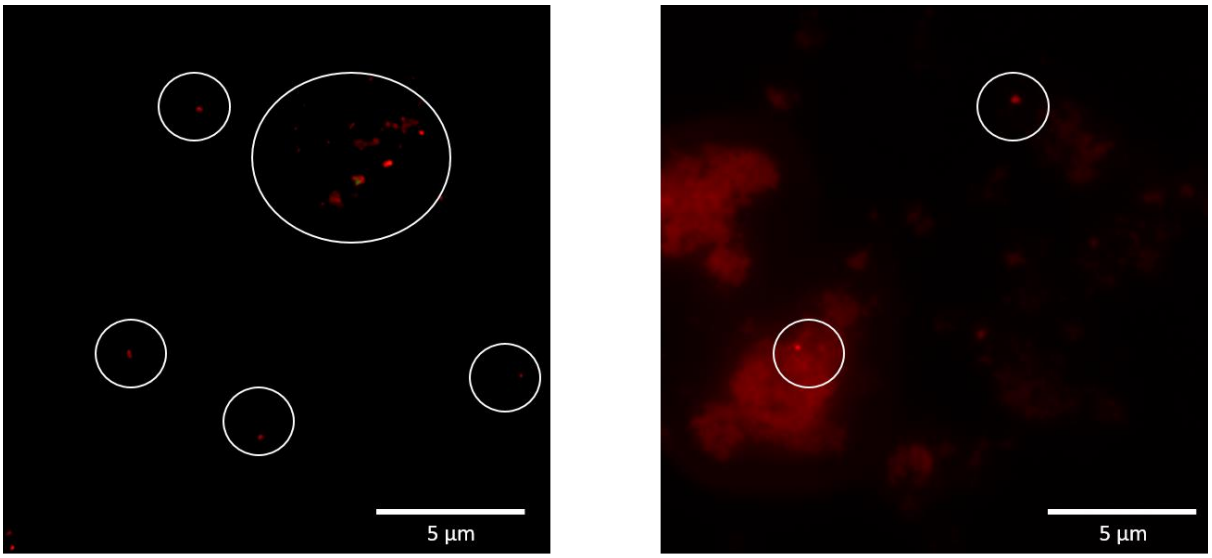

Figure S244 - A selection of DAPI filter images of compound **5** at a concentration of 0.50 mM in DMSO. Evidence of aggregate formations are circled for clarity. Photo bleaching during the imagery lead to a loss of fluorescence emission intensity, therefore some compound aggregates could not be successfully captured in one (or both images).

In-silico modelling

Computational calculations for compounds **1**-**5** were conducted in line with studies reported by Hunter using Spartan 16'' in order to identify primary hydrogen bond donating and accepting sites.[3] Calculations were performed using semi-empirical PM6 methods to model electrostatic potential maps and identify corresponding E_{max} and E_{min} values. PM6 was used over AM1 in line with research conducted by Stewart.[4]

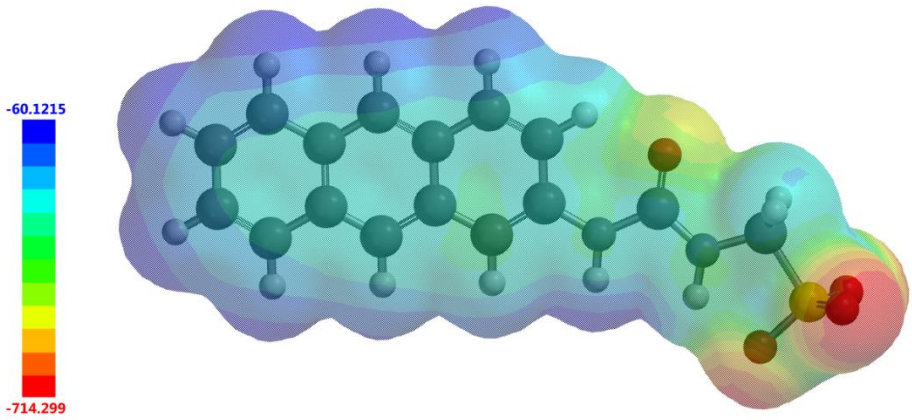

Figure S245 - Electrostatic potential map calculated for **1** using semi-empirical PM6 modelling methods. E_{max} and E_{min} values depicted in the figure legends are given in KJ/mol.

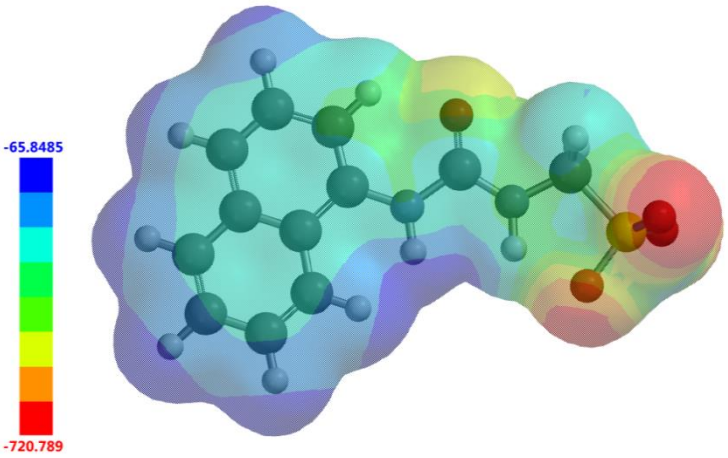

Figure S246 - Electrostatic potential map calculated for **2** using semi-empirical PM6 modelling methods. E_{max} and E_{min} values depicted in the figure legends are given in KJ/mol.

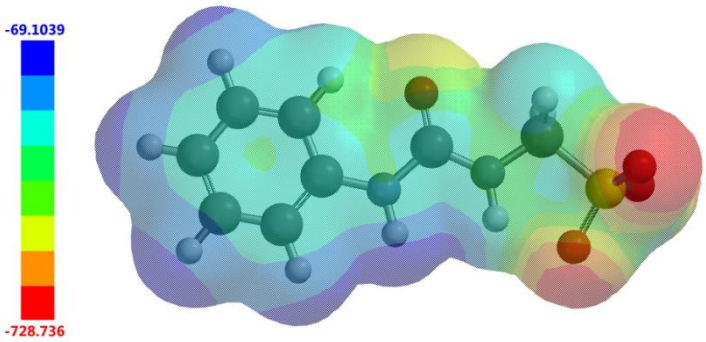

Figure S247 - Electrostatic potential map calculated for **3** using semi-empirical PM6 modelling methods. E_{max} and E_{min} values depicted in the figure legends are given in KJ/mol.

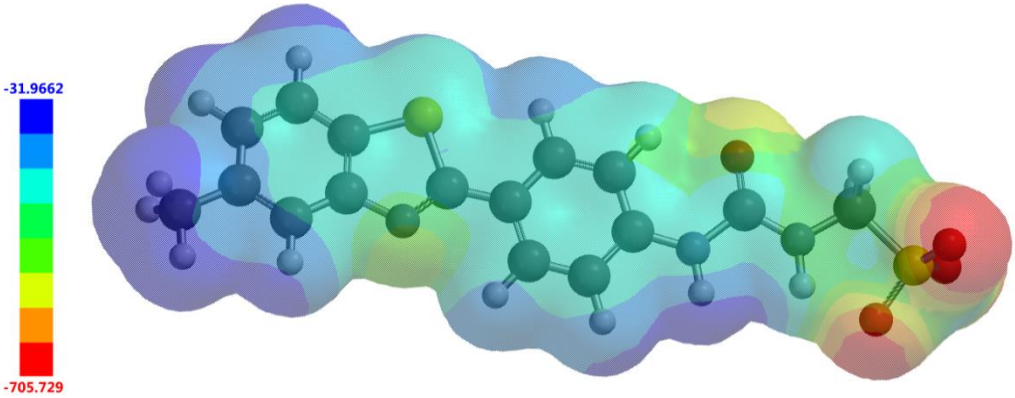

Figure S248 - Electrostatic potential map calculated for **4** using semi-empirical PM6 modelling methods. E_{max} and E_{min} values depicted in the figure legends are given in KJ/mol.

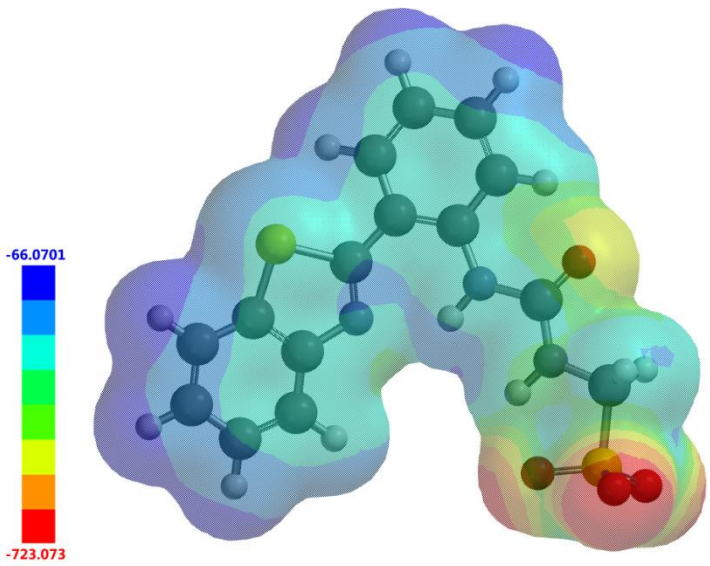

Figure S249 - Electrostatic potential map calculated for **5** using semi-empirical PM6 modelling methods. E_{max} and E_{min} values depicted in the figure legends are given in KJ/mol.

Mass Spectrum Data

Acquisition Parameter					
Source Type	ESI	Ion Polarity	Negative	Set Nebulizer	0.4 Bar
Focus	Not active	Set Capillary	3500 V	Set Dry Heater	180 °C
Scan Begin	100 m/z	Set End Plate Offset	-100 V	Set Dry Gas	4.0 l/min
Scan End	1350 m/z	Set Collision Cell RF	150.0 Vpp	Set Divert Valve	Source

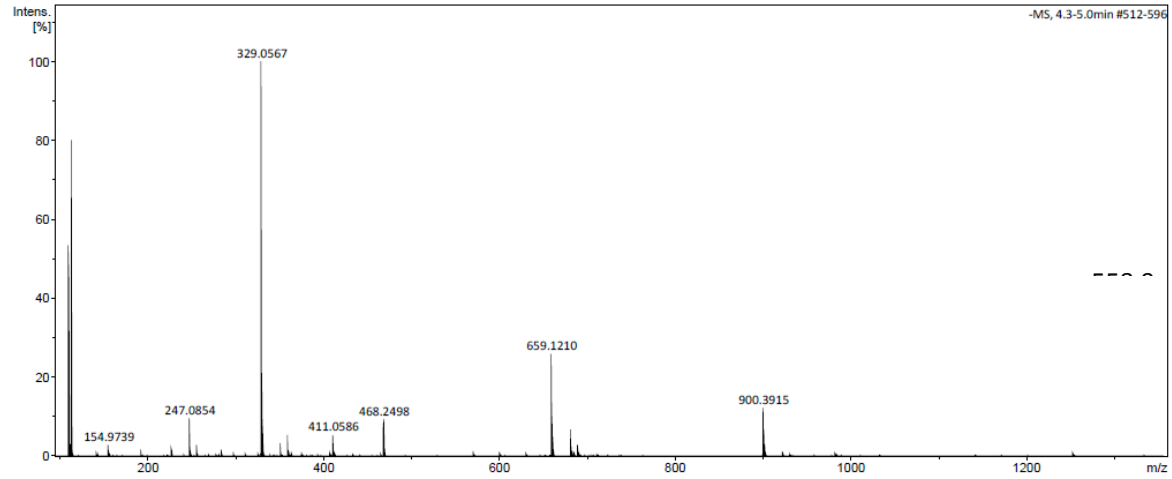

Figure S250 – Mass spectrum collected for compound **1**.

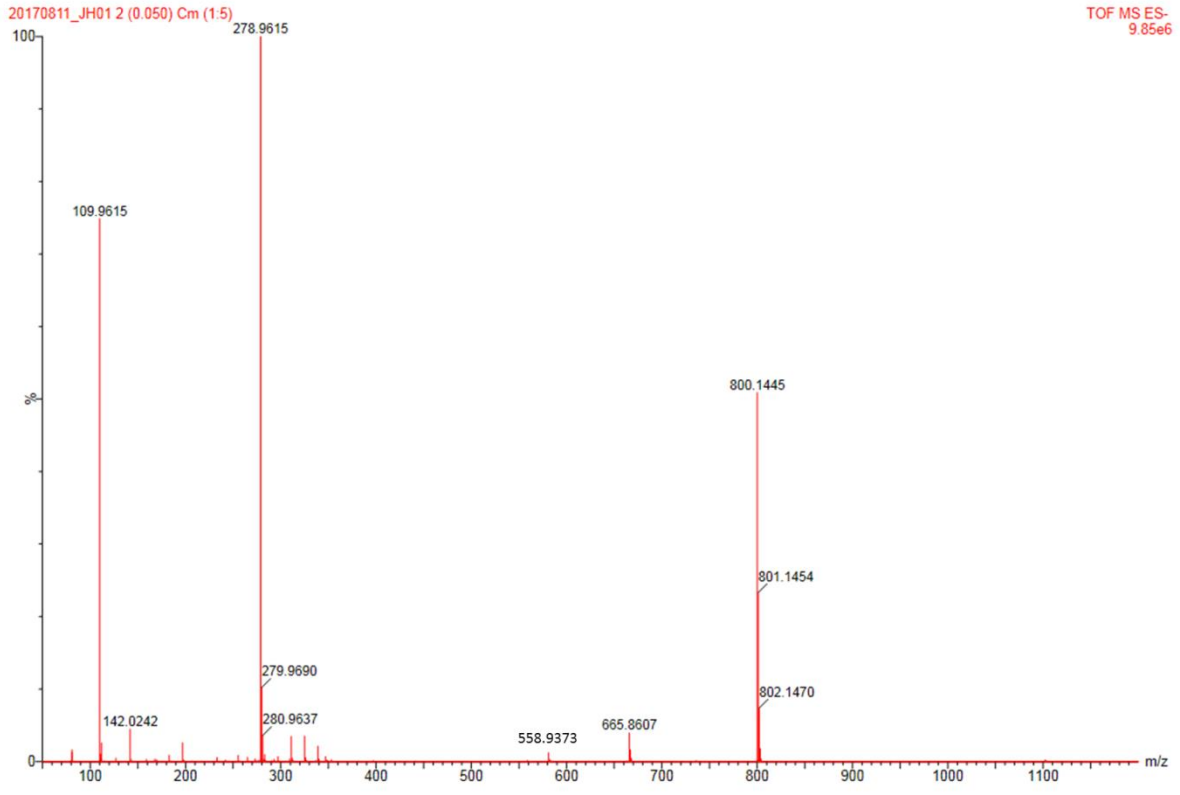

Figure S251 – Mass spectrum collected for compound **2**. Analysed using Mass Lynx software

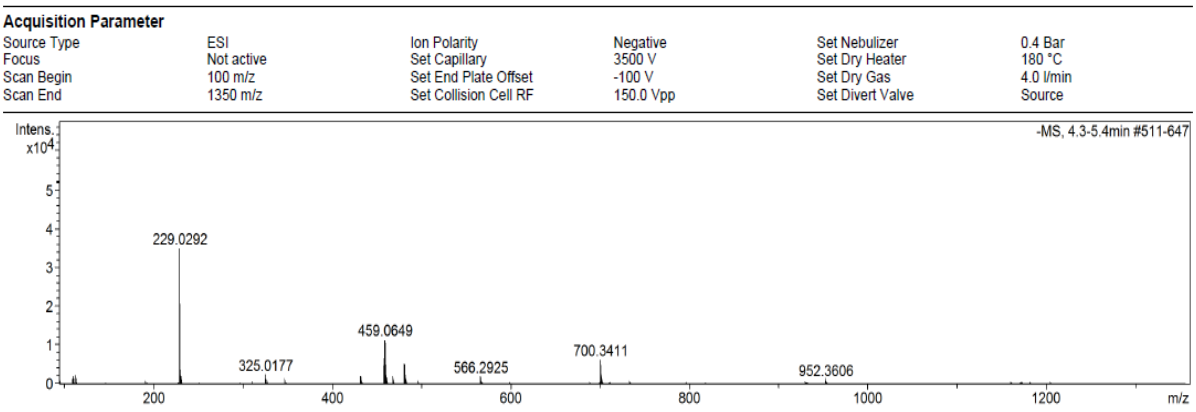

Figure S252 – Mass spectrum collected for compound **3**.

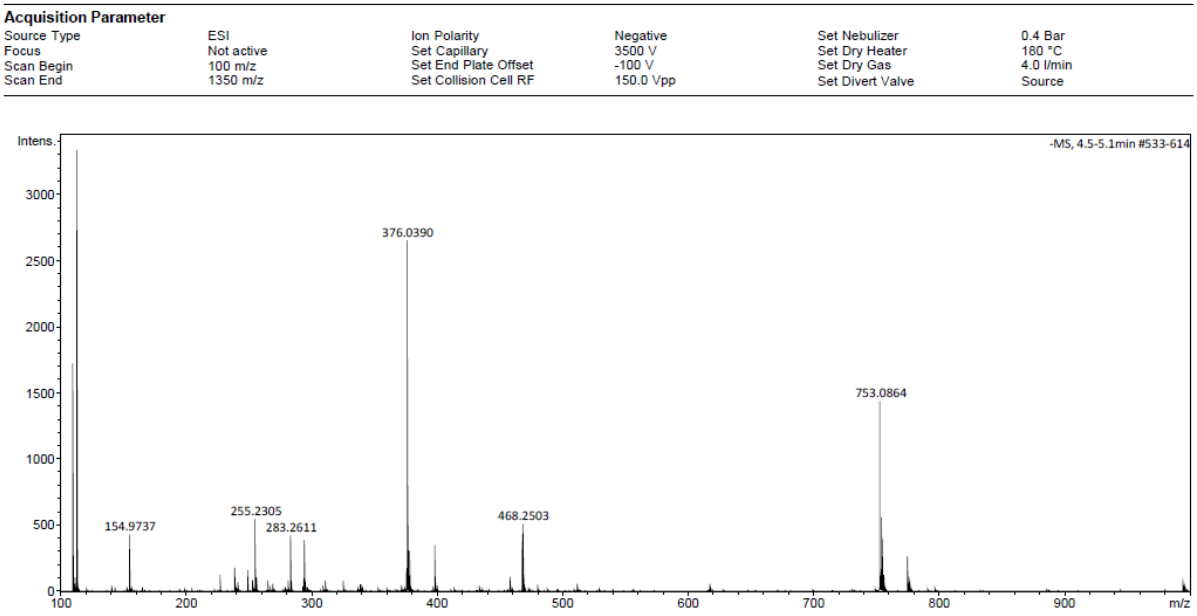

Figure S253 – Mass spectrum collected for compound **4**.

Acquisition Parameter					
Source Type	ESI	Ion Polarity	Negative	Set Nebulizer	0.4 Bar
Focus	Not active	Set Capillary	3500 V	Set Dry Heater	180 °C
Scan Begin	100 m/z	Set End Plate Offset	-100 V	Set Dry Gas	4.0 l/min
Scan End	1350 m/z	Set Collision Cell RF	150.0 Vpp	Set Divert Valve	Source

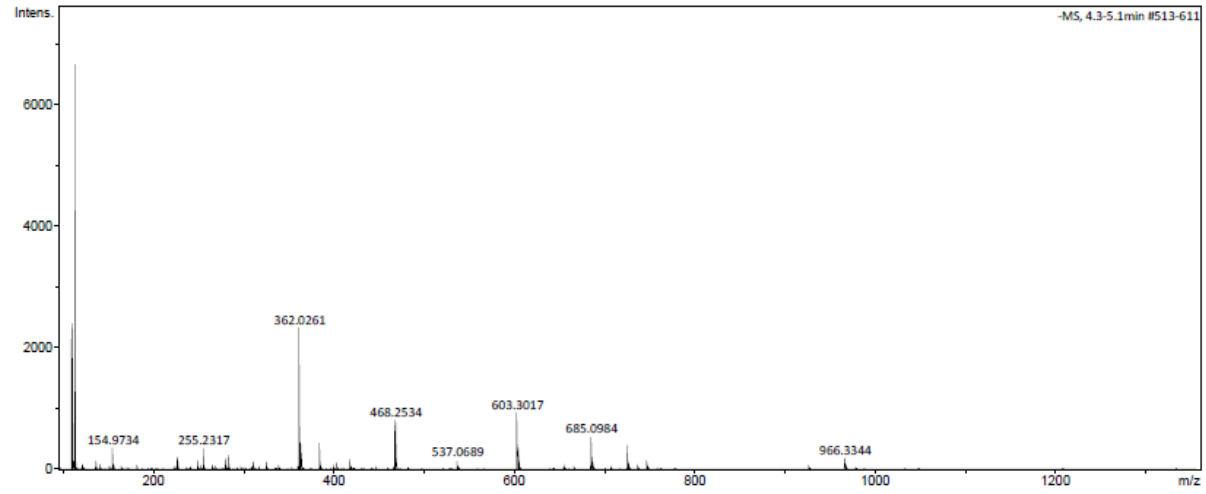

Figure S254 – Mass spectrum collected for compound **5**.

References

1. Levin, P.A. (2002) Light microscopy techniques for bacterial cell biology. In *Methods in Microbiology: Molecular Cellular Microbiology*, Vol. **31**. Sansonetti, P., and Zychlinsky, A. (eds). London: Academic Press Ltd., pp. 115–132.
2. L. R. Blackholly, H. J. Shepherd and J. R. Hiscock, *Crystengcomm*, 2016, **18**, 7021-7028.
3. C. A. Hunter, *Angewandte Chemie-International Edition*, 2004, **43**, 5310-5324.
4. J. J. P. Stewart, *Journal of Molecular Modeling*, 2007, **13**, 1173-1213.